CALCIUM SIGNALING

IN

PSEUDOMONAS AERUGINOSA

By

MANITA GURAGAIN

Masters of Science in Microbiology
Tribhuvan University
Kathmandu, Nepal
2005

Submitted to the Faculty of the
Graduate College of the
Oklahoma State University
in partial fulfillment of
the requirements for
the Degree of
DOCTOR OF PHILOSOPHY
December, 2015

CALCIUM SIGNALING

IN

PSEUDOMONAS AERUGINOSA

Dissertation Approved:

Dr. Marianna A. Patrauchan

Dissertation Adviser

Dr. Edward I. Shaw

Dr. Jeffery A. Hadwiger

Dr. Erika I. Lutter

Dr. Antonius G. Oomens

ACKNOWLEDGEMENTS

I would like to express my sincere gratitude to all individuals who motivated, inspired, helped, supported and encouraged me to reach the height and depth of my doctoral research work.

My first and deepest gratitude goes to my committee chair and advisor Dr. Marianna A. Patrauchan, for giving me an opportunity to pursue doctoral research under her guidance. It would not have been possible to accomplish my dissertation research without her expert advice, continuous support, strong motivations, invaluable suggestions, critical discussions, and unending patience. Dr. Patrauchan, I am equally indebted to you for training and helping me with mentorship, scientific writings, fellowships and award application skills. I would like to dedicate my awards and honors to you, for you believed in me more than myself. I cannot thank you enough for nurturing my research interest, providing a healthy working environment and supporting my graduate career morally and financially. You will continue to be my inspiration for perseverance, enthusiasm, and love for research. I want to express my deepest gratitude for your warm support during the most delicate transitions in my professional and personal life. I feel extremely lucky to find you as my research advisor and mentor.

Acknowledgements reflect the views of the author and are not endorsed by committee members or Oklahoma State University.

I would like to thank all the members of my graduate committee, Dr. Edward I. Shaw, Dr. Jeffery A. Hadwiger, Dr. Erika I. Lutter, and Dr. Antonius G. Oomens for their invaluable suggestions, critical insights, guidance, and support for my research. I am very grateful to all of you for providing collegial and conducive atmosphere during each committee meeting and beyond. A sincere thank you for your precious time spent for critically reviewing my dissertation. I would like to extend special thank you to Dr. Lutter for her invaluable suggestions on extraction of quorum sensing molecules and sharing her protocols, strains, and equipment.

I would also like to thank Dr. William D. Picking and Wendy L. Picking for allowing me to work under their supervision. I am very grateful to both of you for your expert guidance and training on gene cloning, protein purification, immunofluorescence, and cell invasion procedures. I want to specially thank Dr. William D. Picking for making my professional transition smooth despite all the odds and for all the support afterwards.

I would like to acknowledge the Department of Microbiology and Molecular Genetics for accepting me in the graduate program and continuously supporting me financially. I would like to thank Microbiology office staff, past and present for making my graduate journey smooth and enjoyable. My very special thanks go to senior administrative assistant Sallie Robinson, for all her care, help and guidance throughout my graduate career, timely orders and constant reminders about various deadlines. Sallie,

Acknowledgements reflect the views of the author and are not endorsed by committee members or Oklahoma State University.

I am very glad to have you around. Many thanks go to Connie Budd and Dr. Garry Marley for letting me use their facilities and equipment. Thank you both!

A very special thank you goes to the Patrauchan lab members, past and present. I especially want to thank Svetlana, Sharmily, Tammy, Kaylee, Dirk, Amber, Biraj, Michelle, Nitu, Hannah, Afom, Ian, Judson, and Shelby. Thank you all for a friendly and supportive work environment, cooperation, and helpful scientific and non-scientific discussions. I cannot thank you all enough for your help, love, care, and support at some hard times during my graduate career. I will forever cherish your company, gatherings and celebrations as a lab family. My special thanks to Shalaka for her warm welcome in the lab and all her help as a senior colleague and a fine scientist. I never imagined that my graduate career would reward me with a very good friend like you. I miss you and look forward to work with you in future.

I would like to express my sincere gratitude to all scientists whose help make my research efficient and productive. I will like to thank Dr. Steven Hartson (Department of Biochemistry, Oklahoma State University) for letting me use his lab facilities to conduct high performance liquid chromatography (HPLC) analysis. A special thank you for HPLC training, invaluable guidance, critical suggestions, and help with troubleshooting. I would also like to thank Dr. Anthony K. Campbell (School of Pharmacy and Pharmaceutical Sciences, Cardiff, UK) for sharing his expertise and templates for calculating intracellular calcium concentrations, Dr. Delfina Dominguez (University of

Acknowledgements reflect the views of the author and are not endorsed by committee members or Oklahoma State University.

Texas) for sharing *E. coli* strain carrying pMMB66EH plasmid containing , and Dr. Michael Franklin (Montana State University) for successful collaboration

I would like to mention special thanks to my friends Thagendra, Roshani, Nabin, and Sulochana for being my pillar. Thank you for the helping hands being my ultimate backup so that I can focus on my research. I consider myself extremely lucky to find loving and caring friends like you.

Most importantly, I would like to thank my family for helping me become who I am. Words are not enough to appreciate my parent's love, support, encouragement, and dedication throughout my journey. I would like to express immense gratitude to my dad Madhav Prasad Guragain and my mom Januka Guragain for instilling the moral values and nurturing and supporting my decisions. Had it not been your brave decision to let me go away from your sight in a hope of fulfilling my career, I would never be following up my dream. A very special thank goes to my mom for travelling all the way from Nepal to support my graduate career. My dissertation work would not have been as smooth and efficient without you taking care of me and my personal responsibilities. Dear parents, your idea of pursuing any career to the highest peak will definitely drive me to the best opportunities leading to big contributions. Very special thanks to my husband Nirajan Bhattarai for his unconditional love, support, and encouragement. Thank you for making my research a priority above all. A huge thank for your motivation, suggestions, patience, and help. I would also like to thank my brother Manit and sister Mamata for their love,

Acknowledgements reflect the views of the author and are not endorsed by committee members or Oklahoma State University.

care, and support during my graduate career and beyond. A heartfelt thanks goes to my son Nirvaan for bringing joy to our life and filling our lives with positive energy. Coming home and hugging you has been my biggest stress reliever that prepares me for next fresh energetic day!

Finally, I would like to thank everyone else who have helped me in one way or the other during the completion of my doctoral work.

Acknowledgements reflect the views of the author and are not endorsed by committee members or Oklahoma State University.

Name: MANITA GURAGAIN

Date of Degree: DECEMBER, 2015

Title of Study: CALCIUM SIGNALING IN *PSEUDOMONAS AERUGINOSA*

Major Field: MICROBIOLOGYAND MOLECULAR GENETICS

Abstract: *P. aeruginosa* is an opportunistic pathogen and a major cause of hospital acquired infections and severe chronic infections in endocarditis and cystic fibrosis (CF) patients. During such infections, it encounters elevated levels of Ca^{2+}. Ca^{2+} regulates gene expression, physiology, and production of several virulence factors, thereby, enhancing adaptability and virulence of *P. aeruginosa*. This indicates signaling role of Ca^{2+} in *P. aeruginosa*, however, molecular mechanisms involved in Ca^{2+} regulation are yet unknown. In eukaryotes, Ca^{2+} is a well established intracellular signal regulating essential cellular processes. We aim to characterize the molecular mechanisms involved in Ca^{2+} regulation and ultimately test the intracellular signaling role of Ca^{2+} in *P. aeruginosa*. Our studies established that *P. aeruginosa* maintains submicromolar level of intracellular Ca^{2+} ($[Ca^{2+}]_{in}$), which transiently increases in response to external Ca^{2+} . We determined that Ca^{2+} homeostasis is maintained by multiple transporters and putative Ca^{2+} binding proteins, and that *P. aeruginosa* responds to Ca^{2+} by using a two-component regulatory system CarSR, which regulates the expression of genes encoding putative Ca^{2+} binding proteins. These proteins contribute to the maintenance of intracellular Ca^{2+} homeostasis, which, in turn, plays an important role in Ca^{2+} regulation of physiology and virulence. Finally, we showed that Ca^{2+} regulates quorum sensing (QS) signaling in *P. aeruginosa* by affecting the transcription of QS regulatory genes. The ongoing work using Ca^{2+} transient defective mutant is aiming to provide direct experimental evidence for role of Ca^{2+} as a secondary messenger.

TABLE OF CONTENTS

Chapter Page

Chapter Page

LIST OF TABLES

Table Page

LIST OF FIGURES

Figure Page

PREFACE

Dissertation overview

P. aeruginosa is an opportunistic pathogen causing severe acute and chronic infections. As one of the leading pathogens infecting hospitalized and immunocompromised individuals, *P. aeruginosa* poses a serious threat to human health. In addition, remarkable ability of this bacterium to adapt and survive in various environmental conditions, production of multitude of virulence factors, and extremely high antibiotic resistance further aggravates the situation. Consequently, *P. aeruginosa* has attracted a lot of scientific attention in an attempt to understand the regulation of bacterial adaptation and virulence. Despite the existing knowledge of the regulatory mechanisms, *P. aeruginosa* still continues to be an invincible pathogen. Therefore, it is of high importance to understand the currently unknown signaling pathways regulating the adaptation and virulence of *P. aeruginosa.* This knowledge is necessary for developing novel strategies to prevent and treat *P. aeruginosa* infections. This work aimed to (1) establish intracellular Ca^{2+} homeostasis in *P. aeruginosa* PAO1 and elucidate the required mechanisms, (2) identify the molecular mechanisms controlling the Ca^{2+} regulated phenotypes in PAO1, (3) characterize the interrelationship between quorum sensing and Ca^{2+} signaling, and (4) characterize the role of intracellular Ca^{2+} homeostasis in regulating Ca^{2+} induced physiology and virulence.

The experimental work is presented in four chapters preceded by a literature review in chapter 1:

Chapter 1 is a literature review on physiology, virulence, adaptability, and antibiotic resistance *of P. aeruginosa*. It also reviews the current understanding on signaling mechanisms regulating bacterial physiology and virulence, including Ca^{2+} regulation. Part of this review is published in Cell Calcium 2014, where I have provided an exhaustive literature analysis of prokaryotic Ca^{2+} transporters, performed phylogenetic analysis of the P-type ATPases and prepared a diagramed model of bacterial Ca^{2+} network.

Chapter 2 summarizes my first experimental steps towards establishing the role of Ca^{2+} as a secondary messenger in *P. aeruginosa* PAO1. This study aims to characterize intracellular Ca^{2+} homeostasis, identify the responsible mechanisms, and their role in Ca^{2+} dependent physiology. For this, I measured intracellular Ca^{2+} concentration ($[Ca^{2+}]_{in}$) in *P. aeruginosa* PAO1. Further, I predicted Ca^{2+} transporters and characterized their role in maintenance of intracellular Ca^{2+} homeostasis, growth, and swarming motility. The results were published in Cell Calcium, 2013.

Chapter 3 identifies the molecular mechanisms regulating Ca^{2+} induced processes. This is a collaborative work with Dr. Michael J. Franklin in Montana State University, Bozeman, USA. This study characterizes transcriptional response of *P. aeruginosa* strains PAO1 and FRD1 to Ca^{2+} and identifies Ca^{2+} responsive two-component regulatory system CarSR and its regulon. My role in this study was to characterize the role of CarSR and its regulon in the maintenance of intracellular Ca^{2+} homeostasis and Ca^{2+} dependent phenotypes. I also supervised work of Michelle King, an undergraduate

student at the time, who performed bioinformatic analysis, growth and pyocyanin studies. I drafted the manuscript, which has been submitted for publication in Journal of Bacteriology.

Chapter 4 aims to provide direct experimental evidence for the role of Ca^{2+} as a secondary messenger. This study investigates the interrelationship between quorum sensing (QS) and Ca^{2+} signaling systems and identifies a Ca^{2+} influx channel that can be used to prove the signaling role of Ca^{2+}. I predicted and characterized the role of Ca^{2+} leak channel in Ca^{2+} influx, Ca^{2+}-regulated motility, production of pyocyanin, and antibiotic resistance. In addition, I investigated the regulatory effect of Ca^{2+} on QS system and studied the effect of QS molecules on $[Ca^{2+}]_{in}$.

Chapter 5 describes my contributions to other project. This chapter aimed to identify the role of putative calcium-binding protein EfhP in *P. aeruginosa* virulence, Ca^{2+} dependent physiology and intracellular Ca^{2+} homeostasis. My contribution to this project was to measure $[Ca^{2+}]_{in}$ in a mutant lacking *efhP*. The results were published in PLos One in 2014.

CHAPTER I

BACKGROUND AND HISTORICAL REVIEW

Pseudomonas aeruginosa

The first mentioning of *P. aeruginosa* infections was reported before the bacterium was isolated. Blue green coloration of the surgical wound dressings due to infectious agent was described by Sedillot in 1850. The pigment was later extracted and identified as pyocyanin by Fordos (1860). Lucke (1862) described the association of blue-green pigment with rod-shaped bacteria (1). In 1882, Gessard isolated and characterized the infectious agent in pure culture from cutaneous wounds, which was then named *Bacillus pyocyaneus* (2, 3). Based on the physiological characterization, the organism was grouped into the class of Gammaproteobacteria. The bacterium grows optimally at 37 °C, however, it can also grow well in the temperature range of 25 °C to 42 °C (4, 5). This bacterium was given a name of *Pseudomonas aeruginosa* in 1900 only (3). It is ubiquitous and has been isolated from diverse environments like soil and water, as well as from living organisms. Wide distribution of this bacterium can be attributed to its minimal nutritional requirements, diverse metabolic capabilities, multiple mechanisms of resistance, a large repertoire of virulence factors, and extreme adaptability (6). *P. aeruginosa* is well known for its ability to adhere, form biofilms (7) and thus colonize a variety of medically relevant surfaces such as catheters, respiratory therapy equipment, antiseptics, soaps, physiotherapy and hydrotherapy pool, contact lenses and lens solution, humidifiers and many more.

P. aeruginosa's physiological versatility is reflected in its genome. *P. aeruginosa* strain PAO1 is a prototypic wild-type strain isolated from burn wound. The complexity of its 6.26 million base pairs (Mbp) genome is comparable to that of a simple eukaryote like *Sachharomyces cerevisae;* it contains 5,570 predicted open reading frames (ORF). Compared to other sequenced bacteria, it possesses a high number of regulatory genes (468 genes).

***P. aeruginosa* infections**

P. aeruginosa can infect a wide range of hosts, both plants and animals, including humans. *P. aeruginosa* does not belong to a common normal flora. It is an opportunistic pathogen, infecting

individuals of all ages with damaged epithelial barrier and/or compromised immunity. When epithelial cells are damaged, it predisposes *P. aeruginosa* for colonizing and causing severe infections in patients with burns, open wounds, surgical wounds, urinary catheters, mechanical ventilators, endotracheal tubes, and scratched cornea. Initial adhesion of *P. aeruginosa* to altered epithelial barrier allows the direct host-pathogen interactions (8) and triggers the production of virulence factors by the pathogen. Over time, *P. aeruginosa* adapts to the host environment and the infection can progress to chronic form. One of the best studied examples of *P. aeruginosa* chronic infection is lung infection in patients with cystic fibrosis (CF). In addition, *P. aeruginosa* can establish life threatening infections in immunocompromised individuals like patients with HIV infection and cancer (9). Extensive studies on CF lungs infections by *P. aeruginosa* suggest that chronic infections result from inadequate immune response allowing bacteria to persist and damage the host (9). Once established, such infections cannot be eradicated from the host, ultimately making *P. aeruginosa* infections the dominant cause of morbidity and mortality in CF patients (10). During transition from acute to chronic infection, *P. aeruginosa* population becomes physiologically diverse in terms of colony morphology (11), hypermutability (12), antimicrobial susceptibility (13), and virulence (14). This may be caused by regulatory switches or by accumulation of multiple loss-of-function mutations targeting different virulence and antibiotic resistance related genes (15, 16)

P. aeruginosa is also known for causing community- or hospital-acquired infections (9). In fact, it is the most frequently isolated nosocomial pathogen. According to the Center for Disease Control (CDC) reports in 2013, about 51,000 hospital-acquired *P. aeruginosa* infections occur in the United States each year, which leads to approximately 400 deaths. The contributing factors include poor health status of the patients, high prevalence of the multidrug-resistant (MDR) strains, and prior use of broad spectrum antibiotics (17). Most of nosocomial *P. aeruginosa* infections lead to pneumonia (6). According to CDC, multidrug resistant *P. aeruginosa* infections are considered a serious threat in the United States.

P. aeruginosa virulence factors

P. aeruginosa is a challenging pathogen due to its extreme adaptability, multidrug resistance and arsenals of virulence factors, which counteract host defense mechanisms and enhance the bacterial ability to cause a disease. Major virulence factors in *P. aeruginosa* are discussed below.

Type III secretion systems (T3SS)

Studies suggest that expression of T3SS is required for *P. aeruginosa* to cause severe systemic infections, which can result in death or relapse despite the appropriate antibiotic therapy (18, 19). T3SS expression in *P. aeruginosa* is associated with increased risk of infections, severe and systemic disease (18, 20, 21) . T3SS is a complex needle-like machine that injects effector proteins directly into the host cell. Its expression is tightly regulated and requires a direct contact with host cell and depletion of Ca^{2+} in the growth medium (22, 23). Till date, four T3SS effector proteins have been identified in *P. aeruginosa*; ExoS, ExoT, ExoU, and ExoY. The first two are bifunctional toxins with N-terminal GTPase activity and C-terminal ADP-ribosyltransferase activity, both activitiescausing the irreversible disruption of host cell actin cytoskeleton. This causes host cell rounding detachment from cell matrix, and inhibition of cell migration and phagocytosis, which eventually facilitates *P. aeruginosa* penetration through epithelial barriers. ExoU has phospholipase A_2 (PLA_2) activity and hydrolyzes phospholipids, lysophospholipids, and neutral lipids, resulting in cell membrane damage. This causes a rapid loss of plasma membrane integrity and kills host cells. By killing phagocytes and destroying epithelial barrier, ExoU possibly promotes bacterial persistence and dissemination (As reviewed in(9)). ExoY is a secreted adenylyl cyclase. It elevates the concentration of cAMP in host cells and is required for the enhanced expression of Kruppel-like factor KLF6, which is associated with the host cell cytotoxicity (24, 25).

Flagellum and type IV pili

P. aeruginosa has one polar flagellum and multiple, polar, short type IV pili (TFP). Flagellum and TFP are proteinaceous appendages whose structural components are flagellin and

pillin respectively. These filamentous structures are a major means of motility. Flagellum provides swimming motility to *P. aeruginosa* by rotating in a corkscrew motion in an aqueous environment. It is essential for bacterial chemotaxis (26). Polarly localized pilli undergo reversible assembly and disassembly, extend and retract like a grapping hook to allow bacteria to twitch over a solid surface (9, 27). In addition, these proteins serve as major adhesins which allow *P. aeruginosa* attachment to host cells and various surfaces, and subsequently induce host cell signaling and pathogenic events (9). During infection, flagellum binds to the basolateral surface of epithelia and elicits the activation of the host inflammatory response via Toll-like receptor 5 (TLR5) (26). *P. aeruginosa* TFP bind to the apical surface of epithelia, cause bacterial aggregation leading to the formation of microcolonies, an important step in the early biofilm formation. TFP also function as phage receptors (9, 28). *Pillin* interaction with host epithelial receptor asialo-GM1 initiates rapid epithelial inflammatory responses by evoking IL-8 secretion (29). Together, flagellum and TFP facilitates a highly coordinated swarming motility on semi solid surfaces, flagellum being the major driver (9, 30). Swarming motility contributes to early stages of biofilm formation, an important factor contributing to *P. aeruginosa* virulence (31).

Extracellular proteases and lipases

Several proteases secreted by *P. aeruginosa* lead to pathogenic interaction between the bacterium and its host. *P. aeruginosa* produces two extracellular elastases, lasA (Staphyloslysin) and lasB (Elastase). These are secreted via type 2 secretion system (T2SS) and regulated by *las* and *rhl* regulons of quorum sensing system (32). Together, LasA and LasB are believed to play key roles in CF lung infections by destroying elastin and collagen, major components of lung tissues (33-35). *P. aeruginosa* uses LasB, a neutral metalloprotease, to counteract the human immune system by degrading or inactivating human immunoglobulins G and A (36, 37), serum α-1 proteinase inhibitor (38), complement components (39), and opsonizing lungs surfactant proteins A and D (40). LasA is a serine protease which cleaves a wide range of glycine containing proteins, including proteins required

for peptidoglycan stabilization in the cell wall. It has limited elastolytic activity compared to LasB, but enhances the elastolytic activity of other elastases including LasB (41, 42). Presence of zinc and calcium in the growth medium of *P. aeruginosa* promotes the production and processing of LasA and LasB, which results in increased elastase and proteolytic activities (43).

Alkaline protease (AprA) is a zinc metalloprotease secreted by Type I secretion system (TISS). AprA can degrade laminin leading to tissue necrosis in *P. aeruginosa* infections (44). *P. aeruginosa* uses AprA to evade the immune system by degrading cytokines (45, 46) and inhibiting neutrophil function (47). Protease IV is another serine protease secreted by *P. aeruginosa*. It destroys the lungs tissue by degrading the host surfactant proteins A, B, and D. It also enables the bacterium to evade the immune protective response by degrading complement proteins, immunoglobulins and fibrinogen (48).

P. aeruginosa is known to secrete four extracellular phospholipases C (PLC): PlcA, PlcB, PlcH, and PlcN. PLCs degrade the phospholipids such as phosphatidylcholine (PC) and phophatidylethanolamine (PE), major components of lung surfactant and human cell membrane, respectively. All four PLCs can degrade PC, whereas, only PlcB and PlcA can hydrolyze PE. Besides PC and PE, PlcA is shown to hydrolyze phosphoserine. Hydrolysis of phospholipids by PLCs results in destruction of host mucus layer and cell membrane. PlcH is hemolytic and cytotoxic and is shown to be a virulence determinant in a variety of infection models. PlcH also counteracts the host immune response by suppression of neutrophil respiratory burst (49-52). Physiological roles of PlcA, PlcB, and PlcN are not well understood. PlcB is shown to be required for chemotaxis of *P. aeruginosa* towards the phospholipids (52). In addition to PLC, *P. aeruginosa* also produces phospholipase D (PldA). PldA hydrolyses a wide variety of lipids found in lung surfactant and host cell membrane including glycerophospholipids, PC, PE, phosphatidylglycerol, and phosphoserine. PldA is shown to be positively associated with promotion of chronic infection and host cell invasion by *P. aeruginosa* (53).

Biofilm

Biofilm is a different mode of lifestyle than planktonic growth due to differential gene expression resulting in various physiological changes including new metabolic capabilities, enhanced chemical tolerance and increased virulence (54). A highly organized community of bacteria in biofilm are held together on a surface by self-produced extracellular polymeric substances (EPS) (55, 56). EPS is composed of exopolysaccharides, extracellular DNA (eDNA), lipids, and proteins (57). EPS imparts biofilm with stability and characteristic resistance to various physical and chemical factors (58, 59). EPS also forms channels that provide a means of communication and supply of nutrients and oxygen (60). *P. aeruginosa* has a remarkable ability to form biofilms on both abiotic and biotic surfaces. *P. aeruginosa* biofilms can survive and persist inside the host for decades due to its ability to evade host defense mechanisms and antibiotic therapy. Cells in biofilm can, however, disperse from biofilm and return to planktonic mode of growth, which results in recurrence of acute infections. Such recurrent infections in CF lungs lead to fatal lungs failure (61-63). Multiple regulatory mechanisms such as cyclic di-GMP, quorum sensing, two-component regulatory systems, and sigma factors regulate the switch between planktonic and biofilm modes (64-66).

Pyocyanin

Pyocyanin, a blue redox-active toxin, is one of the major virulence factors produced by *P. aeruginosa*. Pyocyanin is associated with several *P. aeruginosa* infections and is required for full virulence of *P. aeruginosa* during airway infections (67). Once secreted, pyocyanin plays a key role in host-pathogen interactions by inducing neutrophil apoptosis (68), ciliary dyskinesia (69), increased IL-8 expression (70), and disturbing Ca^{2+} homeostasis in human lungs epithelia (71). It also controls the colony size, biofilm thickness (72), and eDNA release in *P. aeruginosa* (73). Pyocyanin interaction with molecular oxygen generate reactive oxygen species (ROS), which disturb the redox balance in host cells leading to cell injury and death (74). Besides its roles in host cell damage,

pyocyanin enhances iron availability to the bacterium by reducing ferric ion in complex with host iron-binding protein transferrin (75), which in turn regulates the pycoyanin production (76).

Rhamnolipids

Rhamnolipid is a biosurfactant produced by *P. aeruginosa* in stationary growth phase. *P. aeruginosa* produces heterogenous mixture of rhamnolipids, di-rhamnolipid being the major component (77, 78). Rhamnolipids have important roles during chronic infection in CF patients where they inactivate tracheal cilia so that bacteria avoid ciliary clearance (79, 80). These molecules reduce the surface tension, a key requirement for swarming motility (81). Besides, it plays roles in *P. aeruginosa* biofilm formation and dispersal (82-85).

Other virulence factors

Lipopolysaccharides (LPS) are membrane associated antigenic molecules capable of eliciting immune response. LPS excludes external substances from entering the bacterial cell and mediates bacterial interaction with antibiotics (86). *P. aeruginosa* can modify lipid A portion of LPS in response to environmental stimuli like antimicrobials. Lipid A modifications have been associated with increased resistance to antibiotics and greater severity of lungs disease (9).

Exotoxin A (Exo A) is an ADP-ribosyl transferase enzyme, which blocks host protein synthesis by inhibition of host elongation factor 2 (EF-2), leading to cell death. Other effects of Exo A include reduction of cytokines production and enhanced killing of host cells by apoptosis (87, 88).

Pyoverdin is a siderophore that sequesters iron from host sources in a process of establishing chronic infection. Iron bound pyoverdin also functions as a signaling molecule, leading to upregulation of virulence factors like Exo A, endoproteases, and pyoverdin itself (63).

Cystic fibrosis transmembrane conductance regulator (CFTR) inhibitory factor (Cif) is a recently identified novel virulence factor that causes reduction or loss of CFTR by increasing the ubiquitination and lysosomal degradation of CFTR (89, 90). Cif is an epoxide hydrolase (91) with

possible role in systemic infection (92). It is secreted via SEC secretion system or outer membrane vesicles (OMVs) (91, 93). Cif-mediated reduction of CFTR inhibits bactericidal activity of neutrophils and therefore contributes largely to evasion of innate immune responses (94, 95).

The types of virulence factors and the levels of their production in *P. aeruginosa* differ between acute and chronic infections. Virulence factors like flagellum, TFP, T3SS, extracellular enzymes, and Exo A are mostly associated with acute infections. On the other hand, pyocyanin, pyoverdin, rhamnolipids, lipid A modifications, and Cif are associated with chronic infections. *Pseudomonas* isolates from chronic infections commonly overproduce exopolysaccharides and more readily form biofilms (9).

Signaling systems in *P. aeruginosa*

P. aeruginosa possesses multiple interconnected signaling systems. These systems intricately regulate virulence, persistence, and antimicrobial resistance. Signaling systems detect cellular and environmental stimuli and orchestrate the response by triggering the changes in gene expression (63).

Quorum sensing

Quorum sensing (QS) is a cell density dependent mechanism for cell-to-cell communication, which enables a coordinated response within the entire bacterial community (96). QS is based on the production and detection of chemical signals called autoinducers, whose concentration is proportional to cell density. In *P. aeruginosa*, QS is mediated by three interconnected systems: Las, Rhl, and Pqs. Each system has a synthase gene(s) (*lasI, rhlI, pqsA-E),* synthesizing a specific autoinducer, and a corresponding transcriptional regulator (*lasR, rhlR, and pqsR),* recognizing the specific autoinducer molecule and regulating the response. Two of these systems, Las and Rhl, utilize lactones: N-3-oxo-dodecanoyl homoserine lactone (3-O-C12 HSL) and N-butanoyl homoserine lactone (C4-HSL), respectively. Pqs utilizes 2-heptyl-3-hydroxy-4-quinolone (PQS) (97-99). QS regulates the transcription of more than 6% of *P. aeruginosa* genome, including the genes involved in production

and secretion of toxins, extracellular proteases, and other virulence factors (100, 101). These genes may be controlled by individual or multiple QS systems. For example, Las system regulates production of elastases, ExoA, and AprA; Rhl system regulates production of rhamnolipids and represses assembly and function of T3SS , and PQS system regulates production of pyocyanin (as reviewed in (63)). Furthermore, QS contributes to the regulation of various physiological processes like biofilm formation and cell differentiation, swarming motility, and cell survival in *P.* aeruginosa (102). Finally, QS serves as a global regulator by regulating general metabolism and is intricately connected with other regulatory networks (100).

Two-component regulatory systems

Two component regulatory systems (TCSs) are molecular machineries that are integrated into various signaling circuits and enable bacteria to sense and respond to environmental conditions, thus providing the means for successful adaptation. A typical TCS consists of a membrane bound histidine kinase (HK), which phosphorylates itself as well as a cognate response regulator (RR) in response to stimuli. Upon accepting the phosphate group from the HK, RR undergoes conformational changes enabling its interactions with downstream targets and commonly resulting in transcriptional regulation of multiple genes (103, 104). *P. aeruginosa* possesses 60 TCSs in its genome, a number unusually high compared to other bacteria (103). This large number of TCSs supports the extreme adaptability and variable survival strategies of *P. aeruginosa*. Many TCSs like GacSA, PhoPQ, PmrAB, and BfmSR play major role regulating virulence of *P. aeruginosa* and its interactions with a host during infections. GacSA regulates expression of genes involved in infection and biofilm formation by regulating small regulatory RNAs RsmZ and RsmY (66). PhoPQ and PmrAB regulate antibiotic resistance via lipid A modification as well as expression of virulence factors in response to Mg^{2+} limiting conditions. BfmSR regulates Rhl QS system as well as bacterial adaptation and virulence during chronic infections in CF lungs (105-110).

Cyclic nucleotides

In *P. aeruginosa,* cyclic adenosine monophosphate (cAMP) and cyclic diguanylic acid are two major cyclic nucleotides playing an intracellular signaling role. cAMP is recognized by several transcriptional regulators including the virulence factor regulator (VfR) and a cAMP regulator protein (CRP), which regulate the expression of ExoA, TFP, T3SS, and Las QS system. (111-113). On the other hand, the production of cAMP is regulated by several factors including interactions with surface during adhesion *via* chemotaxis-like chemosensory (Chp) system (114, 115) and in response to various environmental factors *via* anti-sigma factor MucA controlling the production of exopolysaccharide alginate(116, 117).

Another nucleotide, c-di-GMP, is a secondary messenger in many bacteria, including *P. aeruginosa*. This molecule is synthesized by diguanylate cyclase and hydrolyzed by phosphodiesterase activities. 39 genes in *P. aeruginosa* genome contain diguanylate cyclase (GGDEF) domain, or phosphodiesterase EAL-containing domain, or both (118). The intracellular level of c-di-GMP is regulated by *wsp* operon that encodes for a chemotaxis pathway (119). FimX, an important protein for TFP formation, degrades c-di-GMP despite the presence of both GGDEF and EAL domains. . On the other hand, FimX, requires it's both domains for correct subcellular localization (120, 121). FleQ, a major flagellar regulator, lacks both GGDEF and EAL domains, however, still responds to c-di-GMP (122).

Other signals

Fairly new secondary signals are ppGpp and pppGpp. These nucleotide molecules accumulate inside the cells in response to amino acid starvation, and regulate the transition of growing cells to a survival mode (123).

Pyocyanin and pyoverdin may also be recognized as signaling molecules and regulate gene expression in *P. aeruginosa*. For example, iron-bound form of pyoverdin regulates the expression of

regulators PvdS and FpvI, cell surface receptor protein FpvA and the anti-sigma factor FpvR, which results in the production of virulence factors pyoverdin, exotoxins, and PrpL endoproteases (124). Pyocyanin regulates expression of genes involved in efflux, redox balance and iron acquisition in *P. aeruginosa*. Besides, pyocyanin also regulates expression of PQS QS genes, thus contributing to regulating community responses and virulence. Pyocyanin controls expression of many genes via transcriptional regulator SoxR, (as reviewed in (63)) which regulates expression of genes involved in transport (RND efflux pump mexGHI-opmD and a major facilitator protein) and possible redox control (putative monooxygenase) (125)

Antimicrobial resistance in *P. aeruginosa*

The antibiotic resistance threat (ART) published by CDC (2013) reports isolation of clinical strains of *P. aeruginosa* that are resistant to all antibiotics including aminoglycosides, cephalosporin, fluoroquinolones, and carbapenem that are currently used to treat *Pseudomonas* infections. In fact, about 13% (approximately 6,000) of healthcare associated *P. aeruginosa* infections are found multidrug resistant (MDR) every year in the United States. Therefore, *P. aeruginosa* is recognized as a serious threat to public health. Drug-resistant *P. aeruginosa* infections are associated with higher morbidity and mortality, longer hospital stay, and greater need for surgical intervention. Multidrug resistance of *P. aeruginosa* may be caused by multiple mechanisms including intrinsic and acquired resistance, both stable and inheritable, and adaptive resistance, which is transient and non-inheritable (as reviewed in (6)).

Intrinsic antibiotic resistance in *P. aeruginosa* is chromosomally encoded and is based on the outer membrane impermeability, multidrug efflux pumps, chromosomal β-lactamase AmpC. *P. aeruginosa* outer membrane lacks high permeability porins present in other gram negative bacteria. It possesses only low efficiency porins allowing diffusion of small molecules with low efficiency compared to high permeability porins. This makes *P. aeruginosa* membrane less permeable to many hydrophobic antibiotics compared to other Gram-negative bacteria hence, providing protection

against a variety of antibiotics and antimicrobials (126). Multidrug efflux pumps actively export antibiotics from cell, and thus prevent intracellular accumulation of antibiotics to the inhibitory concentrations. Resistance-nodulation-division (RND) efflux pumps are the largest family of efflux pumps in *P. aeruginosa*. Its genome encodes for 12 RND pumps (10) that are composed of three main components and are responsible for efflux of chemically diverse molecules including lipophilic and amphiphilic antibiotics, like β-lactams, chloramphenicol, fluoroquinolones, macrolides, novobiocin, sulfonamides, tetracycline, trimethoprim, and aminoglycosides (127, 128). In addition to RND efflux systems, *P. aeruginosa* employs β-lactamase AmpC to hydrolyze and resist effects of β-lactam antibiotics.

Acquired resistance is based on gene transfer and occurrence of mutations. These mechanisms stabilize and enhance the intrinsic resistance mechanisms. Horizontal transfer of one or multiple antibiotic resistance cassette confers resistance to otherwise effective antibiotics and lead to emergence of MDR strains (reviewed in (129)). For example, acquisition of plasmids containing other than AmpC β-lactamases expands the range and the level of β-lactam resistance in *P. aeruginosa* (130). Mutations in regulatory genes and antibiotic cellular targets also increase resistance as exemplified by mutations in *mexZ* and DNA gyrase. *mexZ* is a negative transcriptional regulator, and once mutated, it will increase the antibiotic resistance of the organism by de-repressing the transcription of *mexXY* efflux pump responsible for removal of tetracycline, erythromycin, and gentamicin(131, 132). DNA gyrase is a target for fluoroquinolones, and therefore mutational modifications of the encoding sequence of DNA gyrase prevent binding and therefore increase resistance to fluoroquinolones (128, 129).

Adaptive resistance is a temporary response to environmental conditions. Environmental stimuli like antibiotics, biocides, polyamines, pH, anaerobiosis, cations, and carbon sources, or association with epithelial surface induce antibiotic resistance by changing gene expression (as reviewed in (129)), which collectively increases the resistance of the organism to a variety of

stressors. For example, in response to limiting Mg^{2+} conditions, exposure to cationic peptides, polymyxin B, or interaction with epithelial cells, the expression of genes responsible for regulating and catalyzing lipid A modification is induced. This subsequently shields the bacterial outer membrane from the interactions with cationic peptides, and protects the cells from damage (106, 107).

Calcium signaling

Calcium signaling in eukaryotes

Calcium ions (Ca^{2+}) serve as perhaps the most versatile intracellular messenger in eukaryotic cells, regulating many cellular processes including cell cycle, transport, motility, gene expression and metabolism (133-138). Cells maintain the intracellular free Ca^{2+} concentration ($[Ca^{2+}]_i$) at the level 10,000-fold lower (10^{-7} nM) than in the extracellular fluid (10^{-3} nM) (138, 139), thus generating a steep gradient. This gradient is then utilized by the cells to generate transient changes in $[Ca^{2+}]_i$ in response to various external stimuli. The transient changes in $[Ca^{2+}]_i$ serve as informational signals relating external stimuli to cellular processes (138). Eukaryotic cells possess several mechanisms to maintain the low cytosolic Ca^{2+} levels. Mitochondria and endoplasmic reticulum sequester Ca^{2+}. There is a number of efflux and influx transport systems that control translocation of Ca^{2+} within the cell, as well as Ca^{2+}-binding proteins (CaBPs), small organic anions, ATP, and metabolites that act as Ca^{2+} reservoirs or buffers (reviewed in (139-141)).

Calcium signaling in bacteria

While the role of Ca^{2+} in eukaryotes has been extensively studied, the role of Ca^{2+} in prokaryotes still remains elusive. A large body of evidence suggest that Ca^{2+} affects various bacterial physiological processes such as spore formation, chemotaxis, heterocyst differentiation, transport and virulence (7, 142-145). Similar to eukaryotes, prokaryotic cells maintain tight control of their cytosolic Ca^{2+}, at the level of 100-300 nM.(146-149). Intracellular Ca^{2+} transients are produced in

response to nitrogen starvation, environmental stress (148, 150), and metabolites of carbohydrate metabolism (151, 152). Moreover, proteomic and transcriptomic analyses in *Escherichia coli*, *Bacillus subtilis* and *Pseudomonas aeruginosa* revealed that the expression of hundreds of genes are modulated by changes in $[Ca^{2+}]_i$ in response to elevated external calcium (152-156). The processes affected by these changes include swarming, type III secretion (157), polysaccharide production, iron acquisition, quinolone signaling and general stress responses (156). These and other findings clearly indicate that environmental Ca^{2+} regulates physiology of prokaryotes. However, the signaling role of Ca^{2+}_i in prokaryotes remains intriguing and indeterminate, and needs to be experimentally confirmed. This requires the direct experimental evidences connecting $[Ca^{2+}]_i$ transients to the regulatory outcomes.

Calcium transporters in bacteria

Earlier studies of Ca^{2+} transport in prokaryotes showed that bacteria possess molecular mechanisms for both uptake and extrusion of Ca^{2+} (158-163). It was proposed that Ca^{2+} enters bacterial cells by means of either non-proteinaceous polyhydroxybutyrate-polyphosphate (PHB-PP) complexes or Ca^{2+} channels, and it is extruded by either Ca^{2+}-translocating ATPases or electrochemical potential driven Ca^{2+} transporters. Several studies (152, 164-166) suggested functional redundancy of Ca^{2+} transporters. The presence of multiple Ca^{2+} transport systems, perhaps, is required for maintenance of Ca^{2+}homeostasis at different environmental conditions, relating to different physiological states. Functional redundancy of Ca^{2+} transporters reflects the physiological importance of cellular Ca^{2+} homeostasis.

Channels

Sequence analyses and the findings of the effect of eukaryotic Ca^{2+} channels inhibitors on the $[Ca^{2+}]_i$ suggest that bacteria possess Ca^{2+} channels. MscL and BsYetJ are the channels that have been functionally characterized for their role in Ca^{2+} transport. A mechanosensitive channel MscL in *Synechocystis* sp. PCC 6803 (166) contributes to translocation of Ca^{2+} down the concentration

gradient in response to membrane depolarization in a temperature dependent manner. An atypical Ca^{2+} leakage channel BsYetJ transports extracellular Ca^{2+} into the cytoplasm of *B. subtilis* in a pH dependent manner (167). This protein is homologous to the human hBI-1 channel, which mediates ER Ca^{2+} leak into the cytoplasm. BsYetJ forms a transmembrane pore, which transiently interacts with Ca^{2+} during its transport into the cytoplasm.

ATPases

Ca^{2+} ATPases are mostly high-affinity Ca^{2+} pumps that export the cation from the cytosol to the extracellular environment by using the energy stored in ATP. Two types of ATPase (P- and F-) have been shown to play role in ATP-dependent Ca^{2+} flux in bacteria and archaea. P-type ATPases form a transient phosphorylated intermediate upon hydrolyzing ATP and thus released energy is used to translocate cations across the membrane (168). Few bacterial P-type ATPases have been characterized for their role in either Ca^{2+} translocation or Ca^{2+}-dependent phosphorylation. PMA1 from *Synechocystis* and Cda from *Flavobacterium odoratum* showed vanadate-sensitive Ca^{2+}-dependent phosphorylation. Based on sequence analysis, PMA1 appears to be closely related to eukaryotic sarcoplasmic reticulum Ca^{2+} ATPases (SERCA) whereas Cda lacks sequence similarity with other P-type ATPases and is proposed to be a new class of ATP-ases closely related to F-type ATPases (169, 170) (171). Two P-type ATPases from *Listeria monocytogenes*, LMCA1 and a LM0818 are structurally and functionally similar to each other as well as to eukaryotic SERCA ATPases (172). LMCA1, however, exhibited different biochemistry including low Ca^{2+} affinity and the ability to counter-transport 1 H^+ in per 1 Ca^{2+} out by electrogenic mechanism (173). Other characterized bacterial P-type ATPases include CaxP from *Streptococcus pneumonia* (145). YloB from *B. subtilis* (174), and PacL from *Synechococcus* sp. (175). The mutants lacking *caxP*, but not *yloB* accumulated intracellular Ca^{2+}. F-type ATPases or ATP synthases are known to reversibly phosphorylate ADP at the expense of the transmembrane electrochemical gradient of, most commonly, protons. So far, only one example of F-type ATPase, β-subunit AtpD in *E. coli*, has been

shown to be required for Ca^{2+} efflux in bacteria (152), which is most likely due to its role in ATP synthesis.

Electrochemical potential driven transporters

Electrochemical potential driven Ca^{2+} transporters are mostly low-affinity Ca^{2+} transport systems that use the energy stored in the electrochemical gradient of ions. Depending on the gradient, exchangers can operate in both directions (uptake and export) (176). Bacterial Ca^{2+} exchangers (CAX) use H^+, Na^+, or PO_4^{3-} to translocate Ca^{2+} across the membrane. Ca^{2+}/H^+ and Ca^{2+}/Na^+ antiporters have been identified in a number of bacterial genera and were thought to serve as a major mechanism for Ca^{2+} transport in prokaryotes. Glu and Asp rich Ca^{2+}/H^+ antiporter (with no name or sequence available) from *B. subtilis* translocates Ca^{2+} in everted membrane vesicles using NADH as an energy source and generates membrane potential (177). The electrogenic mechanism of actions was also shown for several other Ca^{2+}/H^+ exchangers (178, 179), probable Ca^{2+}/Na^+ antiporter (158), as well as $Ca^{2+}/PO_4^{3-}/H^+$ symporter (180). Several studies have shown that Ca^{2+} exchangers (CAX) differ in ion specificity. For example, YftkE (designated as ChaA) from *B. subtilis* as well as ApCAX and SynCAX from cyanobacteria are Ca^{2+}-specific (178, 181), whereas ChaA from *E. coli,* in addition to Ca^{2+}/H^+, exhibits Na^+/H^+ and K^+/H^+ antiport activity (165, 182). Major facilitator superfamily (MFS) transporter, LmrP from *Lactobacillus lactis* is an unique Ca^{2+} transporter and belongs to multidrug transporters known to mediate the extrusion of structurally different molecules, and exports monovalent cationic ethidium (183). In addition, LmrP selectively binds Ca^{2+} and Ba^{2+} and efflux Ca^{2+} via electrogenic exchange (antiport) with three or more protons (184). Specific inorganic phosphate (Pi) transporting systems (PitB in *E.coli*) also translocate Ca^{2+} (as well as other divalent ions) in the form of neutral metal phosphate complex $MeHPO_4$. Identification of several other metal phosphate symporters translocating divalent cations in different bacteria (185, 186) suggests that they may serve as a general mechanism of co-translocating Pi and divalent cations including Ca^{2+}.

Role of calcium in *Pseudomonas aeruginosa* physiology

Ca^{2+} triggers multiple changes in *P. aeruginosa* gene expression and protein production. Addition of Ca^{2+} to the growth medium globally affects gene expression in *P. aeruginosa* (Guragain *et.al*, submitted for publication). Furthermore, Ca^{2+} increases the abundance of proteins involved in iron acquisition, quinolone signaling, nitrogen metabolism, and stress responses (7, 156). On the other hand, it was shown that the low levels of Ca^{2+} are required for transcriptional induction of the type three secretion system (T3SS) in *P. aeruginosa (187)*. Our previous studies showed that growth at elevated Ca^{2+} leads to the formation of thicker biofilm (7), enhanced antibiotic resistance (Khanam *et al*., in preparation), increased production of alginate, pyocyanin, secreted proteases (7) and rhamnolipid (unpublished data). Recent work from our lab has identified a putative Ca^{2+} binding protein EfhP in *P. aeruginosa* (188). The lack of EfhP changes the abundance of proteins related to virulence factors production and stress response at high Ca^{2+}. EfhP regulates the production of several virulence factors including pyocyanin, alginate, and biofilm, at high Ca^{2+} and is required for Ca^{2+} induced virulence of *P. aeruginosa* in plants.

Overall, these observations suggest the regulatory role of external Ca^{2+} in *P. aeruginosa* physiology and virulence. However, whether intracellular Ca^{2+} plays role as second messenger in *P. aeruginosa* is still unknown. To address this question, it is necessary to characterize the molecular mechanisms responsible for intracellular Ca^{2+} homeostasis, identify the systems involved in sensing environmental Ca^{2+} and regulating the responses, and better understand the potential interplay between calcium and other intracellular signals.

CHAPTER II

CALCIUM HOMEOSTASIS IN *PSEUDOMONAS AERUGINOSA* REQUIRES MULTIPLE TRANSPORTERS AND MODULATES SWARMING MOTILITY.

This chapter has been published "**M. Guragain**, D.L. Lenaburg, F.S. Moore, I. Reutlinger, and M. A. Patrauchan. (2013). Calcium homeostasis in *Pseudomonas aeruginosa* requires multiple transporters and modulates swarming motility. *Cell Calcium*, 54, 350-361" and is included in this dissertation with permission from the publisher. (License number: 3687450464671)

Copyright © 2013, Elseiver Ltd.

Abstract

Pseudomonas aeruginosa is an opportunistic human pathogen causing severe acute and chronic infections. Earlier we have shown that calcium (Ca^{2+}) induces *P. aeruginosa* biofilm formation and production of virulence factors. To enable further studies of the regulatory role of Ca^{2+}, we characterized Ca^{2+} homeostasis in *P. aeruginosa* PAO1 cells. By using Ca^{2+}-binding photoprotein aequorin, we determined that the concentration of free intracellular Ca^{2+} ($[Ca^{2+}]_{in}$) is 0.14±0.05 μM. In response to external Ca^{2+}, the $[Ca^{2+}]_{in}$ quickly increased at least 13 fold followed by a multi-phase decline by up to 73%. Growth at elevated Ca^{2+} modulated this response. Treatment with inhibitors known to affect Ca^{2+} channels, monovalent cations gradient, or P-type and F-type ATPases impaired $[Ca^{2+}]_{in}$ response, suggesting the importance of the corresponding mechanisms in Ca^{2+} homeostasis. To identify Ca^{2+} transporters maintaining this homeostasis, bioinformatic and LC-MS/MS-based membrane proteomic analyses were used. $[Ca^{2+}]_{in}$ homeostasis was monitored for seven Ca^{2+}-affected and eleven bioinformatically predicted transporters by using transposon insertion mutants. Disruption of P-type ATPases PA2435, PA3920, and ion exchanger PA2092 significantly impaired Ca^{2+} homeostasis. The lack of PA3920 and vanadate treatment abolished Ca^{2+}- induced swarming, suggesting the role of the P-type ATPase in regulating *P. aeruginosa* response to Ca^{2+}.

Introduction

Calcium (Ca^{2+}) is a well-known signaling molecule that regulates a number of essential processes in eukaryotes (139). Abnormalities in cellular Ca^{2+} homeostasis have been implicated in many human diseases, including diseases associated with bacterial infections, for example, cystic fibrosis (CF) and endocarditis. In addition, Ca^{2+} plays a regulatory role in innate immune response (189), and its intracellular ($[Ca^{2+}]_{in}$) and extracellular ($[Ca^{2+}]_{ex}$) concentrations fluctuate in response to inflammation. For example, the levels of $[Ca^{2+}]$ in pulmonary fluid and nasal secretions of CF patients are increased (190, 191). Altogether the evidence suggests that cellular Ca^{2+} balance in a host may provide an environmental cue for opportunistic pathogenic bacteria and trigger their virulence. In support, in prokaryotes, Ca^{2+} has been implicated in various physiological processes such as spore formation, motility, cell differentiation, transport, and virulence (reviewed in (192)). It has also been shown that Ca^{2+} modulates bacterial gene expression (7, 156, 193), suggesting its regulatory role in prokaryotes. Furthermore, there is growing evidence that Ca^{2+} plays a signaling role in prokaryotes, which requires a tight control of cellular Ca^{2+} homeostasis. Several bacteria including *Escherichia coli* (147), *Propionibacterium acnes* (194), *Streptococcus pneumoniae* (145) *Bacillus subtilis* (146) and cyanobacteria (148) have been shown to maintain intracellular Ca^{2+} at sub-micromolar levels, and produce Ca^{2+} transients in response to environmental and physiological conditions (150, 195). Such responses may play a key role in Ca^{2+}-regulated bacterial physiology and virulence, however, the molecular mechanisms of bacterial Ca^{2+} homeostasis have not been well characterized. Several studies suggest that

bacteria control their $[Ca^{2+}]_{in}$ by using multiple mechanisms of transporting or chelating Ca^{2+} (reviewed in (192)).

Three major types of Ca^{2+} transport systems have been described in prokaryotes: gradient driven Ca^{2+} exchangers, ATP-ases, and non-proteinaceous polyhydroxybutyrate-polyphosphates (PHB-PP) channels. Ca^{2+} exchangers have been identified in a number of bacterial genera and are thought to serve as a major mechanism for Ca^{2+} transport in prokaryotes (176). They are low-affinity Ca^{2+} transporters that use the energy stored in the electrochemical gradient of ions, and, depending on the gradient, can operate in both directions. The specificity of the transporters may vary. For example, YftkE (ChaA) from *B. subtilis* (181) as well as ApCAX and SynCAX from cyanobacteria (178) are Ca^{2+}-specific, whereas ChaA from *E. coli* exhibits Na^+/H^+ and K^+/H^+ antiport activity in addition to Ca^{2+}/H^+ (182). Ca^{2+} exchangers may also play role in cell sensitivity to Ca^{2+} and salt tolerance, as exemplified by cyanobacterial ApCAX and SynCAX (178). ATP-ases are mostly high-affinity pumps that export cations from the cytosol by using the energy of ATP. They include P-type and F-type ATPases. Ca^{2+}- translocating P-type ATPases_ belong to P2A and P2B subgroups, as classified in (196). The former are similar to mammalian sarco(endo)plasmic reticulum (SERCA) Ca^{2+} pumps exporting Ca^{2+} against steep transmembrane gradients, and the latter are similar to plasma membrane (PMCA) calmodulin-binding ATPases. Five characterized prokaryotic P2A-ATPases include PacL from cyanobacteria (197), LMCA1 from *Listeria monocytogenes* (173), YloB from *Bacillus subtilis* (198), CaxP from *Streptococcus penumoniae* (145), and PacL from *Flavobacterium odoratum* (199). Most of them were shown to export Ca^{2+} in membrane vesicles and proposed to play a role in cell protection against high Ca^{2+}.

LMCA1 from *L. monocytogenes* (173) and PacL from *F. odoratum* (197) were shown to undergo Ca^{2+}-dependent phosphorylation required to transport Ca^{2+}. F-type ATPases, or ATP synthases, are known to synthesize ATP at the expense of transmembrane electrochemical gradient of protons (most commonly). So far, only one F-type ATPase AtpD in *E. coli* was shown to play role in Ca^{2+} homeostasis, most likely due to its role in ATP synthesis (152). Overall, although several prokaryotic gradient- and ATP- driven transporters were shown to translocate Ca^{2+} *in-vitro*, only few were tested for their role in cellular Ca^{2+} homeostasis *in-vivo*, of which only ion-exchanger SynCAX in *Synechocystis* sp. PCC6803 was shown to play role in cellular Ca^{2+} efflux (178). The difficulty of identifying the roles of Ca^{2+} transporters *in-vivo* is likely due to their functional redundancy, the molecular basis of which requires further studies.

Pseudomonas aeruginosa is an opportunistic human pathogen, and a major cause of nosocomial infections and severe chronic infections in endocarditis and in CF patients. Earlier, we showed that growth at high Ca^{2+} enhances *P. aeruginosa* biofilm formation and induces biosynthesis of several secreted virulence factors including alginate, extracellular proteases and pyocyanin (7, 156). However, the molecular mechanisms of Ca^{2+} regulation are not defined. To enable studies required to uncover such mechanisms, it is necessary to first characterize cellular Ca^{2+} homeostasis in this organism. Therefore, the aim of this work was to measure the intracellular Ca^{2+} concentration ($[Ca^{2+}]_{in}$) in *P. aeruginosa* cells and characterize its responses to external Ca^{2+}. We employed a recombinant photoprotein aequorin-based reporter system, which has been successfully used to measure $[Ca^{2+}]_{in}$ in live prokaryotic cells (146, 152), and to monitor both short- and long-term $[Ca^{2+}]_{in}$ responses to external Ca^{2+} transients (146, 147) as well as other

environmental and physiological determinants (146, 195). We also aimed to identify Ca^{2+} transporters that play role in maintaining cellular Ca^{2+} homeostasis. The strategy combined bioinformatic and proteomic approaches, followed by characterization of transposon insertion mutants obtained from the University of Washington Genome Center. This study presents the first evidence of Ca^{2+} homeostasis in *P. aeruginosa* and identifies several mechanisms and proteins required for maintaining Ca^{2+} homeostasis and regulating Ca^{2+}-induced swarming motility. In addition, the results provide a basis and excellent tools for further studies of the roles of cellular Ca^{2+} homeostasis in the regulation of Ca^{2+}-modulated physiology and virulence of this important human pathogen.

Materials and methods

Chemicals used in this study are listed in the supplementary information**.** Primers were obtained from Integrated DNA Technologies Inc.

Bacterial strains, plasmids, and media. *P. aeruginosa* strain PAO1, the non-mucoid strain with genome sequence available was used in the study. Biofilm minimal medium (BMM) was made as described in (7). When required, $CaCl_2.2H_2O$ was added to final concentration of 1 or 5 mM. For proteomic studies, PAO1 cells were first grown in 5 ml tubes for 16 h (mid-log), and then used to inoculate (0.1 %) 100 ml fresh medium in 250 ml flasks. The cultures were grown to mid-log growth phase and harvested by centrifugation. Transposon insertion mutants were obtained from the University of Washington Two - Allele library and are listed in Table 2.1. The mutants contained either ISphoA/hah or ISlacZ/hah insertions with tetracycline resistance cassette that disrupted the genes of interest. The mutations were confirmed by two-step PCR: first, transposon

flanking primers were used to verify that the target gene is disrupted, and second, transposon-specific primers were used to confirm the transposon insertion. The primer sequence is available at www.gs.washington.edu. For convenience, the mutants were designated as PA:IS, where PA is the identifying number of the disrupted gene from *P. aeruginosa* PAO1 genome (www.pseudomonas.com).

Sequence analyses. To predict Ca^{2+} transporters in *P. aeruginosa* PAO1 genome, we applied BLASTp sequence alignments, using the National Centre for Biotechnology Information (NCBI) non-redundant database (GenBank release 160.1), as well as functional domains search using Conserved Domain Database (CDD) and PROSITE. Homologous proteins were selected based on at least 25 % identity over the full length of amino acid sequence. For phylogenetic analyses, amino acid sequences of the functionally characterized transporters of Ca^{2+} and other cations were aligned with *P. aeruginosa* putative Ca^{2+} transporters using ClustalW. Thus obtained multiple sequence alignments were then used to build unrooted phylogenetic tree using Neighbor-joining algorithm in the MEGA 5.1 software.

Table 2. 1. Protein prediction and identification. Transposon mutants.

PA ORF[a]	Protein name, gene name[b]	Predicted domain(s)[c]	Best characterized hit in the nr NCBI, Accession #, Organism, % identity [d]	Transposon mutant PW#[e] Mutant Genotype	Mutant Designated Name	Fold difference in abundance in response to calcium[f]
ATP-driven transporters						
PA1429	Probable cation transporting P-Type ATPase	E1-E2 ATPase	P-type Na^+ ATPase, BAF91372.2, *Exiguobacterium aurantiacum*, 45%	PW3596 PA1429-E05::ISlacZ/hah	PA1429::IS	
PA4825	Probable Mg^{2+} transport ATPase, P-Type, *mgtA*	E1-E2 ATPase	Ca^{2+}/Mn^{2+} P-type ATPase PMR1, CAB87245, *Candida albicans*, 25%	PW9116 PA4825-F12::ISphoA/hah	PA4825::IS	New
PA3690	Probable metal-transporting P-type ATPase	E1-E2 ATPase; Heavy metal associated domain	Cd^{2+} /Zn^{2+} transporting ATPase, HMA3 P0CW78.1, *Arabidopsis thaliana*, 32%	PW7241 PA3690-C04::ISlacZ/hah	PA3690::IS	3
PA1634	K^+-transporting ATPase, beta subunit, *kdpB*	E1-E2 ATPase	NA	PW3911 PA1634-E05::ISlacZ/hah	PA1634::IS	5
PA2435	Heavy metal translocating P-type	E1-E2 ATPase		PW5099 PA2435-A02::ISpho	PA2435::IS	

	ATPase, *hmtA*			A/hah		
PA3920	Probable metal transporting P-type ATPase	E1-E2 ATPase; Heavy-metal-associated domain	Cation transporting ATPase, NP_440588, 44%, *Synechocystis* PCC6803, 44%	PW7626 PA3920-G01::ISphoA/hah	PA3920::IS	
PA1549	Probable cation-transporting P-type ATPase	E1-E2 ATPase; Heavy-metal-associated domain	CtpA, AAW66130, *Rubrivivax gelatinosus*, 36%	PW3788 PA1549-G12::ISphoA/hah	PA1549::IS	PA1552 (New)
PA5554	Probable ATPase synthase, beta subunit, *atpD*	F1 ATP synthase	F1F0-ATP synthase β subunit, Q587Q4, *Acidithiobacillus ferroxidans*, 77%	PW10412 PA5554-B01::ISlacZ/hah	PA5554::IS	2 PA5552 (3) PA5553 (New) PA5555 (2) PA5556 (New) PA5560 (2)
PA4496	Probable ABC transporter, substrate binding subunit	Substrate binding component	Dipeptide binding protein chain A, 1DPP_A, *E. coli*, 50%	PW8565 PA4496-F02::ISphoA/hah	PA4496::IS	ND PA4497 (0.2)
PA3400	Hypothetical protein	ABC type transporter	NA	PW6735 PA3400-	PA3400::IS	PA3402 (3)

				H11::ISpho A/hah		
Ion gradient driven exchangers						
PA3963	Probable Transporter	Cation Efflux Superfamily	Zinc transporter, YiiP, 3H90_A, *E.coli* K-12, 45%	PW7707 PA3963-E02::ISpho A/hah	PA3963::IS	
PA2092	Probable major facilitator superfamily transporter	Major Facilitator Superfamily	Purine efflux pump PbuE, Q0GQS6.1, *Bacillus amyloliquefaciens*, 35%	PW4602 PA2092-F01::ISlacZ /hah	PA2092::IS	
PA4292	Probable Phosphate transporter	PO_4^{3-}/SO_4^{2-} permease	NA	PW8230 PA4292-A03::ISpho A/hah	PA4294::IS	
PA0397	Probable cation efflux system protein	Cation efflux family	Znt-like transporter 2, Q8NEW0.1, *Homo sapiens*, 27%	PW1733 PA0397-E03::ISlacZ /hah	PA0397::IS	
Other transporters						
PA2999	Probable Na^+-translocating NADH:ubiquinone oxidoreductase subunit, *nqrA*	NADH-quinone reductase domain	Na^+ translocating NADH ubiquinone oxidoreductase subunit A , ZP_08756125.1, *Haemophilus pittmaniae* HK85,58%	PW6021 PA2999-D10::ISlacZ/hah	PA2999::IS	5
PA4614	Probable	Large-conductance	Mechanosensitive channel	PW8772	PA4614::	4

	conductance mechanosensitive channel, *mscL*	mechanosensitive channel	large, MscL chain A, 3HZQ_A, *Staphylococcus aureus*, 36%	PA4614-B11::ISphoA/hah	IS	
PA5167	Dicarboxylic acid transporter, *dctP*	Bacterial extracellular solute binding		PW9688 PA5167-F06::ISphoA/hah	PA5167::IS	PA5164 (2)
PA4016	Hypothetical protein	Membrane lipoprotein lipid attachment site	NA	PW7791 PA4016-E06::ISphoA/hah	PA4106::IS	PA4017 (4)

[a] Gene identifier in the PAO1 genome available at www. pseudomonas.com.

[b] As annotated in the PAO1 genome.

[c] Domains were predicted by the algorithms in CDD and PROSITE.

[d] The % identity was calculated over the full length of the proteins using transporter proteins encoded in PAO1 genome as a query.

[e] The mutant strain identifier in the UW library of transposon mutants available at www.gs.washington.edu.

Proteomic analysis. Membrane proteins were isolated by carbonate extraction as described in (200). The details are described in supplementary information. Protein concentration was determined using the 2D Quant kit (GE Healthcare). LC-MS/MS-based spectral counting was performed at the OSU Proteomics Facilities using LTQ-OrbitrapXL mass spectrometer. Proteins were identified using Mascot (v.2.2.2 from Matrix Science, Boston, MA, USA) and a database generated by *in silico* digestion of the *P. aeruginosa* PAO1 proteome predicted from the genome. Search results were validated using Scaffold (v.3 from Proteome Software Inc., Portland, OR). Proteins were considered identified if the protein probability threshold was greater than 99 % and at least three peptides were identified, each with 95 % certainty.

Expression and reconstitution of aequorin. PAO1 and transposon mutants were transformed with pMMB66EH (courtesy of Dr. Delfina Dominguez), carrying aequorin (201) and carbenicillin resistance genes, using a heat shock method described in (202). The transformants were selected on Luria bertani (LB) agar containing carbenicillin (300 µg/ml) and, in case of transposon mutants, tetracycline (60 µg /ml) and verified by PCR using aequorin specific primers (For: 5'CTTACATCAGACTTCGACAACCCAAG, Rev: 5'CGTAGAGCTTCTTAGGGCACAG). Aequorin was expressed and reconstituted as described in (147) with modifications. The details are described in supplementary information.

Luminescence measurements and estimation of free intracellular calcium. Cells with reconstituted aequorin were aliquoted (100 µl) in 96 well plate (Griener bio one, Lumitrack 600) and, when required, treated with inhibitors (2, 4 di-nitrophenol at 0.5, 1, or 2 mM; $LaCl_3$ at 300 or 600 µM; gramicidin D at 1 or 10 µg/ml; calcimycin at 5

μM; or vanadate at 2 mM) for 10 min in the dark at room temperature without shaking. Gramicidin D and calcimycin were dissolved in 50 % and 3 % DMSO, respectively. To ensure penetration of gramicidin D and calcimycin through the bacterial outer membrane, we added 10 μg/ml of compound 48/80, known to permeabilize the outer membrane of gram negative bacteria without affecting the cytoplasmic membrane (203). In this case, the corresponding amounts of DMSO and 48/80 were used to treat cells as a negative control. Luminescence was measured at 25 ^{0}C using Synergy Mx Multi-Mode Microplate Reader (Biotek). To measure the basal level of $[Ca^{2+}]_{in}$, the measurements were recorded for 1 min at 4 sec interval, then the cells were challenged with 1 or 5 mM Ca^{2+} (final concentration) injected by using the internal Synergy injectors, mixed for 1 sec, and the luminescence was recorded for 20 min at 4-5 sec interval. Injection of buffer alone was used as a negative control, and did not cause any significant fluctuations in $[Ca^{2+}]_{in.}$ $[Ca^{2+}]_{in}$ was calculated by using the formula $pCa= 0.612 (-\log_{10}k) + 3.745$, where k is a rate constant for luminescence decay (s^{-1}) (147). The excel-based template incorporating the formula and the aequorin standard curve was generously shared by Dr. Anthony Campbell. The results were normalized against the total amount of available aequorin, which was estimated by summing the light detected during an entire experiment and the light detected during discharge. The discharge was performed by permeabilizing cells with 2 % Nonidet 40 (NP40) in the presence of 12.5 mM $CaCl_{2.}$ The luminescence released during the discharge was monitored for 5 min at 4-5 sec interval. The estimated remaining available aequorin was at least 10 % of the total aequorin, unless mentioned otherwise. To control possible cell lysis and aequorin leakage during the procedure,

following the luminescence measurements, the cells were collected by centrifugation, and luminescence was reported for both the supernatants and the cell pellets resuspended in buffer (25 mM HEPES, 1 mM $MgCl_2$, 125 mM NaCl; pH 7.5). The experimental conditions reported here were optimized to prevent any significant cell lysis. The responses to Ca^{2+} challenges were characterized and validated by using curve fitting analysis with IGOR PRO software v.6.3.1.2. (WaveMetrics).

Results

***P. aeruginosa* maintains $[Ca^{2+}]_{in}$ homeostasis.** To study Ca^{2+} homeostasis in *P. aeruginosa* PAO1, we first measured the basal level of free intracellular Ca^{2+} ($[Ca^{2+}]_{in}$), and then monitored the changes in $[Ca^{2+}]_{in}$ in response to externally added 1 and 5 mM Ca^{2+}. Cells grown at no added Ca^{2+} (naïve) or 5 mM Ca^{2+} (induced) were compared. In naïve cells, the $[Ca^{2+}]_{in}$ was 0.14 ± 0.05 µM (Fig. 2.1.A). The addition of 1 mM Ca^{2+} caused a 13 fold increase of $[Ca^{2+}]_{in}$ to 1.86 ± 0.53 µM within 0.6 min (2.92 µM/min) followed by a two-phase decline, validated by the curve fitting analysis. The first, fast, phase proceeded at a rate 0.75 µM/min, lasted for ~2 min, and accounted for 38 % of $[Ca^{2+}]_{in}$ reduction. During the second, slow, phase, $[Ca^{2+}]_{in}$ reduced for another 35% to 0.5 µM at a rate 0.04 µM/min. When the cells were transferred to a fresh buffer containing no Ca^{2+}, a complete recovery to the basal $[Ca^{2+}]_{in}$ level was observed (data not shown). We also monitored $[Ca^{2+}]_{in}$ for additional 70 min and detected a very slow decrease at a rate 1.43 nM/min (data not shown). Considering the minor changes during this extended incubation, $[Ca^{2+}]_{in}$ was monitored during 21 min in all further experiments. Challenging naïve cells with 5 mM Ca^{2+} caused 28 fold increase in $[Ca^{2+}]_{in}$ to 3.93 ± 0.37 µM within 0.92 min (3.88 µM/min) followed by a multi-phase decrease. First, $[Ca^{2+}]_{in}$

dropped similarly to naïve cells by 38 %, but at a lower rate 0.46 µM/min. Then it increased to 3.01 ± 0.34 µM and slowly declined to 2.22 µM, showing a total decrease by 44 %.

In induced cells, the basal $[Ca^{2+}]_{in}$ was 0.22 ± 0.04 µM, which is 57 % higher than in naïve cells (Fig. 2.1.B). Upon exposure to 1 mM Ca^{2+}, the induced cells increased their $[Ca^{2+}]_{in}$ at a rate (3.12 µM/min) similar to naïve cells, but only fivefold (to 1.19 ± 0.11 µM) and during a shorter period of time (0.3 min). The following decrease proceeded with a much lower rate (0.16 µM/min), lasted for ~1.5 min, and accounted for 21 %. In contrast to naïve cells, during the second phase, $[Ca^{2+}]_{in}$ slowly increased with a rate 0.04 µM/min to 1.23 ± 0.45 µM. The response to 5 mM Ca^{2+} in induced cells also showed a multi-phase pattern. Although the first rapid increase brought $[Ca^{2+}]_{in}$ to a similar to naïve cells level (3.66 ± 0.44 µM), it was only 17 fold higher than the basal level. This increase occurred very quickly within 0.08 min at a rate 42.62 µM/min. The following decline was threefold faster than in naïve cells (1.6 µM/min). The second increase was similar to the one in naïve cells elevating $[Ca^{2+}]_{in}$ to 2.9 ± 0.45 µM, followed by a decline to 2.13 ± 0.27 µM with a total decrease by 42 %.

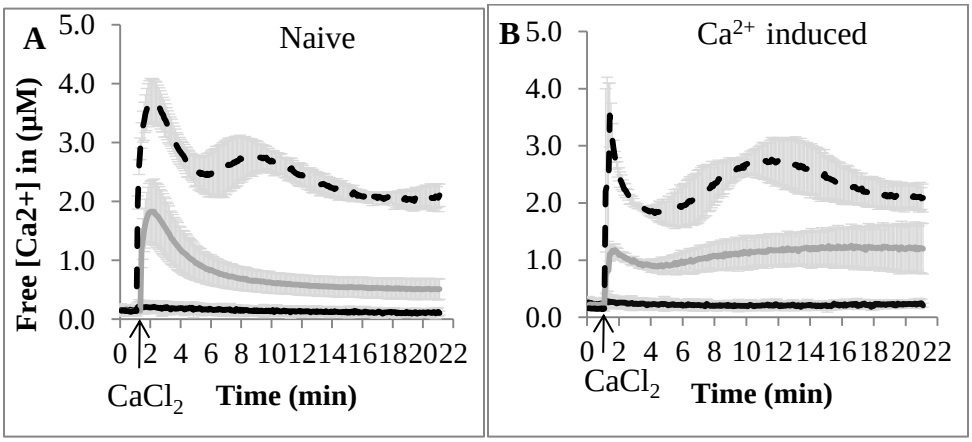

Figure 2.1. The effect of externally added Ca^{2+} on $[Ca^{2+}]_{in}$ in *P. aeruginosa* PAO1. Cells were grown in BMM with no added Ca^{2+} (A) or in the presence of 5 mM Ca^{2+} (B), and challenged with of 0 mM (black), 1mM (dark grey), and 5 mM (dash) Ca^{2+}. The basal level of luminescence was monitored for 1 min. 1 mM or 5 mM $CaCl_2$ was added at the time indicated by the arrow, followed by luminescence for 20 min. Changes in free $[Ca^{2+}]_{in}$ were calculated as described in the Methods section. The averages of at least three independent experiments are plotted.

The PAO1 genome contains multiple homologs of Ca^{2+} transporting ATPases and gradient driven exchangers. Homology searches in the PAO1 genome (www.pseudomonas.com) using amino acid sequences of the characterized prokaryotic Ca^{2+} transporters revealed 18 genes encoding different types of transporters (Table 2.1). Based on sequence similarity and predicted conserved domains, ten were predicted to encode P-, F-type, and ABC-type ATPases, and eight to encode ion exchangers and other types of transporters. They include two earlier characterized proteins: heavy metal translocating P-type ATPase (PA2435) and dicarboxylic acid transporter (PA5167) (204, 205). The comparative sequence analyses revealed that seven predicted P-type ATPases share 13 - 39 % sequence identity and do not have other paralogs in the PAO1 genome. Phylogenetic analysis using functionally characterized prokaryotic P-type ATPases showed that the PAO1 proteins can be grouped into four clades, which coincide with ion specificity: 1) Ca^{2+} (PA1429); 2) Mg^{2+} (PA4825); 3) K^{+} (PA1634); and 4) Pb^{2+}, Cd^{2+}, Zn^{2+}, CO^{2+}, Cu^{2+} (PA2435, PA3920, PA1549, and PA3690) (Fig. 2.S1). Further sequence comparison revealed that PA1429 together with five prokaryotic Ca^{2+}-translocating P-type ATPases in clade 1 are more closely related to the human Ca^{2+} translocating ATPase SERCA than to the human calmodulin-binding ATPase PMCA1 (data not shown). This supports their classification into the subgroup of P2A-ATPases (196). Interestingly, clade 2, including PA4825 and Mg^{2+}-translocating MgtB from *S. typhimurium*, is closely related to PMCA1 (data not shown). Furthermore, considering that PA2435 was shown to uptake both Cu^{2+} and Zn^{2+} (205), we combined Cu^{2+} and heavy metal- translocating proteins into one clade (4). As a result, PA1549, earlier grouped into functionally uncharacterized subfamily FUPA27 (206), was clustered with clade 4 proteins,

suggesting its possible involvement in translocation of these ions. Other predicted transporters have one to four paralogs in the PAO1 genome and share 28 % – 82 % amino acid sequence identity. All the predicted transporters are conserved among ten sequenced pseudomonads and share 19 % – 100 % identity with their corresponding homologs.

Growth at elevated Ca^{2+} alters abundance of PAO1 membrane proteins. The modulated $[Ca^{2+}]_{in}$ response in Ca^{2+} induced cells suggested the involvement of transporters, whose expression is affected by Ca^{2+}. To identify such transporters, membrane proteins from PAO1 cells grown at no added or 5 mM Ca^{2+} were extracted and subjected to LC-MS/MS spectral counting - based comparative analyses. In total, about 500 proteins were identified, of which more than 80 % were transmembrane or membrane-associated proteins. These included seven bioinformatically predicted putative Ca^{2+} transporters, and ten proteins encoded within the same apparent operons (Table 2.1). To estimate the effect of Ca^{2+}, for every protein we calculated a ratio of the total number of fragmentation spectra that map to the peptides of the protein in the samples collected at 5 mM *vs.* no added Ca^{2+}. The results suggest that six predicted Ca^{2+} transporters (shown in bold in Table 2.1) increased abundance at least twofold in response to growth at elevated Ca^{2+}. Considering that apparent operonic genes may have similar expression profile, the results also suggest Ca^{2+} induction for PA3400, PA5167, PA4016, and PA1549. However, PA4496 and PA4497 showed decreased abundance in response to 5 mM Ca^{2+}.

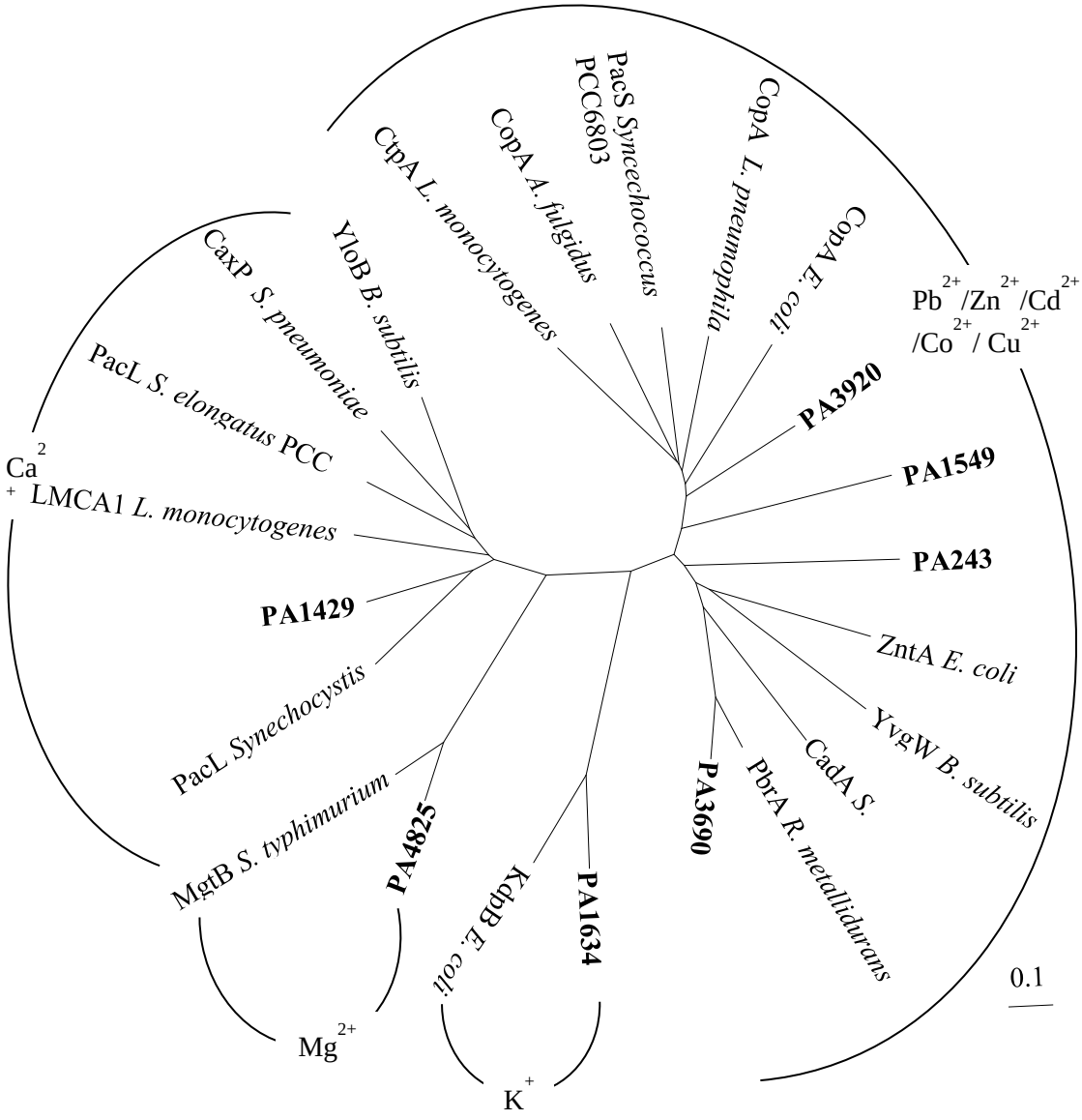

Figure 2.S1. phylogenetic analysis of P-type ATPases. The unrooted neighbor-joining tree was calculated using MEGA5.1 software from the ClustalW alignment of the amino acid sequences of seven predicted P-type ATPases from P. aeruginosa PAO1 (PA1429, PA4825, PA1634, PA3920, PA1549, PA2435, and PA3690) and characterized P-type ATPases: LMCA1, Q8Y8Q5.1; YloB, NP_389448.1; PacL, S36742; PacL,

NP_441217.1; CaxP, YP_001836255.1; KdpB, NP_415225.1; ZntA, NP_417926.1; SERCA, NP_775293.1; PMCA1, NP_001001331.1; MgtB, NP_462662.1; CopA, Q8RNP6; CopA, NP_069309.1; CopA, YP_488775.1; YvgW, YP_006631457.1; PbrA, YP_145622.1. NCBI accession numbers are provided. The letter "G" represents the group number designated based on the [Ca2+]in profile. The cations transported by the characterized ATPases are shown next to the respective cluster.

Ca^{2+} homeostasis in PAO1 involves multiple transporters of different types. To study the role of the predicted transporters in Ca^{2+} homeostasis, we obtained 18 mutants, each with one predicted transporter encoding gene disrupted with either ISphoA/hah or ISlacZ/hah transposon insertion. The mutants were monitored for their $[Ca^{2+}]_{in}$ response to 1 mM Ca^{2+} and compared to the wild type (WT) PAO1 cells. Based on the results they were grouped into four groups (Fig 2.2). Group I (four mutants) showed the initial rapid increase in $[Ca^{2+}]_{in}$ at least twofold higher than in WT cells followed by the recovery to approximately the WT level $[Ca^{2+}]_{in}$. Group II (five mutants) failed the recovery to the WT level $[Ca^{2+}]_{in}$ during 21 min monitoring, and had the remaining $[Ca^{2+}]_{in}$ at the levels at least twofold higher than in PAO1 cells. Group III (four mutants) showed two peaks of $[Ca^{2+}]_{in}$ increase and the remaining $[Ca^{2+}]_{in}$ at the level at least twofold higher than in WT cells. The $[Ca^{2+}]_{in}$ changes less than twofold *vs.* PAO1 were considered not significant (five mutants in group IV).

Among the ten examined mutants with disrupted putative ATP-ases, seven showed significant changes in $[Ca^{2+}]_{in}$ response (Fig 2.2.A). They included mutants lacking six P-type ATPases: PA3690, PA4825 (Group I), PA1429, PA1549 (Group II), PA2435, PA3920 (Group III), and ABC transporter PA3400 (Group II). The group III mutants showed the most drastic changes in $[Ca^{2+}]_{in}$ response, and together with PA1549-lacking mutant failed to significantly decrease the elevated $[Ca^{2+}]_{in.}$ The remaining three ATP-ases: P-type PA1634, F-type PA5554, and ABC transporter PA4496 showed no role in maintaining $[Ca^{2+}]_{in}$ homeostasis (Group IV). Among the eight tested putative ion exchangers and other transporters, disruption of six showed significant changes in $[Ca^{2+}]_{in}$ response (Fig. 2.2.B). They included: three ion exchangers PA3963, PA4292

(Group I), and PA2092 (Group III), dicarboxylic acid transporter PA5167, hypothetical protein PA4016 (Group II), and mechanosensitive channel PA4614 (Group III). Among these proteins, the most significant effect was observed for the mutant lacking a major facilitator type transporter PA2092, that was unable to reduce $[Ca^{2+}]_{in}$ after the initial increase. Ion exchanger PA0397 and probable Na^{+} translocating oxidoreductase PA2999 showed no role in Ca^{2+} homeostasis.

Multiple mechanisms are involved in Ca^{2+} homeostasis in PAO1. To identify the role of different types of transporters in Ca^{2+} homeostasis and better understand the mutants $[Ca^{2+}]_{in}$ profiles, we examined the effect of several inhibitors specifically affecting different mechanisms associated with ion transport, on the maintenance of $[Ca^{2+}]_{in}$. For this, PAO1 cells were treated with the selected inhibitors and monitored for their $[Ca^{2+}]_{in}$ response to 1 mM Ca^{2+}. First, calcimycin, a Ca^{2+} ionophore known to carry Ca^{2+} into the cells (207), was used to test the response of PAO1 cells to Ca^{2+} influx (Fig. 2.3.A). Treatment with 5 µM calcimycin caused a rapid (36 µM/min) uptake of Ca^{2+} and increase of $[Ca^{2+}]_{in}$ to 9.54 ± 0.15 µM followed by an immediate but slower (4.1 µM/min) decline to 2.36 ± 0.33 µM. The second increase in $[Ca^{2+}]_{in}$, although appearing 4 min earlier than in the DMSO control, is most likely due to the presence of DMSO (used to dissolve calcimycin).

To test the role of a proton gradient across the cytoplasmic membrane and intracellular ATP in $[Ca^{2+}]_{in}$ response, 2,4-Dinitrophenol (DNP), a proton ionophore known to disrupt a proton gradient and uncouple oxidative phosphorylation (152), was used (Fig. 2.3.B).

A.

Group I **Group III**

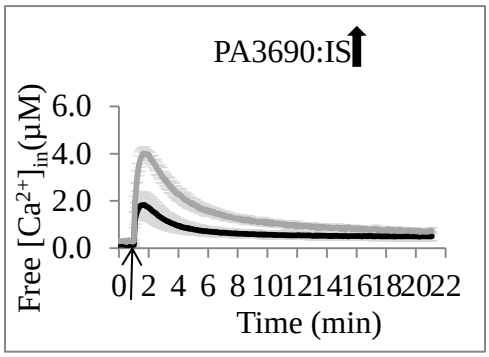

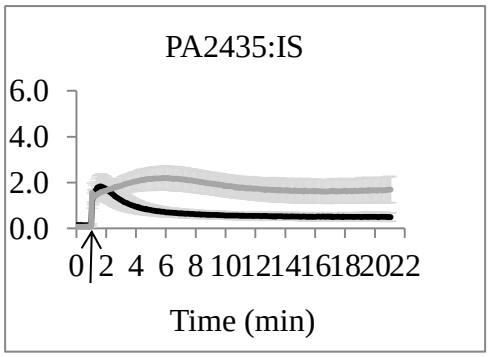

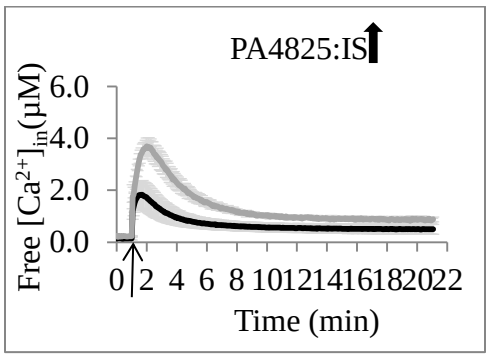

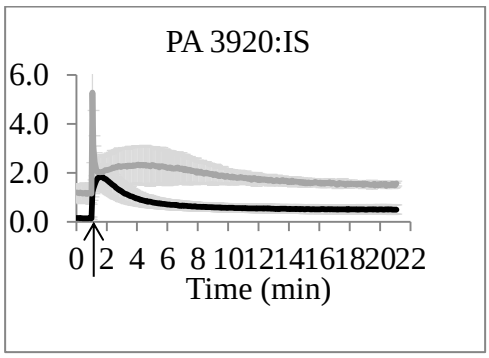

Group II **Group IV**

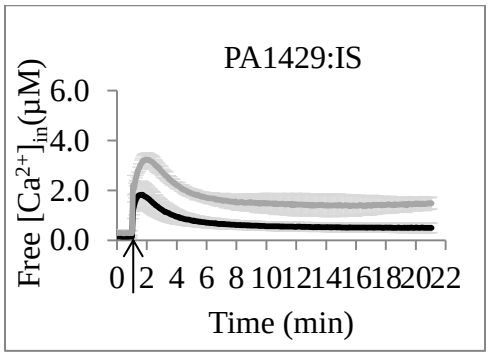

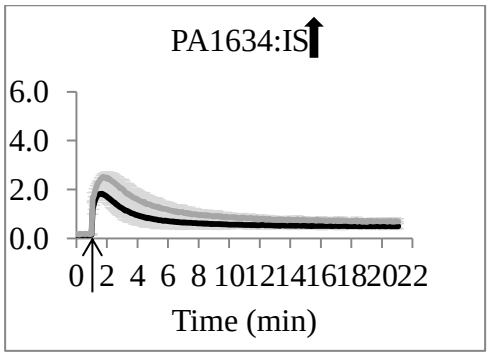

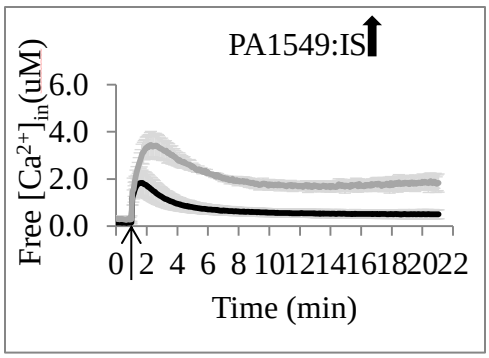

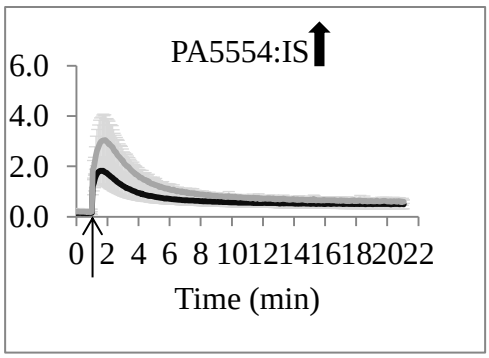

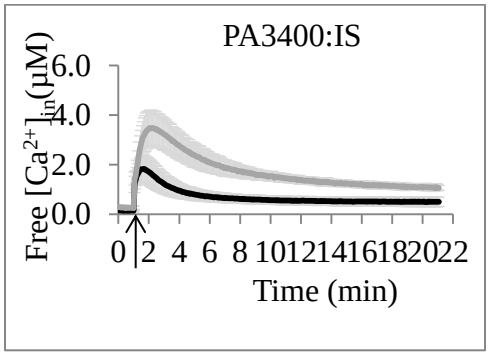

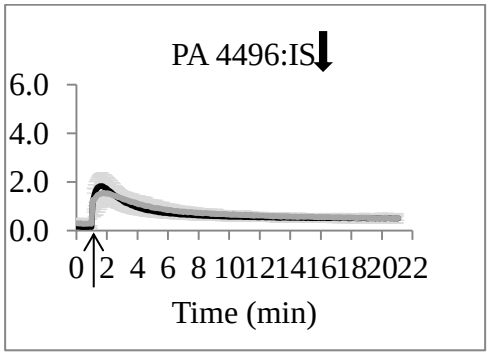

B.

Group I

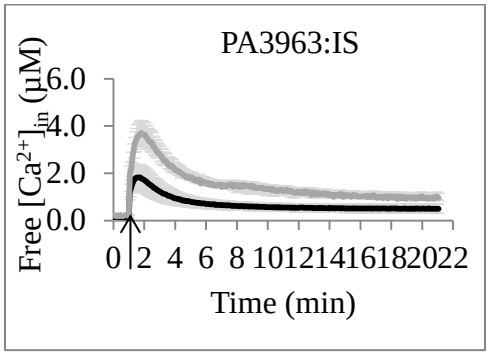

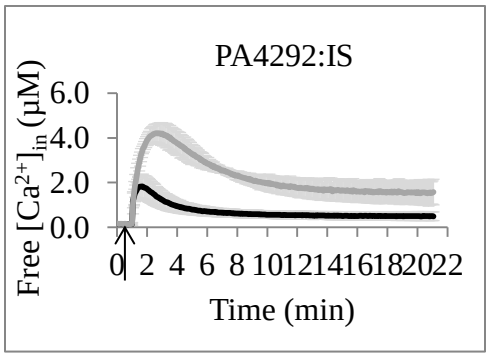

Group III

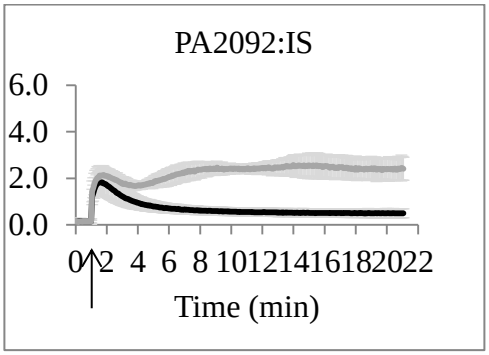

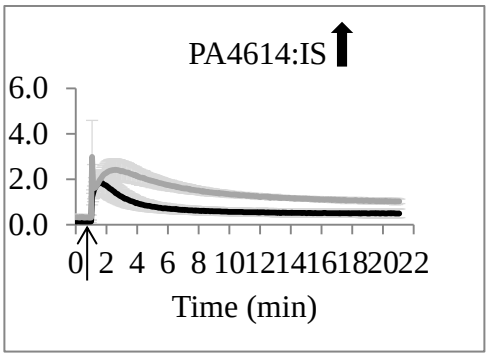

Group II **Group IV**

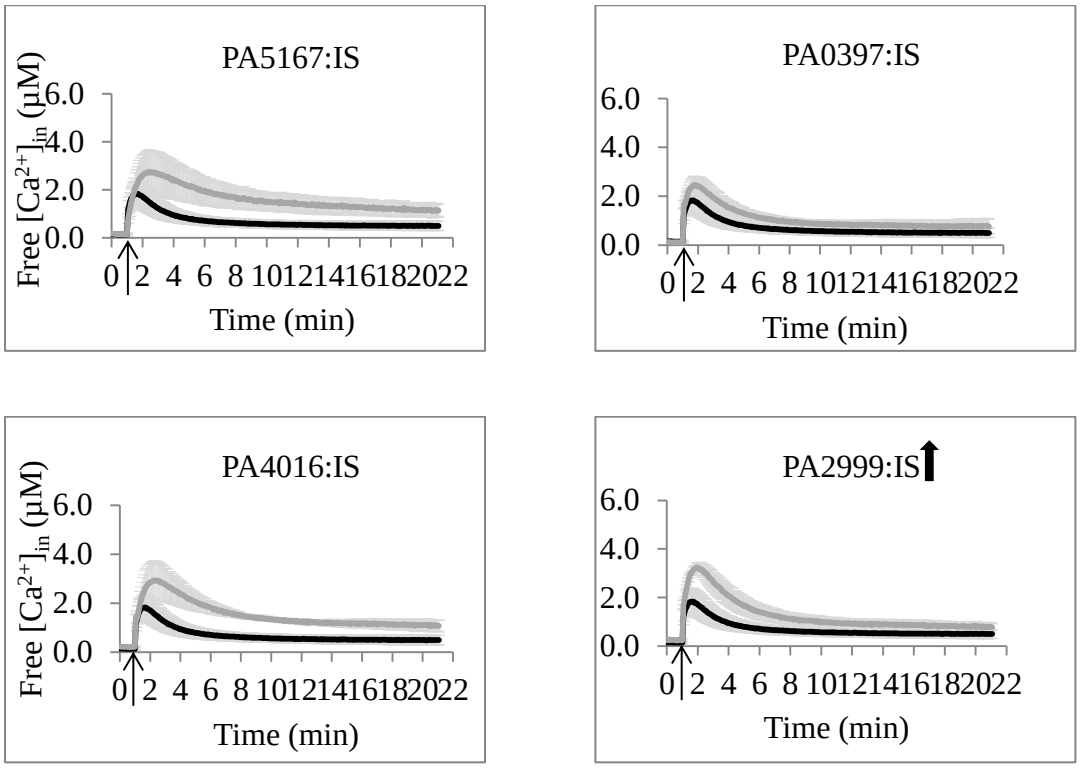

Figure 2.2. Free $[Ca^{2+}]_{in}$ profiles of transposon mutants with disrupted ATP-dependent transporters (A) or ion exchange transporters (B). The mutants were obtained from the University of Washington Two - Allele library. Cells were grown in BMM media with no added Ca^{2+}. The basal level of luminescence was monitored for 1 min. 1 mM $CaCl_2$ was added at the time indicated by the arrow, followed by luminescence measurements for 20 min. Changes in free $[Ca^{2+}]_{in}$ were calculated as described in the Methods section. PA numbers represent the open reading frames in PAO1 genome. Black, PAO1 wild type; grey, transposon mutant. The data is an average of at least three independent experiments. Upward and downward arrows indicate that the protein abundance was increased and decreased, correspondingly, during growth at 5 mM $CaCl_2$.

In a concentration dependent manner, DNP caused a second peak of $[Ca^{2+}]_{in}$ to increase, which at higher levels of DNP appeared to merge with the first peak and reached 7.28 ± 0.74 µM. This level of $[Ca^{2+}]_{in}$ was reached at the rate of 22 fold slower than in calcimycin-treated cells, and was followed by a 32 % decrease. The remaining $[Ca^{2+}]_{in}$ was higher with increasing dose of DNP, and at 2 mM DNP, reached 8.39 ± 1.35 µM.

To examine the role of monovalent cation exchangers in PAO1 Ca^{2+} homeostasis, gramicidin D treatment was used (Fig. 2.3.C). Gramicidin D is known to form channels across the cytoplasmic membrane and dissipate the gradients of H^+, Na^+, and K^+ (208), which may also affect the intracellular ATP pool (209). In a concentration-dependent manner, gramicidin D treatment elevated the initial increase in $[Ca^{2+}]_{in}$ up to 9.06 ± 1.15 µM, which was followed by a decline to 2.49 ± 0.23 µM. The rates of $[Ca^{2+}]_{in}$ increase and decrease were at least twofold higher at 10 µg/ml than at 1 µg/ml gramicidin D. The $[Ca^{2+}]_{in}$ recovery levels were similar in the treated cells and at least fivefold higher than in the untreated cells. The effect of gramicidin D on $[Ca^{2+}]_{in}$ also included the effect caused by DMSO.

Lanthanum (III) is a Ca^{2+} antagonist, known to block Ca^{2+} channels (210). It may also arrest Ca^{2+}-binding ATPases in a phosphorylated form and prevent further conformational changes required for Ca^{2+} translocation (211). The effect of $LaCl_3$ on the level of $[Ca^{2+}]_{in}$ showed two distinct concentration-dependent patterns: a decrease in the initial rise in $[Ca^{2+}]_{in}$ and appearance of the second peak of $[Ca^{2+}]_{in}$ (Fig. 2.3.D). The remaining level of $Ca^{2+}{}_{in}$ was at least fivefold higher in the $LaCl_3$ treated cells than in the untreated.

We also tested the effect of vanadate on Ca^{2+} homeostasis in PAO1 (Fig. 2.3.E). Vanadate is known to inhibit P-type (212) and ABC (213) ATPases, and therefore is expected to block Ca^{2+} uptake or efflux mediated by these transporters. Vanadate treatment increased the initial rise of $[Ca^{2+}]_{in}$ by twofold, and the remaining level of $[Ca^{2+}]_{in}$ by fourfold.

Ca^{2+} homeostasis is not involved in PAO1 tolerance to external Ca^{2+}. To examine whether the putative Ca^{2+} transporters play a role in cell tolerance to high Ca^{2+}, thirteen mutants from groups I - III were grown in the presence of 5 or 100 mM Ca^{2+} and compared to WT. The results showed that at 5 mM Ca^{2+}, neither PAO1 nor mutants showed any growth defects. Similarly, the addition of 100 mM Ca^{2+}, although introduced a 13 h lag phase, did not significantly affect growth of the wild type or the mutants (data not shown).

Ca^{2+} homeostasis is involved in regulating Ca^{2+}-induced swarming motility in PAO1. To determine the role of Ca^{2+} homeostasis in Ca^{2+}- induced swarming motility in PAO1, the group III mutants with abolished ability to maintain Ca^{2+} homeostasis were tested for swarming motility at 5 mM Ca^{2+} *vs.* no added Ca^{2+} (Fig. 2.4. A). The presence of Ca^{2+} induced swarming in PAO1 by sixfold. When this induction was taken as 100 %, two mutants PA3920:IS, with disrupted P-type ATPase, and PA2092:IS, with disrupted major facilitator protein, showed only 27 % and 67 % of Ca^{2+} induction, respectively. PA2435:IS, with disrupted P-type ATPase, showed no significant difference in swarming, and PA4614:IS, with disrupted mechanosensitive channel, swarmed 26 % further in the presence of Ca^{2+} than PAO1.

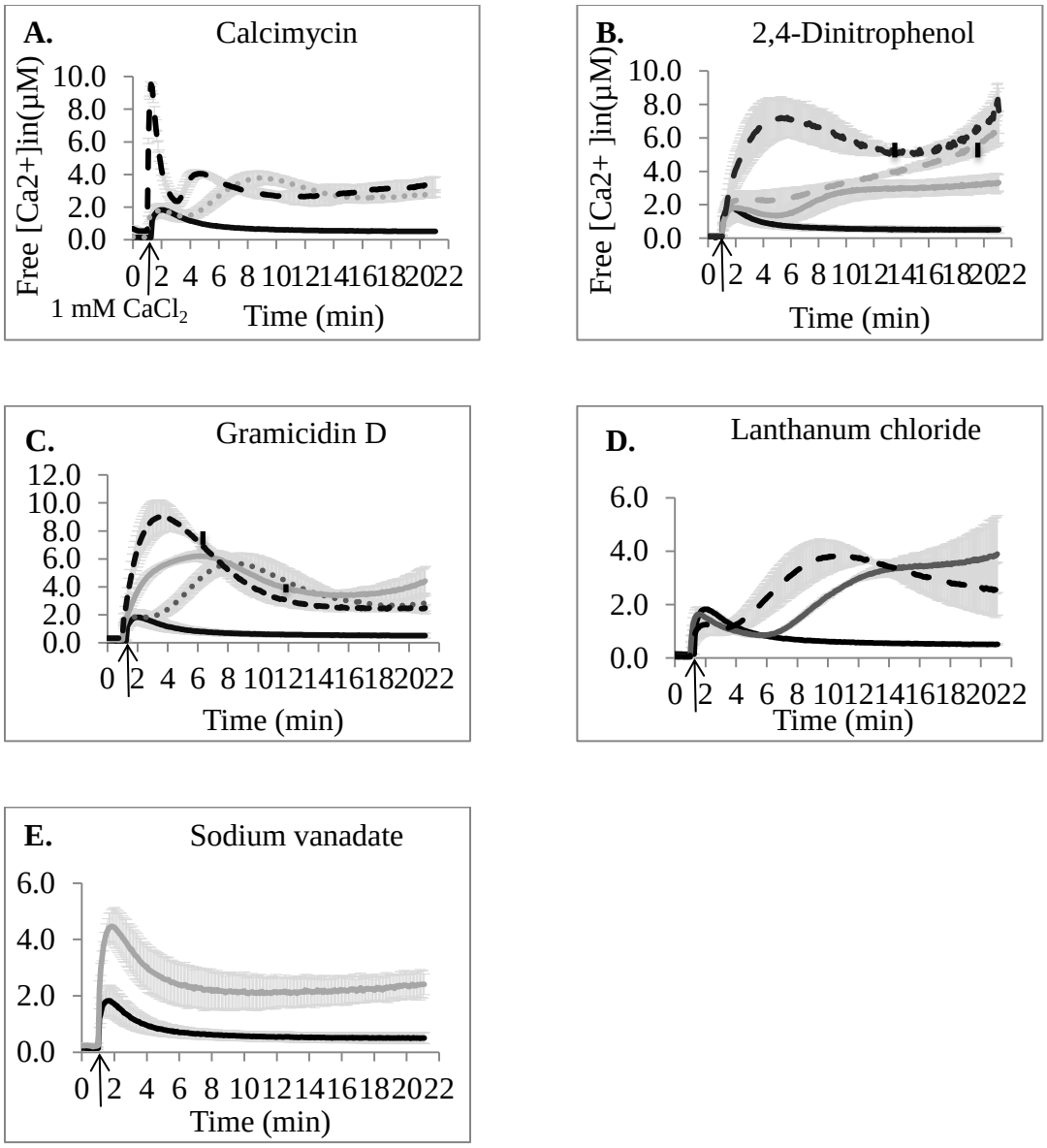

Figure 2.3. Effect of inhibitors on free $[Ca^{2+}]_{in}$ in *P. aeruginosa* PAO1. Cells grown in BMM media containing no added Ca^{2+} were treated with inhibitors for 10 min at room temperature. The basal level of luminescence was monitored for 1 min. 1 mM $CaCl_2$ was added at the time indicated by the arrow, followed by luminescence measurements for 20 min. Changes in free $[Ca^{2+}]_{in}$ were calculated as described in the Methods section. A. Calcimycin. Black, 0 mM; dashed black, 5 μM; small dotted grey, solvent control. B. Cells challenged with 2, 4 dinitrophenol. Black, 0mM; grey, 0.5 mM; dashed grey, 1

mM; dashed black, 2 mM. C. Gramicidin D. Black, 0 µg/ml; small dotted grey, 1 µg/ml; dashed black, 10 µg/ml; and grey, solvent control. Vertical lines on the plots indicate the points, at which the remaining available aequorin reached 10 % of the estimated total aequorin. D. $LaCl_3$. Black, 0 µM; grey, 300 µM, and dashed black, 600 µM. E. Vanadate (2 mM, pH 7.5). The data were averaged from at least three independent experiments.

We also tested the effect of inhibitors targeting P-type and ABC ATPases (vanadate), Ca^{2+} channels ($LaCl_3$), or dissipating H^+, Na^+, and K^+ gradients (gramicidin D) on Ca^{2+}-induced swarming motility (Fig. 2.4.B). All three inhibitors reduced the effect of Ca^{2+} on swarming. The most significant reduction was observed in the presence of 2 mM vanadate, where Ca^{2+} induction reached only 17 % of the induction in untreated PAO1. The presence of 10 µg/ml gramicidin D or 600 µM $LaCl_3$ decreased Ca^{2+} induction by 34% and 63%, respectively. The results for $LaCl_3$ should, however, be taken with a caution, since it precipitated during preparation.

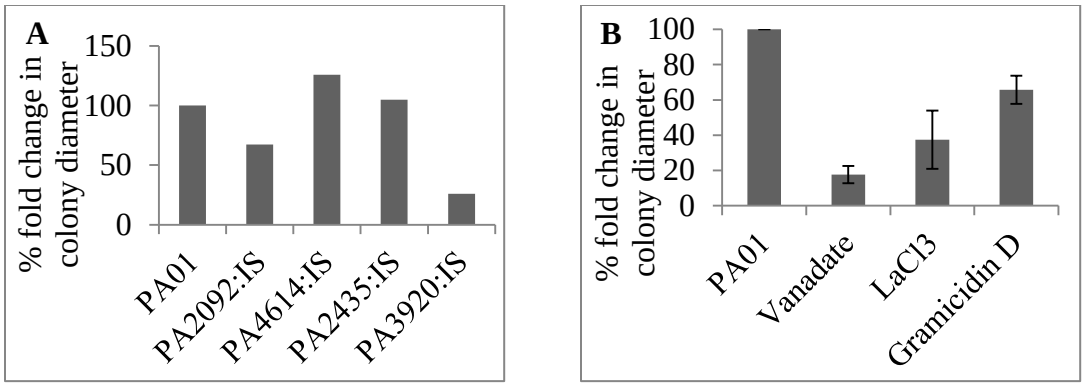

Figure 2.4. Swarming motility. Cells were grown on swarming agar containing 0 mM or 5 mM Ca^{2+}. A. Group III mutants. B. PAO1 cells. Inhibitors: 2 mM vanadate, 600 µm $LaCl_3$, or 10 µg/ml gramicidin D were added to the medium prior to plating. Colony diameters were measured, and fold differences (5 mM *vs*. 0 mM) were calculated using the corresponding controls. The percentage of fold changes was calculated considering that the fold difference in untreated PAO1 was 100 %. The averages of at least three biological replicates were used to calculate the percentage of the fold changes. To avoid bias, in case of mutants, colony diameters were first averaged, and then the fold differences between the mutants and WT were calculated. The standard deviation between replicates was below 10 %.

Discussion

This study establishes that *Pseudomonas aeruginosa* PAO1, a human pathogen with Ca^{2+}- induced virulence, maintains free intracellular Ca^{2+} at sub-micromolar level, which rapidly increases and slowly restores in response to external Ca^{2+}. This process is impaired by blocking monovalent cation gradient or modulating Ca^{2+} uptake, and requires several transporters from the superfamilies of P-type ATPases and ion exchangers. These proteins will make an excellent tool for studying Ca^{2+} regulation and signaling in this organism. Finally, the study showed the role of Ca^{2+} homeostasis in Ca^{2+}- induced swarming motility, suggesting its regulatory role in *P. aeruginosa* response to Ca^{2+}. The intracellular level of $[Ca^{2+}]_{in}$ (0.1 – 0.2 μM) and the magnitude (5-28 fold) of the initial response to external Ca^{2+} (1 - 5 mM) places *P. aeruginosa* among three other bacteria *E. coli* JM109, *Anabaena sp.* PCC7120, and *B. subtilis* (146-148), whose intracellular Ca^{2+} levels have been characterized. In contrast, *Propionibacterium acne*, although has a similar basal level of $[Ca^{2+}]_{in}$, responds to 1mM Ca^{2+} by only twofold increase in $[Ca^{2+}]_{in}$ (194). The results illustrate that *P. aeruginosa* is able to maintain sub-micromolar levels of intracellular Ca^{2+} in the presence of millimolar levels of external Ca^{2+}, suggesting its ability to (1) block Ca^{2+} uptake, (2) pump out Ca^{2+} from the cells against the steep concentration gradient, or (3) chelate Ca^{2+} inside the cells. The first two abilities in prokaryotes were attributed to the function of several mechanisms including ion channels, P- and F-type ATPases and ion gradient driven transporters that were identified using inhibitors (148, 152) or individual proteins (173).

The detected two-phase $[Ca^{2+}]_{in}$ recovery (short-rapid and long-slow) following the challenge with 1 mM Ca^{2+} may suggest the function of distinct efflux mechanisms of

high and low efficiency. The following fluctuations of $[Ca^{2+}]_{in}$ in the presence of 5 mM Ca^{2+} may be a result of continuous cumulative effect of both influx and efflux mechanisms eventually resulting in the recovery of the $[Ca^{2+}]_{in}$ basal level. Comparison of Ca^{2+}-induced and naïve cells revealed multiple differences in $[Ca^{2+}]_{in}$ responses. Lower initial $[Ca^{2+}]_{in}$ responses with elevated rates of the $[Ca^{2+}]_{in}$ initial increase and decrease in the presence of 5 mM Ca^{2+} in induced cells suggest that Ca^{2+} induces adaptation mechanisms. However, the elevated basal level of $[Ca^{2+}]_{in}$ in induced cells and their inability to significantly reduce the increased $[Ca^{2+}]_{in}$ at 1 mM Ca^{2+} indicate that growth at elevated Ca^{2+} possibly sensitizes cells to external Ca^{2+}, as was proposed in *E. coli* (147). Overall, these observations suggest the presence of multiple mechanisms for controlling Ca^{2+} homeostasis in *P. aeruginosa* and their complex regulation in response to different levels of Ca^{2+} in the environment.

Among several types of transporters determined to be involved in the maintenance of $[Ca^{2+}]_{in}$ homeostasis, the most numerous were P-type ATPases. This superfamily of transporters has long been established to transport metals, but was not initially considered to play a major role in Ca^{2+} transport in prokaryotes. Later, several reports described both Ca^{2+}-dependent P-type ATPase activity and ATP-dependent Ca^{2+} transport or transporters, most of which were shown to efflux Ca^{2+} *in-vitro* in membrane vesicles (197, 214). However their role in maintaining cellular Ca^{2+} homeostasis *in-vivo* has not been tested. In this study, out of the seven P-type ATPases predicted in the PAO1 genome, four were induced by Ca^{2+}, and six played a role in $[Ca^{2+}]_{in}$ maintenance. These six were phylogenetically related to divalent cation translocating ATPases, whereas PA1634 clustered with K^{+}-translocating KdpB from *E. coli,* showed no effect on $[Ca^{2+}]_{in}$

homeostasis. P-type ATPases are known to be inhibited by vanadate, functioning as a phosphate analog (212). In agreement, four mutants with disrupted P-type ATPases showed a $[Ca^{2+}]_{in}$ profile similar to the profile of vanadate treated PAO1 cells with increased $[Ca^{2+}]_{in}$ or lowered ability of its recovery. The disruption of two other P-type ATPases PA2435 and PA3920 showed the most significant effect and abolished the ability of PAO1 to reduce $[Ca^{2+}]_{in}$ below 1.5 μM in the presence of 1mM Ca^{2+}. PA2435 has been shown earlier to translocate $Cu^{2+}$and Zn^{2+} (205), but in our phylogenetic analysis, it clustered closer to heavy metal-translocating ATPases, whereas PA3920 was more closely related to Cu^{2+}-translocating transporters. Noteworthy, these two proteins were not detected to be induced by Ca^{2+}, and therefore, likely do not contribute to the increased rate of Ca^{2+} efflux in Ca^{2+}-induced cells. Since the identified P-type ATPases contributing to the detected changes in the intracellular Ca^{2+} do not contain typical Ca^{2+}-binding domains, they are not likely to play a direct role in translocating Ca^{2+}. The ATPases may be involved in controlling transition of metals important for Ca^{2+} translocation or generating an ion gradient that serves as an energy source for Ca^{2+} transporters, as was proposed in *A. vinelandii* (215).

To characterize the contribution of F-type ATPases (ATP synthases) in Ca^{2+} homeostasis, we treated cells with a protonophore 2,4 DNP, known to inhibit ATP synthesis by uncoupling oxidative phosphorylation (152). This treatment raised the level of $[Ca^{2+}]_{in}$ and impaired the ability of PAO1 to decrease it, most likely due to the lack of ATP. The role of ATP in Ca^{2+} efflux has been described in *E. coli*, where the lack of F-type ATP synthase AtpD decreased cellular ATP content and impaired $[Ca^{2+}]_{in}$ efflux (152). However, the disruption of PA5554, the AtpD homolog with 82 % amino acid

sequence identity, although induced by Ca^{2+}, did not affect Ca^{2+} homeostasis. It is possible that two paralogs of PA5554 in the genome: PA1697 and PA1104, with 24 and 28 % amino acid sequence identity, correspondingly, could compensate for the absence of PA5554 and provide ATP required for Ca^{2+} efflux.

Gradient driven Ca^{2+} exchangers have been considered as a major mechanism in bacterial Ca^{2+} efflux that most commonly employs H^+ and Na^+ as coupling ions. In agreement, treating PAO1 with gramicidin D, known to dissipate monovalent ion gradients across the cytoplasmic membrane (207), caused a significant initial accumulation of $[Ca^{2+}]_{in}$, which decreased over time, suggesting the function of alternative efflux mechanisms. We predicted and tested the role of four putative gradient driven exchangers in $[Ca^{2+}]_{in}$ homeostasis, three of which showed a significant impact on Ca^{2+} homeostasis. The disruption of PA2092 showed the most prominent effect, as the mutant was not able to decrease the elevated $[Ca^{2+}]_{in}$ in the presence of 1mM Ca^{2+}. None of the predicted ion exchangers were induced by Ca^{2+}, suggesting that, similarly to P-type ATPases PA2435 and PA3920, they do not play role in the differences between naïve and induced cells. The results suggest that Ca^{2+} translocation may be coordinated by the combined action of both P-type ATPases and ion exchangers as was illustrated for SERCA or PMCA ATPases and Na^+/Ca^{2+} exchangers in mammalian systems (216, 217).

Treating PAO1 cells with a Ca^{2+} channel blocker $LaCl_3$ (210) reduced the initial uptake of Ca^{2+}, confirming the role of La^{3+} sensitive channels in PAO1 Ca^{2+} influx, as has been shown in other bacteria (147, 148). The antagonistic effect of La^{3+} on Ca^{2+} influx in *E. coli* was associated with poly-3-hydroxybutyrate/polyphosphate (PHB-PP) channels (147). However, search of the PAO1 genome for homologs of the functionally defined

PHB-PP genes from *Ralstonia* (218) returned only scattered homologous genes. This may indicate the presence of a non- or low-homology PHB-PP biosynthetic pathway or a different type of La^{3+} sensitive channels in PAO1. Interestingly, in addition to blocking Ca^{2+} influx, $LaCl_3$ treatment caused a secondary $[Ca^{2+}]_{in}$ increase and a plateau at about 3 μM. This suggests that La^{3+} also inhibits Ca^{2+} efflux, which is consistent with the known inhibition effect of La^{3+} on P-type ATPases *via* blocking phosphorylation events (196, 211). Furthermore, we detected that the disruption of PA4614 encoding Ca^{2+}-induced probable mechanosensitive channel MscL caused a very quick uptake of Ca^{2+} followed by a second increase and a slow recovery of $[Ca^{2+}]_{in}$. In *E. coli,* although the expression of the homologous gene was also affected by Ca^{2+}, its disruption showed no effect on Ca^{2+} homeostasis (152). Mechanosensitive channels are known to open in response to membrane tension and protect cells against hypoosmotic shock as reviewed in (219). It is not clear why the lack of the MscL protein caused the increase in Ca^{2+} uptake. We hypothesize that Ca^{2+}-induced MscL may contribute to limiting Ca^{2+} uptake when in a closed state under the tested physiological conditions, and when *mscL* is disrupted, cells become more permeable to Ca^{2+} influx.

Finally, we determined that elevated Ca^{2+} induced swarming motility in PAO1, whereas treatment with vanadate, $LaCl_3$ and gramicidin D decreased this induction. The disruption of P-type ATPase PA3920 and ion exchanger PA2092 also significantly diminished the inducing effect of Ca^{2+} on swarming. The effect of Ca^{2+} on swarming motility varies in different bacteria, for example, Ca^{2+} has been shown to induce swarming in *Vibrio parahaemolyticus* (157), but inhibited this type of motility in fluorescent pseudomonads (220). This study shows for the first time that Ca^{2+}

homeostasis plays an important role in *P. aeruginosa* Ca^{2+} induced swarming, a complex physiological phenomenon known to modulate virulence and antibiotic resistance in this organism (221).

Overall, this study reports that *P. aeruginosa* PAO1 maintains a sub-micromolar basal level of $[Ca^{2+}]_{in}$ using multiple transport mechanisms that most likely require ATP and monovalent cation gradient. Involvement of multiple transport systems in Ca^{2+} influx and efflux has been suggested in *E. coli* (147, 222), and may be differentially regulated by growth conditions. This functional redundancy was also illustrated by the high tolerance of PAO1 cells to external Ca^{2+}, and reflects the physiological importance of the controlled cellular Ca^{2+} homeostasis. The two major aspects of such importance include protecting cells against the toxicity of high $[Ca^{2+}]$ and maintaining low basal level of $[Ca^{2+}]_{in}$ required for Ca^{2+} to play a signaling role. The transient changes in $[Ca^{2+}]_{in}$ (magnitude, length, and frequency) may function to relate external signal(s) to cellular response(s), as has been established in eukaryotes (139) and proposed in prokaryotes (192). We identified at least three transporters that play a major role in $[Ca^{2+}]_{in}$ homeostasis, and will be used in further studies required for experimental confirmation of signaling role of Ca^{2+} in *P. aeruginosa*.

Acknoweldgements

We thank Dr. Anthony Campbell from the School of Pharmacy and Pharmaceutical Sciences, Cardiff University in UK for sharing his expertise and the templates for calculating $[Ca^{2+}]_{in.}$ We thank Dr. Delfina Dominguez from The University of Texas at El Paso for sharing *E. coli* strain carrying pMMB66EH. We thank Dr. Wouter

Hoff from Oklahoma State University for critical review of the manuscript and insightful discussions. We thank Dr. Masato Kumauchi from Oklahoma State University for curve-fitting analysis. Mass spectrometry analyses were performed in the DNA/Protein Resource Facility at Oklahoma State University, using resources supported by the NSF MRI and EPSCoR programs (Award DBI/0722494). This work was supported by the Grant-in-Aid from American Heart Association (Award 09BGIA2330036) and the Research Grant from OCAST (Award HR12-167). Transposon mutants were obtained from the University of Washington Two - Allele library (grant # NIH P30 DK 089507).

Supplementary information.

Chemicals. Coelenterazine was purchased from Life Technologies (California, USA). Compound 48/80, 2, 4 di-nitrophenol, calcimycin, thiourea, tributyl phosphine (TBP), and ASB14 were obtained from Sigma Aldrich (St. Louis, MO). Nitrendipine, sodium orthovanadate, and lanthanum (III) chloride were purchased from Tocris biosciences (Bristol, UK), New England Biolabs (Tozer, MA), and AlfaAesar (Massachusetts, USA), respectively. All chemicals were of analytical grade.

Protein extraction. Cell pellets of PAO1 grown at no or elevated Ca^{2+} were washed in saline (0.14 M NaCl) and resuspended in TE buffer (10 mM Tris/HCl, 1 mM EDTA, pH 8.0), containing Mini Complete protease inhibitor cocktail (1:100 (v/v)). Cells were disrupted by sonication (5 cycles of 30 sec with 1 min interval on ice) using 550 Sonic Dismembrator (Fisher Scientific, Pittsburgh, PA) and centrifuged for 10 min at 4 ^{0}C. The procedure was repeated two times. The supernatants were combined, diluted with ice-cold 0.1 M sodium carbonate followed by gentle stirring for 1h at 4 ^{0}C, and centrifuged at 100 000 x g for 1 h at 4 ^{0}C in a Beckman L8-70M ultracentrifuge. The

pellets were collected, washed twice in 50 mM Tris pH 7.3, and subjected to liquid chromatography–tandem mass spectrometry (LC-MS/MS) – based spectral counting.

Expression and reconstitution of aequorin. Mid-log cultures grown in 5 ml of BMM were inoculated (1 %) into 100 ml of fresh BMM. Cells were grown until mid-log phase at 37^0C, 200 rpm, induced with IPTG (1 mM) for 2 hours for apoaequorin production, and then harvested by centrifugation at 5,500 g for 5 min at 4 ^{0}C. After been washed once in buffer (25 mM HEPES, 1 mM $MgCl_2$, 125 mM NaCl; pH 7.5), the cell pellets were resuspended in 2.5 ml of the same buffer. Aequorin was reconstituted by incubating the cells in the presence of 2.5 μM coelenterazine for 30 min in the dark at room temperature without shaking. The collected cells were washed twice with the buffer, and resuspended in 1 ml of the same buffer. Final cell density was adjusted to OD_{600} of 0.4.

CHAPTER III

THE *PSEUDOMONAS AERUGINOSA* PAO1 TWO-COMPONENT REGULATOR, CARSR, REGULATES CALCIUM HOMEOSTASIS AND CALCIUM-INDUCED VIRULENCE FACTOR PRODUCTION THROUGH ITS REGULATORY TARGETS, CARO AND CARP.

M. Guragain, M. M. King, K. S. Williamson, A. C. Pérez-Osorio, T. Akiyama, S. Khanam, M. A. Patrauchan and M. J. Franklin. (2015). The Pseudomonas aeruginosa PAO1 two-component regulator, CarSR, regulates calcium homeostasis and calcium-induced virulence factor production through its regulatory targets, CarO and CarP.

Abstract

Pseudomonas aeruginosa is an opportunistic human pathogen that causes severe, life threatening infections in patients with cystic fibrosis (CF), endocarditis, wounds, or with artificial implants. During CF pulmonary infections, *P. aeruginosa* often encounters environments where the levels of calcium (Ca^{2+}) are elevated. Previously, we showed that *P. aeruginosa* responds to externally added Ca^{2+} through enhanced biofilm formation, increased production of several secreted virulence factors, and by developing a transient increase in the intracellular Ca^{2+} followed by its removal to the basal sub-micromolar level. However, the molecular mechanisms responsible for regulating Ca^{2+}-induced virulence factor production and Ca^{2+} homeostasis are not known. Here, we characterized the genome-wide transcriptional response of *P. aeruginosa* to elevated [Ca^{2+}] in both planktonic cultures and in biofilms. Among the genes induced by $CaCl_2$ in strain PAO1 was an operon containing the two-component regulator PA2656-PA2657 (here called *carS* and *carR*), while the closely related two-component regulators, *phoPQ* and *pmrAB,* were repressed by $CaCl_2$ addition. To identify the regulatory targets of CarSR, we constructed a deletion mutant of *carR*, and performed transcriptome analysis of the mutant strain at low and high [Ca^{2+}]. Among the genes regulated by CarSR in response to $CaCl_2$ are the predicted periplasmic OB-fold protein, PA0320 (here called *carO*) and the inner membrane-anchored five-bladed □-propeller protein, PA0327 (here called *carP).* Mutations in both *carO* and *carP* affected Ca^{2+} homeostasis, reducing the ability of *P. aeruginosa* to export excess Ca^{2+}. In addition, a mutation in *carP* had a pleotropic effect in a Ca^{2+}-dependent manner, altering swarming motility, pyocyanin production, and tobramycin sensitivity. Overall, the results indicate that the two-

component system CarSR is responsible for sensing high levels of external Ca^{2+}, and responding through its regulatory targets that modulate Ca^{2+} homeostasis, surface-associated motility, and production of the virulence factor, pyocyanin.

Introduction

Pseudomonas aeruginosa, a natural inhabitant of soil and water, is able to infect a variety of hosts, including plants and humans. In humans, it causes severe acute and chronic infections by colonizing respiratory and urinary tracts, burned or wounded epithelia, cornea, and muscles (10, 223, 224). The versatility of *P. aeruginosa* pathogenicity is associated with diverse metabolic capabilities, multiple mechanisms of resistance, a large repertoire of virulence factors, and adaptability, due in part to tightly coordinated regulation of gene expression. A large portion of the *P. aeruginosa* PAO1 genome, approximately 9.4%, encodes transcriptional regulators (103, 225), including two-component regulators (TCS): 89 response regulators, 55 sensor kinases, and 14 sensor-response regulator hybrids (10). The regulatory targets for most of these regulatory systems are unknown.

Calcium plays an important signaling role in both eukaryotic and prokaryotic cells. In prokaryotes, Ca^{2+} is an essential nutrient, since it is a necessary cofactor for many enzymes. However, Ca^{2+} can be toxic to cells at high concentrations, and therefore bacteria maintain a low sub-micromolar intracellular concentration of Ca^{2+} (226). *P. aeruginosa* may encounter environments where external Ca^{2+} levels are in the milimolar range, varying from 10 mM in soil (227) to 40 mM in hypersaline lakes (228). As a plant and human pathogen, *P. aeruginosa* may be exposed to lower but also varying Ca^{2+} levels. For example, in plants, Ca^{2+} concentration ranges from 0.01 to 1 mM in extracellular spaces (229) and from 1 to 10 mM in apoplasts (230). In a human body, Ca^{2+} levels may reach about 1 - 2 mM in extracellular fluids and saliva (231) (232), and 5 mM in blood (233) and human milk (234). In case of disease, for example, during

cystic fibrosis (CF) pulmonary infections, both intracellular and extracellular Ca^{2+} levels fluctuate in response to inflammation (190, 235), and the overall Ca^{2+} levels in nasal secretions and sputum increase at least two fold (232) reaching up to 3-7 mM (236, 237).

In a previous study, we demonstrated that *P. aeruginosa* maintains a sub-micromolar intracellular concentration of Ca^{2+} ($[Ca^{2+}]_{in}$) (226). However, when the cells are exposed to high levels of extracellular Ca^{2+}, characteristic of the environments described above, the cells undergo a transient increase of $[Ca^{2+}]_{in}$. The transient increase is followed by a return to sub-micromolar levels of $[Ca^{2+}]_{in}$ and a maintenance of homeostatic concentration of internal Ca^{2+}, apparently due to the transport of excess Ca^{2+} through Ca^{2+} export pumps. Interestingly, in addition to maintenance of Ca^{2+} homeostasis, *P. aeruginosa* recognizes the external concentration of Ca^{2+} as a physiological signal, and responds through changes in the abundances of intracellular proteins and secreted virulence factors (7, 156). This Ca^{2+} triggered change in *P. aeruginosa* physiology leads to enhanced plant infectivity (238), biofilm formation, and swarming motility, as well as increased production of the virulence factors, alginate, pyocyanin, and secreted proteases (7, 156, 226). Furthermore, Ca^{2+} alters the abundance of *P. aeruginosa* proteins involved in iron acquisition, quinolone signaling, nitrogen metabolism, and stress responses (7, 156). These observations suggest that Ca^{2+} plays an important regulatory role in *P. aeruginosa* virulence. However, the molecular mechanisms responsible for sensing environmental Ca^{2+} and regulating the Ca^{2+}-induced responses are not known. Therefore, the goals of this study were to identify and characterize Ca^{2+}-mediated molecular responses.

Bacteria use two-component regulatory systems (TCSs) to sense and respond to diverse and continuously changing environmental stimuli, including changing cation concentrations. TCSs help regulate responses to Na^{+}, Mg^{2+}, and other cations, and therefore are likely involved in Ca^{2+}-dependent regulation. A typical TCS contains a sensor kinase located partially in the cytoplasmic membrane and a cognate response regulator (239). Upon exposure to a stimulus, the sensor kinase autophosphorylates at histidine residues. The consequent conformation change enables the transfer of a phosphate group to the aspartate residue on the cognate response regulator, which typically results in DNA binding to an activator DNA sequence and changes in gene expression (103, 104). *P. aeruginosa* has many TCSs, and some of these have been characterized. For example, PhoPQ and PmrAB regulate resistance to polymyxin B and antimicrobial peptides *via* lipid A modification at low magnesium (Mg^{2+}) concentration (106, 240-242). PhoPQ also regulates aminoglycoside resistance, twitching and swarming motility, surface attachment, and biofilm formation, ultimately contributing to regulation of virulence (110, 243). PmrAB is induced by cationic antimicrobial peptides including polymyxins (240), whereas PhoPQ is induced by polyamines and low [Mg^{2+}] (244). Other TCSs respond to metals, including the CzcRS and CopRS systems that regulate the resistance to zinc and copper, respectively (245, 246). CzcRS also regulates the transcription of CzcrBCA Resistance-Nodulation-Division (RND) efflux pump, which is responsible for carbapenem resistance (245). GacAS and AlgRZ regulate the production of several virulence factors including pyocyanin, cyanide, lipase, and alginate, as well as systemic virulence and motility (243, 247-251). GacAS also controls the production of the quorum sensing signaling molecule N-butyryl-homoserine lactone (252) and

resistance to diverse antibiotics, including the aminoglycosides, gentamicin, and chloramphenicol (243). Transcription of *gacS* is repressed by sub-inhibitory concentrations of tobramycin, ciprofloxacin, and tetracycline (253). AlgRZ also regulates early stages of biofilm formation (254) and the expression of quorum sensing genes (255). Another TCS, FleRS regulates flagella synthesis, adhesion (256), motility, and antibiotic resistance (257). Five TCS response regulators PA1099, PA3702, PA4547, PA4493, and PA5261 are involved in coordinating the interactions of the bacterium with the host lung epithelium (258). However, most other TCS encoded on the *P. aeruginosa* genome remain uncharacterized, with their signals and regulatory targets yet to be identified.

In this study, we used microarray analysis to characterize the global transcriptional response of *P. aeruginosa* to elevated external Ca^{2+}. From these analyses, we identified the TCS, PA2656-PA2657 (here referred to as calcium regulator, *carSR*), whose transcription is highly induced by elevated Ca^{2+} in planktonic cultures of *P. aeruginosa* PAO1. Using deletion mutations and microarray analysis, we identified the regulatory targets of *carSR*, which include the hypothetical proteins PA0320 and PA0327. Further characterization of PA0320 and PA0327 indicate that they play roles in maintaining Ca^{2+} homeostasis. PA0327 also influences production of the virulence factor, pyocyanin, and swarming motility in a Ca^{2+}-dependent manner.

Materials and Methods

Bacterial strains, plasmids, and media. Strains and plasmids used in this study are listed in Table 3.S1. *P. aeruginosa* PAO1 is a non-mucoid strain with the complete

genome sequence available (10). *P. aeruginosa* FRD1 is a mucoid cystic fibrosis isolate, also with an available genome (259) sequence. Isogenic mutants were constructed in PAO1. The gene PA2657 (*carR*) was deleted from PAO1 using allelic exchange as described previously (7). PAO1 mutants with transposon insertion in PA0320 (PA0320-H07::IS*lacZ*/hah) and PA0327 (PA0327-B11::IS*phoA*/hah) were provide by the University of Washington two-allele library. The sites of transposon insertions were confirmed by two-step PCR, using the primer sequences available at www.gs.washington.edu. For convenience, the transposon mutants were designated as PA::Tn5, where PA is the identifying number of the disrupted gene from the *P. aeruginosa* PAO1 genome (www.pseudomonas.com). Each mutant gene was complemented by cloning the gene behind the arabinose-inducible P_{BAD} promoter in the Tn7 vector, pTJ1 (260) (graciously provided by Dr. Joanna Goldberg). For complementing vectors, PA0320 and PA0327 were amplified using PCR with gene-specific primers listed in Table 3.S1. The PCR products were cloned into TA cloning vectors (Invitrogen). The resulting plasmids were digested with *Nco*I and *Hind*III, and the bands containing PA0320 and PA0327 were ligated into pTJ1, producing plasmids pTA56 and pTA57, respectively. A Tn7-based construct containing both PA2657 and PA2656 was used to complement the PA2657 mutant, to correct for any possible polar effects due to the disruption of PA2657. PA2656 and PA2657 were amplified separately using Phusion® High-Fidelity DNA polymerase (NEB). After addition of 3' A-overhang by *Taq* DNA polymerase, PCR products were cloned into TA cloning vectors. The *Eco*RI-*Eco*RV fragment containing PA2656 was ligated into pTJ1, followed by ligation of the *Eco*RI fragment containing PA2657. The resulting plasmid was labeled pTA104.

The Tn7-based vectors were integrated into the chromosome of the respective *P. aeruginosa* mutant strains using electroporation, along with the Tn7 transposase helper plasmid, pTNS1, with selection for trimethoprim resistance. The trimethoprim resistance marker was then removed using pFLP2 (261). pTNS1 and pFLP2 were graciously provided by Dr. Herbert Schweizer.

For estimation of free intracellular calcium **(**$[Ca^{2+}]_{in}$**),** PAO1 and mutant derivatives were transformed with pMMB66EH-AEQ (graciously provided by Drs. D. Dominguez and A. Campbell), which carries the gene for aequorin (262) and was selected for by carbenicillin resistance (202). The presence of the aequorin gene in the resulting strains was verified by PCR, using the aequorin specific primers (Table 3.S1).

Biofilm and planktonic cultures were cultivated in Biofilm minimal medium (BMM) (7) which contained (per liter): 9.0 mM sodium glutamate, 50 mM glycerol, 0.02 mM $MgSO_4$, 0.15 mM NaH_2PO_4, 0.34 mM K_2HPO_4, and 145 mM NaCl, 20 µl trace metals, 1 ml vitamin solution. Trace metal solution consisted of (per liter of 0.83 M HCl): 5.0 g $CuSO_4.5H_2O$, 5.0 g $ZnSO_4.7H_2O$, 5.0 g $FeSO_4.7H_2O$, 2.0 g $MnCl_2.4H_2O$). Vitamins solution contained (per liter): 0.5 g thiamine and 1mg biotin. The pH of the medium was adjusted to 7.0. When required, $CaCl_2{\cdot}2H_2O$ was added to a final concentration of 10 mM.

Table 3 S1. Bacterial Strains, plasmids and Oligonucleotide Sequences

Strains/Plasmids	Description	Reference
P. aeruginosa		
PAO1	Wild type strain, Alg^-	(10)
FRD1	Cystic Fibrosis isolate, Alg^+	(259)
PA0320-H07::IS*lacZ*/*hah*	PAO1 with Tn5 disruption of PA0320	(263)
PA0327-B11::IS*phoA*/*hah*	PAO1 Tn5 disruption of PA0327	(263)
Δ*carR*::Gm	PAO1 with deletion of *carR* replaced with Gm^r gene	This study
PA0320-H07::IS*lacZ*/*hah*/P_{BAD}-PA0320	Tn5 disruption of PA0320 complemented by P_{BAD}-PA0320	This study
PA0327-B11::IS*phoA*/*hah*/ P_{BAD}-PA0327	Tn5 disruption of PA0320 complemented by P_{BAD}-PA0327	This study
Δ*carR*::Gm/ P_{BAD}-*carRS*	Deletion of *carR* complemented by *cars*	This study
Plasmids		
pTJ1	Tn7 vector containing P_{BAD} promoter, Tm^r	(260)
pMMB66EH-AEQ	pMMB66EH containing aequorin gene from *Aequorea Victoria*	(264)
pTNS1	Helper plasmid for Tn7 transposase, Ap^r	(265)
pFLP2	Helper plasmid for FLP recombinase, Ap^r	(261)
pCR2.1	Cloning vector from Invitrogen, Ap^r, Km^r	Invitrogen
pTA53	PA0320 in pCR2.1	This study
pTA54	PA0327 in PCR2.1	This study
pTA55	P_{BAD}-PA0320 in pTJ1	This study
pTA56	P_{BAD}-PA0327 in pTJ1	This study

pTA57	PA2656 in pCR2.1	This study
pTA99	PA2657 in pCR2.1	This study
pTA104	P_{BAD}-PA2656 and 2657 in pTJ1	This study

Oligonucleotides	
aequorin – For	CTTACATCAGACTTCGACAACCCAAG
aequorin – Rev	CGTAGAGCTTCTTAGGGCACAG
PA0320 NcoI 5'	ACCCATGGAACTTCGTCACCT
PA0320 XbaI 3'	GGTCTAGAAGGGGTTCACCGG
PA0327 NcoI 5'	TGCCATGGCTATCCACGCCCA
PA0327 XbaI 3'	AGTCTAGAGCGGGCCAGGGG
5'PA2657-EcoRI	GCAGAATTCATCCTGAAGGACGAGGAAGACGAC
3'PA2657	GTCCAGTTGCATGCCGTTCG
5'PA2656	CCAGTGCGTGTGCCTGAACG
3'PA2656-EcoRV	CGAGATATCCGGGACTGTCGGCAAATGGT

RT-qPCR Primers	
0320Left_RtPCR	GACACCCCGGTGGTCCTCCA
0320Right_RtPCR	TCGACTTCGCCGGTCAGCTTG
0327Left_RtPCR	CCGGTCGGGATCGAAGGTCA
0327Right_RtPCR	GGTTCGCCGTCCAGGAGTGG
acpLeftRT-PCR2	ACTCGGCGTGAAGGAAGAAG
acpRightRT-PCR2	CGACGGTGTCAAGGGAGT

Growth of planktonic cultures and biofilms. *P. aeruginosa* strains PAO1 and FRD1 were cultured planktonically for 18 h at 37°C, with shaking at 250 rpm, in BMM with 10 mM added $CaCl_2$ or with no added $CaCl_2$. Biofilms were cultured on the surface of silicone tubing at 37°C in a single flow-through system for 72 h with and without 10 mM added $CaCl_2$ as described previously (7). Biofilms were detached from the interior surface of the silicone tubing with the plunger from a 3 ml syringe. For FRD1, the cells were plunged into 150 ml of 110 mM sodium citrate. All resulting cell suspensions were collected by centrifugation at 10,000 rpm at 4°C for three min.

For physiological studies of PAO1 and its mutant derivatives, cells were cultured by inoculating 5 ml of a mid-exponential phase culture into 100 ml of BMM with no added or 10 mM $CaCl_2$. Cultures were incubated at 37^{o}C at 200 rpm with absorbance sampling every 2-4 h in a Biomate 3 spectrophotometer (Thermo Scientific).

RNA extraction, processing, and microarray analysis. RNA was isolated from cells using a hot phenol extraction method (266). Briefly, pelleted cells were suspended in 1.5 ml lysis buffer (0.15 M sucrose, 0.01 M sodium acetate, pH 4.5) and 1.5 ml 2% sodium dodecyl sulfate. Following the addition of 3 ml of water-saturated phenol, the mixture was incubated for 5 min at 65°C with frequent vortexing. 3 ml of chloroform was added, and the mixture was centrifuged for 30 min at 4°C. The aqueous phase was precipitated overnight, washed, and resuspended in RNase-free water. The RNA was cleaned on an RNeasy column (Qiagen) following the manufacturer's mini cleanup protocol and then subjected to two 30 min Turbo DNase (Ambion) treatments before precipitation and resuspension. RNA quality was assessed using an RNA6000 nano assay (Bioanalyzer2100, Agilent Technologies, Palo Alto, CA). Labeled cDNA was

synthesized from 8 micrograms of total RNA according to SOP#M007 (TIGR), using a 2:1 ratio of amino-allyl dUTP to dTTP and Superscript II. cDNA quality and dye incorporation were assessed with the Nanodrop 1000.

Pseudomonas aeruginosa Version 1 glass slide DNA microarrays were obtained from J .Craig Venter Institute (JCVI), formerly The Institute for Genomic Research and prepared according to SOP#M008 (TIGR), with minor modifications. For each condition (PAO1 planktonic, PAO1 biofilm, FRD1 planktonic, and FRD1 biofilm), labeled cDNA from cells grown with 10 mM added $CaCl_2$ and cells grown with no added $CaCl_2$ were cohybridized to the same slide, and a dye swap was performed. In this manner, for each of the four growth conditions, a minimum of four biological samples were hybridized to four microarrays.

Microarray slides were scanned using the GenePix 4000B scanner (Molecular Devices) and emissions at 532 and 650 nm were recorded. GenePix Pro software V 6.0 (Molecular Devices) was used to obtain median pixel intensity values for each spot on the array and generate GenePix Results (gpr) files. Gpr files were imported into Flexarray v 1.6.1 for normalization and analysis. Background correction was performed using the normexp algorithm. The Loess algorithm was used for within-array normalization, followed by scaling for between-array normalization. The Limma TREAT (t-tests relative to a threshold) method was used to generate symmetrical fold change to conservatively assess differential expression due to calcium addition. Empty and reserved spots were not included in the dataset. Replicate spots (three per gene) were averaged and genes with greater than two-fold change at $p < 0.05$ were selected for further analysis.

For validation of the JCVI microarray data, two additional biological replicates of PAO1 were grown planktonically with and without 10 mM added $CaCl_2$ as described above. Affymetrix microarrays were performed with these samples as described previously (267). Transcripts identified as upregulated in two-color arrays (JCVI) were also found to be upregulated on the Affymetrix platform, with 92% (33/36) being greater than two-fold upregulated ($p < 10^{-14}$). Transcripts identified as downregulated in two-color arrays were also downregulated on the Affymetrix platform, with 90% (26/29) greater than two-fold ($p < 10^{-14}$). The microarray data have been deposited in NCBI's Gene Expression Omnibus (Edgar et al., 2002) and are accessible through GEO Series accession number GSE74491 (http://www.ncbi.nlm.nih.gov/geo/query/acc.cgi?acc=GSE74491).

Reverse transcription quantitative polymerase chain reaction (RT-qPCR). At 6, 12, and 24 h, 1 ml aliquots of wild type and □*carR* mutant cells were removed from a 25 ml volume of BMM (with or without 10 mM added $CaCl_2$), pelleted, and frozen at -80°C. RNA was extracted with the hot phenol method, cleaned on RNA Clean & Concentrator-25 Columns (Zymo Research), and turbo DNase treated (Ambion). One step RT-qPCR was performed with the Rotor-Gene SYBR Green RT-PCR kit (Qiagen) as described previously (268). Three biological replicates for each strain, time point, and Ca^{2+} level were assayed in triplicate using primers designed for the *acpP*, PA0320, and PA0327 transcripts (Table 3.S1). Negative controls lacking reverse transcriptase were performed with each of the 36 samples and revealed that samples were free from DNA contamination. RT-qPCR efficiencies, calculated from the slope of standard curves using

Rotor-Gene software, were similar for *acpP* (1.06), PA0320 (0.97), and PAO327 (1.03), with $r^2 > 0.98$ for each. The Relative Expression Software Tool® (REST) (269) was used to calculate mean fold change of PA0320 (*carO*) and PA0327 (*carP*) transcripts due to 10 mM calcium (10 mM /0 mM) using *acpP* as a normalizer. To determine if transcripts were significantly upregulated by calcium, a non-parametric one-tailed Mann-Whitney test, assuming unequal variation, was performed using GraphPad Prism version 6.04 for Windows. This test was also used to determine if there was a significant increase in fold change due to calcium in the wild type strain PAO1 compared to the □*carR* mutant strain.

Measurement of cellular calcium concentration ($[Ca^{2+}]_{in}$). Luminescence measurements and estimation of free $[Ca^{2+}]_{in}$ was done as described previously (226) with slight modification. Briefly, mid-log phase cells were induced with IPTG (1 mM) for 2 h for apoaequorin production, and then harvested by centrifugation at 6000 g for 5 min at 4 ^{0}C. Aequorin was reconstituted by incubating the cells in the presence of 2.5 µM coelenterazine for 30 min. 100 µl of cells with reconstituted aequorin were equilibrated for 10 min in the dark at room temperature. Luminescence was measured using Synergy Mx Multi-Mode Microplate Reader (Biotek). To estimate the basal level of $[Ca^{2+}]_{in}$, the measurements were recorded for 1 min at 5 sec intervals, then the cells were challenged with 1 mM Ca^{2+}, mixed for 1 sec, and the luminescence was recorded for 20 min at 5 sec intervals. Injection of buffer alone was used as a negative control, and did not cause any significant fluctuations in $[Ca^{2+}]_{in.}$ $[Ca^{2+}]_{in}$ was calculated by using the formula $pCa = 0.612 (-\log_{10}k) + 3.745$, where k is a rate constant for luminescence decay (s^{-1}) (147). The results were normalized against the total amount of available aequorin as described (226).

The discharge was performed by permeabilizing cells with 2 % Nonidet 40 (NP40) in the presence of 12.5 mM $CaCl_2$. The luminescence released during the discharge was monitored for 10 min at 5 sec intervals. The estimated remaining available aequorin was at least 10 % of the total aequorin. The experimental conditions reported here were optimized to prevent any significant cell lysis.

Swarming motility assay. Swarming motility was assayed as described in (226). PAO1 and mutants were grown in 5 ml BMM at no added or 10 mM $CaCl_2$. Two µl of the middle-log cultures normalized to the OD_{600} of 0.3 were spot inoculated onto the surface of BM2 agar plates (62 mM potassium phosphate buffer [pH 7], 0.02 mM $MgSO_4$, 10 µM FeSO4, 0.4% [w/v] glucose, 0.5% [w/v] Casamino Acids, and 0.5% [w/v] Difco agar) (248). After inoculation, the plates were incubated for 24 h, then the colony diameters and morphology were recorded.

Pyocyanin analysis. Pyocyanin production was assayed by using chloroform extraction as described (238) with modifications. Briefly, *P. aeruginosa* cultures grown in BMM until late log phase was normalized to OD_{600} of 0.3. Two µl of the normalized culture was inoculated in the middle of a BM2 agar plate (248) and incubated for 24 h at 37°C. Since swarming colonies spread within agar matrix, they were excised from the agar and split in two equal halves, one to be used for pyocyanin extraction and the other for total cellular protein quantification. Agar slices of the same size were used as negative controls. The samples were mashed into fine pieces. Pyocyanin was extracted with 30 ml chloroform followed by 15 ml of 0.2 N HCl. The absorbance of the extract was measured at 520 nm, and the amount of pyocyanin was calculated by using coefficient of extinction 17.1 M^{-1} Cm-^{1} (270) and normalized per mg of total cell protein. The latter was

determined by using the Bradford assay (EMD) following the manufacture's protocol. The data shown represent one of three independent experiments, each including three biological replicates.

Antibiotic susceptibility assays. Antibiotic susceptibility assays were performed using tobramycin and polymyxin B E-strips (Biomerieux). In brief, strains were cultured in BMM medium with no added $CaCl_2$ or 10 mM $CaCl_2$ for 18 h and normalized to an OD_{600} of 0.1. 100 µl of the normalized cultures was then spread on BMM agar plates with or without added $CaCl_2$. E- Strips with tobramycin and Polymyxin B gradients were placed onto the inoculated plates. After 24 h of incubation at 37°C, the MICs were recorded by determining the concentration of antibiotics on the strip at which no bacterial growth was detected. At least three replicates were tested in at least two independent experiments; the reported MICs are the mean values of the collected measurements.

Bioinformatics analyses. Sequence homology searches were performed using the NCBI nr database (Genebank release 160.1). Sequence alignments and phylogenetic analysis of histidine kinases and response regulators were performed using MEGA software (271). Homologous proteins were selected based on at least 25 % identity over the full length of amino acid sequence. Functional domains were predicted using Pfam (272). Protein subcellular localization was predicted using pSORTb v3.0 (273) and Loc tree (274) analysis. Prediction of transmembrane helices and signal peptides were performed using TMHMM (275) and SignalP 4.0, respectively (276). Protein 3D structure was predicted using HHpred (277) and iTASSER (278) and visualized using PyMOL (The PyMOL Molecular Graphics System, Version 1.7.6 Schrödinger, LLC).

Results

Transcriptome response of *P. aeruginosa* to Ca^{2+}. We performed whole genome transcriptome analysis of *P. aeruginosa* strain PAO1 and the mucoid cystic fibrosis strain FRD1, in order to identify *P. aeruginosa* genes whose transcription is positively or negatively regulated by Ca^{2+}. The strains were cultured under low and high $CaCl_2$ conditions (no added or 10 mM added $CaCl_2$) in both planktonic cultures and in biofilms. As with our prior proteomics results (156), the transcriptomics data showed both strain- and condition-specific effects on gene expression due to added Ca^{2+}. Table 3.1 shows genes differentially regulated by Ca^{2+} (at least two-fold change in expression and $p<0.05$) for strain PAO1, and the same genes in strain FRD1. Among the genes upregulated by Ca^{2+} in PAO1 is the operon PA0102-PA0104, encoding a carbonic anhydrase and permease that are likely involved in CO_2-mediated calcification (Patrauchan, unpublished data). The upregulated genes also included PA0320 and PA0327 encoding hypothetical proteins, whose role in calcium-dependent processes is described below. Also significantly upregulated by Ca^{2+} are the genes involved in quorum sensing, *lasI* and *rhlR*, as well as several genes that are regulated by the quorum sensing systems. The latter include *hcnA*, encoding hydrogen cyanide production, and many of the *pvd* genes responsible for pyoverdine biosynthetis. Pyoverdine biosynthetic proteins were shown to increase abundance in response to Ca^{2+} in our prior proteomics study (156).

Table 3.1. P. aeruginosa PAO1 genes affected by high Calcium levels

PA number	Gene/domain	PAO1 planktonic (10mM/0mM $CaCl_2$		PAO1 biofilm (10mM/0mM $CaCl_2$		FRD1 planktonic (10mM/0mM $CaCl_2$		FRD1 biofilm (10mM/0mM $CaCl_2$	
		Fold Change	P-value	Fold Change	P-value	Fold Change	P-value	Fold Change	P-value
Genes upregulated by high Ca during growth in planktonic culture									
PA0102	carbonic anhydrase	7.1	<0.01	1.0	1.00	-1.1	1.00	-1.3	0.91
PA0103	permease	5.6	<0.01	1.1	0.98	1.1	0.98	-1.5	0.83
PA0104	hypothetical	3.5	0.03	1.3	0.91	-1.3	1.00	-1.0	1.00
PA0122	*rahU*	6.0	0.02	1.6	0.74	2.1	0.28	-2.6	0.26
PA0320	OB-fold	17.1	<0.01	1.0	1.00	1.3	0.96	1.8	0.69
PAO327	Ca^{2+}-binding B-Propeller	13.0	<0.01	1.0	1.00	-1.0	1.00	1.0	1.00
PA0940	DUF2024	10.6	<0.01	1.2	0.97	-1.3	1.00	1.1	1.00
PA0941	thioredoxin	10.3	<0.01	1.4	0.89	-1.3	1.00	1.3	0.99
PA0942	DNA binding	2.9	0.04	1.0	1.00	-1.3	0.99	-1.2	1.00
PA1134	DUF393	3.0	0.02	1.9	0.58	-1.2	1.00	1.2	0.99
PA1432	*lasI*	3.1	0.01	1.0	1.00	-1.9	0.54	-1.2	0.97
PA2081	*kynB*	3.3	0.02	1.0	1.00	-2.1	0.34	1.1	1.00
PA2193	*hcnA*	2.4	0.04	1.0	1.00	-1.8	0.72	-1.4	0.89
PA2384	fur-like	3.1	0.02	2.1	0.32	1.0	1.00	1.1	1.00
PA2386	*pvdA*	4.1	<0.01	2.0	0.49	-1.3	0.99	1.1	1.00
PA2397	*pvdE*	2.6	0.02	2.2	0.29	1.1	1.00	-1.2	1.00
PA2412	pyoverdine synthesis	7.6	<0.01	1.9	0.54	-1.1	1.00	1.4	1.00
PA2413	*pvdH*	3.4	<0.01	1.4	0.98	-1.0	1.00	1.1	1.00
PA2424	*pvdL*	2.6	0.03	2.2	0.35	-1.3	0.94	1.8	0.74
PA2425	*pvdG*	4.0	<0.01	2.3	0.21	-1.5	0.92	1.5	0.99
PA2427	hypothetical	3.8	<0.01	1.4	0.89	-1.1	1.00	1.7	0.77
PA2656	histidine kinase	9.7	<0.01	-1.1	1.00	1.1	1.00	1.1	1.00
PA2657	response regulator	12.6	<0.01	-1.5	0.89	1.0	1.00	1.1	1.00
PA2658	PepSY domain	12.1	<0.01	-1.0	1.00	1.1	1.00	1.4	0.98
PA2659	PepSY domain	12.4	<0.01	-1.1	1.00	-1.2	1.00	-1.1	1.00
PA3322	DNA binding	2.8	0.03	1.0	1.00	-1.0	1.00	1.0	1.00
PA3407	*hasAp*	4.2	<0.01	1.1	1.00	1.1	1.00	-1.2	0.99
PA3477	*rhlR*	4.4	0.04	2.0	0.5	1.3	1.00	-1.8	0.79
PA3478	*rhlB*	6.9	0.04	2.1	0.47	1.2	1.00	-1.7	0.81
PA3885	*tpbA*	7.1	<0.01	-1.0	1.00	4.3	0.007	2.4	0.16
PA4141	hypothetical	3.7	0.03	2.4	0.3	2.1	0.41	-1.4	0.94
PA4378	*inaA*	3.1	0.02	-1.3	0.99	2.7	0.05	104	0.93
PA4379	hypothetical	5.1	<0.01	-1.6	0.83	3.8	<0.01	1.9	0.65
PA4469	hypothetical	2.9	0.02	2.8	0.08	1.1	0.89	1.3	1.00
PA4517	DUF1705	5.0	0.01	1.1	1.00	15.0	<0.01	1.1	1.00
PA5530	permease	5.7	<0.01	-1.4	0.79	4.6	<0.01	1.3	1.00

Genes upregulated by Calcium during growth in biofilms									
PA4570	hypothetical	1.0	1.00	4.3	0.01	-2.0	0.37	-1.0	1.00
Genes Down-regulated by high Calcium during planktonic growth									
PA0391	hypothetical	-2.6	0.02	-1.2	0.95	-1.3	0.96	-3.7	0.01
PA0603	transporter	-2.5	0.03	-1.0	1.00	-2.6	0.05	-1.1	1.00
PA0610	*ptrN*	-4.3	0.03	-1.9	0.56	-1.3	1.00	-2.0	0.48
PA0733	pseudouridine synthase	-3.5	0.01	1.0	1.00	1.1	1.00	1.1	1.00
PA0865	*Hpd*	-6.5	<0.01	-1.4	0.86	1.6	0.89	-1.2	0.98
PA1336	histidine kinase	-4.2	<0.01	1.2	1.00	1.1	1.00	1.1	1.00
PA1541	efflux transporter	-2.6	0.03	1.1	1.00	-1.1	1.00	1.3	0.98
PA1559	epimerase	-3.0	0.0.1	-2.0	0.45	-16.6	<0.01	-13.1	<0.01
PA2780	DNA binding	-2.7	0.01	1.1	0.99	1.2	0.99	-1.4	0.94
PA3217	*cyaB*	-2.6	0.03	-1.4	0.76	1.0	1.00	-1.0	1.00
PA4555	*pilY2*	-4.8	0.02	1.3	0.98	1.0	1.00	-1.6	0.9
PA4556	*pilE*	-3.8	0.01	0.2	0.95	1.1	1.00	-1.5	0.92
PA4568	*rpmA*	-2.6	0.04	-1.1	1.00	1.3	1.00	1.3	0.99
PA4699	TPR domain	-2.5	0.03	-1.1	1.00	-1.0	1.00	1.3	0.99
PA4823	hypothetical	-3.3	0.02	-1.2	1.00	-1.4	0.9	1.2	0.99
PA5024	permease	-2.5	0.02	1.3	0.98	1.0	1.00	1.2	0.99
Genes Down-regulated by high Calcium during biofilm growth									
PA0316	*serA*	1.3	1.00	-3.1	<0.01	1.0	1.00	-1.4	0.97
PA0890	*aotM*	1.5	0.98	-4.0	0.01	-5.2	<0.01	-5.6	<0.01
PA1053	hypothetical	-1.4	0.9	-3.2	<0.01	6.7	0.12	-3.0	0.02
PA1927	*metE*	-1.1	1.00	-10.6	<0.01	-23.0	<0.01	-1.5	0.73
PA4453	ABC transporter	1.1	1.00	-2.6	0.03	-1.1	1.00	-1.9	0.65
PA4455	ABC transporter	-1.1	1.00	-3.0	0.03	-1.1	1.00	-1.9	0.65
PA4773	decarboxylase	-1.8	0.72	-9.1	0.01	-27.6	<0.01	-23.1	<0.01
PA4774	spermidine biosynthesis	-2.3	0.28	-12.3	<0.01	-42.9	<0.01	-37.4	<0.01
PA4775	hypothetical	-1.2	1.00	-4.9	0.01	-10.0	<0.01	-13.8	<0.01
PA4776	*pmrA*	-1.3	1.33	-4.3	0.02	-7.4	<0.01	-9.4	<0.01
PA4777	*pmrB*	1.1	1.00	-6.9	<0.01	-5.6	<0.01	-12.5	<0.01
PA4781	response regulator	-1.9	1.00	-3.0	0.03	-1.5	0.98	-2.2	0.14
PA4782	hypothetical	-2.7	0.19	-12.0	<0.01	-11.6	<0.01	-23.4	<0.01
PA4826	hypothetical	-1.1	0.94	-4.7	0.01	-4.9	0.01	-1.3	0.99
Genes Down-regulated by high Calcium during both planktonic and biofilm growth									
PA1178	*oprH*	-58.8	<0.01	-28.2	<0.01	-1.5	0.89	-12.8	0.04
PA1179	*phoP*	-15.1	<0.01	-18.1	<0.01	-1.3	0.98	-11.6	<0.01
PA1180	*phoQ*	-12.5	<0.01	-14.7	<0.01	-1.4	0.96	-11.2	<0.01
PA1343	hypothetical	-12.2	<0.01	-13.5	<0.01	5.5	<0.01	-6.3	0.07
PA3552	*arnB*	-12.5	<0.01	-4.8	<0.01	-5.2	<0.01	-20.3	<0.01

PA3553	*arnC*	-11.1	<0.01	-4.7	<0.01	-8.3	<0.01	-29.4	<0.01
PA3554	*arnA*	-11.5	<0.01	-6.5	0.02	-27.5	<0.01	-43.5	<0.01
PA3556	*arnT*	-5.6	0.01	-5.1	0.01	-22.8	<0.01	-37.1	<0.01
PA3559	*arnG*	-5.2	0.02	-5.9	0.01	-5.9	0.04	-14.4	0.01
PA4010	glycosylase	-4.7	<0.01	-4.3	0.01	-2.9	0.1	-4.7	<0.01
PA4011	hypothetical	-3.5	0.02	-4.1	0.01	-3.2	0.11	-5.1	<0.01
PA4359	transport	-4.2	<0.01	-3.8	0.01	-4.1	0.01	-11.5	<0.01
PA4825	*mgtA*	-4.0	0.05	-3.5	0.12	-3.7	0.06	-1.2	0.95

Ca^{2+} influences the expression of three two-component regulatory systems (TCSs), *carSR*, *phoPQ*, and *pmrAB*. Expression of the novel TCS, PA2656-PA2657 (here termed, *carSR*) increased 10 to 12 fold in response to Ca^{2+}, while the TCSs *phoPQ* and *pmrAB* had significantly reduced expression (Table 3.1). The *carSR* operon contains four genes, which include the histidine kinase, *carS*, and the response regulator, *carR*, as well as two small periplasmic lipoproteins (PA2658 and PA2659), that both contain peptidase propeptide domains with possible protease inhibitory function. Increased expression of this operon was observed during growth of PAO1 in planktonic culture, but not in biofilms, and not in FRD1 cultures. Expression of both *phoPQ* and *pmrAB* TCSs was downregulated by Ca^{2+} in planktonic and biofilms cultures of both PAO1 and FRD1 (Table 3.1). Other studies have shown that PhoPQ affects the expression of the *arn* operon (PA3552-PA3559), which is involved in modification of LPS and enhanced resistance to cationic peptide antibiotics (110, 279). The transcriptomics results here are consistent with those results and indicate that Ca^{2+},also caused reduced expression of the *arn* operon in biofilm and planktonic cultures of both PAO1 and FRD1 (Table 3.1).

P. aeruginosa encodes multiple TCSs from each of the OmpR, NarL, and NtrC subgroups. We performed sequence alignment of paralogs from each of the TCSs clades for both the histidine kinases and the response regulators. The results of the OmpR subclade for the response regulators are shown in Fig. 3.1. Interestingly, although having opposite regulatory responses to Ca^{2+}, CarSR, PhoPQ, and PmrAB are closely related paralogs within the OmpR group, and all involved in divalent cation sensing and osmoregulation (106).

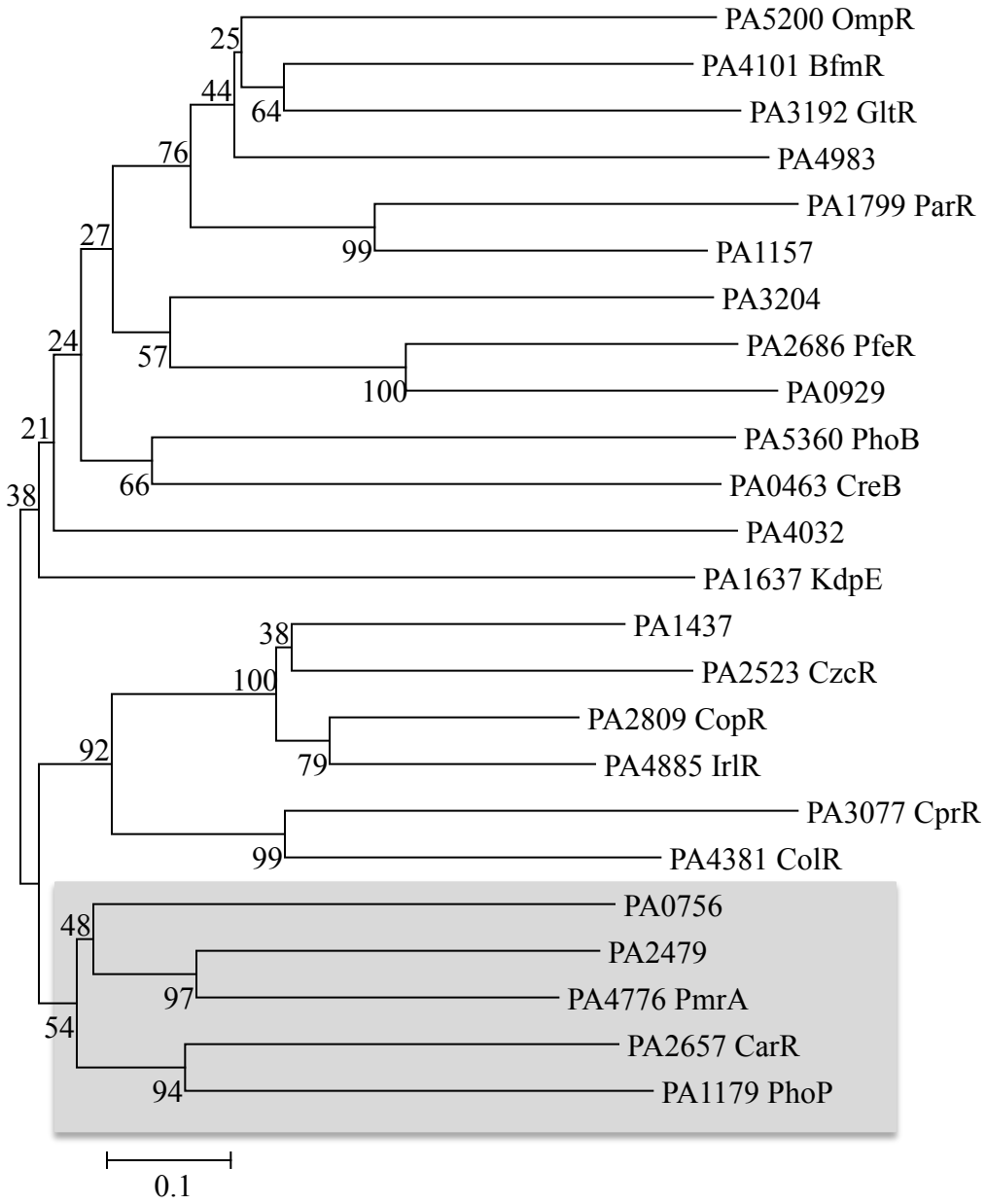

Figure 3.1. Phylogenetic analysis of *P. aeruginosa* response regulators in the OmpR clade of two-component systems. The OmpR response regulator protein sequences were aligned using the MEGA software (57). Phylogenetic relationships were constructed by using neighbor-joining and bootstrapping analysis within the MEGA program. The shaded region shows the subclade that includes PhoP, PmrA, and CarR.

CarSR regulates PA0320 and PA0327 in a Ca^{2+}-dependent manner. To identify the regulatory targets of CarSR, we constructed a deletion mutation of the *carR* response regulator in strain PAO1 and performed transcriptome analysis of the mutant strain with and without adding $CaCl_2$. The results were compared to the responses of wild-type strain PAO1 to Ca^{2+}. Expression of PA0320 and PA0327, which was highly upregulated by Ca^{2+} in PAO1 strain, was unaffected by Ca^{2+} in the Δ*carR* mutant strain, suggesting that CarSR directly (or indirectly) regulates transcription of PA0320 and PA0327 in a Ca^{2+}-dependent manner. To confirm the role of CarSR in regulation of PA0320 and PA0327, we performed RT-qPCR on PAO1 and on PAO1 Δ*carR*, using PA0320 and PA0327 specific primers. The results show that at the 6 h time point, PA0320 and PA0327 were slightly repressed by Ca^{2+} in both strains.(Fig. 3.2 A, B). However, after 12 and 24 h of growth, expression of both PA0320 and PA0327 was induced by Ca^{2+}in strain PAO1, but not in the Δ*carR* mutant. PA0320 had a 4.5 fold mean fold increase in mRNA abundance due to Ca^{2+} at 24 h (p=0.05), and PA0327 had a 4.1 fold increase due to Ca^{2+} (p= 0.05), as determined by a Mann-Whitney test. In the Δ*carR* mutant strain, PA0320 and PA0327 mRNA was slightly reduced by Ca^{2+}, confirming the role of *carR* in the Ca^{2+}-dependent transcription of PA0320 and PA0327.

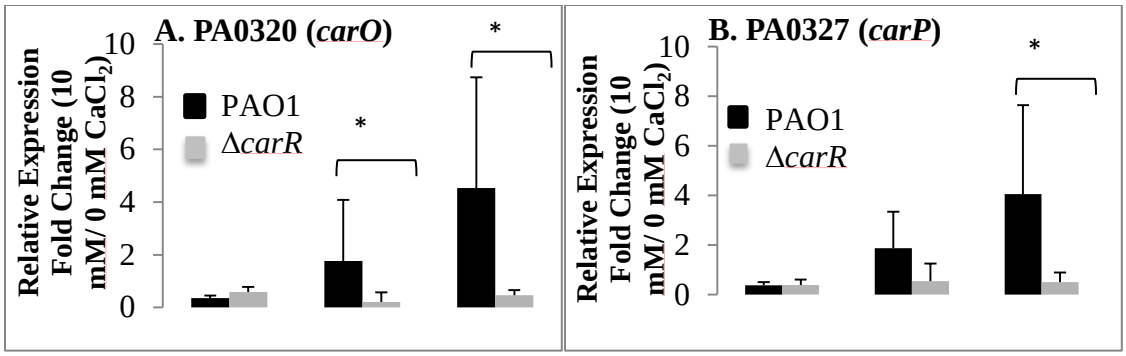

Figure 3.2. Reverse transcription quantitative polymerase chain reaction (RT-qPCR) analysis of PA0320 (*carO)* and PA0327 (*carP*) in *P. aeruginosa* PAO1 and in the *P. aeruginosa* Δ*carR*. (A) Relative expression of *carO* in BMM with 10 mM $CaCl_2$ compared to 0 mM $CaCl_2$ for *P. aeruginosa* PAO1 (black bars) and in *P. aeruginosa DcarR* (grey bars). (B) Relative expression of *carP* in BMM with 10 mM $CaCl_2$ compared to 0 mM $CaCl_2$ for *P. aeruginosa* PAO1 (black bars) and in *P. aeruginosa* Δ*carR* (grey bars). Data show the mean and standard deviation for three biological replicates (two technical replicates for each sample) at each time point. Statistical significance of the difference was calculated using student's T-test. *, $p<0.01$.

Predicted roles of PA0320 and PA0327 based on protein structural models. Structural modeling of PA0320 using HHpred and iTASSER indicates that this protein contains an OB-fold (oligonucleotide/oligosaccharide binding motif) with similarity to YgiW of *E. coli* (280), which is required for cell survival in hydrogen peroxide and cadmium (281). PA0320 is predicted to have a signal peptide for transport of the protein to the periplasm. The 3D structure of PA0327, predicted by HHPred and I-Tasser, forms a 5 bladed β-propeller (Fig. 3.S1). Structural homologs of PA0327, including YjiK, α-L-arabinofuranosidases, hemagglutinin-neuraminidase, and levansucrase, which both require Ca^{2+} for stability (reviewed in (282)). The predicted SdiA-regulated domain is commonly found in TolB proteins, which include Ca^{2+}-dependent phosphotriesterases. Sequence analysis predicts that the N-terminus of PA0327 has an uncleaved transmembrane domain, suggesting that PA0327 is anchored in the cytoplasmic membrane with the rest of the protein facing the periplasm. Overall, the predicted structure of PA0327 suggests that it binds Ca^{2+} in a central pocket, and that Ca^{2+} binding may be required for the protein stability. PAO1 possesses two paralogs of PA0327 (PA0319 and PA2017) with 38-47% amino acid sequence identity. However, expression of PA0319 and PA2017 is not affected by Ca^{2+}. Therefore, although PA0319 is adjacent to and in the same orientation as PA0320, these two genes have different regulatory mechanisms. From the structural predictions, we refer to PA0320 as CarO (calcium-regulated OB-fold protein) and PA0327 as CarP (calcium-regulated □-propeller protein).

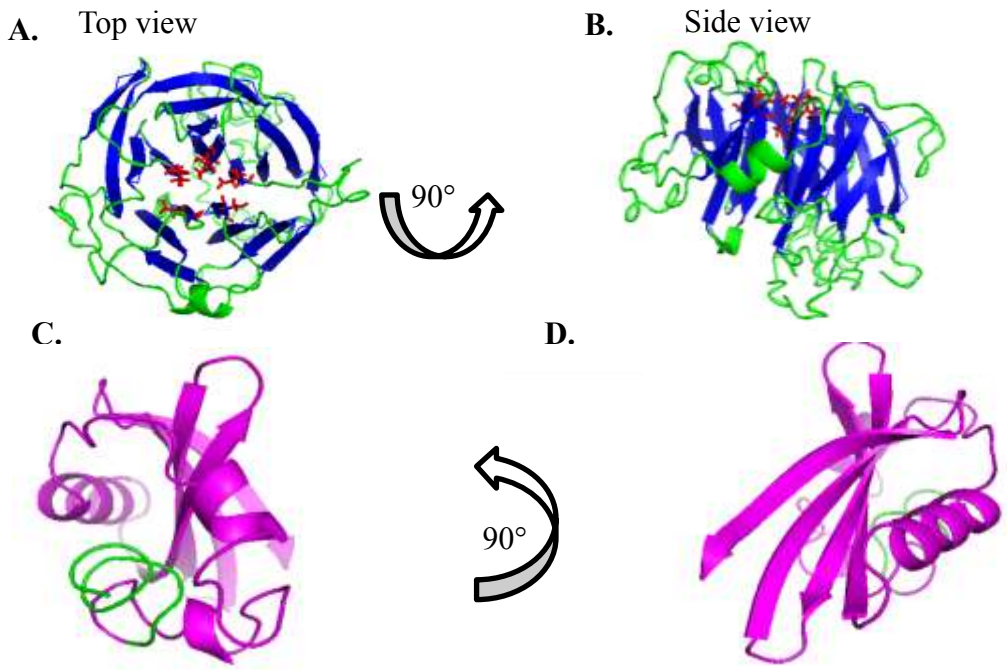

Figure 3.S1. Predicted structure of *P. aeruginosa* PA0327 (CarP) and PA0320 (CarO). Structural predictions were made by using i-TASSER (64) and HHpred (63), and visualized by using PyMOL (The PyMOL Molecular Graphics System, Version 1.7.6 Schrödinger, LLC). The structural predictions for CarP were based on threading onto the *E. coli* YjiK (PDB#3QQZ). CarP is predicted to form a β-propeller, with the β-sheets highlighted in blue. The amino acid residues predicted to bind Ca^{2+} are within the central pocket, and are highlighted in red. (A) Top view of the predicted structure. (B) 90^0 rotation around the x-axis showing the side view of the β-propeller structure. Rotating the structure reveals that the predicted Ca^{2+} binding residues are located at one entrance of the β-propeller tunnel. The structural predictions for CarO is based on threading onto putative lipoprotein of *Clostridium difficile* 630 (PDB#4EXR). Car O is predicted to form a OB fold domain as highlighted in magenta. (C) Predicted structure of CarP. (D) 90^0 rotation around the y-axis.

CarP is required for optimal growth of PAO1 in high [Ca^{2+}] medium. In order to characterize the functional roles of *carO* and *carP* in response to Ca^{2+}, we obtained transposon mutants of each gene from the University of Washington two-allele library (283). Each mutation was complemented by cloning the respective gene into the single-copy Tn7 expression vector, pTJ1 (260). To determine the effect of Ca^{2+} on growth, each mutant strain and its respective complemented counterpart was cultured in BMM with or without 10mM [Ca^{2+}]. The mutations in *carR* and *carO* did not affect growth at either Ca^{2+} level (Fig. 3.3). However, the *carP* mutation caused a defect in growth at high [Ca^{2+}]. The lag phase of *carP*::Tn5 increased by 4 h, and the strain had a twofold decrease in growth rate. The maximum growth yield of the *carP*::Tn5 mutant was also reduced in the presence of 10 mM $CaCl_2$. No effect on growth was observed for the *carP*::Tn5 mutant when no Ca^{2+} was added to the medium. Complementation of *carP* restored the wild-type growth characteristics (Fig. 3.3).

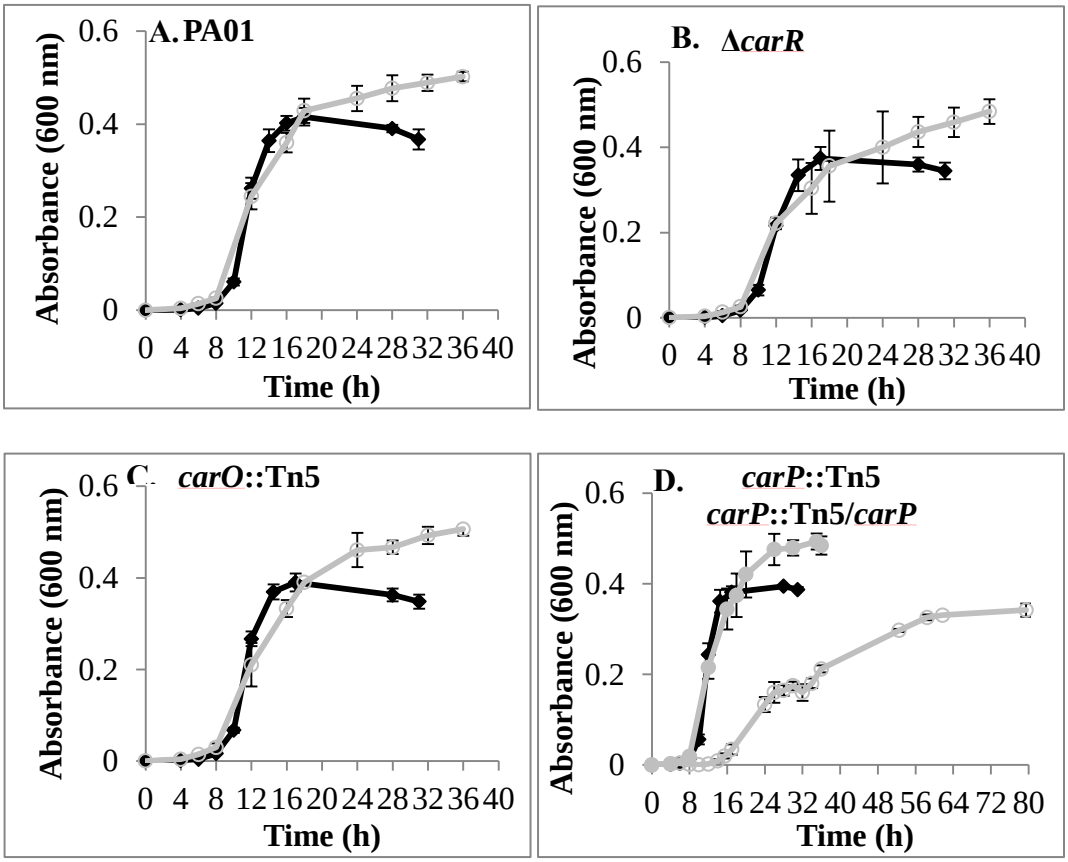

Figure 3.3. Growth of *P. aeruginosa* PAO1 and mutant strains in BMM containing 0 mM $CaCl_2$ (black diamonds) or 10 mM $CaCl_2$ (open gray circle). (A) Growth of *P. aeruginosa* PAO1 in BMM. (B) Growth of *P. aeruginosa* Δ*carR*. (C) Growth of *P. aeruginosa carO*::Tn5. (D) Growth of *P. aeruginosa carP*::Tn5. Filled grey circles show *P. aeruginosa carP*::Tn5, complemented with *carP*. Data show the mean and standard deviation for three biological replicates.

CarSR regulates Ca^{2+} homeostasis in PAO1 through the activities of CarO and CarP. To characterize further the functional roles of CarRS and its regulatory targets, *carO* and *carP*, we measured the intracellular concentration of Ca^{2+} ($[Ca^{2+}]_{in}$) and monitored its changes in response to a rapid increase in extracellular $CaCl_2$. For this, we expressed the recombinant Ca^{2+}-binding luminescence protein, aequorin, in PAO1 and in its corresponding mutant strains. We assayed each strain when first cultured without $CaCl_2$ or with 10 mM $CaCl_2$. In the former case, PAO1 maintained $[Ca^{2+}]_{in}$ at 0.14 ± 0.05 µM, which transiently increased in response to the addition of 1 mM $CaCl_2$ (Fig 3.4. ABC – black lines)(226). The mutations in *carR* or *carO* did not affect the basal level of $[Ca^{2+}]_{in}$. The immediate increase level of $[Ca^{2+}]_{in}$ following the addition of 1 mM $CaCl_2$ external Ca^{2+} was also unaffected by the mutations (Fig. 3.4. A, B – grey lines). However, the recovery of $[Ca^{2+}]_{in}$ was impaired following the addition of 1 mM $CaCl_2$. Recovery from the sudden increase in external Ca^{2+} was sixfold higher in Δ*carR* strain (Fig. 3.4.A) and twofold higher in *carO*:Tn5 (Fig. 3.4. B) than in the wild-type PAO1, suggesting that CarR and CarO play roles in maintaining $[Ca^{2+}]_{in}$ homeostasis. Unlike the Δ*carR* and *carO*::Tn5 mutants, the *carP*::Tn5 strain had a 2.5 fold higher basal level of $[Ca^{2+}]_{in}$ (0.34 ± 0.17 µM) than PAO1 (Fig. 3.4. C inset). Recovery of $[Ca^{2+}]_{in}$ from a sudden increase in external Ca^{2+} was impaired 2.5 fold, in the *carP*::Tn5 strain (Fig.3. 4. C – grey lines).

The intracellular calcium levels were also measured when the strains were first cultured with 10mM $CaCl_2$. For these experimnents, cells were first cultured in BMM with 10 mM $CaCl_2$, then washed to remove excess $CaCl_2$, and assayed for response to rapid addition of 1mM Ca^{2+}. Under these condition, the basal $[Ca^{2+}]_{in}$ for the wild-type strain was 0.35 ± 0.09 µM, or 2.5 fold higher than when cultured in BMM without Ca^{2+}

(Fig 3.4. DEF – black lines) Addition of 1 mM external Ca^{2+} resulted in increased basal $[Ca^{2+}]_{in}$ to 1.38 ± 0.03 µM and only partially recovery of $[Ca^{2+}]_{in}$ after 4 min, followed by a slow increase to 2.17 ± 0.48 µM after 20 min (Fig. 3.4. D – black line). Mutations in *carR* or *carO* did not significantly change the $[Ca^{2+}]_{in}$ profile compared to the wild-type strain, with both strains showing partial recovery at 4 min followed by a slow increase in $[Ca^{2+}]_{in}$ (Fig. 3.4. D,E – grey lines). However, the *carP*::Tn5 mutant strain had a very different response to externally added Ca^{2+} (Fig. 3.4F – grey lines). First, the basal level of $[Ca^{2+}]_{in}$ was threefold higher than in PAO1, at 0.98 ± 0.16 µM (Fig. 3.4. F inset). Second, recovery to basal level following the addition of 1 mM $CaCl_2$ was impaired compared to wild-type, and the $[Ca^{2+}]_{in}$ remained elevated. The results indicate that $[Ca^{2+}]_{in}$ homeostasis was impaired in all three mutant strains when grown at low $[Ca^{2+}]$, and impaired in the *carP*::Tn5 mutant strain when first cultured with high $[Ca^{2+}]$.

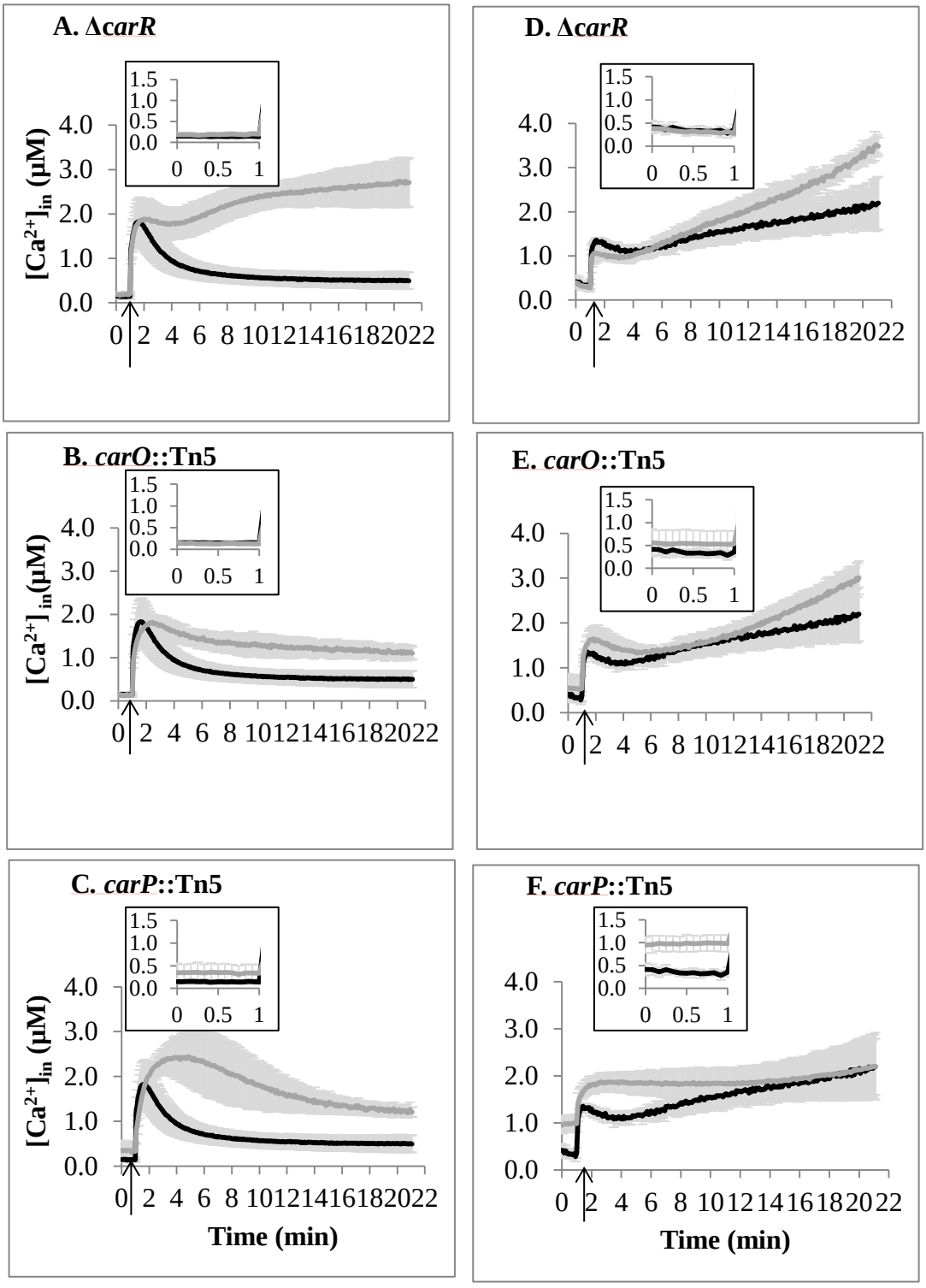
Cells grown at no added CaCl2
Cells grown at 10 mM CaCl2
A. ΔcarR
D. ΔcarR
B. carO::Tn5
E. carO::Tn5
C. carP::Tn5
F. carP::Tn5
[Ca2+]in (µM)
Time (min)

Figure 3.4. Free $[Ca^{2+}]_{in}$ profiles of *P. aeruginosa* wild type strain PAO1 (black line) and mutants (grey line): (A and D), Δ*carR;* (B and E), *carO*::Tn5; (C and F), *carP*::Tn5. Cells were grown in BMM media without added $CaCl_2$ (A, B, and C) or 10 mM $CaCl_2$ (D, E, and F). 1 mM $CaCl_2$ was added at the time indicated by the arrow. Changes in free $[Ca^{2+}]_{in}$ were calculated as described in the Methods section. Insets: Basal level of $[Ca^{2+}]_{in}$ monitored for 1 min before 1 mM Ca^{2+} was added. Data show the mean and standard deviation for three biological replicates.

CarP modulates Ca^{2+}-induced swarming motility and pyocyanin production. In previous work, we noted that Ca^{2+} addition results in phenotypic changes of *P. aeruginosa* (226). In particular, Ca^{2+} results in changes in swarming motility, pyocyanin production, and sensitivity to tobramycin in the wild-type strain. The transcriptome data presented here show that elevated Ca^{2+} also causes an increase in expression of genes for pyocyanin production (Table 3.1). Therefore, to determine if *carR*, *carO*, or *carP* play a role in either of these Ca^{2+}-dependent phenotypes, we assayed the mutant and complemented strains for swarming motility and pyocyanin production at low and high Ca^{2+}. As in the prior study (6), 10 mM Ca^{2+} caused an increase in PAO1 swarming by fivefold (Fig. 3.5 A, B). Mutations of *carR* or *carO* did not have a significant effect on swarming motility at any Ca^{2+} level (Fig. 3.5 C, D, E, F). In contrast, the mutation in *carP* significantly altered the morphology of swarming colonies at elevated [Ca^{2+}], showing multiple branches that extended from the swarming colonies (Fig. 3.5 G, H). Complementation of *carP* restored the wild-type swarming morphology (Fig. 3.5 I). While the Δ*carR* and *carO*::Tn5 mutants had similar pigment production as PAO1 at both low and high Ca^{2+} levels, the *carP*::Tn5 mutant appeared impaired for pigment production in swarming colonies. We extracted and quantified pyocyanin produced by the swarming colonies. Figure 3.6 shows that the Tn5 disruption of *carP* reduced the pyocyanin amount by 72%. The *carP* complemented strain had levels of pyocyanin production that were similar to wild-type.

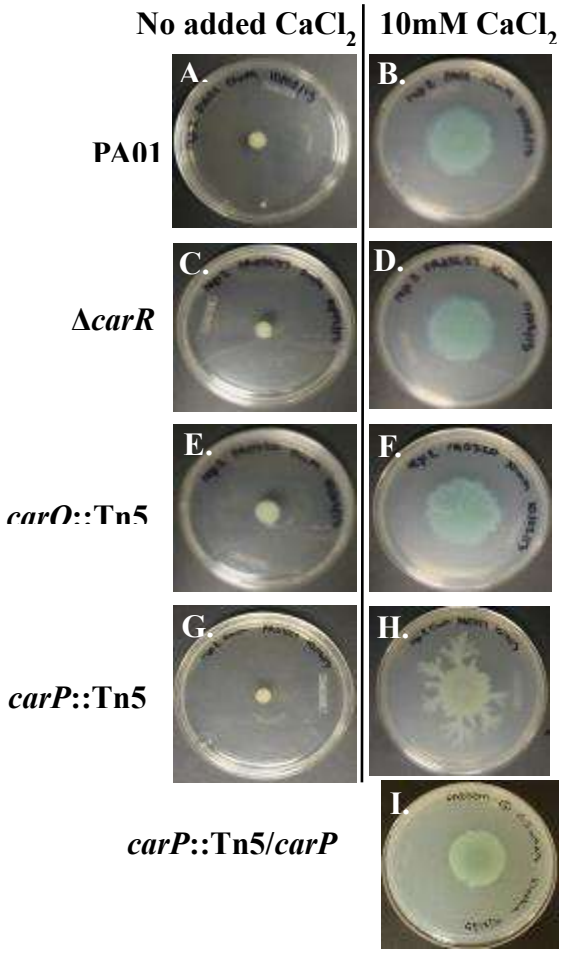

Figure 3.5. Swarming colonies of P. aeruginosa strains growing on BM2 agar containing 0mM (A, C, E, and G) or 10 mM $CaCl_2$ (B, D, F, H, and I). The following strains were tested: PAO1 (A, B), Δ*carR* (C, D), carO::Tn5 (E, F), *carP*::Tn5 (G, H), and *carP*::Tn5/*carP* (I). The latter was grown on BM2 swarm agar containing 10 mM $CaCl_2$ and 0.3 mM arabinose. Diameter and morphology of the colonies were reported after 24 h incubation. The pictures show representative replicates selected from three biological replicates.

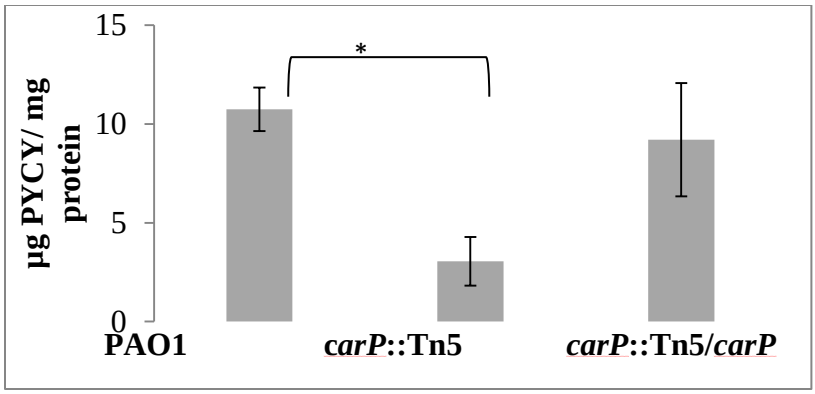

Figure 3.6. Pyocyanin production by P. aeruginosa PAO1, carP::Tn5, and *carP::*Tn5/*carP*. Pyocyanin was extracted from swarming colonies grown on BM2 plates in the presence of 10mM $CaCl_2$. The excised agar plugs containing the colonies were cut into halves. Pyocyanin amounts were quantified from one half of the agar plug, and then normalized to the total cellular protein extracted from the other half of the plug. The data represent the mean and standard deviations for at least three biological replicates in three independent experiments. Statistical significance of the difference was calculated using student's T-test. *, $p<0.01$.

***carO* and *carP* mutations cause increased sensitivity to tobramycin at high [Ca^{2+}].** Our earlier studies showed that growth at elevated Ca^{2+} increases the minimum inhibitory concentration (MIC) of PAO1 to tobramycin and polymyxin B (Khanam, *et.al*, unpublished data). To assess the potential role of *carR*, *carO*, and *carP* in Ca^{2+}-dependent resistance, we assayed each mutant and complemented strain for MIC using E-test strips (Fig. 3.7). In wild type cells, the MIC for tobramycin was eightfold greater than in cells cultured without adding Ca^{2+}. Both *carO*::Tn5 and *carP*::Tn5 strains had twofold reduction in tobramycin MIC when grown at elevated Ca^{2+}. The MIC for tobramycin was restored in these strains to the wild type levels when the mutant genes were complemented. No difference in tobramycin susceptibility was detected in the mutant cells cultured without adding Ca^{2+}. The *ΔcarR* mutation did not affect tobramycin resistance. The MIC of polymyxin B is 32 fold greater for the wild-type strain PAO1, when cells are cultured in the presence of 10 mM $CaCl_2$ than when no $CaCl_2$ is added to the medium. The mutations in *carR*, *carO*, or *carP* had no effect on polymyxin B resistance compared to wild-type at either $CaCl_2$ concentration.

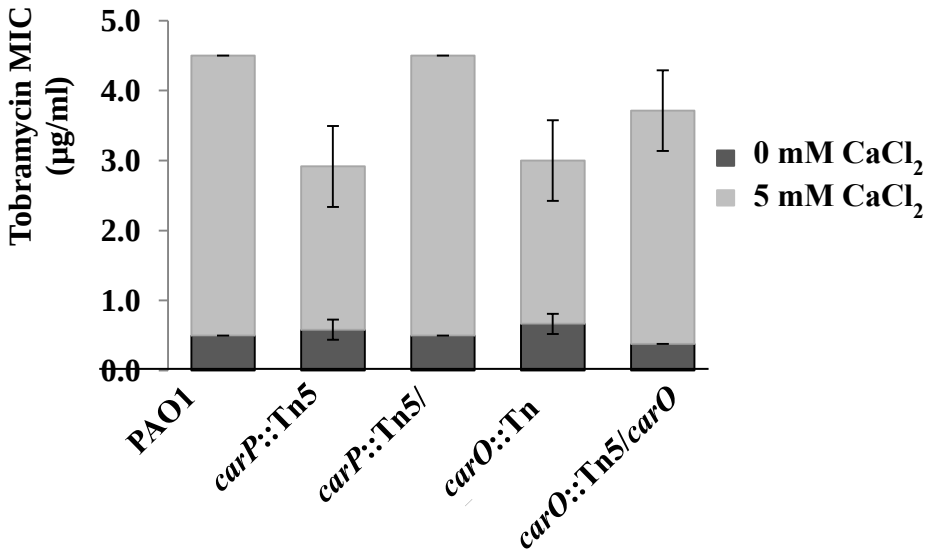

Figure 3.7. Minimum inhibitory concentrations (MICs) of tobramycin for *P. aeruginosa* PAO1, mutants *carO::*Tn5, and *carP::*Tn5, and their complemented counterparts *carO::*Tn5/*carO*, and *carP*::Tn5/*carP* grown on BMM with no added $CaCl_2$ (dark grey bars) or 10 mM $CaCl_2$ (light grey bars). Cells were grown in BMM at no added $CaCl_2$ till mid-log phase, their OD_{600} were normalized to 0.1, and the aliquots of 100 µL were plated onto BMM agar for MIC measurements. E-strips with tobramycin gradient were placed on the bacterial lawns, and the MICs were recorded after 24 h incubation. The data represent the mean and standard deviations of at least three biological replicates from two independent experiments. The coefficient of variation between biological replicates was less than 25%.

Discussion

Our earlier studies showed that Ca^{2+} regulates a number of physiological processes, including virulence, in the opportunistic pathogen *P. aeruginosa* (7, 156, 226, 238). However, the molecular mechanisms responsible for sensing extracellular Ca^{2+} and orchestrating the cellular responses are not known. Here, we applied a genome-wide transcriptome analysis of *P. aeruginosa* to identify genes whose transcription is differentially regulated by Ca^{2+}. Among the genes identified as induced by Ca^{2+} is an operon (PA2656-2659) containing the two-component regulatory system, *carSR*. The CarSR proteins are closely related to other *P. aeruginosa* TCSs, PhoPQ and PmrAB, which are involved in Mg^{2+} sensing (106). Other gram negative bacteria have been shown to recognize or respond to extracellular Ca^{2+} through TCSs. In *Salmonella typhimurium*, the PhoQ kinase of the PhoPQ system binds Ca^{2+}, Mg^{2+} and Mn^{2+} and regulates the transcription of genes, including virulence factors (reviewed in (284)). PhoQ has distinct Ca^{2+} and Mg^{2+} binding sites (285), suggesting an intricate nature of PhoPQ regulation by divalent cations. In *Vibrio cholera*, expression of the CarSR TCS negatively regulates polysaccharide production and biofilm formation in response to elevated Ca^{2+} (154). In *Escherichia coli*, AtoSC is induced by Ca^{2+} and regulates the biosynthesis and the intracellular distribution of cPHB (complexed poly-(R)-3-hydroxybutyrate), building the non-proteinaceous complexes that act as voltage-gated Ca^{2+} channels (286-288). Here, we demonstrate that expression of the *P. aeruginosa* TCS, CarSR, increases in response to high levels of external Ca^{2+}. CarSR in turn regulates transcription of *carO* and *carP* genes, that are involved in Ca^{2+}-dependent

responses. Based on these results, we propose that CarSR is a Ca^{2+}-regulated TCS in *P. aeruginosa* PAO1.

In addition to inducing the transcription of *carSR*, elevated Ca^{2+} represses the transcription of two closely related TCSs, *phoPQ* and *pmrAB*. McPhee et al. showed that *phoPQ* and *pmrAB* are also downregulated by elevated Mg^{2+} (106, 240). Changes in Mg^{2+} concentrations in the media did not affect the transcription of *carSR* (106). The transcriptional response of the TCSs due to Ca^{2+} addition is affected by the mode of growth. Expression of *carSR* is induced only in planktonic cultures, whereas expression of *pmrAB* and *phoPQ* is reduced in biofilms and in planktonic cultures. The results suggest an additional level of regulation coordinating responses to Ca^{2+} during a switch from planktonic to biofilm growth.

Comparison of the Ca^{2+}-induced regulon reported here and the Mg^{2+}-induced regulon reported in (106) revealed that 36 PAO1 genes are positively regulated by elevated Ca^{2+}, but not by elevated Mg^{2+}. These genes include PA0102-0104 encoding for carbonic anhydrase and permease, hypothetical proteins PAO320 (here named CarO) and PA0327 (here named *C*arP) that are regulated by *carSR*, and quorum sensing systems *las* and *rhl*, together with 14 genes regulated by these quorum sensing proteins (289-291). The latter include *rahU* involved in modulating biofilm formation and interaction with host innate immunity, *hcnA* involved in hydrogen cyanide production, *kynB* involved in the anthranilate pathway, *rhlB* essential for rhamnolipid biosynthesis, and *pvd* genes involved in pyoverdine biosynthesis. This comparison found no genes that were significantly induced by elevated levels of both Ca^{2+} and Mg^{2+}. However twenty genes were downregulated by both cations. Most of these downregulated genes belong to the

regulons of PhoPQ and PmrAB, including the *arn* operon (110, 240), which is involved in modification of LPS with arabinose groups. The *arn*-mediated LPS modifications were shown to increase *P. aeruginosa* resistance to polymyxin B (242). However, here we observed a decreased transcription of the *arn* operon, and an increase in resistance to polymyxin B in response to elevated Ca^{2+}. This result suggests that *P. aeruginosa* possesses an alternative mechanism for resistance to polymyxin B that is positively regulated by Ca^{2+}, and independent of Arn modification of LPS.

The Ca^{2+}-induced TCS, CarSR, regulates expression of *carO* and *carP* in a Ca^{2+}-dependent manner. CarSR, CarO, and CarP are all required for *P. aeruginosa* PAO1 response to elevated Ca^{2+} levels. In particular, CarSR, CarO, and CarP are all required to maintain intracellular [Ca^{2+}] at a low level when cells are grown at low [Ca^{2+}]. In addition, CarP is required for maintaining low cytosolic [Ca^{2+}] and for optimal growth when cells are exposed to high [Ca^{2+}]. CarP is also involved in other processes that are influenced by high [Ca^{2+}], including modulating the amount of pyocyanin production and affecting swarming motility. Both CarO and CarP also contribute to Ca^{2+}-induced resistance to tobramycin.

The molecular roles of CarO and CarP in Ca^{2+}-dependent processes are presently unknown. Since CarO and CarP are located primarily in the periplasm, they are likely not involved in the direct biosynthesis of pyocyanin, flagella, flagella motor or chemotaxis system. However, they may allow the cells to sense or modulate the periplasmic levels of Ca^{2+}, which itself plays a role in regulating production of these factors either directly or *via* reducing the intracellular concentration of Ca^{2+}. Intracellular [Ca^{2+}] may in turn affect expression of genes required for pyocynin production or

swarming motility. Whether their activities are direct or indirect, CarO and CarP are important for *P. aeruginosa* responses to high levels of Ca^{2+}, since the phenotypes observed for the *carO* and *carP* mutants occur primarily at high [Ca^{2+}].

The results presented here indicate that the two component system CarSR is responsible for *P. aeruginosa* sensing elevated levels of external Ca^{2+}, and is responding through induction of its regulatory targets, *carO* and *carP*. CarO and CarP affect intracellular Ca^{2+} homeostasis, surface-associated motility, resistance to tobramycin, and production of the virulence factor pyocyanin.

Acknowledgements

The authors thank Jessica Richards for her help with the bioinformatics analysis. We also thank Dr. Anthony Campbell from the School of Pharmacy and Pharmaceutical Sciences, Cardiff University in UK for sharing his expertise and the templates for calculating $[Ca^{2+}]_{in,}$ and Dr. Delfina Dominguez from The University of Texas at El Paso for sharing *E. coli* strain carrying pMMB66EH. This work was supported in part by NIH/NIAID award AI113330 (M.J.F.) and OCAST Award HR12-167 (M.A.P).

CHAPTER IV

A LINK BETWEEN QUORUM SENSING AND INTRACELLULAR CLACIUM SIGNALING IN *PSEUDOMONAS AERUGINOSA.*

M. Guragain, S. Khanam, A. E. Price, H. Wendelbo and M. A. Patrauchan

Abstract

Pseudomonas aeruginosa is a ubiquitous bacterium that is able to successfully inhabit diverse environments ranging from soil, to eukaryotic hosts. It possesses multiple signaling and regulatory systems to recognize and coordinate its responses to a multitude of different environmental stimuli. Elevated environmental calcium (Ca^{2+}) and quorum sensing (QS) signaling molecules regulate multiple physiological processes in *P. aeruginosa,* some of which overlap. This raises an intriguing question about possible relationship between the two signaling systems. Our earlier genome-wide proteomic and transcriptomic studies suggested that Ca^{2+} regulates the expression of QS genes. Here we applied promoter activity assay and confirmed that growth at elevated Ca^{2+} differentially regulates the transcription of QS regulators, *lasR, rhlR,* and *pqsR*. Rapid changes in external Ca^{2+} also cause intracellular Ca^{2+} transients. To test whether the latter are involved in mediating Ca^{2+} regulation, we identified a putative Ca^{2+} leak channel encoded by PA2604 that is responsible for generating the intracellular Ca^{2+} transients. Transposon disruption of PA2604 abolished QS- and Ca^{2+}-dependent pyocyanin production and impaired QS- and Ca^{2+}-regulated swarming motility. This provides the first experimental evidence of the regulatory role of the intracellular Ca^{2+} transients, and strongly supports the role of Ca^{2+} as a secondary messenger in *P. aeruginosa*. Since the addition of QS signaling molecules did not generate intracellular Ca^{2+} transients, we conclude that environmental Ca^{2+} regulates QS *via* transient changes of intracellular Ca^{2+} in *P. aeruginosa*.

Introduction

Bacterial survival in diverse habitats is a result of continuous adaptation to constantly changing environmental conditions, which requires a synchronized regulation of various cellular processes. Ubiquitous bacteria like *Pseudomonas aeruginosa* that successfully inhabit such diverse environments as soil, water, or eukaryotic host, have evolved intricately coordinated molecular mechanisms allowing them to recognize and respond to highly variable environmental stimuli. These mechanisms include sensors relaying the environmental signals to cognate regulators either directly or through intracellular (secondary) signaling systems, which collectively form complex regulatory networks. *P. aeruginosa* possess several secondary signaling systems including quorum sensing (QS), cyclic adenosine monophosphate (cAMP), cyclic-di-guanosine monophosphate (c-di-GMP), alarmones guanosine tetraphosphate (ppGpp), and guanosine pentaphosphate (pppGpp) (63).

QS, a well-studied signaling system in *P. aeruginosa,* regulates collective behavior of cell population by synchronizing gene expression in response to cell density (96). *P. aeruginosa* possesses three QS systems, Las, Rhl, and PQS that utilize 3-O-C12 homoserine lactone (3-O-C12 HSL), C4 homoserine lactone (C4 HSL), and pseudomonas quinolone signaling (PQS) as autoinducer molecules, respectively (99, 292, 293). More than 6% of *P. aeruginosa* PAO1 genome, including genes involved in production and secretion of toxins, extracellular proteases, pyocyanin, and rhamnolipids, are regulated by QS (100, 101). Overall, QS signaling coordinates the regulation of community behavior such as swarming motility and biofilm formation in *P. aeruginosa* (102). It also regulates the transition between avirulent environmental state and highly virulent pathogenic state of the organism, thus enabling successful physiological adaptation during host invasion.

The regulation of QSs was shown to be intricately interconnected with the global regulatory network of *P. aeruginosa* (294). A variety of environmental factors trigger changes in the expression of QS genes *via* so called global transcriptional regulators controlling the expression of multiple pathways. For example, nitrogen and iron starvation was shown to regulate QS signaling *via* transcriptional activation of alternative sigma factor RpoN (Las and Rhl) and small regulatory RNAs (srNA) PrrF (PQS), respectively. Limiting phosphate conditions are recognized by two component regulatory system PhoB/R, which in turn regulates Rhl and PQS response. Low magnesium induces the production of *lasI* and PQS biosynthetic genes. Low nutrient availability causes premature induction of Las and Rhl genes as a result of catabolite repression involving a cAMP receptor, NitVfr. QS systems are also regulated by several two-component regulatory systems (TCSs) and transcriptional regulators. A TCS GacA/S induces the expression of *lasI* and *rhlI via* sRNAs, RmsY and RmsZ, and transcriptional regulator *qscR*. Besides GacAS, two other sensor kinases LadS and GecS control Las and Rhl QS systems *via* sRNAs. Finally, the transcriptional regulators controlling expression of QS systems in *P. aeruginosa* include RsaL, QteE, QslA, MvaT, GibA, PmpR, AlgQ, AlgR, VqsM, PA1196, PpyR, PtxR, QscR, and VqsR that are also regulating diverse physiological processes including biosynthesis of alginate, pyocyanin, and rhamnolipid (reviewed in (63, 295)). This complex and interconnected regulation enables fine tuning of metabolism and behavior of *P. aeruginosa* allowing successful adaptation to environmental challenges. It also illustrates the responsiveness of QS-based regulation to environmental factors, which may include calcium.

Calcium ions (Ca^{2+}) represent one of the most essential secondary messenger in eukaryotes, which regulates many vital cellular processes including cell cycle, apoptosis, transport, motility, gene expression, and metabolism (reviewed in (296)). In prokaryotes,

however, the role of Ca^{2+} is not well characterized. It has been shown that growth at elevated Ca^{2+} regulates many physiological processes including spore formation, chemotaxis, heterocyst differentiation, transport, and virulence in several bacterial species (7, 142-144). Our earlier genome-wide microarrays and proteomic studies in *P. aeruginosa* showed that Ca^{2+} modulates the expression of a large number of genes including those responsible for iron acquisition, oxidative stress response, alginate and phenazine biosynthesis, production of extracellular proteases, nitrogen metabolism, antibiotic resistance, and quorum sensing signaling (156) (Guragain *et al.* submitted). We also determined that growth in high Ca^{2+} enhances biofilm formation (7), swarming motility (297), and plant infectivity of *P. aeruginosa* (188). However, the mechanisms of Ca^{2+} regulation remain elusive. To address this question, we identified Ca^{2+}-regulated two-component system CarSR regulating several putative Ca^{2+} -binding proteins in a Ca^{2+} -dependent manner. One of these proteins, CarP, is responsible for cell tolerance to high Ca^{2+} and Ca^{2+}-induced swarming and pyocyanin production (Guragain *et al*., submitted). The remaining question is whether Ca^{2+} plays role as a secondary messenger in prokaryotes. To address this, we established that *P. aeruginosa* maintains submicromolar level of intracellular Ca^{2+} ($[Ca^{2+}]_{in}$), which is transiently increased in response to elevated external Ca^{2+} and identified at least four putative Ca^{2+} transporters required for $[Ca^{2+}]_{in}$ homeostasis (297). Altogether these data suggest that Ca^{2+} serves as both primary (external) and secondary (intracellular) messenger in *P. aeruginosa*. The latter, however, requires experimental confirmation.

Our microarray and proteomic analyses suggested that growth at elevated external Ca^{2+} increased the expression of genes involved in QS in *P. aeruginosa* (7, 156, 188) (Guragain *et al*, submitted). Furthermore, comparison of the characterized Ca^{2+} regulon with the regulons of QS systems (100, 101, 298) revealed a number of physiological processes commonly regulated by

both Ca^{2+} and QS (Table 4.1). These observations suggest a possible interplay between Ca^{2+} and QS regulatory networks. We hypothesized that either externally elevated Ca^{2+} regulates the production of QS signaling molecules triggering a response, or sensing QS molecules generates intracellular Ca^{2+} transients regulating the downstream effects. In order to characterize a possible relationship between QS and Ca^{2+} signaling in *P. aeruginosa*, we applied transcriptional analysis and studied the effect of Ca^{2+} on the production of QS signal molecules. We also determined whether $[Ca^{2+}]_{in}$ is transiently changed in response to externally added QS molecules, and characterized the role of Ca^{2+} in regulating QS-dependent swarming motility in *P. aeruginosa*. This study demonstrates that Ca^{2+} regulates QS signaling in *P. aeruginosa*. We also identified a probable Ca^{2+} influx channel and characterized its role in $[Ca^{2+}]_{in}$ homeostasis and Ca^{2+}-dependent swarming and production of virulence factor, pyocyanin. Finally, we provide the first experimental evidence that transient changes in the intracellular $[Ca^{2+}]$ are required for regulating Ca^{2+}-dependent processes, such as biosynthesis of pyocyanin, and therefore support that intracellular Ca^{2+} plays a signaling role in *P. aeruginosa*.

Table 4.1. Genes/proteins regulated by elevated Ca^{2+} in *P. aeruginosa*

Gene/Protein Name, PAORF	QS system	Reference
RahU, PA0122	Las/Rhl	(100, 101)
Autoinducer synthesis protein (LasI), PA1432	Las/Rhl	(100, 101)
Kynurenine foramidase (KynB), PA2081	Las/Rhl	(100, 101)
Hydrogen cyanide synthase (HcnA), PA2193	Las/Rhl	(100, 101)
PvdL, PA2424	Las/Rhl	(101)
Hypothetical protein, PA3322	Las/Rhl	(100, 101)
RhlR, PA3477	Las/Rhl/PQS	(100, 101, 299)
RhlB, PA3478	Las/Rhl	(100, 101)
Hypothetical protein, PA4141	Las/Rhl/PQS	(100, 101, 291)
5-methyltetrahydropteroyltriglutamate-homocysteine S-methyltransferase (MetE), PA1927	Las/Rhl	(101)
Fur like, PA2384	PQS	(291)
L-ornithine N5-oxygenase (PvdA), PA2386	PQS	(291)
Hypothetical protein, PA2412	PQS	(291)
Hypothetical protein, PA2427	PQS	(291)
Hypothetical protein, PA4469	PQS	(291)
Hypothetical protein, PA4570	PQS	(291)

Materials and Methods

Bacterial strains, plasmids and media. Strains and plasmids used in this study are listed in Table 4.2. *P. aeruginosa* strain PAO1 used in this study is the non-mucoid strain with genome sequence available. Strain PA0214 (ΔlasI) was generously provided by Dr. Erika Lutter (Department of Microbiology and Molecular Genetics, Stillwater, OK). Transposon insertion mutants were obtained from the University of Washington Two - Allele library (300). The mutants contained ISphoA/hah or ISlacZ/hah insertions with tetracycline resistance cassette that disrupted the genes of interest. The mutations were confirmed by two-step PCR: first, transposon flanking primers were used to verify that the target gene is disrupted, and second, transposon-specific primers were used to confirm the transposon insertion. The primer sequence is available at www.gs.washington.edu. For convenience, the mutants were designated as PA::Tn5, where PA is the identifying number of the disrupted gene from *P. aeruginosa* PAO1 genome (www.pseudomonas.com).

Biofilm minimal media (BMM) (7) contained (per liter): 9.0 mM sodium glutamate, 50 mM glycerol, 0.02 mM $MgSO_4$, 0.15 mM NaH_2PO_4, 0.34 mM K_2HPO_4, and 145 mM NaCl, 20 µl trace metals, 1 ml vitamin solution. Trace metal solution (per liter of 0.83 M HCl): 5.0 g $CuSO_4.5H_2O$, 5.0 g $ZnSO_4.7H_2O$, 5.0 g $FeSO_4.7H_2O$, 2.0 g $MnCl_2.4H_2O$). Vitamins solution (per liter): 0.5 g thiamine, 1 mg biotin. The pH of the medium was adjusted to 7.0. Cells were first grown in 5 ml tubes for 16 h (mid-log) and then used to inoculate (0.1%) 100 ml fresh medium in 250 ml flasks. The cultures were grown to mid-log or stationary phase and harvested by centrifugation.

Table 4.2. Strains and plasmids used in this study

Strains/Plasmids	Description	Reference
Strains		
P. aeruginosa PAO1	Wild type sequenced strain	(10)
PAOJP2	*lasI-rhlI* double mutant of PAO1	(301)
PAO214	*lasI* knockout mutant of PAO1	(301)
PA1430::Tn5	*lasR* transposon mutant of PAO1	(300)
	PW 3597	
	PA1430-B10::ISlacZ/hah	
PA3476::Tn5	*rhlI* transposon mutant of PAO1	(300)
	PW6880	
	PA3476::ISPhoA/hah	
PA3477::Tn5	*rhlR* transposon mutant of PAO1	(300)
	PW 6882	
	PA3477-B10::ISlacZ/hah	
PA0996::Tn5	*pqsA* transposon mutant of PAO1	(300)
	PW 2798	
	PA0996-H05::ISlacZ/hah	
PA1003::Tn5	*pqsR* transposon mutant of PAO1	(300)
	PW2812	
	PA1003-G11::ISlacZ/hah	
PA2604::Tn5	PW5376	(300)
	PA2604-G04::ISPhoA/hah	
Plasmids		
pMS402	Expression reporter plasmid carrying the promoterless *luxCDABE* gene, *ori* of pRO1615 (302)	(303)
pKD204	pMS402 containing *lasR* promoter cloned upstream of promoterless *luxCDABE* gene in pMS402	(304)

pKD205	pMS402 containing *rhlR* promoter cloned upstream of promoterless *luxCDABE* gene in pMS402	(304)
pKD-*pqsR*	pMS402 containing *pqsR* promoter cloned upstream of promoterless *luxCDABE* gene in pMS402	(305)
pMMB66EH-AEQ	pMMB66EH plasmid containing aequorin gene from *Aequorea victoria*	(306)

Assessment of gene transcription. A *lux*-based reporter system was used for monitoring the promoter activities of QS regulator and synthase encoding genes. For this, the 282-940 bp regions upstream of *lasR, rhlR, pqsR, lasI, rhlI, and pqsA* genes were cloned upstream of a promoterless *luxCDABE* operon in the pMS402 plasmid as described in (303). The reporter plasmids were kindly provided by Dr. Kangmin Duan (Department of Microbiology and Infectious diseases, University of Calgary, Calgary, Alberta, Canada) and Dr. Lin Chen (The College of Life Sciences, Northwestern University, Xi'an, China) and transformed into PAO1 cells using a electroporation approach (307). Promoter activity assays were carried out in 96-well white luminescent plates with clear bottom (Greinerbio). For this, mid-log cultures of the reporter strains were normalized to OD600 of 0.3 amd inoculated (1%) into 200 µl BMM containing no added or 5 mM Ca^{2+}. Lids were treated with 0.04 % triton solution to avoid condensation. The plates were incubated in a Synergy Mx Multi-Mode Microplate Reader (Biotek) at 37°C with shaking set at "fast". Luminescence and cell density at OD600 was measured for 14 h every 2 h. Promoter activity was measured as a relative light intensity (RLUs) and normalized by the respective values of OD600 nm and the luminescence produced by empty vector controls. The effect of Ca^{2+} was obtained by calculating fold difference between the data collected at 5 mM *vs* no added Ca^{2+}. Every experiment was done with at least three biological replicates, and was repeated at least twice.

Estimation of Free Intracellular Calcium ($[Ca^{2+}]_{in}$). PAO1 and mutants were transformed with pMMB66EH (courtesy of Dr. Delfina Dominguez and Dr. Anthony Campbell), carrying aequorin (308) and carbenicillin resistance genes, using a heat shock method described in (202). The transformants were selected on Luria bertani (LB) agar containing carbenicillin (300 µg/ml) and verified by PCR using aequorin specific primers (For:

5′CTTACATCAGACTTCGACAACCCAAG, Rev: 5′CGTAGAGCTTCTTAGGGCACAG). Aequorin was expressed and reconstituted as described in (297). Briefly, mid-log phase cells were induced with IPTG (1 mM) for 2 h for apoaequorin production, and then harvested by centrifugation at 5,232 g for 5 min at 4°C. Aequorin was reconstituted by incubating the cells in the presence of 2.5 µM coelenterazine for 30 min.

Luminescence measurements and estimation of free $[Ca^{2+}]_{in}$ were performed as described in (297) with slight modifications. Briefly, 100 µl of cells with reconstituted aequorin were equilibrated for 10 min in the dark at room temperature. Luminescence was measured using Synergy Mx Multi-Mode Microplate Reader (Biotek) at the interval of 5 min. For basal level of $[Ca^{2+}]_{in}$, the measurements were recorded for 1 min, then the cells were challenged with 1 mM Ca^{2+} and monitored for another 6 min followed by challenge with QS signal molecules at appropriate concentrations, mixed for 1 sec, and the luminescence was recorded for next 20 min. Injection of buffer alone with respective solvent concentration was used as a negative control. $[Ca^{2+}]_{in}$ was calculated by using the formula $pCa = 0.612(-\log_{10}k)+3.745$, where k is a rate constant for luminescence decay (s^{-1}) (147). The aequorin standard curve was shared by Dr. Anthony Campbell. The results were normalized against the total amount of available aequorin as described in (297). The discharge was performed by permeabilizing cells with 2% Nonidet 40 (NP40) in the presence of 12.5 mM $CaCl_2$. The luminescence released during the discharge was monitored for 10 min at 5 sec interval. Injection of buffer alone was used as a negative control, and did not cause any significant fluctuations in $[Ca^{2+}]_{in.}$ The estimated remaining available aequorin was at least 10% of the total aequorin. The experimental conditions reported here were optimized to prevent any significant cell lysis.

Swarming motility assay. Swarming motility was assayed as described in (297). PAO1 and mutants were grown in BM2 swarm agar at no added or 5 mM Ca^{2+}. 2 µl of the mid-log cultures normalized to the OD600 of 0.3 were spot inoculated onto the surface of BM2 swarm agar (248). After inoculation, the plates were incubated for 15 h and the colony diameters were measured. The effect of Ca^{2+} was calculated as a fold difference (ratio) between the diameters of the colonies grown at 5 mM and no added Ca^{2+}.

Antibiotic sensitivity assay. *P. aeruginosa* resistance to tobramycin and polymyxin B was assayed as described in (Khanam *et. al*., in preparation). PAO1 and PA2604::Tn5 were grown in BMM at no added or 5 mM Ca^{2+}. 100 µl of the mid-log cultures normalized to the OD600 of 0.1 were spread inoculated onto the surface of BMM agar containing no added or 5 mM Ca^{2+}. E-test strips for tobramycin or Polymyxin B (Biomeurix) were placed on the surface of the inoculated plates and incubated for 24 h. The minimum inhibitory concentration (MIC) was measured as a point at which the edge of the zone of inhibition crosses the e-test strip. The effect of Ca^{2+} was calculated as a fold difference (ratio) between the MIC at 5mM *vs*. no added Ca^{2+}.

Results

Bioinformatic search for proteins required for Ca^{2+} uptake in *P. aeruginosa* PAO1. Previous studies identified two types of Ca^{2+} influx channels in bacteria: Polyhydroxybutyrate polyphosphate (PHB-PP), a non-proteinaceous Ca^{2+} influx channel in *E. coli* (147) and YetJ, a pH sensitive Ca^{2+} leak channel in *B. subtilis* (167, 309). Sequence analysis of PAO1 genome revealed no closely clustered homologs of PHB synthesis genes characterized in *E. coli*. However, it was shown that *P. aeruginosa* PAO1 produces medium chain length polyhydroxy alkanoate (PHA) (310). Biosynthesis of PHA requires two PHA synthases: PA5056 and PA5058

(310). Further, it was shown that *P. aeruginosa* is able to synthesize and accumulate polyphosphates (PP), and the level of cellular PP is regulated by exopolyphosphatase PA5241 and polyphosphate kinase PA5242 (311, 312). Based on the above, we hypothesized that PAO1 produces PHA-PP channel that may serve to uptake Ca^{2+}.

Search for homologs of YetJ identified one homolog PA2604 that shares 23% amino acid sequence identity with YetJ in *B. subtilis* and contain the functional domain transmembrane Bax inhibitor motif. We hypothesized that similarly to *B. subtilis*, PA2604 encodes a putative Ca^{2+} leak channel, which is also involved in Ca^{2+} uptake in *P. aeruginosa*.

PA2604 is required for generating transient increase in $[Ca^{2+}]_{in}$. Earlier we showed that *P. aeruginosa* generates transient changes in $[Ca^{2+}]_{in}$ in response to elevated external Ca^{2+}. We assumed that if a protein is responsible for Ca^{2+} uptake, it would also be responsible for the transient increase in $[Ca^{2+}]_{in}$ in response to externally added Ca^{2+}. Therefore, the four candidates predicted to uptake Ca^{2+}, PA5056, PA5058, PA5241, and PA2604 were tested for their role in increasing the $[Ca^{2+}]_{in}$. For this, transposon mutants with the corresponding genes disrupted with either ISphoA/hah or ISlacZ/pho were obtained, confirmed, and subjected to the measurements of $[Ca^{2+}]_{in}$ in response to the addition of 1 mM Ca^{2+}, and compared to the wild type PAO1 cells (Fig 3.4.1, A,B,C,D).

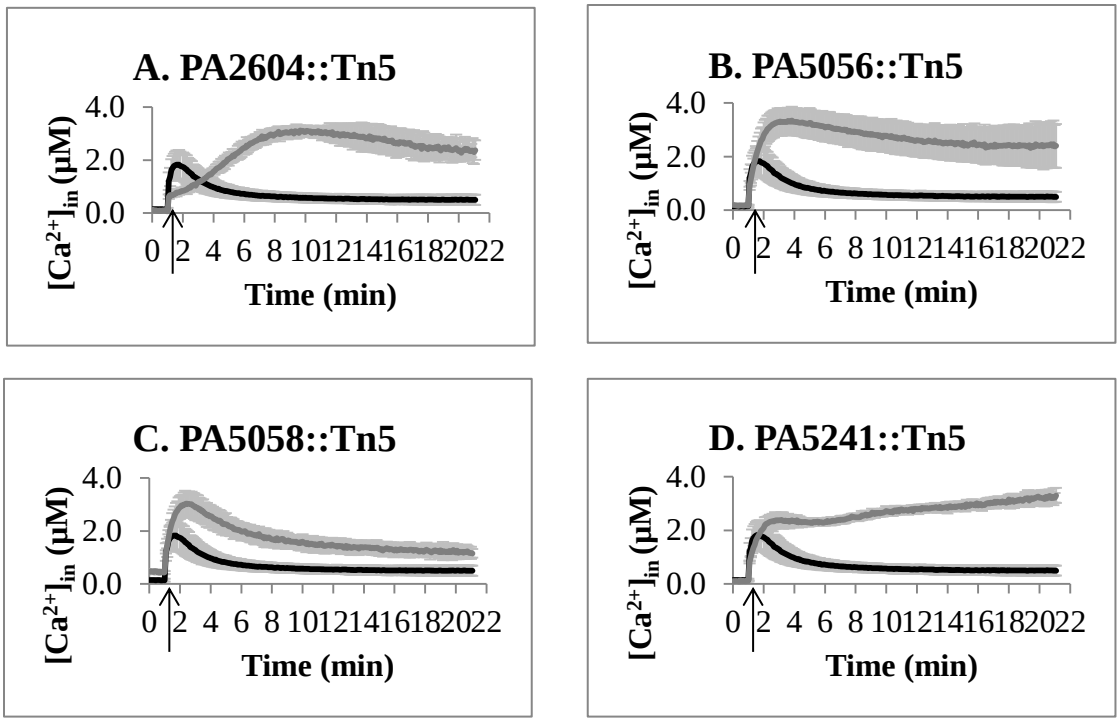

Figure 4.1. Free $[Ca^{2+}]_{in}$ profiles of transposon mutant with disrupted putative Ca^{2+} channels. The mutants were obtained from the University of Washington Two - Allele library. Cells were grown in BMM media with no added Ca^{2+}. The basal level of luminescence was monitored for 1 min. 1 mM $CaCl_2$ was added at the time indicated by the arrow, followed by luminescence measurements for 20 min. Changes in free $[Ca^{2+}]_{in}$ were calculated as described in the Methods section. PA numbers represent the open reading frames in PAO1 genome. (A) PA2604::Tn5. (B) PA5056::Tn5. (C) PA5058::Tn5. (D) PA5241::Tn5. Black, PAO1 wild type; grey, transposon mutant. The data is an average of at least three independent experiments.

Earlier we showed that PAO1 maintains $[Ca^{2+}]_{in}$ at the level of 0.14 ± 0.05 μM which transiently increases to 1.86 ± 0.53 μM over the period of 0.6 min in response to 1 mM external Ca^{2+} (297). The mutants with disrupted PHA synthases, PA5056 and PA5058, or exopolyphosphatase, PA5241 did not exhibit any reduction in the initial increase of $[Ca^{2+}]_{in}$ in response to rapid Ca^{2+} addition **(**Fig. 4.1 B,C,D). On contrary, all three of them showed a greater $[Ca^{2+}]_{in}$ increase and a significantly reduced (PA5058::Tn5) or abolished (PA5056::Tn5, PA5241::Tn5) recovery to the $[Ca^{2+}]_{in}$ basal level. Thus, while the WT cells recovered their $[Ca^{2+}]_{in}$ to 0.05 ± 0.19, PA5058::Tn5 - only to 1.18±0.2 μM, PA5056::Tn5 – showed no recovery, and PA5241::Tn5 – further increased the $[Ca^{2+}]_{in}$ to 3.24 ± 0.23 μM. The disruption of PA2604 reduced the increase of $[Ca^{2+}]_{in}$ three fold. This short increase to only 0.62±0.09 μM in 0.08 min **(**Fig. 4.1 A**)**. was not followed by a recovery to the basal level, but instead was followed by a second wave of $[Ca^{2+}]_{in}$ increase reaching 3.26 ± 0.27 μM over 9.66 min, and then a slow decline to 2.34±0.37μM, which is fivefold above the recovery level in WT cells. Thus, the PA2604::IS does not develop a transient increase of $[Ca^{2+}]_{in}$ in response to rapid addition of external Ca^{2+}; instead, the level of $Ca^{2+}{}_{in}$ in the mutant undergoes a two-phase increase.

PA2604 regulates Ca^{2+} induced swarming motility and pyocyanin production. Our previous study showed that swarming motility and production of pyocyanin in *P. aeruginosa* was induced in the presence of elevated Ca^{2+} (7, 297). To test whether the transient increase of $[Ca^{2+}]_{in}$ is involved is regulating this cellular response to Ca^{2+}, swarming motility and pyocyanin production in PAO1 and PA2604::Tn5 were tested in the presence of 5 mM or at no added $CaCl_2$. Confirming our previous observations, 5 mM Ca^{2+} induced swarming motility in the wild type PAO1. However, mutation in PA2604, although did not affect swarming motility at no

added Ca^{2+}, reduced the diameter of the swarming colony by about 50 % and caused the formation of branches at elevated Ca^{2+} (Fig. 4.2 A, B).

We also confirmed that the addition of Ca^{2+} enhances the production of pyocyanin in the wild type PAO1. Disruption of PA2604 abolished Ca^{2+} induction of pyocyanin production in liquid cultures (Fig. 4.3). Interestingly, this difference was not observed in cultures grown on the surface of agar media.

PA2604 doesn't regulate Ca^{2+} induced antibiotic resistance. Earlier we showed that growth at elevated Ca^{2+} enhances PAO1 resistance to tobramycin and polymyxin B (Khanam *et.al*, in preparation). To test whether the development of $[Ca^{2+}]_{in}$ transient increase is involved in regulating Ca^{2+} induced antibiotic resistance, the MICs of the two antibiotics for PA2604::IS mutant were determined by using E-test strips. However, no changes in Ca^{2+} induced tobramycin or polymyxin B resistance were observed in the mutant (Fig 4. S1).

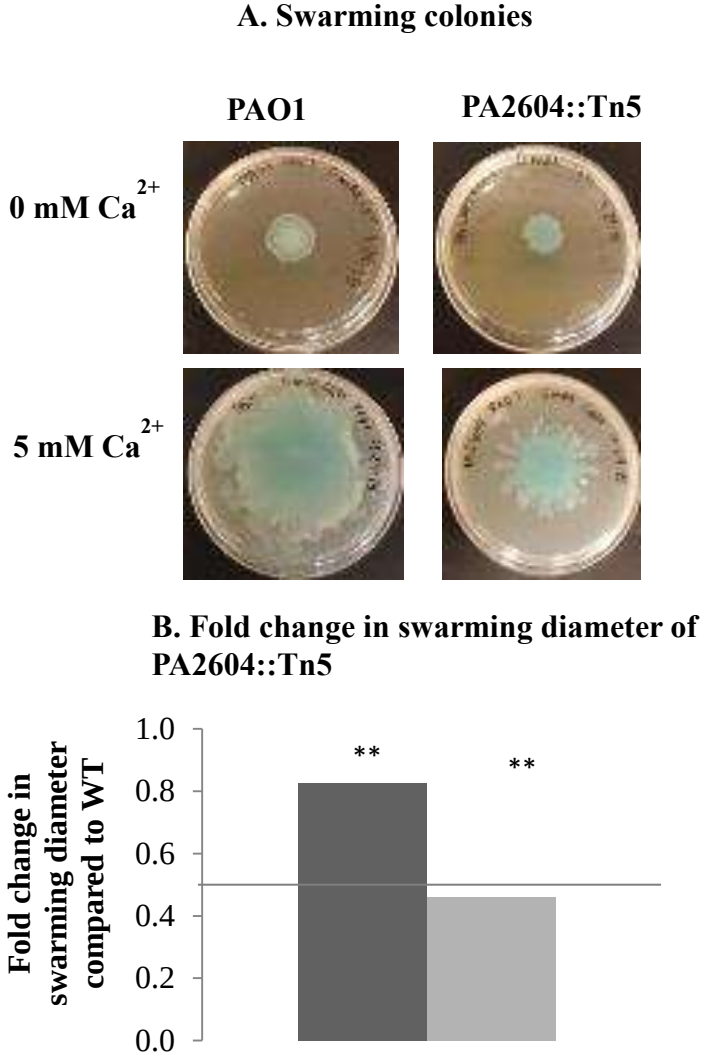

Figure 4.2. Swarming motility. PAO1 and PA2604::IS cells were grown on BM2 swarm agar with no added or 5 mM $CaCl_2$.(A) Representative photographs of swarming colonies. Colony diameters were measured, and fold differences (5 mM *vs*. 0 mM) were calculated. (B) Fold change in diameters of the swarming colonies grown at 5 mM $CaCl_2$ *vs* no added $CaCl_2$. The averages of at least three biological replicates were used to calculate the fold changes. Statistical significance of the difference was calculated using student's T-test. **$p \leq 0.01$.

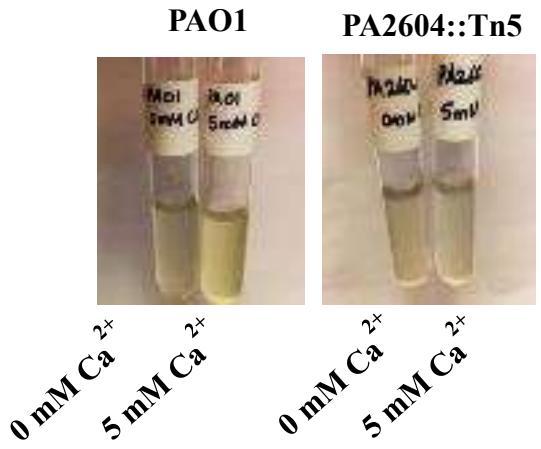

Figure 4.3. Pycoycanin production. PAO1 and PA2604::IS cells were grown on BMM with no added or 5 mM $CaCl_2$. Representative photographs of bacterial growth.

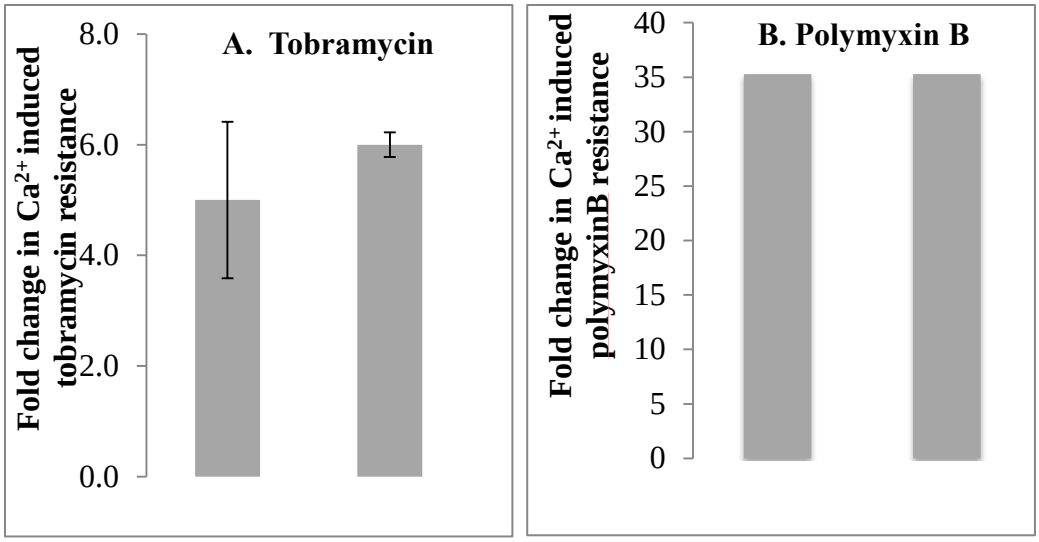

Figure 4.S1. Antibiotic resistance. Cells were grown on BMM agar plates containing no added or 5 mM $CaCl_2$. MIC was measured using E-test strips for (A) tobramycin or (B) polymyxinB (Biomeurix) as the concentration, at which the zone of growth inhibition crosses the e-test strip. The effect of Ca^{2+} was calculated as a fold difference (ratio) between the MIC determined at 5mM $CaCl_2$ and no added $CaCl_2$. The presented data represent the averages of at least two biological replicates.

Ca^{2+} regulates promoter activity of QS genes. Genome-wide microarray analysis determined that 10 mM Ca^{2+} upregulates the transcription of genes encoding *rhl* and *las* systems of QS at least twofold, whereas *pqsA* was slightly downregulated (Table 4.3). In order to confirm the regulatory role of Ca^{2+} in QS gene expression, the activity of promoters of QS regulatory and synthase genes was measured in cells growing at 5 mM $CaCl_2$ or no added $CaCl_2$ by using *lux*-based reporter constructs (Fig. 4.4). The activity of *lasR* promoter was increased during early phases of growth with the maximum activity reached during middle exponential phase, whereas the activities of *rhlR* and *pqsR* promoters were elevated during the transition from the exponential to stationary phase, which the maximum activity observed during early stationary phase of growth (Fig 4.4 B, 4.4 C**)**. The presence of 5 mM Ca^{2+} increased the activity of *lasR* promoter by at least two fold during the exponential growth (Fig. 4.4 A), whereas *rhlR* and *pqsR* promoter activities were downregulated by Ca^{2+} (Fig. 4.4 B, 4.4 C).

Externally added QS molecules do not affect $[Ca^{2+}]_{in}$. To determine if externally added QS signal molecules trigger changes in $[Ca^{2+}]_{in}$ in PAO1, we expressed the recombinant Ca^{2+}-binding luminescence protein aequorin in the wild-type PAO1 strain, and exposed these cells to 10, 25, and 50 µM C4 HSL or 3-O-C12 HSL, and 10, and 20 µM PQS. In order to provide a source of cellular Ca^{2+}, we used two approaches. In the first approach, Ca^{2+} was provided during growth by addition of 1 mM $CaCl_2$ in the growth medium. In the second, Ca^{2+} was not provided during growth, but1 mM $CaCl_2$ was added to the cells 6 min prior to the addition of QS molecules. No effect of QS molecules on the $[Ca^{2+}]_{in}$ was detected in either case (Figure 4.S2).

Table 4.3. Calcium regulation of QS genes in PAO1 during planktonic growth.

QS system/Gene name, PAORF	Protein Name	Fold change in expression by Ca^{2+}		Reference
		Gene	Protein	
Las				
lasI, PA1432	LasI, autoinducer synthesis protein	3	2	(156, 313)
lasR, PA1430	LasR, Transcriptional regulator	2.4	N/A	(313)
Rhl				
rhlI, PA3476	RhlI, Autoinducer synthasis protein	3.5	N/A	(313)
rhlR, PA3477	RhlR, Transcriptional regulator	4	3	(156, 313)
Pqs				
pqsA PA0996	PqsA, Probable coenzyme A ligase,	0.8	N/A	(313)
mvfR PA1003	MvfR, Transcripional regulator,	2	N/A	(313)

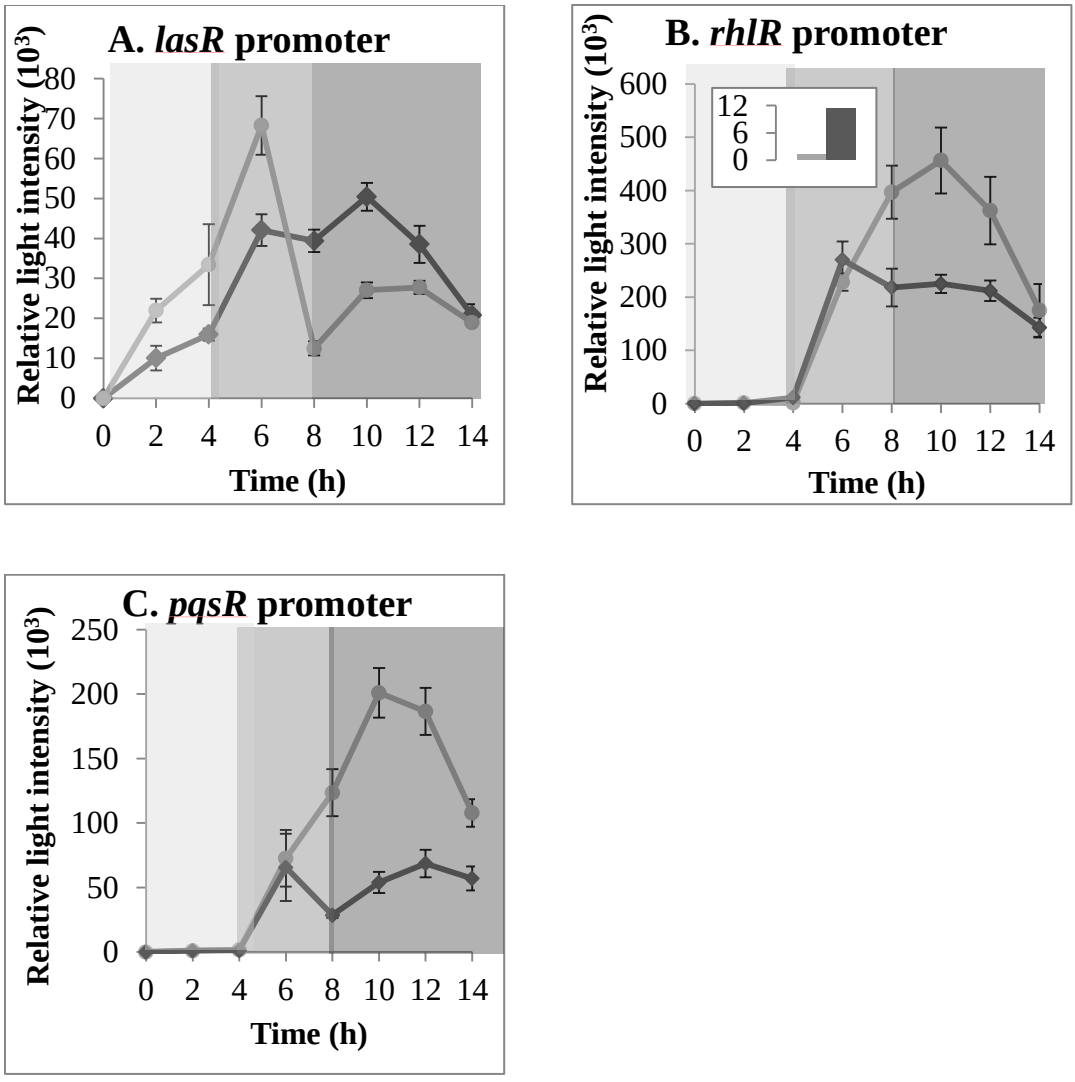

Figure 4.4. Promoter activity of QS genes. Cells were grown in BMM media containing no added or 5 mM $CaCl_2$. Promoter activity was measured as relative intensity of luminescence (RLUs). (A) *lasR* promoter activity. (B) *rhlR* promoter activity. (C) *pqsA* promoter activity. Gray line, no added Ca^{2+}; black line, 5 mM Ca^{2+}. The data is an average of at least four biological replicates. Shaded area, growth phases;light gray, lag; medium gray, log, dark gray, stationary.

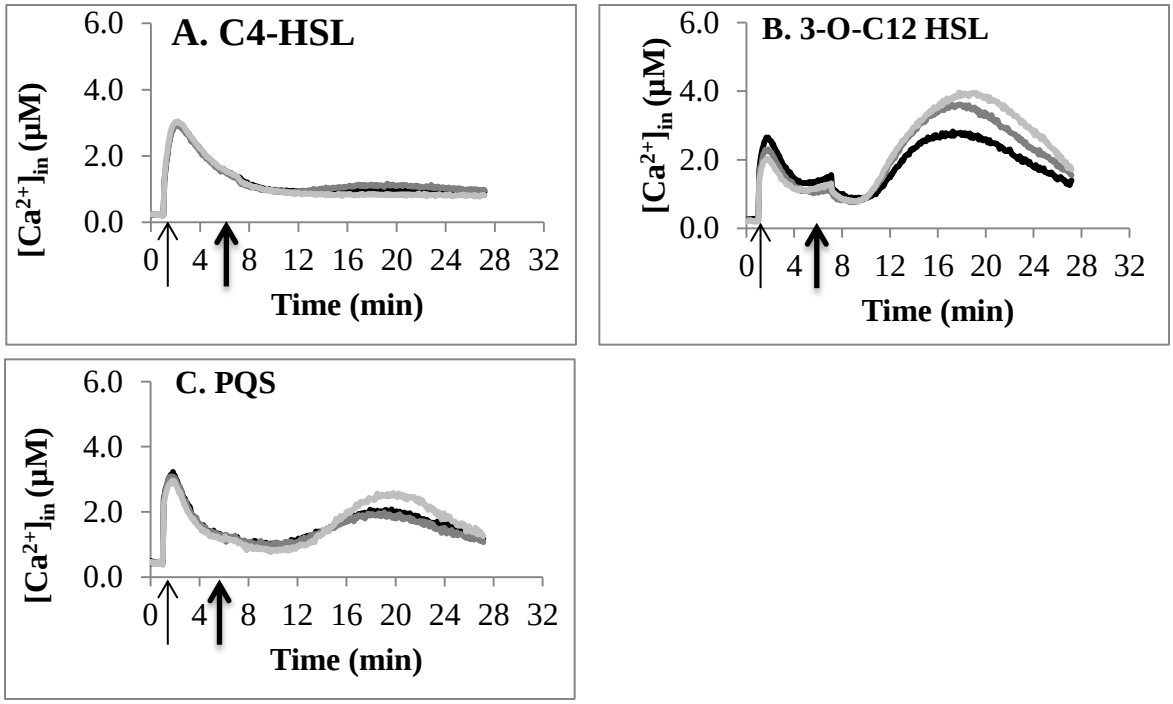

Figure 4. S2. Free $[Ca^{2+}]_{in}$ profiles of PAO1in response to QS signal molecules. Cells were grown in BMM media with no added Ca^{2+}. The basal level of luminescence was monitored for 1 min. 1 mM $CaCl_2$ was added at the time indicated by black arrow, followed by luminescence measurements for 6 min. QS molecules were added at the time indicated by bold black arrow. Changes in free $[Ca^{2+}]_{in}$ were calculated as described in the Methods section. (A) C4 HSL. Black, HEPES buffer; grey, 50 µM; light gray, 100 µM. (B) 3-O-C12 HSL. Black, 0.5% methanol in HEPES buffer; grey, 50 µM; light gray, 100 µM. (C) PQS. Black, HEPES buffer with 0.2% methanol; grey, 10 µM; light gray, 20 µM. Data presented is a representative of at least two biological replicates.

Ca^{2+} regulates QS-controlled swarming motility in PAO1. It was shown that swarming motility in *P. aeruginosa* is controlled by QS signaling. Thus, mutations in *lasI* or *lasR* reduce swarming motility in *P.* aeruginosa, mutations in *rhlI* or *rhlR* completely abolish swarming (314), whereas mutations in *pqsA* enhance it (315). To test whether elevated external Ca^{2+} affects the QS-mediated swarming in PAO1, we tested the abilities of PAO1 and the QS mutants to swarm in the presence of 5 mM $CaCl_2$ or at no added $CaCl_2$ (Fig. 4.5). As shown before (297), 5 mM Ca^{2+} induced swarming motility and the formation of multiple branches in PAO1. At no added $CaCl_2$, deletion of *lasI* caused 74% reduction in PAO1 swarming, which was restored to the WT level by the addition of 5 mM Ca^{2+}. Supporting previous observations (315), disruption of *pqsA* increased swarming motility by 43% in WT growing at no Ca^{2+}, whereas addition of Ca^{2+} increased the swarming diameter of *pqsA* mutant only by 23%. Interestingly, elevated Ca^{2+} did not restore the WT branching morphology in both *lasI* and *pqsA* mutants. As anticipated, disruption of *rhlI* completely abolished the swarming motility, and elevating Ca^{2+} levels did not restore this loss of motility.

A.

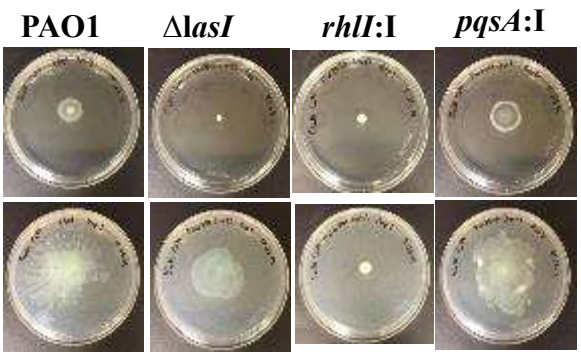

B.

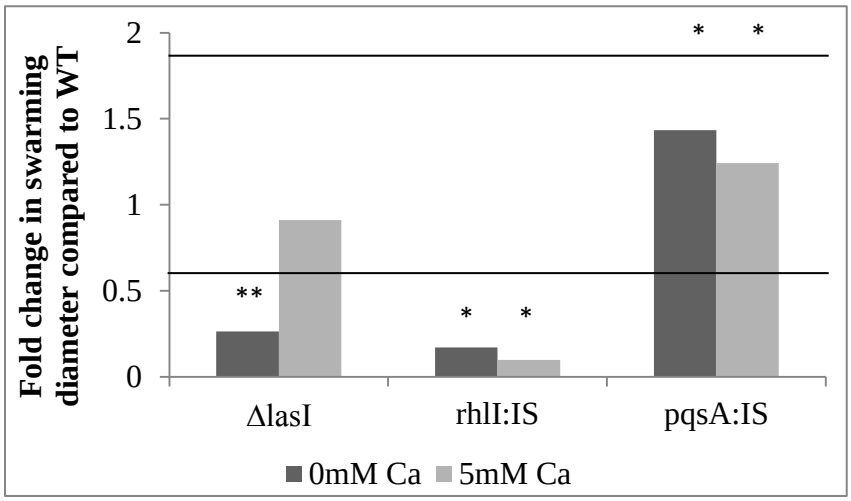

Figure 4.5. Swarming motility. Cells were grown on BM2 swarm agar containing 5 mM or no added $CaCl_2$. A. Representative photos of swarming colonies. B. Fold difference in swarming diameter in mutants *vs* PAO1 at 5 mM or no added $CaCl_2$. The averages of at least three biological replicates were used to calculate the fold changes. Statistical significance was calculated using student T-test. * $p<0.05$; ** $p\leq0.01$.

Discussion

Both Ca^{2+} and QS regulate physiology and virulence of *P. aeruginosa*. However, the interrelationship between the two signaling systems has not been characterized. Earlier, we observed that Ca^{2+} regulates the expression of QS genes (313), suggesting possible regulatory link. This study investigates the mechanism of Ca^{2+} regulation of QS signaling and explores a possibility of QS signals to be recognized by Ca^{2+} signaling *via* changing the $[Ca^{2+}]_{in}$. We also aimed to generate an experimental proof that Ca^{2+} plays a role of intracellular messenger, whose levels in cytoplasm respond to environmental stimuli and in turn regulate the downstream physiological response. This required a mutant that would not be able to generate intracellular transients of Ca^{2+}. The identified Ca^{2+} influx channel in *P. aeruginosa* was shown to play role in the production of intracellular Ca^{2+} transient, and its mutation impaired Ca^{2+}regulated swarming and pyocyanin production, confirming the role of intracellular Ca^{2+} transients in Ca^{2+} regulation.

When aiming to identify proteins required for Ca^{2+} influx, which is required for generating transient increase in $[Ca^{2+}]_{in}$, we considered two categories of Ca^{2+} influx channels that have been described in bacteria: PHB-PP voltage gated Ca^{2+}channel in *E. coli* (147) and a Ca^{2+} leak channel in *B. subtilis* (167, 309). Since no clustered homologs of PHB-PP biosynthetic genes were identified in the PAO1 genome, and considering the reported ability of *P. aeruginosa* to produce medium chain length polyhydroxyalkanoate (PHA) and polyphosphate (PP) (ref), we hypothesized a possibility that the organism forms PHA-PP channels instead, which may play role in uptaking Ca^{2+}. However, the mutants with disrupted PHA synthases and PP phosphatases showed no difference in Ca^{2+} uptake. Neverthless, the lack of PHA synthase PA5056 and PP phosphatase PA5058 significantly impaired the intracellular Ca^{2+} homeostasis and abolished the recovery of the basal level of $[Ca^{2+}]_{in}$. This finding strongly suggests that even if PHA and PP do

not form a channel, they play an important role in maintaining $[Ca^{2+}]_{in}$ possibly due to their ability to bind Ca^{2+} in the cytoplasm enabled by their negative charge.

A pH dependent Ca^{2+} leak channel in *B. subtilis* forms a pore in the bacterial inner membrane that transports Ca^{2+} at neutral pH (167). Disruption of its homolog PA2604 impairs *P. aeruginosa*'s ability to produce immediate transient increase $[Ca^{2+}]_{in}$ in response to rapid change in external Ca^{2+}, suggesting its role in Ca^{2+} influx. The significantly reduced transient increase was not followed by any recovery of the basal $[Ca^{2+}]_{in}$, but instead was followed by a slow increase in $[Ca^{2+}]_{in,}$ suggesting the presence of an alternative channel allowing slow Ca^{2+} influx. Importantly, the defect in transient increase in $[Ca^{2+}]_{in}$ in PA2604::IS mutant lead to impaired Ca^{2+}-regulated swarming motility and pyocyanin production. This strongly supports the hypothesis that intracellular Ca^{2+} plays role as a secondary messenger Ca^{2+}. Intracellular Ca^{2+} signaling appears to regulate only selected Ca^{2+}-regulated processes as it does not affect Ca^{2+}-induced antibiotic resistance. The latter must employing an alternative mechanism of relaying the environmental Ca^{2+} signal, and thus differentiating the distinct roles of Ca^{2+} as a primary and secondary messenger.

P. aeruginosa is known to have multiple signaling pathways, including quorum sensing, c-di-GMP, cAMP, other small nucleotides, and pigments pyocyanin and pyoverdin, which interact with each other. Regulation of QS genes expression by Ca^{2+} suggests the interaction between Ca^{2+} and QS signaling systems. Promoter activity assays confirmed that Ca^{2+} exerts its regulatory role at the transcriptional level for QS regulatory genes. In agreement with our earlier proteomic and microarray analyses, we observed that elevated external Ca^{2+} increases the activity of *lasR* promoter during the exponential growth phase, however the activities of *pqsR* and *rhlR* promoters were mostly inhibited by Ca^{2+}, with only a transient brief increase for *rhlR* promoter

during the transition to exponential growth phase. The negative regulation of *rhlR* and *pqsR* promoter activities by Ca^{2+} is in contrast with our previous observations, although it may be due to different Ca^{2+} concentrations used in the two studies (10 mM earlier and 5 mM here) or the presence of additional level of regulation responding to Ca^{2+}. To validate the collected proteomic and transcriptomic data, we aimed to measure the production of QS molecules in PAO1 cultures grown at different Ca^{2+}. However, the employed HPLC approach did not detect any QS molecules in the collected samples, indicating a need for an alternative higher sensitivity technique, i.e. mass spectrometry.

It was shown that acyl homoserine lactones (AHLs) may induce intracellular Ca^{2+} transients in both bacteria and eukaryotes. The addition of N-hexanoyl-L- homoserine lactone to *Serratia liquefaciens* cells caused transient changes in their $[Ca^{2+}]_{in}$ (316), however, the molecular mechanisms of this effect have not been studied. *P. aeruginosa* 3-O-C12 HSL elevate cytosolic Ca^{2+} in human epithelial cells (317, 318), as well as *Arabidopsis thaliana* root cells (319). In contrast, our observations did not detect any changes in $[Ca^{2+}]_{in}$ in response to the addition of C4-HSL, 3-O-C12 HSL, and PQS in *P. aeruginosa*. Although it is possible that QS molecules induce the $[Ca^{2+}]_i$ changes under the conditions different than the ones tested, it is more likely that QS signaling is not affecting the intracellular $[Ca^{2+}]$ in this bacterium, changing the balance towards Ca^{2+} regulating QS signaling and not the other way around. This further emphasizes the selectivity of the intracellular Ca^{2+} signaling in *P. aeruginosa*.

Swarming motility is a complex community behavior regulated by both QS and Ca^{2+}. Our observations suggest that QS regulation of swarming motility is controled by Ca^{2+}. 3-O-C12-HSL synthase, LasI, is known to positively regulate swarming motility in *P aeruginosa* (314). In agreement, we observed inhibition of swarming motility in the transposon mutant with disrupted

lasI, which however, was restored by adding Ca^{2+} to growth medium. It is possible that Ca^{2+} addition regulates some other mechanism complimenting the negative effect of *lasI* disruption, including, for example, upregulation of Rhl system involved in producing rhamnolipid, which is required for swarming (314). This is in agreement with our earlier microarray and proteomic studies (156, 313), showing a positive effect of elevated Ca^{2+} on the expression of Rhl system, but in contrast with the presented data showing a decreased promoter activity of *rhlR* in the presence of Ca^{2+}. This intriguing disagreement raises a possibility of additional level of regulation differentially mediated by Ca^{2+} or a mode of growth (planktonic *vs* biofilm). As expected, the disruption of *rhlI*, preventing biosynthesis of rhamnolipid, completely abolished the swarming and could not be restored by the addition of Ca^{2+}, whereas earlier reported negative regulation of swarming motility by *pqsA* (315)was not significantly affected by Ca^{2+}. Better understanding of the regulatory roles of Ca^{2+} on the transcription of QS synthase genes and the production of QS molecules will provide further insight into the complex relationship of Ca^{2+} and QS signaling systems and their role in regulating swarming motility.

This study reports Ca^{2+} regulation of QS signaling system in *P. aeruginosa* exerted by controling the transcription of QS regulatory genes, hence, suggesting the interaction between QS and Ca^{2+} signaling systems enabling fine tuning of the bacterial adaptation to environment. This study also identified a Ca^{2+} influx channel PA2604 required to produce immediate transient increase in $[Ca^{2+}]_{in}$ in response to rapid changes of external Ca^{2+}, and demonstrated the regulatory role of $[Ca^{2+}]_{in}$ homeostasis in *P. aeruginosa* physiology and virulence.

Acknowledgements

We thank Dr. Kangmin Duan (Department of Microbiology and Infectious diseases, University of Calgary, Calgary, Alberta, Canada) and Dr. Lin Chen (The College of Life

Sciences, Northwestern University, Xi'an, China) for providing the promoter activity plasmid constructs. We also thank Dr. Erika I. Lutter (Department of Microbiology and Molecular Genetics, Oklahoma State University, OK, USA) for Δ*lasI* strain, Dr. Ronald Rahaim and Mr. Sajan Silwal (Department of Chemistry, Oklahoma State University, OK, USA) for sharing the rotovap. We thank Dr. Anthony Campbell (School of Pharmacy and Pharmaceutical Sciences, Cardiff University, UK) for sharing his expertise and the templates for calculating $[Ca^{2+}]_{in.}$ We thank Dr. Delfina Dominguez from The University of Texas at El Paso for sharing *E. coli* strain carrying pMMB66EH. DNA/Protein Resource Facility at Oklahoma State University provided resources supported by the NSF MRI and EPSCoR programs (Award DBI/0722494). We thank Dr. Steven Hartson for HPLC instrumentation and guidance. This work was supported by OCAST Award HR12-167.

CHAPTER V

SIDE PROJECT

A *PSEUDOMONAS AERUGINOSA* EF-HAND PROTEIN, EhfP (PA4107), MODULATES STRESS RESPONSES AND VIRULENCE AT HIGH CALCIUM CONCENTRATION

Part of this chapter has been published "S. A. Sarkisova, S. R. Lotlikar, **M. Guragain**, R. Kubat, J. Cloud, M. J. Franklin and M. A Patrauchan. (2014). A *Pseudomonas aeruginosa* EF-Hand Protein, EfhP (PA4107), Modulates Stress Responses and Virulence at High Calcium Concentration. *PLoS ONE* 9(6): e98985" and is included in this dissertation under Creative Commons Attribution (CCBY) license from the publisher.

Copyright © 2014, PLoS ONE

Introduction

Pseudomonas aeruginosa is a facultative pathogen and a leading cause of severe nosocomial infections in both immunocompetent and immunocompromised patients (320). (321), including patients in intensive care units. *P. aeruginosa* is one of the primary organisms that forms biofilms on airway mucosal epithelium of patients with cystic fibrosis (CF) where it contributes to airway blockage and cellular damage. *P. aeruginosa* also causes infective endocarditis and device-related infections with high morbidity and mortality rates (322), (323), (324). *P. aeruginosa* biofilm infections are increasingly difficult to treat with traditional antibiotic therapy, and are often not eradicated by host defensive processes (325), (326).

Calcium (Ca^{2+}) is a well-known signaling molecule that regulates a number of essential processes in eukaryotes (327). Slight abnormalities in cellular Ca^{2+} homeostasis have been implicated in many human diseases, including diseases associated with bacterial infections, such as CF pulmonary infections and endocarditis. Ca^{2+} metabolism is recognized to be central to the pathology of CF (328). Ca^{2+} is a part of a hyperinflamatory host response to bacterial infection, and accumulates in airway epithelia, pulmonary and nasal liquids of CF patients (190), (191). There is growing evidence suggesting that Ca^{2+} also plays a significant role in the physiology of certain bacteria, affecting maintenance of cell structure, motility, chemotaxis, cell division and differentiation, gene expression, transport, and spore formation (192), (146), (329), (150), (330). Several bacteria including *P. aeruginosa* have been shown to maintain intracellular Ca^{2+} at sub-micromolar levels and produce Ca^{2+} transients in response to environmental and physiological factors (150, 195, 297). However, molecular mechanisms of Ca^{2+} regulation in prokaryotes are not well defined.

In eukaryotes, the regulatory effects of Ca^{2+} are carried out by Ca^{2+}-binding proteins (CaBPs), which may function as Ca^{2+} sensors, signal transducers, Ca^{2+} buffers or Ca^{2+}-stabilized proteins. Prokaryotic genomes also encode CaBPs with different Ca^{2+}-binding motifs, including the EF-hand motif (192, 331), which typically consists of a Ca^{2+}-binding loop flanked by two α-helices. Acidic amino acids in the loop are preferentially bound by Ca^{2+} (332), and are responsible for Ca^{2+} - induced conformational changes required for function (333). Bacterial EF-hand proteins constitute a majority of all studied CaBPs (334), and include the Ca^{2+} transducer calsymin CasA from *Rhizobium etli* (335), putative Ca^{2+} buffers and stabilizers calerythrin from *Saccharopolyspora erythraea* (336), and CabC (337) CabB (338) from *Streptomyces coelicolor*, and *Escherichia coli* transglycosylase MltB (339). Most bacterial proteins containing Ca^{2+}-binding motifs are classified as hypothetical proteins with unknown physiological functions.

Previously, we showed that Ca^{2+} modulates proteome profiles of *P. aeruginosa*, influences biofilm architecture, and alters production of several secreted virulence factors (156), (7)Michiels et al (340) screened 31 bacterial genomes for CaBPs, and predicted that the *P. aeruginosa* hypothetical protein, PA4107, contains EF-hand Ca^{2+}-binding motifs. We also identified PA4107 as having sequence similarity within the EF-hand motif to CasA of *R. etli*. Here, we further analyzed PA4107, which we designate EfhP (EF hand protein) and hypothesized that it is a Ca^{2+} binding protein. We characterized the effect of *efhP* mutation on intracellular Ca^{2+} homeostasis. The results indicate that EfhP is involved in maintenance of intracellular Ca^{2+} homeostasis.

Materials and Methods

Bacterial strains, media, and growth conditions. *Pseudomonas aeruginosa* PAO1 was used in this study. *P. aeruginosa* PAO1 is the non-mucoid strain used for the original genome

sequencing study (10). Biofilm minimal medium (BMM) (7) contained (per liter): 9.0 mM sodium glutamate, 50 mM glycerol, 0.02 mM $MgSO_4$, 0.15 mM NaH_2PO_4, 0.34 mM K_2HPO_4, and 145 mM NaCl, 20 µl trace metals, 1 ml vitamin solution. Trace metal solution (per liter of 0.83 M HCl): 5.0 g $CuSO_4.5H_2O$, 5.0 g $ZnSO_4.7H_2O$, 5.0 g $FeSO_4.7H_2O$, 2.0 g $MnCl_2.4H_2O$). Vitamins solution (per liter): 0.5 g thiamine, 1mg biotin. The pH of the medium was adjusted to 7.0. The level of Ca^{2+} in BMM was below the detection level when measured by QuantiChrom™ calcium assay kit.

Estimation of free intracellular calcium ($[Ca^{2+}]_{in}$). PAO1 and its *efhP* lacking mutant PAO1043 were transformed with pMMB66EH (courtesy of Dr. Delfina Dominguez), carrying aequorin (201) and carbenicillin resistance genes, using a heat shock method described in (202). The transformants were selected on Luria bertani (LB) agar containing carbenicillin (300 µg/ml) and verified by PCR using aequorin specific primers (For: 5'CTTACATCAGACTTCGACAACCCAAG, Rev: 5'CGTAGAGCTTCTTAGGGCACAG). Aequorin was expressed and reconstituted as described in (297). Briefly, mid-log phase cells were induced with IPTG (1 mM) for 2 h for apoaequorin production, and then harvested by centrifugation at 6000 g for 5 min at 4 ^{0}C. Aequorin was reconstituted by incubating the cells in the presence of 2.5 µM coelenterazine for 30 min.

Luminescence measurements and estimation of free $[Ca^{2+}]_{in}$ was performed as described in (297) with slight modifications. Briefly, 100 µl of cells with reconstituted aequorin were equilibrated for 10 min in the dark at room temperature. Luminescence was measured using Synergy Mx Multi-Mode Microplate Reader (Biotek). For basal level of $[Ca^{2+}]_{in}$, the measurements were recorded for 1 min at 5 sec interval, then the cells were challenged with 1 mM Ca^{2+}, mixed for 1 sec, and the luminescence was recorded for 20 min at 5 sec interval.

Injection of buffer alone was used as a negative control, and did not cause any significant fluctuations in $[Ca^{2+}]_{in.}$ $[Ca^{2+}]_{in}$ was calculated by using the formula pCa= 0.612 ($-\log_{10}k$) + 3.745, where k is a rate constant for luminescence decay (s^{-1}) (147). The results were normalized against the total amount of available aequorin as described in (297). The discharge was performed by permeabilizing cells with 2 % Nonidet 40 (NP40) in the presence of 12.5 mM $CaCl_{2.}$ The luminescence released during the discharge was monitored for 10 min at 5 sec interval. The estimated remaining available aequorin was at least 10 % of the total aequorin. The experimental conditions reported here were optimized to prevent any significant cell lysis.

Results and Discussion

EfhP contributes to maintenance of intracellular Ca^{2+} ($[Ca^{2+}]_{in}$) homeostasis in *P. aeruginosa* PAO1. The role of EfhP in maintaining intracellular Ca^{2+} homeostasis was studied using recombinant Ca^{2+}-binding luminescence protein aequorin (**Fig. 5.1**). The lack of *efhP* did not affect the basal level of $[Ca^{2+}]_{in}$ (0.19 ± 0.01 µM) or the initial increase in response to 1 mM Ca^{2+} (1.99 ± 0.14 µM). In contrast, however, this increase was not followed by the recovery of $[Ca^{2+}]_{in}$ to nearly basal WT level, as observed in WT PAO1 cells. Instead, the $[Ca^{2+}]_{in}$ continued to raise and in 20 min reaching 3.66 ± 0.41 µM, which is almost seven fold higher than in PAO1. This suggests that EfhP is involved in maintaining intracellular Ca^{2+} homeostasis, which supports its predicted Ca^{2+}-binding capabilities.

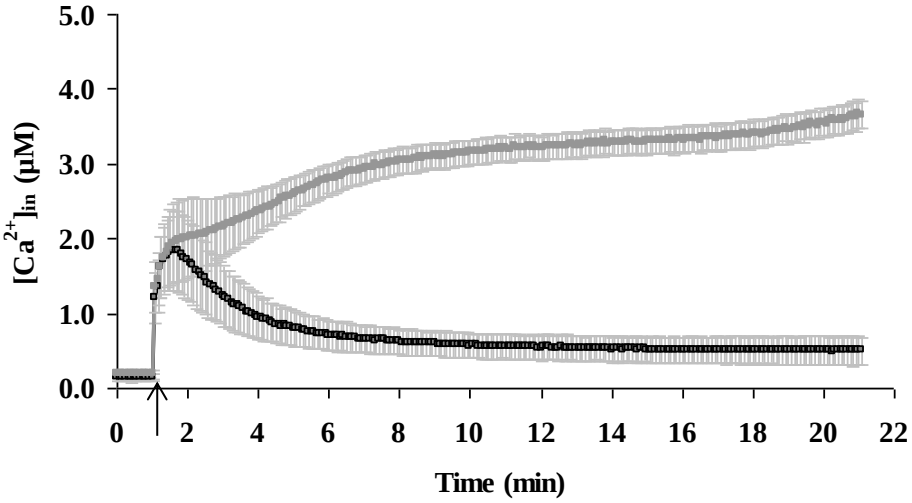

Figure 5.1. Free $[Ca^{2+}]_{in}$ profiles of PAO1 WT (black line) and *efhP* mutant strain PAO1043 (grey line). Cultures were grown in 0 mM Ca^{2+}. After the basal level of $[Ca^{2+}]_{in}$ was monitored for 1 min, 1mM Ca^{2+} was added (indicated by the arrow) followed by further $[Ca^{2+}]_{in}$ measurement for 20 min.

Conclusions.

Sequence analyses (by co-author S.R. Lotlikar) predicted that EfhP is a Ca^{2+}-binding protein spanning the inner membrane, with the two EF-hand domains facing the periplasm. Deletions of e*fhP* in two *P. aeruginosa* strains causes multiple changes in the cytosolic proteome of both strains, but with more changes occurring in the CF pulmonary isolate FRD1. The effects of the *efhP* deletions only occurred when the cells were exposed to elevated [Ca^{2+}] and included reduced abundance of virulence factors and stress response proteins. Author S. Sarkisova investigated the physiological role of *efhP* and showed that the lack of e*fhP* abolished production of pyocyanin, and reduced the degree of infection, biofilm formation, and resistance to oxidative stress in FRD1 at high [Ca^{2+}]. The mutant also lost the ability to produce alginate at no iron and high [Ca^{2+}]. Finally, the lack of EfhP abolished the ability of *P. aeruginosa* to maintain intracellular Ca^{2+} homeostasis. These findings suggest that EfhP is important for Ca^{2+} homeostasis and plays role in Ca^{2+}- triggered virulence and resistance of *P. aeruginosa* in high Ca^{2+} environments.

CHAPTER VI

DISCUSSION

This research aimed to establish the signaling role of Ca^{2+} in bacteria using a human pathogen *P. aeruginosa* as a model organism. Through this study, we have established that the organisms maintains intracellular Ca^{2+} homeostasis, identified Ca^{2+} transporters and Ca^{2+}-sensing two component regulatory system (TCS) in *P. aeruginosa.* We also characterized the molecular and physiological responses of the pathogen to both external Ca^{2+} and transiently changing intracellular Ca^{2+} (Ca^{2+}_{in}). We investigated possible relationships between $[Ca^{2+}]_{in}$ and other secondary messengers in the organism. The genes identified in this study likely form the Ca^{2+} regulatory network and provide a model system that can be used to investigate the detailed molecular mechanisms of Ca^{2+} signaling in bacteria. Utilization of environmental Ca^{2+} as a cue can be well suited for the adaptation and survival in the opportunistic pathogen *P. aeruginosa* which may encounter changing Ca^{2+} concentrations in the diverse environments it occupies, for example, in CF lungs. Based on the previous research, we hypothesized that intracellular Ca^{2+} transients are produced in response to elevated environmental Ca^{2+} and other factors, which allows the bacterium to respond by regulating the multitude of physiological responses. A better understanding of Ca^{2+} regulatory network in a human pathogen may provide new targets for developing novel strategies for combating *Pseudomonas* infections that are currently recognized as a national threat due to their multidrug resistance. Overall, this study identifies several components of calcium regulatory network in *P. aeruginosa* and provides evidence supporting that bacteria use intracellular Ca^{2+} signaling for regulating their physiology and enhancing their adaptation strategies.

Signaling role of Ca^{2+} roots from its chemistry. Ca^{2+} binds water less tightly than Mg^{2+} which enables it to be freely available for binding with several cellular structures and molecules. On the other hand, Ca^{2+} can be toxic to cells by binding negatively charged molecules. For

example, Ca^{2+} can bind and precipitate phosphate leading to cellular conditions incompatible with life. Therefore, cells evolved to acquire mechanisms to exclude high Ca^{2+} from the cytosol. This creates a Ca^{2+} gradient, which can drive Ca^{2+} back into cytosol and thus serve for Ca^{2+} signaling. Other features that make Ca^{2+} unique in its capacity to be used as a signaling entity, but different from other cations include its flexible coordination. This allows interactions between Ca^{2+} and receptor proteins. Finally, affinity of Ca^{2+} for receptor proteins lie within micromolar ranges, thus allowing the physiologically reversible reaction(138).

The fact that bacteria possess all the essential components of Ca^{2+} informational system such as Ca^{2+} transporters, Ca^{2+} storage structures, and calmodulin like Ca^{2+} binding proteins suggests that bacteria may be able to use a prototype of eukaryotic Ca^{2+} signaling. In eukaryotes, intracellular Ca^{2+} signaling connects extracellular stimuli to intracellular responses *via* transient increases in $[Ca^{2+}]_{in}$. The source of Ca^{2+} for its transient increases in the cytosol is provided by releasing the ion from the intracellular storage compartments, which include mitochondria and endoplasmic reticulum (ER) (reviewed in (139)). Ca^{2+} is transported by several types of transporters including channels, ATPases, and gradient driven exchangers. One of the well-studied intracellular Ca^{2+} signal transduction pathways is IP3-mediated intracellular Ca^{2+} signaling. Upon binding to a stimulus, a plasma membrane bound G-protein coupled receptor activates the phospholipase C (PLC). PLC produces IP3 at the cytoplasmic membrane, which then diffuses into the cytosol and binds to the IP3-sensing Ca^{2+} channels in the ER membrane. Consequently, the channels bind Ca^{2+}, switch to an open state, and allow the ER Ca^{2+} to flow down its steep concentration gradient (20,000 fold) into the cytosol. Ca^{2+} released into the cytosol is then actively extruded by Ca^{2+} ATPases like Sarcoplasmic reticulum Ca^{2+} ATPases (SERCA) and Plasms membrane Ca^{2+} ATPases (PMCA). A sequence of these events generates

cytosolic fluctuations of Ca^{2+} levels, the amplitude and frequency of which is recognized as a signal. Ca^{2+} depletion inside the ER is restored *via* slow and highly selective store operated Ca^{2+} channels from the extracytoplasmic space (reviewed in (341)). During all the molecular events involved in Ca^{2+} signaling, Ca^{2+} binding proteins play vital roles of recognizing Ca^{2+}, transducing the signal, and acting as Ca^{2+} buffers. Classic example of Ca^{2+} binding protein transducing Ca^{2+} signal is calmodulin. Calmodulin binds Ca^{2+} within its EF-hand domains, which leads to conformational changes in the protein that in turn releases autoinhibition, remodels active site, and increases the hydrophobicity of the protein exterior, which promotes its interactions with binding partners - target proteins with calmodulin recruitment sites (342).

Several lines of evidence clearly show that extracellular Ca^{2+} regulates bacterial physiology *via* transcriptional, translational, and post-translational changes, hence, establishing that Ca^{2+} serves as a primary signal in bacteria. Ca^{2+} affects the expression of many genes and proteins in *Pseudomonas aeruginosa* (156), *Vibrio parahaemolyticus* (157), *Vibrio cholerae* (154), *Escherichiacoli* (152), and *Bacillus subtilis* (153, 155). Ca^{2+} regulated genes and proteins are related to various processes including general metabolism (electron transport chain, RNA synthesis, protein synthesis/degradation, post translational modifications, and carbohydrate metabolism), lifestyle switch and physiological adaptations (spore formation, heterocyst formation, chemotaxis, swarming motility, transcriptional regulation, biofilm formation and stability, iron acquisition and storage, oxidative stress response, and quorum sensing), transport (carrier proteins mediated transport), and virulence (T3SS, extracellular proteases, alginate, and toxins) (7, 142, 144, 145, 343).

In order for Ca^{2+} to serve as a secondary messenger, its intracellular homeostasis should be tightly regulated, and the basal cytoplasmic levels kept low. Similarly to eukaryotes, bacteria

control their intracellular Ca^{2+} homeostasis and maintain the cytosolic concentration of the ion at sub-micromolar levels despite its steep concentration gradient cross the plasma membrane (147, 149, 344, 345). The second essential component of Ca^{2+} signaling is the generation of transient spikes in the intracellular Ca^{2+}concentration in response to environmental stimuli. So far it has been shown that bacteria are able to do so in response to nitrogen starvation (346), environmental stress (344, 345, 347), and metabolites of carbohydrate (151). The final essential attribute of Ca^{2+} signaling is the regulation of cellular response *via* transcriptional, translational, posttranslational, or functional changes. Although such Ca^{2+}-dependent modifications of cellular physiology have been described in bacteria, there is still no direct experimental evidence supporting the regulatory link between these processes and transient changes in the intracellular Ca^{2+} levels. Ca^{2+} homeostasis in *E. coli* has been studied in more detail than in other bacteria. Thus, *E.coli* maintains intracellular Ca^{2+} homeostasis and keeps the $[Ca^{2+}]_{in}$ low in the range of 100 - 200 nM (143, 147). Ca^{2+} is imported into the cytoplasm by PHB-PP channels (147). Ca^{2+} efflux requires ATP, thus ATP synthase AtpD, is required for maintenance of Ca^{2+} homeostasis (152). Interestingly, PHB-PP synthesis is regulated by Ca^{2+} *via* AtoSC two component system (286). Various stimuli induce intracellular Ca^{2+} transients in *E. coli*. These include extracellular Ca^{2+}, metabolites of carbohydrate (149, 195), chemoattractants and chemorepellents (143), and host complements (149). In high $[Ca^{2+}]$ environment, *E. coli* concentrates Ca^{2+} in the periplasm to the level several folds higher than in the extracellular milieu. However, as stated above, there is still no direct evidence proving the regulatory role of $[Ca^{2+}]_{in}$ transients .

Our research pioneered Ca^{2+} signaling studies in *P. aeruginosa,* a bacterium successfully adapted to survival in a broad variety of ecological niches ranging from soil to a human body. We demonstrated that *P. aeruginosa* is capable of regulating intracellular Ca^{2+} homeostasis and

maintains the $[Ca^{2+}]_{in}$ at the nanomloar level, which is comparable to that in eukaryotes and other studied bacteria (reviewed in (192)). Further, our results showed that $[Ca^{2+}]_{in}$ transiently changes in response to rapidly changing external Ca^{2+} . The addition of methanol and DMSO also modulates the $[Ca^{2+}]_{in}$ response (Guragain *et. al*, unpublished data) further supporting the role of Ca^{2+} as a secondary messenger.

Since maintenance of Ca^{2+} homeostasis requires functional Ca^{2+} transporters, Ca^{2+} binding proteins, and Ca^{2+} storage compartments, we aimed to identify these components in *P. aeruginosa*. We identified seven ATPases, six gradient driven exchangers, and one mechanosensitive channel, and demonstrated their role in Ca^{2+}efflux in the organism. Among these, four transporters belonging to P-ATPases, gradient driven exchangers, and a mechanosensitive channel are required. The fact that multiple proteins from different families of transporters are involved in controlling Ca^{2+} efflux does not suggest functional redundancy, but indicates 1) the physiological importance of $[Ca^{2+}]_{in}$ control and 2) multiple routes of regulation of this process in response to variable environmental conditions, thereby, demonstrating fine tuning of Ca^{2+} homeostasis. Considering that most well characterized Ca^{2+}translocating ATPases are high affinity and low capacity systems, we hypothesize that these proteins function in response to minute and possibly rapid changes of Ca^{2+} concentration in the environment. Whereas gradient driven exchangers are low affinity, high capacity transporters (139), and therefore are likely to be involved in heavy duty translocation of Ca^{2+} during long-term exposure to high Ca^{2+}. Together, Ca^{2+} pumps and exchangers complement each other in the maintenance of cellular Ca^{2+} homeostasis. Further biochemical characterization of the individual Ca^{2+} transporters is needed to identify their roles in controlling Ca^{2+} levels under diverse environmental and physiological conditions.

We also aimed to identify a mechanism responsible for Ca^{2+} influx. Identification of such mechanism would enable a new line of research targeting to prove the regulatory role of intracellular Ca^{2+} and thus needed to confirm that Ca^{2+} serves as a secondary messenger. We targeted two possible mechanisms of regulated Ca^{2+} uptake: channeling Ca^{2+} *via* voltage gated channel composed of Polyhydroxy butyrate polyphosphate (PHB-PP) complexes (348) or conventional Ca^{2+} channel, For this, we performed sequence analysis of *P. aeruginosa* genome and identified putative proteins involved in biosynthesis of polyhydroxy alkanoate (PHA) (since *P. aeruginosa* does not produce PHB) and polyphosphate (PP), as well as a homolog of Ca^{2+} leak channel characterized in *E. coli* (147). We studied the role of these proteins in maintaining Ca^{2+} homeostasis by using the corresponding mutants. Our results indicate that the disruption of one of the two PHA synthases PA5056, PA5058, and PP phosphatase PA5241 cause intracellular accumulation of Ca^{2+}, but do not affect Ca^{2+} uptake. It is possible that *P. aeruginosa* does not produce PHA-PP-type Ca^{2+} channels or that such channels are involved in Ca^{2+} efflux instead of uptake. Alternatively, negatively charged cytoplasmically located PHA and PP may bind Ca^{2+} and thus contribute to the maintenance of cellular Ca^{2+} homeostasis by either dynamic (bind-release mode) or static (bind only mode) storage of Ca^{2+} in the cytoplasm.

There is evidence for cytosolic Ca^{2+} storage in bacteria. For example, similarly to eukaryotic acidic organelles, acidocalcisomes serving as major storage of Ca^{2+} (349), *Rhodospirillum rubrum* possess negatively charged compartments also shown to store Ca^{2+} in the cytoplasm (350). Another example is storage of Ca^{2+} in the periplasm: when exposed to millimolar concentration of Ca^{2+}, *E.coli* was shown to accumulate Ca^{2+} in the periplasm at the levels several magnitudes higher than in the environment. It was suggested that Ca^{2+} can bind to periplasmic oligosaccharides and anionic proteins (348). These mechanisms may provide both

the intracellular storage of Ca^{2+} needed for signaling and cellular protection against Ca^{2+} toxicity (145). Aiming to characterize such mechanisms in *P. aeruginosa,* we identified a gene *carP,* encoding a periplasmic protein, whose predicted 3D structure contains negatively charged pockets. Disruption of *carP* doubled the level of intracellular Ca^{2+} in the cells grown at elevated Ca^{2+}, suggesting the protein may bind Ca^{2+} in the periplasm and reduce the local concentration of free Ca^{2+} available for translocation into the cytoplasm. In such case, the periplasmic space in *P. aeruginosa* may act as a Ca^{2+} storage compartment or Ca^{2+} sink, as suggested in *E. coli* (348). The mutation in *carP* also lead to defective $[Ca^{2+}]_{in}$ homeostasis, which suggest the role of CarP in Ca^{2+} homeostasis likely by regulating efflux mechanisms. Finally, periplasmic binding of Ca^{2+} may also serve to protect the bacterium against Ca^{2+} toxicity. Wild type *P. aeruginosa* can tolerate the presence of extracellular Ca^{2+} at the level as high as 100 mM, suggesting the existence of high capacity Ca^{2+} binding systems in addition to functional Ca^{2+} efflux mechanisms. We showed that *carP* is required for cellular tolerance to 10 mM Ca^{2+} and its expression is increased during growth in high Ca^{2+}. Finally, the lack of *carP* affected *P. aeruginosa* response to elevated Ca^{2+} by abolishing Ca^{2+} induction of pyocyanin production and causing changes in swarming motility at high Ca^{2+}, Overall, the observations suggest that by binding Ca^{2+} in the periplasm or by regulating Ca^{2+} efflux, CarP may play multiple roles: cellular tolerance against Ca^{2+} toxcity, maintenance of intracellular Ca^{2+} homeostasis and regulation of . Ca^{2+} induced processes. Ca^{2+}-dependent expression of *carP* is positively regulated by the Ca^{2+} induced two-component regulatory system (TCS), CarSR. TCSs are known to sense the environmental stimuli and relay the message towards physiological responses mostly *via* transcriptional regulation. It is possible that CarP is a component of the Ca^{2+} regulatory network connecting the external Ca^{2+} signal to intracellular Ca^{2+} signaling *via* changes in $[Ca^{2+}]_{in}$

transients or binding protein signaling partners. Further studies aiming to understand the relationship between periplasmic and cytoplasmic Ca^{2+} homeostasis will provide an answer to whether periplasm serves as a Ca^{2+} sink or a source of free Ca^{2+} for transient increases in cytosolic Ca^{2+}, or both depending on the environmental conditions.

In addition to a possibility of a PHB-PP voltage gated channel, *P. aeruginosa* may possess a Ca^{2+} leakage channel. The genome sequence analysis revealed PA2604 homologous to BsYetJ in *Bacillus subtilis* (167). The mutant with transposon-disrupted PA2604 showed almost abolished $[Ca^{2+}]_{in}$ transient in response to rapid change in external Ca^{2+}, which, however, was followed by a steady increase of cytosolic Ca^{2+}. This suggests that PA2604 is involved in generating $[Ca^{2+}]_{in}$, but there are alternative compensatory mechanisms of Ca^{2+} uptake. This agrees with the earlier suggestion of multiple Ca^{2+} influx systems in *E. coli* (151). Although the disruption of PA2604 did not completely abolish $[Ca^{2+}]_{in}$ transient, the latter was decreased by almost 66%, which makes it possible to use this mutant to study the regulatory role of intracellular Ca^{2+}. We hypothesized that Ca^{2+}-dependent processes requires $[Ca^{2+}]_{in}$ transient and hence will be impaired in this mutant.

Calmodulin-like Ca^{2+} binding proteins act as major Ca^{2+} signal transducers in eukaryotes. These proteins possess EF-hand motifs responsible for binding Ca^{2+}. Upon binding Ca^{2+} , the proteins undergo conformational changes enabling further interactions with their regulatory targets (139). A number of EF-hand proteins have been reported in bacteria and shown to mediate various processes. For example, calsymin CasA from *Rhizobium etli* was proposed to act as a Ca^{2+} signal transducer and play role in symbiotic relationship between the bacterium and its plant host (335). Several EF-hand proteins were identified in *Streptomyces coelicolor*; CabC (337), CabB (338), and CabA (351), however, their role in Ca^{2+} signaling was not demonstrated.

CabC is suggested to act as a Ca^{2+} buffer. Ca^{2+} binding doesn't induce its conformational change, but regulates $[Ca^{2+}]_{in}$ as well as affects physiology (337). CabB, on the other hand, undergoes large conformational changes upon binding Ca^{2+} and regulates the cellular tolerance to high Ca^{2+} (338). Our lab (188) identified a putative Ca^{2+} binding protein EfhP in *P. aeruginosa* (188). EfhP was predicted to span the inner membrane and face the EF hands into the periplasm. We showed that EfhP is required for intracellular Ca^{2+} homeostasis and regulates Ca^{2+}-dependent changes in *P. aeruginosa* physiology, including virulence factor production and infectivity. Based on these data, we hypothesize that EfhP binds Ca^{2+} within its EF-hand motif, and directly or indirectly mediates Ca^{2+} signaling. However, it is also possible that EfhP is buffering Ca^{2+} in the periplasm, contributing to the maintenance of cellular Ca^{2+} homeostasis, which ultimately regulates responses to Ca^{2+}. It is also possible that Ca^{2+} regulates the function of Ca^{2+} binding proteins by providing them with structural stability. Further detailed biochemical studies of Ca^{2+} binding proteins are necessary for understanding their role in Ca^{2+} signaling.

Finally, it is important to establish whether intracellular Ca^{2+} transients are used to regulate responses to other than extracellular Ca^{2+} stimuli. We showed that $[Ca^{2+}]_{in}$ changes in response to the addition of membrane disturbing compounds including DMSO and methanol. However, it is not clear whether the effect is due to transient membrane permeabilization. Another intriguing question is whether Ca^{2+} signaling is interplaying with quorum sensing signaling (QS), which plays a major role in regulating *P. aeruginosa* virulence in cell communities. Although QS molecules were reported to cause $[Ca^{2+}]_{in}$ changes in eukaryotes (317, 352) and in bacterium *Serratia liquefaciens* (316), we observed no $[Ca^{2+}]_{in}$ changes to rapid additions of QS molecules: C4-HSL, 3-O-C12 HSL, and PQS Nevertheless, our earlier global proteomic and transcriptomic studies showed that growth at elevated Ca^{2+} induces the gene

expression of all three QS systems in *P. aeruginosa.* We further supported these data with promoter activity assays of QS regulatory genes. Although it is possible that QS signals induce the $[Ca^{2+}]_{in}$ changes under conditions different than our experimental conditions, it is more likely that it is changes in Ca^{2+} that serve as a signal that is recognized by QS-mediated regulatory network. Considering the importance of QS signaling in regulating *P. aeruginosa* virulence and pathogenicity and the elevated Ca^{2+} levels in CF pulmonary liquids, it is necessary to understand the regulatory interrelationship between the two signaling systems, which may provide new directions in searching for therapeutic strategies of combating *P. aeruginosa* infections.

Overall, our findings further support that *P. aeruginosa* utilizes all the main components of eukaryotic Ca^{2+} signaling. We demonstrated that the transient changes in intracellular Ca^{2+} are required for regulating Ca^{2+}dependent production of virulence factor pyocyanin. This is the first experimental evidence confirming that transient changes in intracellular Ca^{2+} are involved in regulating cellular response to changes in extracellular Ca^{2+}. Based on all our observations, we propose a model for Ca^{2+} signaling network in *P. aeruginosa* (Fig. 6.1). *P. aeruginosa* maintains low level of $[Ca^{2+}]_{in}$. Extracellular Ca^{2+} is transported into the periplasm, where it is recognized by two component sensor CarS transducing the signal to the regulator CarR, controlling Ca^{2+}-dependent expression of at two periplasmic Ca^{2+} binding proteins CarP and CarO. Upon binding to Ca^{2+}, these two proteins as well as EF hand protein EfhP either directly or indirectly transduce Ca^{2+} signal further towards the regulatory circuits. They may also contribute to buffering periplasmic Ca^{2+} and protecting cell from the excess of Ca^{2+}. Free periplasmic Ca^{2+} is transported into the cytoplasm *via* Ca^{2+} channels including Ca^{2+} leak channel, which increases the intracellular $[Ca^{2+}]_{in}$. To maintain the low intracellular $[Ca^{2+}]$, several efflux mechanisms including ATPases, gradient driven exchangers, and channels export the excessive Ca^{2+} out of

the cytosol. In addition, negatively charged compounds including PHA and PP may bind the excess of cytosolic free Ca^{2+}. Together, these mechanisms ensure intracellular Ca^{2+} homeostasis so that free intracellular Ca^{2+} is only transiently available for signaling or other Ca^{2+}-dependent processes. Ca^{2+} signaling ultimately regulates physiology and virulence of *P. aeruginosa* and endows the bacterium with the ability to successfully adapt to diverse environments, including a human host. This knowledge is essential in our efforts to fully understand the regulation of *P. aeruginosa* virulence and to discover novel strategies for preventing or treating infections caused by this pathogen.

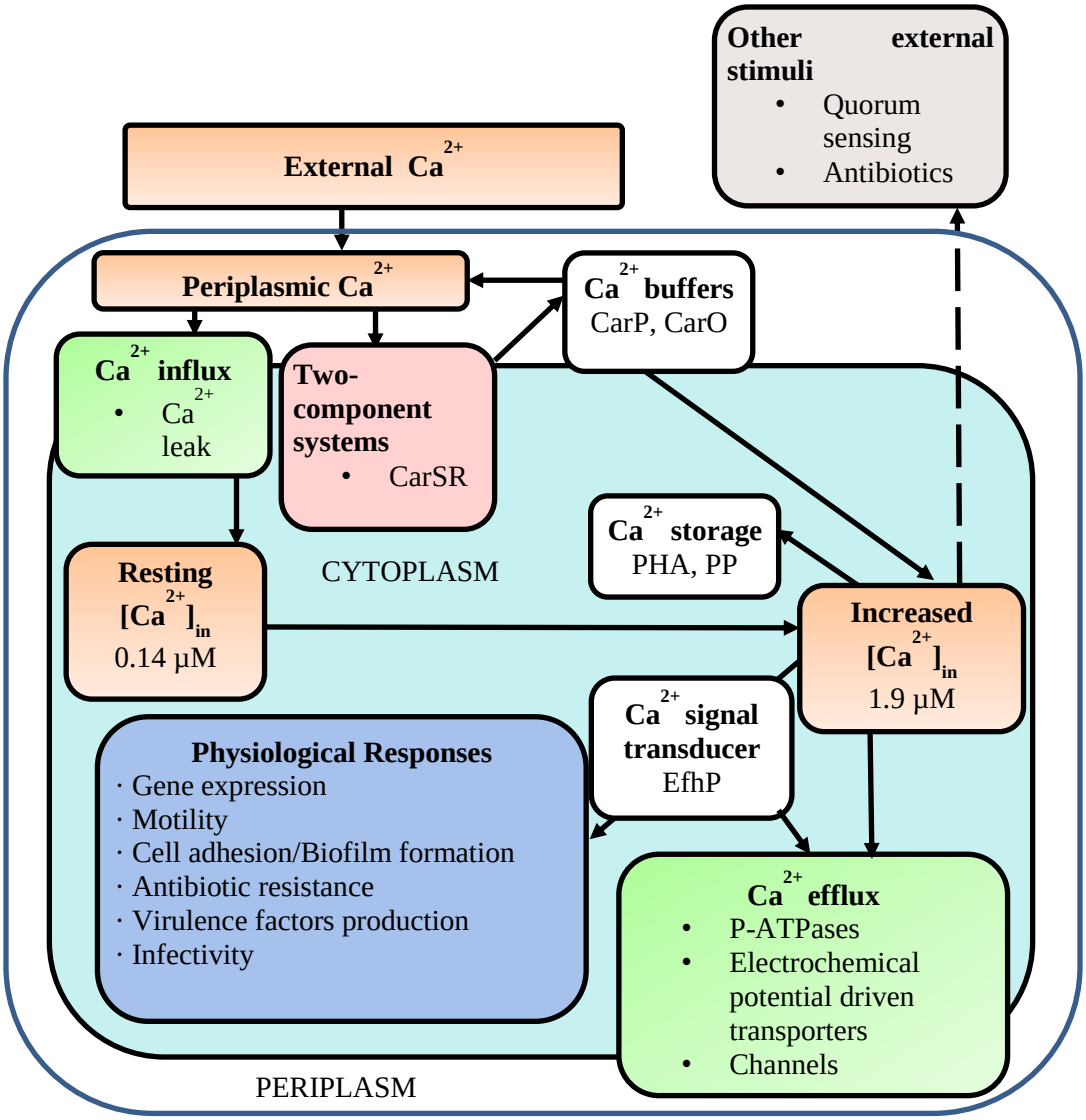

Figure 6.1. Calcium signal transduction pathway in *P. aeruginosa*

CHAPTER VI

MATERIALS AND METHODS

Materials. Coelenterazine was purchased from Life Technologies (California, USA). Nitrendipine, sodium orthovanadate, and lanthanum (III) chloride were purchased from Tocris biosciences (Bristol, UK), New England Biolabs (Tozer, MA), and AlfaAesar (Massachusetts, USA), respectively. Gel red was purchased from Phoenix research. Deoxynucleotide (dNTP) and Taq polymerase were purchased from New England Biolabs (Ipswich, MA). Crystal violet, 2 M MgCl2 solution, was purchased from Thermo Scientific (Pittsburgh, PA). E. coli NovaBlue™. QIAprep Mini-spin kit, was purchased from Qiagen (Valencia, CA). Oligonucleotide primers were obtained from Integrated DNA Technologies (Coralville, IA). Transposon insertion mutants were purchased from the University of Washington Two-Allele library (grant # NIH P30 DK089507) (283). Coelenterazine was purchased from Life Technologies (California, USA). N-(3-Oxododecanoyl)- N-butyryl-L-Homoserine lactone was purchased from Cayman chemicals. The fused inert vials for HPLC were purchased from Thermo Scientific. All reagents and chemicals used during QS molecules extraction and purification were HPLC grade. All reagent-grade chemicals were purchased from Thermo-Fisher Scientific (Waltham, MA) or Sigma-Aldrich (St. Louis, MO), unless otherwise indicated.

Buffers and Reagents. All buffers were made with ultrapure deionized water from Barnstead-thermolyne deionization system at resistance of 18.2 MΩ. See Appendix A for buffer compositions, media and other recipes. When needed pH was adjusted by concentrated hydrochloric acid (HCl) or 1 N sodium hydroxide (NaOH).

Bacterial strains, media, and growth conditions. The bacterial strains and plasmids used in this study are listed in Table 7.1. The transposon insertion mutants obtained from UW were confirmed using two-step PCR: first, transposon flanking primers were used to verify that the gene of interest was disrupted, and second, transposon-specific primers were used to confirm the

transposon insertion. The primer sequence is available at www.gs.washington.edu. PAO1 and transposon mutants were grown at 37 °C in biofilm minimal medium (BMM; See Appendix A) with shaking at 200 rpm (7). When needed, 1 mM - 10 mM $CaCl_2$.2H2O was added to the medium. For DNA manipulations, *E. coli* and *P. aeruginosa* cultures were grown in Luria–Bertani (LB) (Appendix A) broth at 37 ^{0}C with shaking at 200 rpm. Antibiotics used for *E. coli* were (per ml) 100 µg Ampicillin (Ap) or 50 µg kanamycin (Km); for *P. aeruginosa*, (per ml) 300 µg carbenicillin (Cb), 60 µg tetracycline (Tc) or 300 µg trimethoprim (Tm) (Appendix A).

Standard DNA procedures. Established DNA manipulation procedures were employed as described in (261) (353). Plasmid DNA was isolated using the QIAprep mini-spin kit. DNA concentration was determined spectrophotometrically (A260 nm). DNA transformation into *E. coli* DH5α and *P. aeruginosa* PAO1 was performed using heat shock protocol and electroporation protocol, as described in (261, 307, 353).

Polymerase chain reaction (PCR) using Taq polymerase. For colony PCR cells were grown on a LB plate and incubated overnight at 37 ^{0}C to obtain single isolated colonies. Template DNA used was either genomic DNA or was prepared by adding small amount of the bacterial colony to 20 µl of sterile nuclease free water in a 0.2 ml microfuge tube. A 25 µl reaction was initiated by adding 15.5 µl of nuclease free water, 2.5 µl of 25 mM $MgCl_2$, 2 µl of 2.5 mM dNTP, 2 µl of 10 x PCR buffer, 0.5 µl of 10 µM forward primer, 0.5 µl of 10 µM reverse primer, 0.5 µl of template (gDNA or colony template DNA), 1.5 µl of 100 % DMSO and 0.25 µl of Taq DNA polymerase. The regular reaction was then subjected to conditions in a T3 Thermocycler (Whatman Biometra, Gottingen, Germany): Initial denaturation at 94 °C for 5 min (1 cycle), denaturation at 94 °C for 45 s, annealing (5 °C lower than the lowest temperature of the primer) for 40 s, extension at 72 °C for 1 min 30s (1 kb/min); step 2-4 repeat for 30 cycles;

final extension at 72 °C for 10 min (1 cycle); and 15 °C indefinitely. The amplified DNA was ran on 1% agarose gel (Agarose gel; See Appendix A) at 120 V and post-stained using Gel red and visualized using GelDoc-It® Imager (UVP, Upland, CA).

Preparation of chemically competent *E. coli* DH5α cells using $CaCl_2$. E. coli DH5α cells were inoculated in 5 ml of LB broth from a frozen glycerol stock and incubated for ~ 14 hours at 37 °C with shaking at 200 rpm. The main culture was inoculated in 1 liter Erlenmeyer flask containing 500 ml LB and incubated at 37 ^{0}C with shaking at 200 rpm. After approximately 3.5 – 4h at an A600 of 0.5-0.6, the culture was transferred to 2 x 500 ml centrifuge bottles and chilled on ice for 10 min with shaking. The cells were then centrifuged at 6,000 g for 5 min at 4 °C and supernatant was discarded completely. Each pellet was resuspended in 125 ml ice cold 0.1 M $CaCl_2$ and combined into a single 500 ml centrifuge bottle. The resuspended cells were centrifuged at 6,000 g for 5 min at 4 ^{0}C. Cell pellet was resuspended in 250 ml ice cold 0.1 M $CaCl_2$ and chilled on ice for 30 min. Cell pellet was harvested by centrifugation at 6,000 g for 5 min at 4 ^{0}C. Post centrifugation, cell pellet was resuspended in 20 ml of ice cold buffer containing 0.1 M $CaCl_2$ and 15% glycerol. 100 µl of cells suspension was aliquoted in each chilled sterile microfuge tubes and stored at -80 ^{0}C.

Table 7.1. Bacterial strains and plasmids used in this study

Strain/plasmid	Relevant Characteristics	Source
Strains		
Escherichia coli		
E. coli DH5α	General purpose cloning strain; *Δ(lacZ)M15*	New England Biolabs
Pseudomonas aeruginosa		
PAO1	Wild type prototroph	(354)
PW3596	PA1429-E05::ISlacZ/hah	(283)
PW9116	PA4825-F12::ISphoA/hah	(283)
PW7241	PA3690-C04::ISlacZ/hah	(283)
PW3911	PA1634-E05::ISlacZ/hah	(283)
PW5099	PA2435-A02::ISphoA/hah	(283)
PW7626	PA3920-G01::ISphoA/hah	(283)
PW3788	PA1549-G12::ISphoA/hah	(283)
PW10412	PA5554-B01::ISlacZ/hah	(283)
PW8565	PA4496-F02::ISphoA/hah	(283)
PW6735	PA3400-H11::ISphoA/hah	(283)
PW7707	PA3963-E02::ISphoA/hah	(283)
PW4602	PA2092-F01::ISlacZ/hah	(283)
PW8230	PA4292-A03::ISphoA/hah	(283)
PW1733	PA0397-E03::ISlacZ/hah	(283)
PW6021	PA2999-D10::ISlacZ/hah	(283)
PW8772	PA4614-B11::ISphoA/hah	(283)
PW9688	PA5167-F06::ISphoA/hah	(283)
PW7791	PA4016-E06::ISphoA/hah	(283)

Δ*carR*::Gm	PAO1 with deletion of *carR* replaced with Gm^r gene	This study
PW1592	PA0320-H07::ISlacZ/hah	(283)
PW1607	PA0327-B11::ISphoA/hah	(283)
PA0327-B11::IS*phoA*/*hah*/ P_{BAD}-PA0327	Tn5 disruption of PA0320 complemented by P_{BAD}-PA0327	This study
PAOJP2	PAO1:: Δ*lasI-rhlI*	(301)
PAO214	PAO1: Δ*lasI*	(301)
PW 3597	PA1430-B10::ISlacZ/hah	(283)
PW6880	PA3476::ISPhoA/hah	(283)
PW 6882	PA3477-B10::ISlacZ/hah	(283)
PW 2798	PA0996-H05::ISlacZ/hah	(283)
PW2812	PA1003-G11::ISlacZ/hah	(283)
PW5376	PA2604-G04::ISPhoA/hah	(283)
pMMB66EH-AEQ	Plasmid containing aequorin gene from *Aequorea victoria*	(306)
pTJ1	Tn7 vector containing P_{BAD} promoter, Tm^r	(355)
pMS402	Expression reporter plasmid carrying the promoterless *luxCDABE* gene, *ori* of pRO1615	(356)
pKD204	pMS402 containing *lasR* promoter cloned upstream of promoterless *luxCDABE* gene in pMS402	(304)
pKD205	pMS402 containing *rhlR* promoter cloned upstream of promoterless *luxCDABE* gene in pMS402	(304)
pKD-*pqsR*	pMS402 containing *pqsR* promoter cloned upstream of promoterless *luxCDABE* gene in pMS402	(305)

Heat-shock transformation into competent *E. coli* cells. Heat shock competent strains of E. coli were transformed with the plasmid construct by the addition of 100 ng of plasmid to 100 µl of E. coli heat shock competent cells and mixed gently by finger flicking. The cells were then incubated on ice for 30 min, heat shocked at 42 °C for exactly 30 s, and then returned to ice for 5 min. Then, 1000 µl of LB was added to the cells, recovered for 1h and 100 µl mix was plated onto an LB-Kn or LB-Ap. Selected transformants were screened for gene of interest by colony PCR using appropriate gene specific primers. The verified *E. coli* clones were grown in 5 ml (LB broth; See Appendix A) containing Kn to generate a permanent stock (750 µl 20 % skim milk plus 750 ml broth culture) which was stored at -80 °C for plasmid maintenance.

Preparation of chemically competent *P. aeruginosa* PAO1 cells using $MgCl_2$. *P. aeruginosa* PAO1 cells were inoculated from frozen stock in LB agar (Appendix A) at 37ºC for 24 h. An overnight culture was started from isolated colony in 5 ml LB broth (Appendix A) at 37 °C for ~ 16hrs with shaking at 200 rpm. 1.25 ml of overnight culture was inoculated into the 250 ml LB in 500 ml Erlenmeyer flask and incubated at 37ºC with shaking at 200 rpm. After approximately 3.5 – 4h at an A600 of 0.5-0.6, the culture was transferred to 250 ml centrifuge bottle and chilled on ice to 4 °C for 10 min. The cells were then centrifuged at 6,000 g for 5 min at 4 °C and supernatant was discarded completely. Cell pellet was washed twice with ice cold 150 mM $MgCl_2$, first with 250 ml and finally with 125 ml. Cell pellets were resuspended in 125 ml of ice cold 150 mM $MgCl_2$ followed by incubation on ice with gentle shaking for 1h. Cells were harvested by centrifugation at 6,000 g for 5 min at 4 ºC. Cell pellet was finally resuspended in 10 ml ice cold 150 mM $MgCl_2$ containing 15% glycerol and mixed gently. The cells were prepared as 500 µl aliquots in sterile microfuge tubes and incubated at 4 ºC for 12-24h. The

competent cells were flash frozen by storing for 1h in pre-chilled ethanol -80 ºC. Cells were then stored at -80 ºC until use.

Heat-shock transformation into competent *P. aeruginosa* cells. Heat shock competent strains of *P. aeruginosa* were transformed with the plasmid construct by the addition of 1µg of plasmid to 200 µl of *E. coli* heat shock competent cells and mixed gently by finger flicking. The cells were then incubated on ice for 1h, heat shocked at 50 °C for exactly 3 min, and then returned to ice for 5 min. Then, 1 ml of LB was added to the cells, recovered for 1h and 100 µl mix was plated onto an LB-Cb or LB-Tm. Selected transformants were screened for gene of interest by colony PCR using appropriate gene specific primers. The verified *P. aeruginosa* clones were grown in 5 ml LB broth (Appendix A) containing Kn to generate a permanent stock (750 µl 20 % skim milk plus 750 ml broth culture) which was stored at -80 °C for plasmid maintenance.

Preparation of electro-competent *P. aeruginosa* cells. *P. aeruginosa* PAO1 cells were grown in 5 ml of LB broth (Appendix A) for ~ 14 hours. Cells were divided in four microcentrifuge tubes in 1.5 ml aliquots and harvested by centrifugation for 2 min at 13,000 rpm at R.T. Each cell pellet was washed twice with 1 ml of 300 mM sucrose at room temperature (RT). Two pellets were combined in a total of 100 µl 300 mM sucrose. Competent cells were stored at RT until transformed with DNA.

Electroporation of electro-competent *P. aeruginosa* cells. For electroporation, 300-500 ng of non-replicative plasmid DNA was added to previously described 100 µl of electro-competent cells and transfer to a 2 mm gap width electroporation cuvette kept at R.T. A pulse at settings: 25 µF; 200 Ohm; 2.5 kV (Setting EC2) was applied on to a Bio-Rad Gene Pulser X

cell™. After pulsing, 1 ml of LB medium was added at once to recover the cells from the electric shock and transferred to a 17 × 100 mm glass tube incubated for 1 h at 37 °C. 100 µl of these cells were spread plated on LB-Tm or LB-Cb for selection of transformed DNA. Selected transformants were screened for verification of desired genotype by colony PCR using appropriate primers. The verified clones were grown in 5 ml LB to generate a permanent stock (750 µl 20 % skim milk plus 750 ml broth culture) which was stored at -80 °C.

Expression and reconstitution of aequorin. *P. aeruginosa* containing aequorin was grown in 5ml BMM (Appendix A) at 37°C, 200 rpm for 12 h. 100 ml sterile BMM in 500 ml flask was inoculated with 1ml overnight culture of OD600 0.25 and incubated at 37°C, 200 rpm until mid-log phase. 1 ml of 100 mM IPTG (Appendix A) was added to the growing culture and incubated for 37°C, 200 rpm for 2 h. Cell pellet was collected by centrifugation at 6,000g for 5 min at 4°C. Cell pellet was washed two times with 100ml ice cold HEPES buffer (Appendix A). Cells were then resuspended in 1.25 ml HEPES buffer. 1 ml cell suspension was aliquoted into fresh microfuge tube and 5 µl of mM coelenterazine was added. Cells were incubated in dark at room temperature for 30 minutes without shaking. Cell pellet was harvested by centrifugation at 6000 g for 5 min at 4°C. Cell pellets were washed two time with 1 ml HEPES buffer and resupended in1ml HEPES buffer. Final cell density was adjusted to OD 600 of 0.4 in a dilution of 1:10 fold.

Table 7.1. PCR primers used in this study.

Name	Sequence (5' → 3')
Aeq-Forward	CTTACATCAGACTTCGACAACCCAAG
Aeq-Reverse	CGTAGAGCTTCTTAGGGCACAG
3393F.f	GAGGCATGGCAACTGGAG
3393F.fr	GACGAAGAACAGCGACAACA
55614R.f	AGCGAACATGAACGCCTC
55614R.r	AAACCACCCTCACCAATGTC
1776F.f	CTGGCTGGACTGGATCTACC
1776F.r	CAGACCGTTGAACACCACC
4904R.f	GCAAGCCTTCGTCAAGCTC
4904R.r	GACGATCGACTTGCCTTCC
40832R.f	GATCAGGATACCGTGGCG
40832R.r	AGTCAAGCAGATCTGGGAGC
29869F.f	GGTGCAGTTCGTCATCGG
29869F.r	GGTGGATGATCTGCGGTC
14969F.f	CCTTCGTCACGGAACTTCTC
14969F.r	TTGAGAACAACGCCTGTGAG
35645R.f	GCCGGTCTTGTCGAAGATTA
35645R.r	TGTGGATCCAGGTGATGATG
32242F.f	CCTGGAAAGCTCCGACTTC
32242F.r	ATTTGGAGAAGTTGTTGCCG
50822R.f	CGGCAGAAGGTGTAGCTGA
50822R.r	CCAGATCCAGCAGGACATCT
45527F.f	CGGTGCACTATTCGCTACG
45527F.r	TTTCTTCGACGACGGCTACT
15965F.f	CTGATCGGCGAGTTCTGG

15965F.r	AGCTCTCGTACATCAGGCGT
33236F.f	CGGTCGACTAGACTCCCAAC
33236F.r	TTTTGTGCATCTTCGACAGC
4823F.f	GAGATCACCTACGAGGACGC
4823F.r	CCTATCCTGTAGGCTGGTGC
15226R.f	ATCGGGCCGTATTCGTACTT
15226R.r	TGCTGTTCACCGACAAGAAG
52423F.f	GCTCCTAATGGCTTGTCAGG
52423F.r	ATGAACCTCAGTCTGACCCG
15226R.f	ATCGGGCCGTATTCGTACTT
15226R.r	TGCTGTTCACCGACAAGAAG
30996F.f	GGACACCCGTCCTCTTCATA
30996F.r	GTGACCTCGTCCATGGTCTT
30095F.f	CCGGCTGGACTACGACAAC
30095F.r	CTCAGGGCATAGAGTTCGCT
5120F.f	CAGCTTCATCAGCCTGCTC
5120F.r	ACTTCAACTACCCACTGGCG
44509F.f	CCAGAGCTTCCGGGTCTT
44509F.r	TCGTCCTTGCTGAAGACGTA
17281R.f	CCGAATCCATATTTGGCTGA
17281R.r	TCAGAGCAATGGCTTCACAC
32454R.f	ACGAGATGGCGGAATGACT
32454R.r	TTCCACCACAAGAACATCCA
3452R.f	GCGTCGAACTTCTTCTGGAT
3452R.r	GTTGTCATAGGGAGGGGGAT
1932F.f	CGCCTCGAACTGTGAGATTT

1932F.r	GAGAAATCGTCGAGCAAAGG
1638R.f	CTGCATGCTGGAATTGCTC
1638R.r	ACTGAAGATCTCCCGCTTCA
49172F.f	GGAAGAGTCTCCCCTTCGAC
49172F.r	TAGAAGAACAGGCGGACGAT
lasR forward	CTGCTCGAGCCGGGCTCGGCCTGTTCT
lasR reverse	CGGGATCCGGATGGCGCTCCACTCCA
rhlR forward	CATGCGCGAGCAGGAGTTGC
rhlR reverse	TAGGGATCCTAATCGAAGCCCAGGCGC
pqsR forward	GGAAGATCTGCGGTGTGCGACTTGCGC
pqsR reverse	ATACTCGAGCGATGCTCGGCGCTCTCC

Luminescence measurements and estimation of free intracellular calcium. 100 µl cell supsension with reconstituted aequorin was aliquoted in 96 well plate. When required, cells were treated with inhibitors (2, 4 di-nitrophenol at 0.5, 1, or 2 mM; $LaCl_3$ at 300 or 600 µM; gramicidin D at 1 or 10 µg/ml; calcimycin at 5 µM; or vanadate at 2 mM) for 10 min in the dark at room temperature without shaking. Gramicidin D and calcimycin were dissolved in 50 % and 3 % DMSO, respectively. To ensure penetration of gramicidin D and calcimycin through the bacterial outer membrane, 10 µg/ml of compound 48/80 was added. Luminescence was recorded for 1 min at 25 ^{0}C at 4 sec interval. After 1 min, 20 µl of 6 mM $CaCl_2$ was injected into each well by using the internal Synergy injectors, mixed for 1 sec, and the luminescence was recorded for 20 min at 5 sec interval. Injection of buffer alone was used as a negative control in $[Ca^{2+}]_{in.}$ $[Ca^{2+}]_{in}$ was calculated by using the formula pCa= 0.612 ($-\log_{10}k$) + 3.745, where k is a rate constant for luminescence decay (s^{-1}) (147). The excel-based template incorporating the formula and the aequorin standard curve was generously shared by Dr. Anthony Campbell. The results were normalized against the total amount of available aequorin. Total aequorin was estimated by summing the light detected during an entire experiment and the light detected during discharge. The discharge was performed by permeabilizing cells by adding 120 µl of discharge buffer (Appendix A). Luminescence was monitored for 5 min at 5 sec interval. The responses to Ca^{2+} challenges were characterized and validated by using curve fitting analysis with IGOR PRO software v.6.3.1.2. (WaveMetrics).

Swarming motility Assay. *P. aeruginosa g*rowing on LB agar plates was inoculated to 5ml of BMM (Appendix A) and incubated at 37°C, 200 rpm for 16 h. Cell density was normalized to OD_{600} of 0.3 using BMM in a final volume of 1ml. Cell suspension was mixed gently to homogeneity. 2µl of the normalized cell culture was spot inoculated in the center of

swarming agar plate containing 0 mM or 5 mM $CaCl_2$ (Appendix A). Plates were incubated up right at 37°C for 12-24h. Pictures of the swarming plates were captured. Five measurements of the diameter of each colony were taken and average diameter was calculated. The effect of Ca^{2+} was calculated as a fold difference (ratio) between the diameters of the colonies grown at 5 mM and 0 mM Ca^{2+}. The mutants and treatments were compared to their corresponding controls using the mean percentage of fold difference from at least three independent experiments.

Calcium tolerance assay in liquid media. Isolated colonies of *P. aeruginosa* were inoculated in 5 ml BMM (Appendix A) and incubated at 37°C, shaking at 200 rpm for 16 h. Cell density of overnight culture was normalized to OD600 of 0.3 using BMM to a final volume of 1 ml. 100 µl (0.1%) of normalized culture was inoculated into 100 ml of fresh BMM in 250 ml flask. Whenever required, $CaCl_2X2H_2O$ was added to a final concentration of 10 mM. Cultures were incubated at 37°C, shaking at 200 rpm in a MaxQ 5000 floor-model shaker (Thermoscientific). Absorbance at 600 nm was recorded every 2- 4 h using a Biomate 3 spectrophotometer (Thermoscientific).

Pyocyanin analysis. *P. aeruginosa g*rowing on LB agar plates was inoculated to 5ml of BMM (Appendix A) and incubated at 37°C, 200 rpm for 16-18 h. Cell density was normalized to OD_{600} of 0.3 using BMM in a final volume of 1ml. Cell suspension was mixed gently to homogeneity. 2µl of the normalized cell culture was spot inoculated in the center of swarming agar plate containing 0 mM or 5 mM $CaCl_2$ (Appendix A). Plates were incubated up right at 37°C for 12-24h. Swarming colonies were excised from the agar. Colony growing on agar was split in two equal halves. One half of the agar was used for pyocyanin extraction and other half for total cell protein estimation. Agar slices of the same size were used as negative controls. For pyocyanin extraction, agar pieces were transferred to a fresh empty plate and 5 ml saline was

added to it. Agar was mashed into fine pieces. Agar pieces were transferred into chloroform resistant scintillation vials. Masher and the plate were washed with 10 ml saline and collected in the same scintillation vial. To the vials, equal volume (15 ml) of chloroform was added and shaken well for 15 min. The vials were left undisturbed for 10 min to allow complete separation of organic and inorganic layers. Top organic phase was collected in fresh vial. Bottom aqueous phase was used for extraction with chloroform two more times. To the collected organic phase, 0.2 N HCl was added in the ratio of 1:3 of HCl:Chloroform. The vials were shaken well for 15 min and left undisturbed for another 15 min to allow the complete separation of organic and inorganic phases. 200 µl of top HCl extract was collected in a 96-well plate and absorbance was measured at 520 nm. Amount of pyocyanin was calculated by using coefficient of extinction 17.1 M^{-1} Cm^{-1} (357) and normalized per mg of total cell protein. The latter was determined by using Bradford assay (EMD) following the manufacture's protocol.

Total cellular protein estimation in agar culture. Half of the swarming agar growth mentioned above was used for protein estimation. For protein extraction, agar pieces were transferred to a fresh empty plate and 5 ml saline was added to it. Agar was mashed into fine pieces and transferred to a 50 ml falcon tube. Masher and the plate were washed with 10 ml saline and collected in the same conical tube. Cell suspension in conical tube was sonicated in water bath sonicator (Branson, 2800) for 5 min followed by brief vortex mix. Sonication and vortex mix was repeated for total of three times. Cell suspension was centrifuged at 2000 rpm for 2 min at 4^0C. Supernatant was collected in a fresh 50ml falcon tube. 15 ml saline was added to the remaining agar pellets followed by sonication and vortex mix as mentioned before. The agar wash was done for total three times. The collected supernatant was filtered through Whatman No. 1 filter paper and collected in a 50 ml centrifuge tube. Finally, the cells were harvested by

centrifugation at 13,000 rpm for 10 min. To the cell suspension, 1.5 ml of 1M NaOH (Appendix A) was added and heated at 90^0C for 10 min. Samples were centrifuged at 10,000 rpm for 5 min and protein sample in the supernatant was collected and diluted 10 fold . The total cellular protein from *P. aeruginosa* was quantified using Bradford protein assay using Bradford reagent (Appendix A) in a 96-well microplate. Protein standards using Bovine serum albumin (BSA) were prepared in the range from 0 µg/ml-125 µg/ml of BSA in water. Briefly, 200 µl of Bradford reagent was added to all wells. For standard and *P. aeruginosa* cellular protein determination, 20 µl of appropriate BSA standards and cellular protein extracts were added to the wells and mixed well. *P. aeruginosa* cellular extracts were diluted appropriately, as needed for the absorbance values to be in the range of the BSA standards. The 96-well plate was incubated at RT for 5 min and absorbance measured at 595 nm using a Synergy 2 Multi-Mode Microplate Reader (BioTek, Winooski, VT). The amount (µg) of total cellular protein from *P. aeruginosa* was estimated by applying the linear equation generated using BSA standards in Microsoft excel.

Extraction and purification of QS signal molecules. *P. aeruginosa* colony *g*rowing on LB agar plates was inoculated to 5 ml of BMM (Appendix A) and incubated at 37°C, 200 rpm for 16 h. Cell density was normalized to OD_{600} of 0.3 using BMM in a final volume of 1 ml. 100 ml sterile BMM in 250 ml flask was inoculated with 100 µl norrmalized overnight culture and incubated at 37°C, 200 rpm until the stationary phase (usually 24 h). When required, $CaCl_2x2H_2O$ was added to a final concentration of 5 mM. Culture was centrifuged at 10,000 rpm for 5 min at 4^0C and 75 ml supernatant was transferred to 250 ml glass separation funnel. The collected supernatant was mixed with equal volume of acidified ethyl acetate (Appendix A) and vigorously shaken for 30 s. The separation funnel was left undisturbed for 10 min so as to allow complete separation of top organic and bottom aqueous phases. Bottom aqueous phase was

collected in a clean flask and top organic phase was collected for sample in a 250 ml bottle. Collected aqueous phase was transferred back to the separation funnel and used for re-extraction with acidified ethyl acetate for two more times. All the organic phases were pooled together in a round bottom flask (RBF). The extract in RBF was evaporated using a rotary evaporator until it dried down to 10-20 ml. Remaining organic phase was transferred to the glass vials and dried down completely using rotary evaporator. Dried extracts were stored in dark at -20^0C until use.

Quantification of QS signal molecules using high performance liquid chromatography (HPLC). 3-O-C12-HSL, C4-HSL, and PQS molecules were separated using HPLC. Dried ethyl acetate extracts from previous step were resuspended in 200 µl of acidified methanol (0.1% acetic acid) (Appendix A). 20 µl sample was injected into C18 reverse phase column (Phenomenex, Gemini, 5µM pore size, 110 A^0 particle size, 150 mm X 2 mm) at a flow rate of 0.2 ml/min. The mobile phase consisted of methanol containing 0.1% v/v glacial acetic acid (solvent B) and water containing 0.1% v/v glacial acetic acid (solvent A) (Appendix A). A gradient elution method was utilized. For C4 HSL detection, gradient started at 5% solvent B and went to 95% solvent B over 30 min and remained isocratic at 95% solvent B for 15 min. For C12 HSL detection, gradient started at 60% solvent B and went to 95% solvent B over --- min and remained isocratic at 95% solvent B for – min. For PQS detection, gradient started at 60% solvent B and went to 100% solvent B over --- min and remained isocratic at ---% solvent B for 15 min. For detection, the following absorbance max were used: 205 nm (for 3-O-C12-HSL and C4-HSL) and 340 nm (for PQS). The standard solutions were prepared by diluting methanol stocks of standards into 300, 100, 50, 25, and 10 uM. Standard curves were generated by plotting the absorbance area value of the standard against the concentration.

Total cellular protein estimation in liquid culture. The total cellular protein from *P. aeruginosa* PAO1 cells was quantified using Bradford protein assay using Bradford reagent (Bradford reagent; See Appendix A) in a 96-well microplate. Protein standards using Bovine serum albumin (BSA) were prepared in the range from 0 µg/ml-750 µg/ml of BSA in 20 mM Tris buffer (pH 8.3) or an appropriate protein storage buffer. Briefly, 200 µl of Bradford reagent was added to all wells. For standard and *P. aeruginosa* PAO1 cellular protein determination, 10 µl of appropriate BSA standards and cellular protein extracts were added to the wells and mixed well. PAO1 cellular extracts were diluted appropriately, as needed for the absorbance values to be in the range of the BSA standards. The 96-well plate was incubated at R.T for 5 min and absorbance measured at 595 nm using a Synergy 2 Multi-Mode Microplate Reader (BioTek, Winooski, VT). The amount (µg) of total cellular protein from *P. aeruginosa* was estimated by applying the linear equation generated using BSA standards in Microsoft excel.

Assessment of gene expression. Isolated colonies of *P. aeruginosa* strains containing *lux*-based reporter plasmids were inoculated in 5 ml BMM (Appendix A) and incubated at 37°C, 200 rpm for 12 h. Cell density was normalize to OD600 of 0.3 by using BMM in final volume of 1 ml. 1ml of fresh BMM was inoculated with 1% (10µl) of normalized overnight culture and mixed well. In order to prevent the evaporation during incubation, lids were treated with triton solution (Appendix A). 10 ml of triton solution was poured over inner side of the lid. Lid was tilted properly to make sure that that entire surface was coated. After draining the triton solution, plate and lid were exposed to UV- light for 20 min. 200 µl of the inoculated culture was aliquoted in white luminescent plates with clear bottom (Greinerbio). Whenever needed, $CaCl_2X2H_2O$ was added to a final concentration of 5 mM. The plates were incubated in a Synergy Mx Multi-Mode Microplate Reader (Biotek) at 37°C in a fast shaking speed. Luminescence and cell density at

OD600 was measured at 2 h interval for 24 h. Gene expression was measured as a relative light intensity (RLUs) and normalized by the respective values of OD600 nm. The resultant expression profiles of mutants were compared to that of the WT using mean fold difference between no added and 5 mM $Ca^{2+}$from at least three biological replicates.

Antibiotic sensitivity assay. *P. aeruginosa* resistance to tobramycin and polymyxin B was assayed as described in (313). PAO1 and PA2604:IS were grown in BMM at no added or 5 mM Ca^{2+}. 100 µl of the mid-log cultures normalized to the OD600 of 0.1 were spread inoculated onto the surface of BMM agar containing no added or 5 mM Ca^{2+}. E-test strips for tobramycin or polymyxin B (Biomeurix) were placed on the surface of the inoculated plates and incubated for 24 h. The minimum inhibitory concentration (MIC) was measured as a point at which the edge of the zone of inhibition crosses the e-test strip. The effect of Ca^{2+} was calculated as a fold difference (ratio) between the MIC in no added or 5mM Ca^{2+}.

REFERENCES

1. **Pitt TL.** 1998. Pseudomonas, Burkholderia, and related genera, vol 2. Oxford University Press Inc., New York, NY.
2. **C. G.** 1984. Classics in infectious diseases. On the blue and green coloration that appears on bandages. Reviews of Infectious Diseases **6:**2.
3. **Lapage SP, Sneath PH, Lessel EF, Skerman V, Seeliger H, Clark W.** 1992. International code of nomenclature of bacteria: bacteriological code, 1990 revision. ASM Press.
4. **Robert S. Breed EGDM, Nathan R. Smith, .** 1957. Bergey's manual of determinative bacteriology, 7 ed. THE WILLIAMS & WILKINS COMPANY, Baltimore.
5. **Tsuji A, Kaneko Y, Takahashi K, Ogawa M, Goto S.** 1982. The effects of temperature and pH on the growth of eight enteric and nine glucose non-fermenting species of gram-negative rods. Microbiol Immunol **26:**15-24.
6. **Lister PD, Wolter DJ, Hanson ND.** 2009. Antibacterial-resistant Pseudomonas aeruginosa: clinical impact and complex regulation of chromosomally encoded resistance mechanisms. Clin Microbiol Rev **22:**582-610.
7. **Sarkisova S, Patrauchan MA, Berglund D, Nivens DE, Franklin MJ.** 2005. Calcium-induced virulence factors associated with the extracellular matrix of mucoid *Pseudomonas aeruginosa* biofilms. J Bacteriol **187:**4327-4337.
8. **Engel J, Eran Y.** 2011. Subversion of mucosal barrier polarity by Pseudomonas aeruginosa. Frontiers in Microbiology **2**.
9. **Gellatly SL, Hancock RE.** 2013. Pseudomonas aeruginosa: new insights into pathogenesis and host defenses. Pathog Dis **67:**159-173.
10. **Stover CK, Pham XQ, Erwin AL, Mizoguchi SD, Warrener P, Hickey MJ, Brinkman FS, Hufnagle WO, Kowalik DJ, Lagrou M, Garber RL, Goltry L, Tolentino E, Westbrock-Wadman S, Yuan Y, Brody LL, Coulter SN, Folger KR, Kas A, Larbig K, Lim R, Smith K, Spencer D, Wong GK, Wu Z, Paulsen IT, Reizer J, Saier MH, Hancock RE, Lory S, Olson MV.** 2000. Complete genome sequence of *Pseudomonas aeruginosa* PAO1, an opportunistic pathogen. Nature **406:**959-964.
11. **Govan JRW, Deretic V.** 1996. Microbial pathogenesis in cystic fibrosis: Mucoid Pseudomonas aeruginosa and Burkholderia cepacia. Microbiological Reviews **60:**539-+.
12. **Oliver A, Canton R, Campo P, Baquero F, Blazquez J.** 2000. High frequency of hypermutable Pseudomonas aeruginosa in cystic fibrosis lung infection. Science **288:**1251-1253.
13. **von Gotz F, Haussler S, Jordan D, Saravanamuthu SS, Wehmhoner D, Strussmann A, Lauber J, Attree I, Buer J, Tummler B, Steinmetz I.** 2004. Expression analysis of a highly adherent and cytotoxic small colony variant of Pseudomonas aeruginosa isolated from a lung of a patient with cystic fibrosis. Journal of Bacteriology **186:**3837-3847.
14. **Fothergill JL, Panagea S, Hart CA, Walshaw MJ, Pitt TL, Winstanley C.** 2007. Widespread pyocyanin over-production among isolates of a cystic fibrosis epidemic strain. Bmc Microbiology **7**.
15. **Smith EE, Buckley DG, Wu ZN, Saenphimmachak C, Hoffman LR, D'Argenio DA, Miller SI, Ramsey BW, Speert DP, Moskowitz SM, Burns JL, Kaul R, Olson MV.** 2006. Genetic adaptation by Pseudomonas aeruginosa to the airways of cystic fibrosis patients. Proceedings of the National Academy of Sciences of the United States of America **103:**8487-8492.

16. **Martin D, Schurr M, Mudd M, Govan J, Holloway B, Deretic V.** 1993. Mechanism of conversion to mucoidy in Pseudomonas aeruginosa infecting cystic fibrosis patients. Proceedings of the National Academy of Sciences **90:**8377-8381.
17. **Otter JA, Yezli S, French GL.** 2011. The Role Played by Contaminated Surfaces in the Transmission of Nosocomial Pathogens. Infection Control and Hospital Epidemiology **32:**687-699.
18. **Roy-Burman A, Savel RH, Racine S, Swanson BL, Revadigar NS, Fujimoto J, Sawa T, Frank DW, Wiener-Kronish JP.** 2001. Type III protein secretion is associated with death in lower respiratory and systemic Pseudomonas aeruginosa infections. Journal of Infectious Diseases **183:**1767-1774.
19. **El Solh AA, Akinnusi ME, Wiener-Kronish JP, Lynch SV, Pineda LA, Szarpa K.** 2008. Persistent infection with Pseudomonas aeruginosa in ventilator-associated pneumonia. American journal of respiratory and critical care medicine **178:**513-519.
20. **Ledizet M, Murray TS, Puttagunta S, Slade MD, Quagliarello VJ, Kazmierczak BI.** 2012. The Ability of Virulence Factor Expression by Pseudomonas aeruginosa to Predict Clinical Disease in Hospitalized Patients. Plos One **7**.
21. **Hauser AR, Cobb E, Bodi M, Mariscal D, Valles J, Engel JN, Rello J.** 2002. Type III protein secretion is associated with poor clinical outcomes in patients with ventilator-associated pneumonia caused by Pseudomonas aeruginosa. Critical Care Medicine **30:**521-528.
22. **Yahr TL, Hovey AK, Kulich SM, Frank DW.** 1995. Transcriptional analysis of the Pseudomonas aeruginosa exoenzyme S structural gene. Journal of bacteriology **177:**1169-1178.
23. **Urbanowski ML, Brutinel ED, Yahr TL.** 2007. Translocation of ExsE into Chinese hamster ovary cells is required for transcriptional induction of the Pseudomonas aeruginosa type III secretion system. Infection and immunity **75:**4432-4439.
24. **Yahr TL, Vallis AJ, Hancock MK, Barbieri JT, Frank DW.** 1998. ExoY, an adenylate cyclase secreted by the Pseudomonas aeruginosa type III system. Proc Natl Acad Sci U S A **95:**13899-13904.
25. **O'Grady EP, Mulcahy H, O'Callaghan J, Adams C, O'Gara F.** 2006. Pseudomonas aeruginosa infection of airway epithelial cells modulates expression of Kruppel-like factors 2 and 6 via RsmA-mediated regulation of type III exoenzymes S and Y. Infect Immun **74:**5893-5902.
26. **Feuillet V, Medjane S, Mondor I, Demaria O, Pagni PP, Galan JE, Flavell RA, Alexopoulou L.** 2006. Involvement of Toll-like receptor 5 in the recognition of flagellated bacteria. Proc Natl Acad Sci U S A **103:**12487-12492.
27. **Mattick JS.** 2002. Type IV pili and twitching motility. Annu Rev Microbiol **56:**289-314.
28. **Bucior I, Pielage JF, Engel JN.** 2012. Pseudomonas aeruginosa pili and flagella mediate distinct binding and signaling events at the apical and basolateral surface of airway epithelium. PLoS Pathog **8:**e1002616.
29. **DiMango E, Zar HJ, Bryan R, Prince A.** 1995. Diverse Pseudomonas aeruginosa gene products stimulate respiratory epithelial cells to produce interleukin-8. Journal of Clinical Investigation **96:**2204.
30. **Partridge JD, Harshey RM.** 2013. Swarming: flexible roaming plans. J Bacteriol **195:**909-918.

31. **Shrout JD, Chopp DL, Just CL, Hentzer M, Givskov M, Parsek MR.** 2006. The impact of quorum sensing and swarming motility on Pseudomonas aeruginosa biofilm formation is nutritionally conditional. Molecular microbiology **62:**1264-1277.
32. **Williams P, Camara M.** 2009. Quorum sensing and environmental adaptation in Pseudomonas aeruginosa: a tale of regulatory networks and multifunctional signal molecules. Curr Opin Microbiol **12:**182-191.
33. **K. Morihara JYH.** 1985. Pseudomonas proteases. CRC Press, Boca Raton, Fla.
34. **Voynow JA, Fischer BM, Zheng S.** 2008. Proteases and cystic fibrosis. Int J Biochem Cell Biol **40:**1238-1245.
35. **Heck LW, Morihara K, Mcrae WB, Miller EJ.** 1986. Specific Cleavage of Human Type-Iii and Iv Collagens by Pseudomonas-Aeruginosa Elastase. Infection and Immunity **51:**115-118.
36. **Heck LW, Alarcon PG, Kulhavy RM, Morihara K, Russell MW, Mestecky JF.** 1990. Degradation of Iga Proteins by Pseudomonas-Aeruginosa Elastase. Journal of Immunology **144:**2253-2257.
37. **Doring G, Obernesser HJ, Botzenhart K.** 1981. [Extracellular toxins of Pseudomonas aeruginosa. II. Effect of two proteases on human immunoglobulins IgG, IgA and secretory IgA (author's transl)]. Zentralbl Bakteriol A **249:**89-98.
38. **Morihara K, Tsuzuki H, Oda K.** 1979. Protease and elastase of Pseudomonas aeruginosa: inactivation of human plasma alpha 1-proteinase inhibitor. Infect Immun **24:**188-193.
39. **Schultz DR, Miller KD.** 1974. Elastase of Pseudomonas aeruginosa: inactivation of complement components and complement-derived chemotactic and phagocytic factors. Infect Immun **10:**128-135.
40. **Mariencheck WI, Alcorn JF, Palmer SM, Wright JR.** 2003. Pseudomonas aeruginosa elastase degrades surfactant proteins A and D. Am J Respir Cell Mol Biol **28:**528-537.
41. **Kessler E, Safrin M, Abrams WR, Rosenbloom J, Ohman DE.** 1997. Inhibitors and specificity of Pseudomonas aeruginosa LasA. J Biol Chem **272:**9884-9889.
42. **Peters JE, Park SJ, Darzins A, Freck LC, Saulnier JM, Wallach JM, Galloway DR.** 1992. Further-Studies on Pseudomonas-Aeruginosa Lasa - Analysis of Specificity. Molecular Microbiology **6:**1155-1162.
43. **Olson JC, Ohman D.** 1992. Efficient production and processing of elastase and LasA by Pseudomonas aeruginosa require zinc and calcium ions. Journal of bacteriology **174:**4140-4147.
44. **Heck LW, Morihara K, Abrahamson DR.** 1986. Degradation of Soluble Laminin and Depletion of Tissue-Associated Basement-Membrane Laminin by Pseudomonas-Aeruginosa Elastase and Alkaline Protease. Infection and Immunity **54:**149-153.
45. **Horvat RT, Parmely MJ.** 1988. Pseudomonas-Aeruginosa Alkaline Protease Degrades Human Gamma-Interferon and Inhibits Its Bioactivity. Infection and Immunity **56:**2925-2932.
46. **Parmely M, Gale A, Clabaugh M, Horvat R, Zhou WW.** 1990. Proteolytic Inactivation of Cytokines by Pseudomonas-Aeruginosa. Infection and Immunity **58:**3009-3014.
47. **Kharazmi A, Hoiby N, Doring G, Valerius NH.** 1984. Pseudomonas-Aeruginosa Exoproteases Inhibit Human Neutrophil Chemi-Luminescence. Infection and Immunity **44:**587-591.

48. **Malloy JL, Veldhuizen RA, Thibodeaux BA, O'Callaghan RJ, Wright JR.** 2005. Pseudomonas aeruginosa protease IV degrades surfactant proteins and inhibits surfactant host defense and biophysical functions. Am J Physiol Lung Cell Mol Physiol **288:**L409-418.
49. **Ochsner UA, Snyder A, Vasil AI, Vasil ML.** 2002. Effects of the twin-arginine translocase on secretion of virulence factors, stress response, and pathogenesis. Proc Natl Acad Sci U S A **99:**8312-8317.
50. **Schmiel DH, Miller VL.** 1999. Bacterial phospholipases and pathogenesis. Microbes Infect **1:**1103-1112.
51. **Terada LS, Johansen KA, Nowbar S, Vasil AI, Vasil ML.** 1999. Pseudomonas aeruginosa hemolytic phospholipase C suppresses neutrophil respiratory burst activity. Infection and immunity **67:**2371-2376.
52. **Barker AP, Vasil AI, Filloux A, Ball G, Wilderman PJ, Vasil ML.** 2004. A novel extracellular phospholipase C of Pseudomonas aeruginosa is required for phospholipid chemotaxis. Molecular Microbiology **53:**1089-1098.
53. **Spencer C, Brown HA.** 2015. Biochemical Characterization of a Pseudomonas aeruginosa Phospholipase D. Biochemistry **54:**1208-1218.
54. **Watnick P, Kolter R.** 2000. Biofilm, city of microbes. J Bacteriol **182:**2675-2679.
55. **Donlan RM.** 2002. Biofilms: microbial life on surfaces. Emerg Infect Dis **8**.
56. **Karatan E, Watnick P.** 2009. Signals, regulatory networks, and materials that build and break bacterial biofilms. Microbiology and Molecular Biology Reviews **73:**310-347.
57. **Flemming H-C, Wingender J.** 2010. The biofilm matrix. Nature Reviews Microbiology **8:**623-633.
58. **Sutherland IW.** 2001. Biofilm exopolysaccharides: a strong and sticky framework. Microbiology **147:**3-9.
59. **Swartjes JJ, Das T, Sharifi S, Subbiahdoss G, Sharma PK, Krom BP, Busscher HJ, van der Mei HC.** 2013. A functional DNase I coating to prevent adhesion of bacteria and the formation of biofilm. Advanced Functional Materials **23:**2843-2849.
60. **Flemming HC, Wingender J.** 2001. Relevance of microbial extracellular polymeric substances (EPSs)--Part II: Technical aspects. Water Sci Technol **43:**9-16.
61. **Høiby N, Ciofu O, Bjarnsholt T.** 2010. Pseudomonas aeruginosa biofilms in cystic fibrosis. Future microbiology **5:**1663-1674.
62. **Bjarnsholt T.** 2013. The role of bacterial biofilms in chronic infections. APMIS **121:**1-58.
63. **Jimenez PN, Koch G, Thompson JA, Xavier KB, Cool RH, Quax WJ.** 2012. The multiple signaling systems regulating virulence in Pseudomonas aeruginosa. Microbiology and Molecular Biology Reviews **76:**46-65.
64. **Heydorn A, Ersboll BK, Hentzer M, Parsek MR, Givskov M, Molin S.** 2000. Experimental reproducibility in flow-chamber biofilms. Microbiology **146 (Pt 10):**2409-2415.
65. **de Kievit TR.** 2009. Quorum sensing in Pseudomonas aeruginosa biofilms. Environ Microbiol **11:**279-288.
66. **Mikkelsen H, Sivaneson M, Filloux A.** 2011. Key two-component regulatory systems that control biofilm formation in Pseudomonas aeruginosa. Environ Microbiol **13:**1666-1681.

67. **Lau GW, Ran HM, Kong FS, Hassett DJ, Mavrodi D.** 2004. Pseudomonas aeruginosa pyocyanin is critical for lung infection in mice. Infection and Immunity **72:**4275-4278.
68. **Muller M.** 2006. Premature cellular senescence induced by pyocyanin, a redox-active Pseudomonas aeruginosa toxin. Free Radical Biology and Medicine **41:**1670-1677.
69. **Wilson R, Pitt T, Taylor G, Watson D, MacDermot J, Sykes D, Roberts D, Cole P.** 1987. Pyocyanin and 1-hydroxyphenazine produced by Pseudomonas aeruginosa inhibit the beating of human respiratory cilia in vitro. Journal of Clinical Investigation **79:**221.
70. **Denning GM, Wollenweber LA, Railsback MA, Cox CD, Stoll LL, Britigan BE.** 1998. Pseudomonas pyocyanin increases interleukin-8 expression by human airway epithelial cells. Infection and immunity **66:**5777-5784.
71. **Denning GM, Railsback MA, Rasmussen GT, Cox CD, Britigan BE.** 1998. Pseudomonas pyocyanine alters calcium signaling in human airway epithelial cells. American Journal of Physiology-Lung Cellular and Molecular Physiology **274:**L893-L900.
72. **Ramos I, Dietrich LE, Price-Whelan A, Newman DK.** 2010. Phenazines affect biofilm formation by Pseudomonas aeruginosa in similar ways at various scales. Research in microbiology **161:**187-191.
73. **Das T, Manefield M.** 2012. Pyocyanin promotes extracellular DNA release in Pseudomonas aeruginosa.
74. **Price-Whelan A, Dietrich LE, Newman DK.** 2006. Rethinking'secondary'metabolism: physiological roles for phenazine antibiotics. Nature chemical biology **2:**71-78.
75. **Cox CD.** 1986. Role of pyocyanin in the acquisition of iron from transferrin. Infect Immun **52:**263-270.
76. **Vasil ML, Ochsner UA.** 1999. The response of Pseudomonas aeruginosa to iron: genetics, biochemistry and virulence. Mol Microbiol **34:**399-413.
77. **Arino S, Marchal R, Vandecasteele J-P.** 1996. Identification and production of a rhamnolipidic biosurfactant by a Pseudomonas species. Applied Microbiology and Biotechnology **45:**162-168.
78. **Sim L, Ward O, Li Z.** 1997. Production and characterisation of a biosurfactant isolated from Pseudomonas aeruginosa UW-1. Journal of Industrial Microbiology and Biotechnology **19:**232-238.
79. **Hastie AT, Hingley ST, Higgins ML, Kueppers F, Shryock T.** 1986. Rhamnolipid from Pseudomonas aeruginosa inactivates mammalian tracheal ciliary axonemes. Cell Motil Cytoskeleton **6:**502-509.
80. **Kownatzki R, Tummler B, Doring G.** 1987. Rhamnolipid of Pseudomonas aeruginosa in sputum of cystic fibrosis patients. Lancet **1:**1026-1027.
81. **Deziel E, Comeau Y, Villemur R.** 2001. Initiation of biofilm formation by Pseudomonas aeruginosa 57RP correlates with emergence of hyperpiliated and highly adherent phenotypic variants deficient in swimming, swarming, and twitching motilities. J Bacteriol **183:**1195-1204.
82. **Boles BR, Thoendel M, Singh PK.** 2005. Rhamnolipids mediate detachment of Pseudomonas aeruginosa from biofilms. Mol Microbiol **57:**1210-1223.
83. **Pamp SJ, Tolker-Nielsen T.** 2007. Multiple roles of biosurfactants in structural biofilm development by Pseudomonas aeruginosa. J Bacteriol **189:**2531-2539.

84. **Patriquin GM, Banin E, Gilmour C, Tuchman R, Greenberg EP, Poole K.** 2008. Influence of quorum sensing and iron on twitching motility and biofilm formation in Pseudomonas aeruginosa. J Bacteriol **190:**662-671.
85. **Schooling S, Charaf U, Allison D, Gilbert P.** 2004. A role for rhamnolipid in biofilm dispersion. Biofilms **1:**91-99.
86. **King JD, Kocíncová D, Westman EL, Lam JS.** 2009. Review: lipopolysaccharide biosynthesis in Pseudomonas aeruginosa. Innate immunity **15:**261-312.
87. **Schultz MJ, Speelman P, Zaat SA, Hack CE, van Deventer SJ, van der Poll T.** 2000. The effect of pseudomonas exotoxin A on cytokine production in whole blood exposed to Pseudomonas aeruginosa. FEMS Immunol Med Microbiol **29:**227-232.
88. **Du X, Youle RJ, FitzGerald DJ, Pastan I.** 2010. Pseudomonas exotoxin A-mediated apoptosis is Bak dependent and preceded by the degradation of Mcl-1. Mol Cell Biol **30:**3444-3452.
89. **Swiatecka-Urban A, Moreau-Marquis S, MacEachran DP, Connolly JP, Stanton CR, Su JR, Barnaby R, O'Toole GA, Stanton BA.** 2006. Pseudomonas aeruginosa inhibits endocytic recycling of CFTR in polarized human airway epithelial cells. American Journal of Physiology-Cell Physiology **290:**C862-C872.
90. **Bomberger JM, Ely KH, Bangia N, Ye SY, Green KA, Green WR, Enelow RI, Stanton BA.** 2014. Pseudomonas aeruginosa Cif Protein Enhances the Ubiquitination and Proteasomal Degradation of the Transporter Associated with Antigen Processing (TAP) and Reduces Major Histocompatibility Complex (MHC) Class I Antigen Presentation. Journal of Biological Chemistry **289:**152-162.
91. **MacEachran DP, Ye S, Bomberger JM, Hogan DA, Swiatecka-Urban A, Stanton BA, O'Toole GA.** 2007. The Pseudomonas aeruginosa secreted protein PA2934 decreases apical membrane expression of the cystic fibrosis transmembrane conductance regulator. Infection and immunity **75:**3902-3912.
92. **Ye S, MacEachran DP, Hamilton JW, O'Toole GA, Stanton BA.** 2008. Chemotoxicity of doxorubicin and surface expression of P-glycoprotein (MDR1) is regulated by the Pseudomonas aeruginosa toxin Cif. American Journal of Physiology-Cell Physiology **295:**C807-C818.
93. **Bahl CD, MacEachran DP, O'Toole GA, Madden DR.** 2009. Purification, crystallization and preliminary X-ray diffraction analysis of Cif, a virulence factor secreted by Pseudomonas aeruginosa. Acta Crystallographica Section F: Structural Biology and Crystallization Communications **66:**26-28.
94. **Painter RG, Bonvillain RW, Valentine VG, Lombard GA, LaPlace SG, Nauseef WM, Wang G.** 2008. The role of chloride anion and CFTR in killing of Pseudomonas aeruginosa by normal and CF neutrophils. Journal of leukocyte biology **83:**1345-1353.
95. **Bonvillain RW, Painter RG, Adams DE, Viswanathan A, Lanson NA, Wang G.** 2010. RNA interference against CFTR affects HL60-derived neutrophil microbicidal function. Free Radical Biology and Medicine **49:**1872-1880.
96. **Waters CM, Bassler BL.** 2005. Quorum sensing: cell-to-cell communication in bacteria. Annu Rev Cell Dev Biol **21:**319-346.
97. **Gambello MJ, Iglewski BH.** 1991. Cloning and characterization of the Pseudomonas aeruginosa lasR gene-Aeruginosa Lasr Gene, a Transcriptional Activator of Elastase Expression. Journal of Bacteriology **173:**3000-3009.

98. **Pearson JP, Passador L, Iglewski BH, Greenberg EP.** 1995. A second N-acylhomoserine lactone signal produced by Pseudomonas aeruginosa. Proc Natl Acad Sci U S A **92:**1490-1494.
99. **Pesci EC, Milbank JB, Pearson JP, McKnight S, Kende AS, Greenberg EP, Iglewski BH.** 1999. Quinolone signaling in the cell-to-cell communication system of Pseudomonas aeruginosa. Proc Natl Acad Sci U S A **96:**11229-11234.
100. **Schuster M, Lostroh CP, Ogi T, Greenberg EP.** 2003. Identification, timing, and signal specificity of Pseudomonas aeruginosa quorum-controlled genes: a transcriptome analysis. J Bacteriol **185:**2066-2079.
101. **Wagner VE, Bushnell D, Passador L, Brooks AI, Iglewski BH.** 2003. Microarray analysis of Pseudomonas aeruginosa quorum-sensing regulons: effects of growth phase and environment. J Bacteriol **185:**2080-2095.
102. **Juhas M, Eberl L, Tummler B.** 2005. Quorum sensing: the power of cooperation in the world of Pseudomonas. Environmental Microbiology **7:**459-471.
103. **Gooderham WJ, Hancock RE.** 2009. Regulation of virulence and antibiotic resistance by two-component regulatory systems in *Pseudomonas aeruginosa*. FEMS Microbiol Rev **33:**279-294.
104. **Hoch JA.** 2000. Two-component and phosphorelay signal transduction. Curr Opin Microbiol **3:**165-170.
105. **Cao Q, Wang Y, Chen F, Xia Y, Lou J, Zhang X, Yang N, Sun X, Zhang Q, Zhuo C.** 2014. A Novel signal transduction pathway that modulates rhl quorum sensing and bacterial virulence in Pseudomonas aeruginosa.
106. **McPhee JB, Bains M, Winsor G, Lewenza S, Kwasnicka A, Brazas MD, Brinkman FS, Hancock RE.** 2006. Contribution of the PhoP-PhoQ and PmrA-PmrB two-component regulatory systems to Mg2+-induced gene regulation in *Pseudomonas aeruginosa*. J Bacteriol **188:**3995-4006.
107. **McPhee JB, Lewenza S, Hancock RE.** 2003. Cationic antimicrobial peptides activate a two-component regulatory system, PmrA-PmrB, that regulates resistance to polymyxin B and cationic antimicrobial peptides in Pseudomonas aeruginosa. Mol Microbiol **50:**205-217.
108. **Moskowitz SM, Ernst RK, Miller SI.** 2004. PmrAB, a two-component regulatory system of Pseudomonas aeruginosa that modulates resistance to cationic antimicrobial peptides and addition of aminoarabinose to lipid A. Journal of bacteriology **186:**575-579.
109. **Miller AK, Brannon MK, Stevens L, Johansen HK, Selgrade SE, Miller SI, Høiby N, Moskowitz SM.** 2011. PhoQ mutations promote lipid A modification and polymyxin resistance of Pseudomonas aeruginosa found in colistin-treated cystic fibrosis patients. Antimicrobial agents and chemotherapy **55:**5761-5769.
110. **Gooderham WJ, Gellatly SL, Sanschagrin F, McPhee JB, Bains M, Cosseau C, Levesque RC, Hancock RE.** 2009. The sensor kinase PhoQ mediates virulence in *Pseudomonas aeruginosa*. Microbiology **155:**699-711.
111. **Albus AM, Pesci EC, Runyen-Janecky LJ, West SE, Iglewski BH.** 1997. Vfr controls quorum sensing in Pseudomonas aeruginosa. J Bacteriol **179:**3928-3935.
112. **Beatson SA, Whitchurch CB, Sargent JL, Levesque RC, Mattick JS.** 2002. Differential regulation of twitching motility and elastase production by Vfr in Pseudomonas aeruginosa. Journal of bacteriology **184:**3605-3613.

113. **Dasgupta N, Ferrell EP, Kanack KJ, West SE, Ramphal R.** 2002. fleQ, the gene encoding the major flagellar regulator of Pseudomonas aeruginosa, is σ70 dependent and is downregulated by Vfr, a homolog of Escherichia coli cyclic AMP receptor protein. Journal of bacteriology **184:**5240-5250.
114. **Fulcher NB, Holliday PM, Klem E, Cann MJ, Wolfgang MC.** 2010. The Pseudomonas aeruginosa Chp chemosensory system regulates intracellular cAMP levels by modulating adenylate cyclase activity. Molecular microbiology **76:**889-904.
115. **Inclan YF, Huseby MJ, Engel JN.** 2011. FimL regulates cAMP synthesis in Pseudomonas aeruginosa.
116. **Jones AK, Fulcher NB, Balzer GJ, Urbanowski ML, Pritchett CL, Schurr MJ, Yahr TL, Wolfgang MC.** 2010. Activation of the Pseudomonas aeruginosa AlgU regulon through mucA mutation inhibits cyclic AMP/Vfr signaling. Journal of bacteriology **192:**5709-5717.
117. **Diaz MR, King JM, Yahr TL.** 2011. Intrinsic and extrinsic regulation of type III secretion gene expression in Pseudomonas aeruginosa. Frontiers in Microbiology **2**.
118. **Kulasekara HD, Ventre I, Kulasekara BR, Lazdunski A, Filloux A, Lory S.** 2005. A novel two-component system controls the expression of Pseudomonas aeruginosa fimbrial cup genes. Molecular Microbiology **55:**368-380.
119. **Hickman JW, Tifrea DF, Harwood CS.** 2005. A chemosensory system that regulates biofilm formation through modulation of cyclic diguanylate levels. Proceedings of the National Academy of Sciences of the United States of America **102:**14422-14427.
120. **Kaufmann GF, Sartorio R, Lee S-H, Mee JM, Altobell LJ, Kujawa DP, Jeffries E, Clapham B, Meijler MM, Janda KD.** 2006. Antibody interference with N-acyl homoserine lactone-mediated bacterial quorum sensing. Journal of the American Chemical Society **128:**2802-2803.
121. **Kazmierczak BI, Lebron MB, Murray TS.** 2006. Analysis of FimX, a phosphodiesterase that governs twitching motility in Pseudomonas aeruginosa. Molecular microbiology **60:**1026-1043.
122. **Hickman JW, Harwood CS.** 2008. Identification of FleQ from Pseudomonas aeruginosa as ac-di-GMP-responsive transcription factor. Molecular microbiology **69:**376-389.
123. **Kim HY, Schlictman D, Shankar S, Xie Z, Chakrabarty A, Kornberg A.** 1998. Alginate, inorganic polyphosphate, GTP and ppGpp synthesis co-regulated in Pseudomonas aeruginosa: implications for stationary phase survival and synthesis of RNA/DNA precursors. Molecular microbiology **27:**717-725.
124. **Beare PA, For RJ, Martin LW, Lamont IL.** 2003. Siderophore-mediated cell signalling in Pseudomonas aeruginosa: divergent pathways regulate virulence factor production and siderophore receptor synthesis. Molecular microbiology **47:**195-207.
125. **Dietrich LEP, Price-Whelan A, Petersen A, Whiteley M, Newman DK.** 2006. The phenazine pyocyanin is a terminal signalling factor in the quorum sensing network of Pseudomonas aeruginosa. Molecular Microbiology **61:**1308-1321.
126. **Hancock RE.** 1998. Resistance mechanisms in Pseudomonas aeruginosa and other nonfermentative gram-negative bacteria. Clinical Infectious Diseases **27:**S93-S99.
127. **Livermore DM.** 2002. Multiple mechanisms of antimicrobial resistance in Pseudomonas aeruginosa: our worst nightmare? Clin Infect Dis **34:**634-640.

128. **Schweizer HP.** 2003. Efflux as a mechanism of resistance to antimicrobials in Pseudomonas aeruginosa and related bacteria: unanswered questions. Genet Mol Res **2:**48-62.
129. **Breidenstein EBM, de la Fuente-Nunez C, Hancock REW.** 2011. Pseudomonas aeruginosa: all roads lead to resistance. Trends in Microbiology **19:**419-426.
130. **Sacha P, Wieczorek P, Hauschild T, Zórawski M, Olszańska D, Tryniszewska E.** 2008. Metallo-beta-lactamases of Pseudomonas aeruginosa--a novel mechanism resistance to beta-lactam antibiotics. Folia Histochemica et cytobiologica **46:**137-136.
131. **Matsuo Y, Eda S, Gotoh N, Yoshihara E, Nakae T.** 2004. MexZ-mediated regulation of mexXY multidrug efflux pump expression in Pseudomonas aeruginosa by binding on the mexZ-mexX intergenic DNA. FEMS Microbiol Lett **238:**23-28.
132. **Masuda N, Sakagawa E, Ohya S, Gotoh N, Tsujimoto H, Nishino T.** 2000. Contribution of the MexX-MexY-oprM efflux system to intrinsic resistance in Pseudomonas aeruginosa. Antimicrob Agents Chemother **44:**2242-2246.
133. **Permyakov EA, Kretsinger RH.** 2009. Cell signaling, beyond cytosolic calcium in eukaryotes. J Inorg Biochem **103:**77-86.
134. **Ikura M, Osawa M, Ames JB.** 2002. The role of calcium-binding proteins in the control of transcription: structure to function. Bioessays **24:**625-636.
135. **Berridge MJ, Bootman MD, Roderick HL.** 2003. Calcium signalling: dynamics, homeostasis and remodelling. Nat Rev Mol Cell Biol **4:**517-529.
136. **Berridge MJ, Lipp P, Bootman MD.** 2000. The versatility and universality of calcium signalling. Nat Rev Mol Cell Biol **1:**11-21.
137. **Sanders D, Brownlee C, Harper JF.** 1999. Communicating with calcium. Plant Cell **11:**691-706.
138. **Campbell AK.** 1983. Intracellular calcium, its universal role as regulator. Wiley, Chichester, New York.
139. **Clapham DE.** 2007. Calcium signaling. Cell **131:**1047-1058.
140. **Zampese E, Pizzo P.** 2012. Intracellular organelles in the saga of Ca^{2+} homeostasis: different molecules for different purposes? Cell Mol Life Sci **69:**1077-1104.
141. **Gilabert JA.** 2012. Cytoplasmic calcium buffering. Adv Exp Med Biol **740:**483-498.
142. **Straley SC, Plano GV, Skrzypek E, Haddix PL, Fields KA.** 1993. Regulation by Ca2+ in the Yersinia low-Ca2+ response. Mol Microbiol **8:**1005-1010.
143. **Tisa LS, Adler J.** 1995. Cytoplasmic free-Ca2+ level rises with repellents and falls with attractants in Escherichia coli chemotaxis. Proc Natl Acad Sci U S A **92:**10777-10781.
144. **Hu Y, Zhang X, Shi Y, Zhou Y, Zhang W, Su XD, Xia B, Zhao J, Jin C.** 2011. Structures of Anabaena calcium-binding protein CcbP: insights into Ca2+ signaling during heterocyst differentiation. J Biol Chem **286:**12381-12388.
145. **Rosch JW, Sublett J, Gao G, Wang YD, Tuomanen EI.** 2008. Calcium efflux is essential for bacterial survival in the eukaryotic host. Mol Microbiol **70:**435-444.
146. **Herbaud ML, Guiseppi A, Denizot F, Haiech J, Kilhoffer MC.** 1998. Calcium signalling in Bacillus subtilis. Biochim Biophys Acta **1448:**212-226.
147. **Jones HE, Holland IB, Baker HL, Campbell AK.** 1999. Slow changes in cytosolic free Ca2+ in *Escherichia coli* highlight two putative influx mechanisms in response to changes in extracellular calcium. Cell Calcium **25:**265-274.

148. **Torrecilla I, Leganes F, Bonilla I, Fernandez-Pinas F.** 2000. Use of recombinant aequorin to study calcium homeostasis and monitor calcium transients in response to heat and cold shock in cyanobacteria. Plant Physiol **123:**161-176.
149. **Knight MR, Campbell AK, Smith SM, Trewavas AJ.** 1991. Recombinant Aequorin as a Probe for Cytosolic Free Ca^{2+} in *Escherichia coli*. FEBS Lett **282:**405-408.
150. **Leganes F, Forchhammer K, Fernandez-Pinas F.** 2009. Role of calcium in acclimation of the cyanobacterium *Synechococcus elongatus* PCC 7942 to nitrogen starvation. Microbiology **155:**25-34.
151. **Campbell AK, Naseem R, Wann K, Holland IB, Matthews SB.** 2007. Fermentation product butane 2,3-diol induces Ca2+ transients in E. coli through activation of lanthanum-sensitive Ca2+ channels. Cell Calcium **41:**97-106.
152. **Naseem R, Wann KT, Holland IB, Campbell AK.** 2009. ATP regulates calcium efflux and growth in *E. coli*. J Mol Biol **391:**42-56.
153. **Oomes SJ, Jonker MJ, Wittink FR, Hehenkamp JO, Breit TM, Brul S.** 2009. The effect of calcium on the transcriptome of sporulating B. subtilis cells. Int J Food Microbiol **133:**234-242.
154. **Bilecen K, Yildiz FH.** 2009. Identification of a calcium-controlled negative regulatory system affecting *Vibrio cholerae* biofilm formation. Environ Microbiol **11:**2015-2029.
155. **Dominguez DC, Lopes R, Holland IB, Campbell AK.** 2011. Proteome analysis of B. subtilis in response to calcium

J Anal Bioanal Techniques doi:10.4172/2155-9872.S6-001**:**1-9.
156. **Patrauchan MA, Sarkisova SA, Franklin MJ.** 2007. Strain-specific proteome responses of *Pseudomonas aeruginosa* to biofilm-associated growth and to calcium. Microbiology **153:**3838-3851.
157. **Gode-Potratz CJ, Chodur DM, McCarter LL.** 2010. Calcium and iron regulate swarming and type III secretion in *Vibrio parahaemolyticus*. J Bacteriol **192:**6025-6038.
158. **Trombe MC.** 1993. Characterization of a calcium porter of Streptococcus pneumoniae involved in calcium regulation of growth and competence. J Gen Microbiol **139:**433-439.
159. **Tisa LS.** 1998. Calcium transport by Frankia sp. strain EAN1pec. Curr Microbiol **37:**12-16.
160. **Matsushita T, Hirata H, Kusaka I.** 1989. Calcium channels in bacteria: purification and characterization. Ann N Y Acad Sci **560:**426-429.
161. **Kanamaru K, Kashiwagi S, Mizuno T.** 1993. The cyanobacterium, *Synechococcus* sp. PCC7942, possesses two distinct genes encoding cation-transporting P-type ATPases. FEBS Lett **330:**99-104.
162. **Ambudkar SV, Lynn AR, Maloney PC, Rosen BP.** 1986. Reconstitution of ATP-Dependent calcium transport from streptococci. J Biol Chem **261:**15596-15600.
163. **Houng HS, Lynn AR, Rosen BP.** 1986. ATP-driven calcium transport in membrane vesicles of Streptococcus sanguis. J Bacteriol **168:**1040-1044.
164. **Naseem R, Holland IB, Jacq A, Wann KT, Campbell AK.** 2008. pH and monovalent cations regulate cytosolic free $Ca^{(2+)}$ in *E. coli*. Biochim Biophys Acta **1778:**1415-1422.
165. **Ohyama T, Igarashi K, Kobayashi H.** 1994. Physiological role of the chaA gene in sodium and calcium circulations at a high pH in Escherichia coli. J Bacteriol **176:**4311-4315.

166. **Nazarenko LV, Andreev IM, Lyukevich AA, Pisareva TV, Los DA.** 2003. Calcium release from Synechocystis cells induced by depolarization of the plasma membrane: MscL as an outward Ca2+ channel. Microbiology **149:**1147-1153.
167. **Chang Y, Bruni R, Kloss B, Assur Z, Kloppmann E, Rost B, Hendrickson WA, Liu Q.** 2014. Structural basis for a pH-sensitive calcium leak across membranes. Science **344:**1131-1135.
168. **Palmgren MG, Axelsen KB.** 1998. Evolution of P-type ATPases. Biochim Biophys Acta **1365:**37-45.
169. **Geisler M, Koenen W, Richter J, Schumann J.** 1998. Expression and characterization of a Synechocystis PCC 6803 P-type ATPase in E. coli plasma membranes. Biochim Biophys Acta **1368:**267-275.
170. **Geisler M, Richter J, Schumann J.** 1993. Molecular cloning of a P-type ATPase gene from the cyanobacterium Synechocystis sp. PCC 6803. Homology to eukaryotic Ca(2+)-ATPases. J Mol Biol **234:**1284-1289.
171. **Peiffer WE, Desrosiers MG, Menick DR.** 1996. Cloning and expression of the unique Ca2+-ATPase from Flavobacterium odoratum. J Biol Chem **271:**5095-5100.
172. **Hein KL, Nissen P, Morth JP.** 2012. Purification, crystallization and preliminary crystallographic studies of a PacL homologue from Listeria monocytogenes. Acta Crystallogr Sect F Struct Biol Cryst Commun **68:**424-427.
173. **Faxen K, Andersen JL, Gourdon P, Fedosova N, Morth JP, Nissen P, Moller JV.** 2011. Characterization of a Listeria monocytogenes Ca(2+) pump: a SERCA-type ATPase with only one Ca(2+)-binding site. J Biol Chem **286:**1609-1617.
174. **Raeymaekers L, Wuytack E, Willems I, Michiels CW, Wuytack F.** 2002. Expression of a P-type $Ca^{(2+)}$-transport ATPase in *Bacillus subtilis* during sporulation. Cell Calcium **32:**93.
175. **Berkelman T, Garret-Engele P, Hoffman NE.** 1994. The pacL gene of Synechococcus sp. strain PCC 7942 encodes a Ca(2+)-transporting ATPase. J Bacteriol **176:**4430-4436.
176. **Rosen BP.** 1987. Bacterial calcium transport. Biochim Biophys Acta **906:**101-110.
177. **Matsushita T, Ueda T, Kusaka I.** 1986. Purification and characterization of Ca2+/H+ antiporter from Bacillus subtilis. Eur J Biochem **156:**95-100.
178. **Waditee R, Hossain GS, Tanaka Y, Nakamura T, Shikata M, Takano J, Takabe T, Takabe T.** 2004. Isolation and functional characterization of Ca2+/H+ antiporters from cyanobacteria. J Biol Chem **279:**4330-4338.
179. **Brey RN, Rosen BP.** 1979. Cation/proton antiport systems in Escherichia coli. Properties of the calcium/proton antiporter. J Biol Chem **254:**1957-1963.
180. **van Veen HW, Abee T, Kortstee GJ, Konings WN, Zehnder AJ.** 1994. Translocation of metal phosphate via the phosphate inorganic transport system of Escherichia coli. Biochemistry **33:**1766-1770.
181. **Fujisawa M, Wada Y, Tsuchiya T, Ito M.** 2009. Characterization of Bacillus subtilis YfkE (ChaA): a calcium-specific Ca2+/H+ antiporter of the CaCA family. Arch Microbiol **191:**649-657.
182. **Radchenko MV, Tanaka K, Waditee R, Oshimi S, Matsuzaki Y, Fukuhara M, Kobayashi H, Takabe T, Nakamura T.** 2006. Potassium/proton antiport system of *Escherichia coli*. J Biol Chem **281:**19822-19829.

183. **Bolhuis H, van Veen HW, Brands JR, Putman M, Poolman B, Driessen AJ, Konings WN.** 1996. Energetics and mechanism of drug transport mediated by the lactococcal multidrug transporter LmrP. J Biol Chem **271:**24123-24128.
184. **Schaedler TA, Tong Z, van Veen HW.** 2012. The multidrug transporter LmrP protein mediates selective calcium efflux. J Biol Chem **287:**27682-27690.
185. **Van Veen HW, Abee T, Kortstee GJ, Konings WN, Zehnder AJ.** 1993. Characterization of two phosphate transport systems in Acinetobacter johnsonii 210A. J Bacteriol **175:**200-206.
186. **Kay WW, Ghei OK.** 1981. Inorganic cation transport and the effects on C4 dicarboxylate transport in *Bacillus subtilis*. Can J Microbiol **27:**1194-1201.
187. **Dasgupta N, Ashare A, Hunninghake GW, Yahr TL.** 2006. Transcriptional induction of the Pseudomonas aeruginosa type III secretion system by low Ca2+ and host cell contact proceeds through two distinct signaling pathways. Infect Immun **74:**3334-3341.
188. **Sarkisova SA, Lotlikar SR, Guragain M, Kubat R, Cloud J, Franklin MJ, Patrauchan MA.** 2014. A Pseudomonas aeruginosa EF-Hand Protein, EfhP (PA4107), Modulates Stress Responses and Virulence at High Calcium Concentration. Plos One **9**.
189. **Liu L, Ridefelt P, Hakansson L, Venge P.** 1999. Regulation of human eosinophil migration across lung epithelial monolayers by distinct calcium signaling mechanisms in the two cell types. Journal of immunology (Baltimore, Md **163:**5649-5655.
190. **Halmerbauer G, Arri S, Schierl M, Strauch E, Koller DY.** 2000. The relationship of eosinophil granule proteins to ions in the sputum of patients with cystic fibrosis. Clinical and Experimental Allergy **30:**1771-1776.
191. **Lorin MI, Gaerlan PF, Mandel ID, Denning CR.** 1976. Composition of nasal secretion in patients with cystic fibrosis. J Lab Clin Med **88:**114-117.
192. **Dominguez DC.** 2004. Calcium signalling in bacteria. Mol Microbiol **54:**291-297.
193. **Dominguez DC, Lopes R, Holland IB, Campbell AK.** 2011. Proteome analysis of B. subtilis in response to calcium

J Anal Bioanal Techniques **S6**.
194. **Futsaether CM, Johnsson A.** 1994. Using fura-2 to measure intracellular free calcium in *Propionibacterium acnes*. Can J Microbiol **40:**439-445.
195. **Campbell AK, Naseern R, Holland IB, Matthews SB, Wann KT.** 2007. Methylglyoxal and other carbohydrate metabolites induce lanthanum-sensitive Ca^{2+} transients and inhibit growth in *E.coli*. Archives of Biochemistry and Biophysics **468:**107-113.
196. **Palmgren MG, Nissen P.** 2011. P-type ATPases. Annu Rev Biophys **40:**243-266.
197. **Berkelman T, Garret-engele P, Hoffman NE.** 1994. The Pacl gene of *Synechococcus* Sp strain Pcc-7942 encodes a Ca^{2+}-transporting Atpase. J Bacteriol **176:**4430-4436.
198. **Raeymaekers L, Wuytack EY, Willems I, Michiels CW, Wuytack F.** 2002. Expression of a P-type Ca^{2+}-transport ATPase in *Bacillus subtilis* during sporulation. Cell Calcium **32:**93-103.
199. **Desrosiers MG, Gately LJ, Gambel AM, Menick DR.** 1996. Purification and characterization of the Ca^{2+}-ATPase of *Flavobacterium odoratum*. J Biol Chem **271:**3945-3951.
200. **Nouwens AS, Cordwell SJ, Larsen MR, Molloy MP, Gillings M, Willcox MD, Walsh BJ.** 2000. Complementing genomics with proteomics: the membrane subproteome of Pseudomonas aeruginosa PAO1. Electrophoresis **21:**3797-3809.

201. **Campbell AK S-NG (ed).** 1993. Bioluminescent and chemiluminescent indicators for molecular signalling and function in living cells. Academic Press, New York.
202. **Irani VR, Rowe JJ.** 1997. Enhancement of transformation in *Pseudomonas aeruginosa* PAO1 by Mg2+ and heat. Biotechniques **22:**54-56.
203. **Katsu T, Kobayashi H, Fujita Y.** 1986. Mode of Action of Gramicidin S on *Escherichia coli* Membrane. Biochim Biophys Acta **860:**608-619.
204. **Valentini M, Storelli N, Lapouge K.** 2011. Identification of C(4)-dicarboxylate transport systems in *Pseudomonas aeruginosa* PAO1. J Bacteriol **193:**4307-4316.
205. **Lewinson O, Lee AT, Rees DC.** 2009. A P-type ATPase importer that discriminates between essential and toxic transition metals. Proceedings of the National Academy of Sciences of the United States of America **106:**4677-4682.
206. **Chan H, Babayan V, Blyumin E, Gandhi C, Hak K, Harake D, Kumar K, Lee P, Li TT, Liu HY, Lo TC, Meyer CJ, Stanford S, Zamora KS, Saier MH, Jr.** 2010. The p-type ATPase superfamily. J Mol Microbiol Biotechnol **19:**5-104.
207. **Pressman BC.** 1976. Biological application of ionophores. Annual Review of Biochemistry **45:**501-530.
208. **Burkhart BM, Langs DA, Pangborn WA, Duax WL, Pletnev V, Gassman RM.** 1999. Gramicidin D conformation, dynamics and membrane ion transport. Biopolymers **51:**129-144.
209. **Jarrell KF, Hamilton EA.** 1985. Effect of gramicidin on methanogenesis by various methanogenic bacteria. Appl Environ Microbiol **50:**179-182.
210. **Reusch RN, Huang RP, Bramble LL.** 1995. Poly-3-hydroxybutyrate polyphosphate complexes from voltage activated Ca2+ channels in the plasma membranes of *Escherichia coli*. Biophysical Journal **69:**754-766.
211. **Luterbacher S, Schatzmann HJ.** 1983. The site of action of La^{3+} in the reaction cycle of the human red cell membrane Ca^{2+}-pump ATPase. Experientia **39:**311-312.
212. **Kuhlbrandt W.** 2004. Biology, structure and mechanism of P-type ATPases. Nature Reviews Molecular Cell Biology **5:**282-295.
213. **Pezza RJ, Villarreal MA, Montich GG, Argarana CE.** 2002. Vanadate inhibits the ATPase activity and DNA binding capability of bacterial MutS. A structural model for the vanadate-MutS interaction at the Walker A motif. Nucleic Acids Res **30:**4700-4708.
214. **Gambel AM, Desrosiers MG, Menick DR.** 1992. Characterization of a P-type $Ca^{(2+)}$-ATPase from *Flavobacterium odoratum*. J Biol Chem **267:**15923-15931.
215. **Bhattacharyya P, Barnes EM, Jr.** 1976. ATP-dependent calcium transport in isolated membrane vesicles from *Azotobacter vinelandii*. J Biol Chem **251:**56-14-59.
216. **Bers DM, Eisner DA, Valdivia HH.** 2003. Sarcoplasmic reticulum Ca^{2+} and heart failure - Roles of diastolic leak and Ca^{2+} transport. Circulation Research **93:**487-490.
217. **Magyar CE, White KE, Rojas R, Apodaca G, Friedman PA.** 2002. Plasma membrane Ca^{2+}-ATPase and NCX1 Na^{+}/Ca^{2+} exchanger expression in distal convoluted tubule cells. Am J Physiol Renal Physiol **283:**F29-40.
218. **Budde CF, Mahan AE, Lu J, Rha C, Sinskey AJ.** 2010. Roles of multiple acetoacetyl coenzyme A reductases in polyhydroxybutyrate biosynthesis in *Ralstonia eutropha* H16. J Bacteriol **192:**5319-5328.
219. **Booth IR, Edwards MD, Black S, Schumann U, Miller S.** 2007. Mechanosensitive channels in bacteria: signs of closure? Nat Rev Microbiol **5:**431-440.

220. **Sakai M, Futamata H, Kanazawa S.** 2003. Effects of high concentrations of inorganic salts on swarming ability in fluorescent *Pseudomonas* strains. Bioscience Biotechnology and Biochemistry **67:**1479-1484.
221. **Yeung AT, Torfs EC, Jamshidi F, Bains M, Wiegand I, Hancock RE, Overhage J.** 2009. Swarming of *Pseudomonas aeruginosa* is controlled by a broad spectrum of transcriptional regulators, including MetR. J Bacteriol **191:**5592-5602.
222. **Ambudkar SV, Zlotnick GW, Rosen BP.** 1984. Calcium efflux from *Escherichia coli*. Evidence for two systems. J Biol Chem **259:**6142-6146.
223. **Zhao GJ, Hong GL, Liu JQ, Lu Y, Lu ZQ.** 2014. Septic shock due to community-acquired *Pseudomonas aeruginosa* necrotizing fasciitis: A case report and literature review. Experimental and Therapeutic Medicine **7:**1545-1548.
224. **Lakkis C, Fleiszig SM.** 2001. Resistance of *Pseudomonas aeruginosa* isolates to hydrogel contact lens disinfection correlates with cytotoxic activity. J Clin Microbiol **39:**1477-1486.
225. **Silby MW, Winstanley C, Godfrey SA, Levy SB, Jackson RW.** 2011. Pseudomonas genomes: diverse and adaptable. FEMS Microbiol Rev **35:**652-680.
226. **Guragain M, Lenaburg DL, Moore FS, Reutlinger I, Patrauchan MA.** 2013. Calcium homeostasis in Pseudomonas aeruginosa requires multiple transporters and modulates swarming motility. Cell Calcium **54:**350-361.
227. **Anderson S, Appanna VD, Huang J, Viswanatha T.** 1992. A novel role for calcite in calcium homeostasis. FEBS Lett **308:**94-96.
228. **Glunk C, Dupraz C, Braissant O, Gallagher KL, Verrecchia EP, Visscher PT.** 2011. Microbially mediated carbonate precipitation in a hypersaline lake, Big Pond (Eleuthera, Bahamas). Sedimentology **58:**720-738.
229. **Steinhorst L, Kudla J.** 2013. Calcium - a central regulator of pollen germination and tube growth. Biochim Biophys Acta **1833:**1573-1581.
230. **Bose J, Pottosin, II, Shabala SS, Palmgren MG, Shabala S.** 2011. Calcium efflux systems in stress signaling and adaptation in plants. Front Plant Sci **2:**85.
231. **Robertson WG, Marshall RW, Bowers GN.** 1981. Ionized calcium in body-fluids. Crc Critical Reviews in Clinical Laboratory Sciences **15:**85-125.
232. **Blomfiel.J, Warton KL, Brown JM.** 1973. Flow-rate and inorganic components of submandibular saliva in cystic-fibrosis. Archives of Disease in Childhood **48:**267-274.
233. **Berg JM, Tymoczko, J. L., and Stryer, L.** 2002. Biochemistry, vol 5. W. H. Freeman.
234. **Vitolo MR, Valente Soares LM, Carvalho EB, Cardoso CB.** 2004. Calcium and magnesium concentrations in mature human milk: influence of calcium intake, age and socioeconomic level. Arch Latinoam Nutr **54:**118-122.
235. **Lorin MI, Gaerlan PF, Mandel ID, Denning CR.** 1976. Composition of Nasal Secretion in Patients with Cystic-Fibrosis. Journal of Laboratory and Clinical Medicine **88:**114-117.
236. **Sanders NN, Franckx H, De Boeck K, Haustraete J, De Smedt SC, Demeester J.** 2006. Role of magnesium in the failure of rhDNase therapy in patients with cystic fibrosis. Thorax **61:**962-968.
237. **Smith DJ, Anderson GJ, Bell SC, Reid DW.** 2014. Elevated metal concentrations in the CF airway correlate with cellular injury and disease severity. J Cyst Fibros **13:**289-295.
238. **Sarkisova SA, Lotlikar SR, Guragain M, Kubat R, Cloud J, Franklin MJ, Patrauchan MA.** 2014. A *Pseudomonas aeruginosa* EF-hand protein, EfhP (PA4107),

modulates stress responses and virulence at high calcium concentration. PLoS One **9:**e98985.
239. **Stock AM, Robinson VL, Goudreau PN.** 2000. Two-component signal transduction. Annual review of biochemistry **69:**183-215.
240. **McPhee JB, Lewenza S, Hancock REW.** 2003. Cationic antimicrobial peptides activate a two-component regulatory system, PmrA-PmrB, that regulates resistance to polymyxin B and cationic antimicrobial peptides in *Pseudomonas aeruginosa*. Molecular Microbiology **50:**205-217.
241. **Moskowitz SM, Ernst RK, Miller SI.** 2004. PmrAB, a two-component regulatory system of *Pseudomonas aeruginosa* that modulates resistance to cationic antimicrobial peptides and addition of aminoarabinose to lipid A. J Bacteriol **186:**575-579.
242. **Miller AK, Brannon MK, Stevens L, Johansen HK, Selgrade SE, Miller SI, Hoiby N, Moskowitz SM.** 2011. PhoQ mutations promote lipid A modification and polymyxin resistance of *Pseudomonas aeruginosa* found in colistin-treated cystic fibrosis patients. Antimicrob Agents Chemother **55:**5761-5769.
243. **Brinkman FSL, MacFarlane ELA, Warrener P, Hancock REW.** 2001. Evolutionary relationships among virulence-associated histidine kinases. Infection and Immunity **69:**5207-5211.
244. **Kwon DH, Lu CD.** 2006. Polyamines induce resistance to cationic peptide, aminoglycoside, and quinolone antibiotics in *Pseudomonas aeruginosa* PAO1. Antimicrobial Agents and Chemotherapy **50:**1615-1622.
245. **Perron K, Caille O, Rossier C, van Delden C, Dumas JL, Kohler T.** 2004. CzcR-CzcS, a two-component system involved in heavy metal and carbapenem resistance in *Pseudomonas aeruginosa*. Journal of Biological Chemistry **279:**8761-8768.
246. **Teitzel GM, Geddie A, De Long SK, Kirisits MJ, Whiteley M, Parsek MR.** 2006. Survival and growth in the presence of elevated copper: Transcriptional profiling of copper-stressed *Pseudomonas aeruginosa*. Journal of Bacteriology **188:**7242-7256.
247. **Rahme LG, Ausubel FM, Cao H, Drenkard E, Goumnerov BC, Lau GW, Mahajan-Miklos S, Plotnikova J, Tan MW, Tsongalis J, Walendziewicz CL, Tompkins RG.** 2000. Plants and animals share functionally common bacterial virulence factors. Proc Natl Acad Sci U S A **97:**8815-8821.
248. **Overhage J, Lewenza S, Marr AK, Hancock RE.** 2007. Identification of genes involved in swarming motility using a *Pseudomonas aeruginosa* PAO1 mini-Tn5-lux mutant library. J Bacteriol **189:**2164-2169.
249. **Whitchurch CB, Alm RA, Mattick JS.** 1996. The alginate regulator AlgR and an associated sensor FimS are required for twitching motility in *Pseudomonas aeruginosa*. Proc Natl Acad Sci U S A **93:**9839-9843.
250. **Carterson AJ, Morici LA, Jackson DW, Frisk A, Lizewski SE, Jupiter R, Simpson K, Kunz DA, Davis SH, Schurr JR, Hassett DJ, Schurr MJ.** 2004. The transcriptional regulator AlgR controls cyanide production in *Pseudomonas aeruginosa*. J Bacteriol **186:**6837-6844.
251. **Lizewski SE, Lundberg DS, Schurr MJ.** 2002. The transcriptional regulator AlgR is essential for *Pseudomonas aeruginosa* pathogenesis. Infection and Immunity **70:**6083-6093.
252. **Reimmann C, Beyeler M, Latifi A, Winteler H, Foglino M, Lazdunski A, Haas D.** 1997. The global activator GacA of *Pseudomonas aeruginosa* PAO positively controls

the production of the autoinducer N-butyryl-homoserine lactone and the formation of the virulence factors pyocyanin, cyanide, and lipase. Mol Microbiol **24:**309-319.

253. **Linares JF, Gustafsson I, Baquero F, Martinez JL.** 2006. Antibiotics as intermicrobial signaling agents instead of weapons. Proceedings of the National Academy of Sciences of the United States of America **103:**19484-19489.
254. **Whitchurch CB, Erova TE, Emery JA, Sargent JL, Harris JM, Semmler ABT, Young MD, Mattick JS, Wozniak DJ.** 2002. Phosphorylation of the *Pseudomonas aeruginosa* response regulator AlgR is essential for type IV fimbria-mediated twitching motility. Journal of Bacteriology **184:**4544-4554.
255. **Morici LA, Carterson AJ, Wagner VE, Frisk A, Schurr JR, Bentrup KHZ, Hassett DJ, Iglewski BH, Sauer K, Schurr MJ.** 2007. *Pseudomonas aeruginosa* AlgR represses the Rhl quorum-sensing system in a biofilm-specific manner. Journal of Bacteriology **189:**7752-7764.
256. **Ritchings BW, Almira EC, Lory S, Ramphal R.** 1995. Cloning and Phenotypic Characterization of Fles and Fler, New Response Regulators of *Pseudomonas aeruginosa* Which Regulate Motility and Adhesion to Mucin. Infection and Immunity **63:**4868-4876.
257. **Breidenstein EBM, Khaira BK, Wiegand I, Overhage J, Hancock REW.** 2008. Complex Ciprofloxacin Resistome Revealed by Screening a *Pseudomonas aeruginosa* Mutant Library for Altered Susceptibility. Antimicrobial Agents and Chemotherapy **52:**4486-4491.
258. **Hurley BP, Goodman AL, Mumy KL, Murphy P, Lory S, McCormick BA.** 2010. The two-component sensor response regulator RoxS/RoxR plays a role in *Pseudomonas aeruginosa* interactions with airway epithelial cells. Microbes Infect **12:**190-198.
259. **Silo-Suh LA, Suh SJ, Ohman DE, Wozniak DJ, Pridgeon JW.** 2015. Complete genome sequence of *Pseudomonas aeruginosa* mucoid strain FRD1, isolated from a cystic fibrosis patient. Genome Announc **3**.
260. **Damron FH, McKenney ES, Schweizer HP, Goldberg JB.** 2013. Construction of a broad-host-range Tn7-based vector for single-copy PBAD-controlled gene expression in Gram-negative bacteria. Applied and environmental microbiology **79:**718-721.
261. **Hoang TT, Karkhoff-Schweizer RR, Kutchma AJ, Schweizer HP.** 1998. A broad-host-range Flp-FRT recombination system for site-specific excision of chromosomally-located DNA sequences: application for isolation of unmarked Pseudomonas aeruginosa mutants. Gene **212:**77-86.
262. **Campbell AKS-NGS.** 1993. Bioluminescent and chemiluminescent indicators for molecular signalling and function in living cells. Academic Press, New York.
263. **Held K, Ramage E, Jacobs M, Gallagher L, Manoil C.** 2012. Sequence-verified two-allele transposon mutant library for Pseudomonas aeruginosa PAO1. J Bacteriol **194:**6387-6389.
264. **Watkins NJ, Knight MR, Trewavas AJ, Campbell AK.** 1995. Free Calcium Transients in Chemotactic and Non-Chemotactic Strains of Escherichia-Coli Determined by Using Recombinant Aequorin. Biochemical Journal **306:**865-869.
265. **Choi KH, Gaynor JB, White KG, Lopez C, Bosio CM, Karkhoff-Schweizer RR, Schweizer HP.** 2005. A Tn7-based broad-range bacterial cloning and expression system. Nat Methods **2:**443-448.
266. **Lenz AP, Williamson KS, Pitts B, Stewart PS, Franklin MJ.** 2008. Localized gene expression in *Pseudomonas aeruginosa* biofilms. Appl Environ Microbiol **74:**4463-4471.

267. **Stewart PS, Franklin MJ, Williamson KS, Folsom JP, Boegli L, James GA.** 2015. Contribution of stress responses to antibiotic tolerance in *Pseudomonas aeruginosa* biofilms. Antimicrob Agents Chemother **59:**3838-3847.
268. **Williamson KS, Richards LA, Perez-Osorio AC, Pitts B, McInnerney K, Stewart PS, Franklin MJ.** 2012. Heterogeneity in *Pseudomonas aeruginosa* biofilms includes expression of ribosome hibernation factors in the antibiotic-tolerant subpopulation and hypoxia-induced stress response in the metabolically active population. J Bacteriol **194:**2062-2073.
269. **Pfaffl MW, Horgan GW, Dempfle L.** 2002. Relative expression software tool (REST) for group-wise comparison and statistical analysis of relative expression results in real-time PCR. Nucleic Acids Res **30:**e36.
270. **Kurachi M.** 1958. Studies on the biosynthesis of pyocyanine. (II): Isolation and determination of pyocyanine. Bulletin of Institute for Chemical Research, Kyoto University **36:**13.
271. **Tamura K, Dudley J, Nei M, Kumar S.** 2007. MEGA4: Molecular Evolutionary Genetics Analysis (MEGA) software version 4.0. Mol Biol Evol **24:**1596-1599.
272. **Punta M, Coggill PC, Eberhardt RY, Mistry J, Tate J, Boursnell C, Pang N, Forslund K, Ceric G, Clements J, Heger A, Holm L, Sonnhammer EL, Eddy SR, Bateman A, Finn RD.** 2012. The Pfam protein families database. Nucleic Acids Res **40:**D290-301.
273. **Yu NY, Wagner JR, Laird MR, Melli G, Rey S, Lo R, Dao P, Sahinalp SC, Ester M, Foster LJ, Brinkman FS.** 2010. PSORTb 3.0: improved protein subcellular localization prediction with refined localization subcategories and predictive capabilities for all prokaryotes. Bioinformatics **26:**1608-1615.
274. **Nair R, Rost B.** 2005. Mimicking cellular sorting improves prediction of subcellular localization. J Mol Biol **348:**85-100.
275. **Moller S, Croning MD, Apweiler R.** 2001. Evaluation of methods for the prediction of membrane spanning regions. Bioinformatics **17:**646-653.
276. **Petersen TN, Brunak S, von Heijne G, Nielsen H.** 2011. SignalP 4.0: discriminating signal peptides from transmembrane regions. Nat Methods **8:**785-786.
277. **Biegert A, Mayer C, Remmert M, Söding J, Lupas AN.** 2006. The MPI Bioinformatics Toolkit for protein sequence analysis. Nucleic acids research **34:**W335-W339.
278. **Yang J, Yan R, Roy A, Xu D, Poisson J, Zhang Y.** 2015. The I-TASSER Suite: protein structure and function prediction. Nat Methods **12:**7-8.
279. **Macfarlane EL, Kwasnicka A, Ochs MM, Hancock RE.** 1999. PhoP-PhoQ homologues in Pseudomonas aeruginosa regulate expression of the outer-membrane protein OprH and polymyxin B resistance. Mol Microbiol **34:**305-316.
280. **Fukushima K, Kumar SD, Suzuki S.** 2012. YgiW homologous gene from *Pseudomonas aeruginosa* 25W is responsible for tributyltin resistance. J Gen Appl Microbiol **58:**283-289.
281. **Lee J, Hiibel SR, Reardon KF, Wood TK.** 2010. Identification of stress-related proteins in Escherichia coli using the pollutant cis-dichloroethylene. J Appl Microbiol **108:**2088-2102.
282. **Chen CK, Chan NL, Wang AH.** 2011. The many blades of the beta-propeller proteins: conserved but versatile. Trends Biochem Sci **36:**553-561.

283. **Jacobs MA, Alwood A, Thaipisuttikul I, Spencer D, Haugen E, Ernst S, Will O, Kaul R, Raymond C, Levy R, Chun-Rong L, Guenthner D, Bovee D, Olson MV, Manoil C.** 2003. Comprehensive transposon mutant library of *Pseudomonas aeruginosa*. Proc Natl Acad Sci U S A **100:**14339-14344.
284. **Prost LR, Miller SI.** 2008. The Salmonellae PhoQ sensor: mechanisms of detection of phagosome signals. Cellular Microbiology **10:**576-582.
285. **Vescovi EG, Ayala YM, Di Cera E, Groisman EA.** 1997. Characterization of the bacterial sensor protein PhoQ. Evidence for distinct binding sites for Mg2+ and Ca2+. J Biol Chem **272:**1440-1443.
286. **Theodorou MC, Panagiotidis CA, Panagiotidis CH, Pantazaki AA, Kyriakidis DA.** 2006. Involvement of the AtoS-AtoC signal transduction system in poly-(R)-3-hydroxybutyrate biosynthesis in *Escherichia coli*. Biochim Biophys Acta **1760:**896-906.
287. **Reusch RN, Huang R, Bramble LL.** 1995. Poly-3-hydroxybutyrate/polyphosphate complexes form voltage-activated Ca2+ channels in the plasma membranes of *Escherichia coli*. Biophys J **69:**754-766.
288. **Theodorou MC, Tiligada E, Kyriakidis DA.** 2009. Extracellular Ca2+ transients affect poly-(R)-3-hydroxybutyrate regulation by the AtoS-AtoC system in *Escherichia coli*. Biochem J **417:**667-672.
289. **Wagner VE, Bushnell D, Passador L, Brooks AI, Iglewski BH.** 2003. Microarray analysis of *Pseudomonas aeruginosa* quorum-sensing regulons: effects of growth phase and environment. Journal of bacteriology **185:**2080-2095.
290. **Schuster M, Lostroh CP, Ogi T, Greenberg E.** 2003. Identification, timing, and signal specificity of *Pseudomonas aeruginosa* quorum-controlled genes: a transcriptome analysis. Journal of bacteriology **185:**2066-2079.
291. **Bredenbruch F, Geffers R, Nimtz M, Buer J, Häussler S.** 2006. The *Pseudomonas aeruginosa* quinolone signal (PQS) has an iron-chelating activity. Environmental microbiology **8:**1318-1329.
292. **Ochsner UA, Koch AK, Fiechter A, Reiser J.** 1994. Isolation and characterization of a regulatory gene affecting rhamnolipid biosurfactant synthesis in Pseudomonas aeruginosa. J Bacteriol **176:**2044-2054.
293. **Seed PC, Passador L, Iglewski BH.** 1995. Activation of the Pseudomonas aeruginosa lasI gene by LasR and the Pseudomonas autoinducer PAI: an autoinduction regulatory hierarchy. J Bacteriol **177:**654-659.
294. **Schuster M, Greenberg EP.** 2006. A network of networks: quorum-sensing gene regulation in Pseudomonas aeruginosa. Int J Med Microbiol **296:**73-81.
295. **Frederix M, Downie AJ.** 2011. Quorum sensing: regulating the regulators. Advances in microbial physiology **58:**23-80.
296. **Dominguez DC, Guragain M, Patrauchan M.** 2015. Calcium binding proteins and calcium signaling in prokaryotes. Cell Calcium **57:**151-165.
297. **Guragain M, Lenaburg DL, Moore FS, Reutlinger I, Patrauchan MA.** 2013. Calcium homeostasis in Pseudomonas aeruginosa requires multiple transporters and modulates swarming motility. Cell Calcium **54:**350-361.
298. **Whiteley M, Lee KM, Greenberg EP.** 1999. Identification of genes controlled by quorum sensing in Pseudomonas aeruginosa. Proc Natl Acad Sci U S A **96:**13904-13909.
299. **Jensen V, Löns D, Zaoui C, Bredenbruch F, Meissner A, Dieterich G, Münch R, Häussler S.** 2006. RhlR expression in Pseudomonas aeruginosa is modulated by the

Pseudomonas quinolone signal via PhoB-dependent and-independent pathways. Journal of bacteriology **188:**8601-8606.

300. **Jacobs MA, Alwood A, Thaipisuttikul I, Spencer D, Haugen E, Ernst S, Will O, Kaul R, Raymond C, Levy R.** 2003. Comprehensive transposon mutant library of Pseudomonas aeruginosa. Proceedings of the National Academy of Sciences **100:**14339-14344.
301. **Pearson JP, Pesci EC, Iglewski BH.** 1997. Roles of Pseudomonas aeruginosa las and rhl quorum-sensing systems in control of elastase and rhamnolipid biosynthesis genes. Journal of Bacteriology **179:**5756-5767.
302. **Olsen RH, DeBusscher G, McCOMBIE WR.** 1982. Development of broad-host-range vectors and gene banks: self-cloning of the Pseudomonas aeruginosa PAO chromosome. Journal of bacteriology **150:**60-69.
303. **Duan K, Dammel C, Stein J, Rabin H, Surette MG.** 2003. Modulation of Pseudomonas aeruginosa gene expression by host microflora through interspecies communication. Mol Microbiol **50:**1477-1491.
304. **Duan K, Surette MG.** 2007. Environmental regulation of Pseudomonas aeruginosa PAO1 las and rhl quorum-sensing systems. Journal of Bacteriology **189:**4827-4836.
305. **Liang H, Li L, Dong Z, Surette MG, Duan K.** 2008. The YebC family protein PA0964 negatively regulates the Pseudomonas aeruginosa quinolone signal system and pyocyanin production. J Bacteriol **190:**6217-6227.
306. **Watkins NJ, Knight MR, Trewavas AJ, Campbell AK.** 1995. Free calcium transients in chemotactic and non-chemotactic strains of *Escherichia coli* determined by using recombinant aequorin. Biochem J **306 (Pt 3):**865-869.
307. **Choi K-H, Kumar A, Schweizer HP.** 2006. A 10-min method for preparation of highly electrocompetent Pseudomonas aeruginosa cells: application for DNA fragment transfer between chromosomes and plasmid transformation. Journal of microbiological methods **64:**391-397.
308. **Sala-Newby G, Kendall J, Jones H, Taylor K, Badminton M, Llewellyn D, Campbell A.** 1999. Bioluminescent and chemiluminescent indicators for molecular signalling and function in living cells. Fluorescent and Luminescent Probes for Biological Activity **2**.
309. **Bultynck G, Kiviluoto S, Methner A.** 2014. Bax inhibitor-1 is likely a pH-sensitive calcium leak channel, not a H+/Ca2+ exchanger. Science signaling **7:**pe22-pe22.
310. **Qi Q, Rehm BH, Steinbüchel A.** 1997. Synthesis of poly (3-hydroxyalkanoates) in Escherichia coli expressing the PHA synthase gene phaC2 from Pseudomonas aeruginosa: comparison of PhaC1 and PhaC2. FEMS microbiology letters **157:**155-162.
311. **Miyake T, Shiba T, Kameda A, Ihara Y, Munekata M, Ishige K, Noguchi T.** 1999. The gene for an exopolyphosphatase of Pseudomonas aeruginosa. DNA Research **6:**103-108.
312. **Ishige K, Kameda A, Noguchi T, Shiba T.** 1998. The polyphosphate kinase gene of Pseudomonas aeruginosa. DNA Research **5:**157-162.
313. **M. Guragain MMK, K. S. Williamson, A. C. Pérez-Osorio, T. Akyama, S. Khanam, M. A. Patrauchan and M. J. Franklin.** 2015. Role of the two-component regulator, CarSR, in regulating Pseudomonas aeruginosa calcium homeostasis and calcium-induced virulence factor production. Submitted for publication.

314. **Köhler T, Curty LK, Barja F, Van Delden C, Pechère J-C.** 2000. Swarming of Pseudomonas aeruginosa is dependent on cell-to-cell signaling and requires flagella and pili. Journal of bacteriology **182:**5990-5996.
315. **Ha DG, Merritt JH, Hampton TH, Hodgkinson JT, Janecek M, Spring DR, Welch M, O'Toole GA.** 2011. 2-Heptyl-4-Quinolone, a Precursor of the Pseudomonas Quinolone Signal Molecule, Modulates Swarming Motility in Pseudomonas aeruginosa. Journal of Bacteriology **193:**6770-6780.
316. **Werthen M, Lundgren T.** 2001. Intracellular Ca(2+) mobilization and kinase activity during acylated homoserine lactone-dependent quorum sensing in Serratia liquefaciens. J Biol Chem **276:**6468-6472.
317. **Schwarzer C, Wong S, Shi J, Matthes E, Illek B, Ianowski JP, Arant RJ, Isacoff E, Vais H, Foskett JK, Maiellaro I, Hofer AM, Machen TE.** 2010. Pseudomonas aeruginosa Homoserine lactone activates store-operated cAMP and cystic fibrosis transmembrane regulator-dependent Cl- secretion by human airway epithelia. J Biol Chem **285:**34850-34863.
318. **Vikstrom E, Bui L, Konradsson P, Magnusson KE.** 2010. Role of calcium signalling and phosphorylations in disruption of the epithelial junctions by Pseudomonas aeruginosa quorum sensing molecule. European Journal of Cell Biology **89:**584-597.
319. **Song SS, Jia ZH, Xu JZ, Zhang Z, Bian ZR.** 2011. N-butyryl-homoserine lactone, a bacterial quorum-sensing signaling molecule, induces intracellular calcium elevation in Arabidopsis root cells. Biochemical and Biophysical Research Communications **414:**355-360.
320. **Falagas ME, Bliziotis IA.** 2007. Pandrug-resistant Gram-negative bacteria: the dawn of the post-antibiotic era? International journal of antimicrobial agents **29:**630-636.
321. **Kaye KS, Kanafani ZA, Dodds AE, Engemann JJ, Weber SG, Carmeli Y.** 2006. Differential effects of levofloxacin and ciprofloxacin on the risk for isolation of quinolone-resistant Pseudomonas aeruginosa. Antimicrobial agents and chemotherapy **50:**2192-2196.
322. **Bicanic TA, Eykyn SJ.** 2002. Hospital-acquired, native valve endocarditis caused by Pseudomonas aeruginosa. The Journal of infection **44:**137-139.
323. **Ishiwada N, Niwa K, Tateno S, Yoshinaga M, Terai M, Nakazawa M.** 2005. Causative organism influences clinical profile and outcome of infective endocarditis in pediatric patients and adults with congenital heart disease. Circulation journal **69:**1266-1270.
324. **Komshian SV, Tablan OC, Palutke W, Reyes MP.** 1990. Characteristics of left-sided endocarditis due to Pseudomonas aeruginosa in the Detroit Medical Center. Reviews of infectious diseases **12:**693-702.
325. **Jesaitis AJ, Franklin MJ, Berglund D, Sasaki M, Lord CI, Bleazard JB, Duffy JE, Beyenal H, Lewandowski Z.** 2003. Compromised host defense on *Pseudomonas aeruginosa* biofilms: Characterization of neutrophil and biofilm interactions. Journal of Immunology **171:**4329-4339.
326. **Walters MC, 3rd, Roe F, Bugnicourt A, Franklin MJ, Stewart PS.** 2003. Contributions of antibiotic penetration, oxygen limitation, and low metabolic activity to tolerance of Pseudomonas aeruginosa biofilms to ciprofloxacin and tobramycin. Antimicrob Agents Chemother **47:**317-323.

327. **Carafoli E.** 2002. Calcium signaling: a tale for all seasons. Proceedings of the National Academy of Sciences of the United States of America **99:**1115-1122.
328. **von Ruecker AA, Bertele R, Harms HK.** 1984. Calcium metabolism and cystic fibrosis: mitochondrial abnormalities suggest a modification of the mitochondrial membrane. Pediatric research **18:**594-599.
329. **Borriello G, Werner E, Roe F, Kim AM, Ehrlich GD, Stewart PS.** 2004. Oxygen limitation contributes to antibiotic tolerance of Pseudomonas aeruginosa in biofilms. Antimicrob Agents Chemother **48:**2659-2664.
330. **Zhao Y, Shi Y, Zhao W, Huang X, Wang D, Brown N, Brand J, Zhao J.** 2005. CcbP, a calcium-binding protein from *Anabaena* sp. PCC 7120, provides evidence that calcium ions regulate heterocyst differentiation. Proc Natl Acad Sci U S A **102:**5744-5748.
331. **Norris V, Grant S, Freestone P, Canvin J, Sheikh FN, Toth I, Trinei M, Modha K, Norman RI.** 1996. Calcium signalling in bacteria. J Bacteriol **178:**3677-3682.
332. **Kretsinger RH.** 1976. Calcium-binding proteins. Annu Rev Biochem **45:**239-266.
333. **Chazin WJ.** 2011. Relating form and function of EF-hand calcium binding proteins. Accounts of chemical research **44:**171-179.
334. **Zhou Y, Yang W, Kirberger M, Lee HW, Ayalasomayajula G, Yang JJ.** 2006. Prediction of EF-hand calcium-binding proteins and analysis of bacterial EF-hand proteins. Proteins **65:**643-655.
335. **Xi C, Schoeters E, Vanderleyden J, Michiels J.** 2000. Symbiosis-specific expression of *Rhizobium etli* casA encoding a secreted calmodulin-related protein. Proc Natl Acad Sci U S A **97:**11114-11119.
336. **Tossavainen H, Permi P, Annila A, Kilpelainen I, Drakenberg T.** 2003. NMR solution structure of calerythrin, an EF-hand calcium-binding protein from *Saccharopolyspora erythraea*. Eur J Biochem **270:**2505-2512.
337. **Wang SL, Fan KQ, Yang X, Lin ZX, Xu XP, Yang KQ.** 2008. CabC, an EF-hand calcium-binding protein, is involved in Ca^{2+}-mediated regulation of spore germination and aerial hypha formation in *Streptomyces coelicolor*. J Bacteriol **190:**4061-4068.
338. **Yonekawa T, Ohnishi Y, Horinouchi S.** 2005. A calmodulin-like protein in the bacterial genus *Streptomyces*. FEMS Microbiol Lett **244:**315-321.
339. **van Asselt EJ, Dijkstra BW.** 1999. Binding of calcium in the EF-hand of Escherichia coli lytic transglycosylase Slt35 is important for stability. Febs Letters **458:**429-435.
340. **Michiels J, Xi C, Verhaert J, Vanderleyden J.** 2002. The functions of $Ca^{(2+)}$ in bacteria: a role for EF-hand proteins? Trends Microbiol **10:**87-93.
341. **Thurley K, Skupin A, Thul R, Falcke M.** 2012. Fundamental properties of Ca2+ signals. Biochim Biophys Acta **1820:**1185-1194.
342. **Hoeflich KP, Ikura M.** 2002. Calmodulin in action: diversity in target recognition and activation mechanisms. Cell **108:**739-742.
343. **Tisa LS, Olivera BM, Adler J.** 1993. Inhibition of Escherichia coli chemotaxis by omega-conotoxin, a calcium ion channel blocker. Journal of bacteriology **175:**1235-1238.
344. **Herbaud M-L, Guiseppi A, Denizot F, Haiech J, Kilhoffer M-C.** 1998. Calcium signalling in Bacillus subtilis. Biochimica et Biophysica Acta (BBA)-Molecular Cell Research **1448:**212-226.
345. **Torrecilla I, Leganes F, Bonilla I, Fernandez-Pinas F.** 2000. Use of recombinant aequorin to study calcium homeostasis and monitor calcium transients in response to heat and cold shock in cyanobacterial. Plant Physiol **123:**161-175.

346. **Leganés F, Forchhammer K, Fernández-Piñas F.** 2009. Role of calcium in acclimation of the cyanobacterium Synechococcus elongatus PCC 7942 to nitrogen starvation. Microbiology **155:**25-34.
347. **Torrecilla I, Leganes, F., Bonilla, I., and Fernandez-Pinas.** 2001. Calcium transients in response to salinity and osmotic stress in the nitrogen-fixing cyanobacterium *Anabaena* sp. PCC7120, expressing cytosolic apoaequorin. Plant cell and Environment **24:**641-648.
348. **Jones HE, Holland IB, Campbell AK.** 2002. Direct measurement of free Ca(2+) shows different regulation of Ca(2+) between the periplasm and the cytosol of Escherichia coli. Cell Calcium **32:**183-192.
349. **Docampo R, de Souza W, Miranda K, Rohloff P, Moreno SNJ.** 2005. Acidocalcisomes - Conserved from bacteria to man. Nat Rev Microbiol **3:**251-261.
350. **Seufferheld M, Lea CR, Vieira M, Oldfield E, Docampo R.** 2004. The H(+)-pyrophosphatase of Rhodospirillum rubrum is predominantly located in polyphosphate-rich acidocalcisomes. J Biol Chem **279:**51193-51202.
351. **Yonekawa T, Ohnishi Y, Horinouchi S.** 2001. A calcium-binding protein with four EF-hand motifs in *Streptomyces ambofaciens*. Biosci Biotech Bioc **65:**156-160.
352. **Song S, Jia Z, Xu J, Zhang Z, Bian Z.** 2011. N-butyryl-homoserine lactone, a bacterial quorum-sensing signaling molecule, induces intracellular calcium elevation in Arabidopsis root cells. Biochem Biophys Res Commun **414:**355-360.
353. **Joseph S, David WR.** 2001. Molecular cloning: a laboratory manual. Cold Spring Harbor Laboratory Press, Cold Spring Harbor, New York **2**.
354. **Holloway B, Krishnapillai V, Morgan A.** 1979. Chromosomal genetics of Pseudomonas. Microbiological reviews **43:**73.
355. **Damron FH, McKenney ES, Schweizer HP, Goldberg JB.** 2013. Construction of a broad-host-range Tn7-based vector for single-copy P(BAD)-controlled gene expression in gram-negative bacteria. Appl Environ Microbiol **79:**718-721.
356. **Duan KM, Dammel C, Stein J, Rabin H, Surette MG.** 2003. Modulation of Pseudomonas aeruginosa gene expression by host microflora through interspecies communication. Molecular Microbiology **50:**1477-1491.
357. **Kurachi M.** 1958. Studies on the Biosynthesis of Pyocyanine.(II): Isolation and determination of pyocyanine.

APPENDICES

Appendix A: Recipes

Antibiotics:

Ampicillin stock solution (100 mg/ml)

1 g Ampicillin
10 ml Nano-pure water
Sterilize using 0.22 µm pore-size filter. Store in 1 ml aliquots at -20 °C.

Carbenicillin stock solution (300 mg/ml)

3 g Carbenicillin
10 ml Nano-pure water
Sterilize using 0.22 µm pore-size filter. Store in 1 ml aliquots at -80 °C, dark.

Tetracycline hydrochloride stock solution (20mg/ml)

200 mg Tetracycline
10 ml Nano-pure water
Sterilize using 0.22 µm pore-size filter. Store in 1 ml aliquots at -20 °C, dark.

Note: Solubility limit of Tetracycline hydrochloride in water is 20 mg/ml.

Trimethoprim stock solution (50mg/ml)

500 mg Trimethoprim
10 ml of chloroform:ethanol = 1:1
Sterilize using 0.22 µm pore-size filter. Store in 1 ml aliquots at -20 °C, dark.

Note: Trimethoprim is hard to dissolve. Solubility can be enhanced by vortexing and leaving at room temperature for 15 -30 min.

Kanamycin stock solution (50mg/ml)

500 mg Kanamycin
10 ml Nano-pure water
Sterilize using 0.22 µm pore-size filter. Store in 1 ml aliquots at -20 °C, dark.

Buffers:

Discharge buffer (5 ml)

12.5 mM $CaCl_2$
62.5 µl CaCl2 (1M)

2% NP40 (70%)
143 µl NP40 (70%)

Coelenterazine (50mM)

250 µg coelenterazine
1.136 ml ethanol (95%)

HEPES buffer (1000ml)

25 mM HEPES
5.96 g HEPES

125 mM NaCl
7.3 g NaCl

1mM $MgCl_2$
0.0952 g $MgCl_2$

Adjust pH to 7.5 with 1M NaOH

Potassium Phosphate buffer (20mM)

Solution 1:

620 mM $K2HPO_4$
107.99 g $K2HPO_4$
Q.S to 1 L

Solution 2:

620 mM KH_2PO_4
84.37g KH_2PO_4
Q.S to 1 L

Mix 615 ml of solution 1 and 385 ml of solution 2

The ratio ensures that the pH of the buffer is pH 7.0.

50 X TAE (running buffer for agarose gel DNA electrophoresis)

242 g Trisma base
57.1 ml Glacial acetic acid
100 ml 0.5 M EDTA, pH – 8.0
Q.S. to 1 L
Dilute to 1X for running DNA-agarose gel.

Calcium transport inhibitors:

300 mM $LaCl_3$ solution

0.073 g $LaCl_3$
1 ml Nano-pure water
Aliquot in 100 µl volume. Store at 4 ^oC.

20mg/ml Gramicidin D solution

0.02 g Gramicidin D
1 ml DMSO (100%)
Aliquot in 100 µl volume. Store at 4 ^oC.

50mg/ml compound 48/80 solution

0.1 g Gramicidin D
2 ml Nano-pure water
Aliquot in 100 µl volume. Store at 4 ^oC

2,4 dinitrophenol solution

0.0159 g Gramicidin D
1 ml Nano-pure water
Aliquot in 100 µl volume. Store at 4 ^oC

0.058 mM Calcimycin solution

Solution A: 0.58 mM calcimycin
1 g calcimycin
1 ml DMSO (100%)

Dilute solution A 10 fold.
100 µl solution A
900 µl DMSO (100%)
Aliquot in 100 µl volume. Store at 4 ^oC

QS molecules extraction and HPLC buffers:

0.1% acidified ethyl acetate

1 ml glacial acetic acid
999 ml ethyl acetate

0.1% acidified methanol

1 ml glacial acetic acid
999 ml methanol

0.1% acidified water

1 ml glacial acetic acid
999 ml water

Media:

1x Biofilm Minimal Media (BMM)

This bacterial growth medium is well defined and supports excellent growth of *P. aeruginosa.*

9mM Monosodium Glutamate
50mM Glycerol (w/v)
0.15 mM Sodium Phosphate Monobasic
0.34 mM Dipotassium phosphate
145 mM Sodium Chloride
pH: 7
Q.S. to 1 L and Autoclave

After cooling down add the following:
1 ml of Vitamin solution
200 µl of Trace Metal Solution
0.02 mM (20 µl) of Magnesium sulfate solution

Luria-Bertani (LB) Broth

10 g Bacto-Tryptone
5 g Yeast Extract
5 g Sodium Chloride
Q.S. to 1 L. Autoclave.

LB Agar

10 g Bacto-Tryptone
5 g Yeast Extract
5 g Sodium Chloride
15 g Agar
Q.S. to 1 L. Autoclave.

Swarming agar (1 L)

0.4g glucose
0.5g casamino acids
62 mM potassium phosphate buffer
100 ml of 620 mM potassium phosphate buffer

Q.S to 990 ml L and autoclave

After cooling down add the following:
10 µM $FeSO_4$
10 ml of 1 mM $FeSO_4$

0.02 mM Mg SO_4
1 ml of 20 mM Mg SO_4

Using 25 ml pipette, transfer 20 ml swarming agar to sterile petri plates.

Stock Solutions:

Biotin Stock Solution (BSS)

1 mg Biotin
Q.S. to 10 ml
Filter Sterilize

Vitamin Solution for BMM (100 ml)

50 mg Thiamine
1 ml BSS
Q.S. to 100 ml
Filter Sterilize

Trace Metal Solution for BMM (100 ml)

0.5g Copper (II) sulfate pentahydrate
0.5 g Zinc sulfate heptahydrate
0.5 g Ferrous sulfate heptahydrate
0.2 g Manganese chloride tetrahydrate
0.83 M Hydrochloric acid (10 ml)
Q.S to 100 ml
Filter sterilize

1 M Magnesium Sulfate Solution for BMM

24.65 g of Magnesium sulfate heptahydrate
Q.S. to 100 ml
Filter Sterilize

1 M Calcium chloride solution ($CaCl_2.2H_2O$)

11.098 g Calcium chloride
Q.S. to 100 ml

20 mM $MgSO_4$ solution (200 ml)

0.9858 g $MgSO_4$
Q.S to 200 ml
Sterilize using 0.22 µm pore-size filter. Store at 4 °C.

1 mM $FeSO_4$ solution (200 ml)

0.0559 g $FeSO_4$
Q.S to 200 ml
Sterilize using 0.22 µm pore-size filter. Store at 4 °C.

500 mM IPTG stock solution (isopropyl β-D-1- thiogalactpyranoside)

0.24 g IPTG
10 ml diH2O
Filter through 0.22 µm filter. Store at -20 °C in 1 ml aliquots.

300 mM Sucrose stock solution

51.34 g Sucrose
Q.S to 500 ml.
Sterilize using 0.22 µm pore-size filter. Store at 4 °C.

0.1% (w/v) Crystal violet solution

0.5 g Crystal violet
330 ml glacial acetic acid
Q.S to 1 L

Saline solution (0.85 % NaCl)

8.5 g NaCl
Q.S to 1 L
Autoclave. Store at R.T

1N Sodium hydroxide (NaOH) solution

40 g NaOH
Q.S to 1 L

Bradford Reagent

50 mg of Coomassie Blue G-250
50 ml of methanol
} A
100 ml of 85% Phosphoric acid
Add the above solution into 500 ml of H_2O and mix
Filter using Whatman filter paper 1 to remove precipitates
Q.S to 1 L
Store at 4 ^{o}C.

Ethylenediaminetetraacetic acid (EDTA) solution (0.5 M)

73. 06 g EDTA
Add 300 ml of water
Adjust pH to 8 with 1N NaOH
Q.S to 500 ml

<u>Other receipes:</u>

Agarose gel for DNA electrophoresis

50 ml 1 X TAE
0.5 g agarose (electrophoresis grade)
Final concentration of agarose (1 % w/v)

Triton solution (10 ml)

5 µl Triton X-100
2.5 ml ethanol
Q.S to 10 ml with sterilized Nano-pure water

VITA

Manita Guragain

Candidate for the Degree of

Doctor of Philosophy

Thesis: CALCIUM SIGNALING IN *PSEUDOMONAS AERUGINOSA*.

Major Field: Microbiology and Molecular Genetics

Biographical:

Education:

Completed the requirements for the Doctor of Philosophy in Microbiology and Molecular Genetics at Oklahoma State University, Stillwater, Oklahoma in December, 2015.

Completed the requirements for the Master of Science in Microbiology at Tribhuvan University, Kathmandu, Nepal in 2005.

Completed the requirements for the Bachelor of Science in Microbiology at Tribhuvan University, Kathmandu, Nepal in 2003.

Experience and Selected Awards:

Four published peer-reviewed manuscripts (one first-author)
One manuscript submitted for publication in a peer-reviewed journal (first author)
Eight awards for excellence in research, presentation, or academics
Four presentations at national professional meetings
Sixteen presentations at regional/local professional meetings
Graduate Research Assistant at Oklahoma State University 2010-2015
Graduate Teaching Assistant at Oklahoma State University Fall 2009, Spring 2010, Summer 2011 and Spring 2012.

Professional Memberships:

American Society for Microbiology
American Society for Microbiology Missouri Valley Branch